ANALYSIS AND CHARACTERIZATION OF GENERAL SECURITY REGIONS IN POWER NETWORKS

by

© M. Hadi Banakar, B.Sc. (Iran), M.Eng.

A thesis submitted to the Faculty of Graduate Studies and Research in partial fulfillment of the requirements for the degree of Doctor of Philosophy.

Department of Electrical Engineering,
McGill University,
Montreal, Canada.

September, 1980.

ANALYSIS AND CHARACTERIZATION OF GENERAL SECURITY REGIONS IN POWER NETWORKS

by

M. Hadi Banakar, B.Sc. (Iran), M.Eng.

Department of Electrical Engineering

McGill University,

Montreal, Canada.

September, 1980.

ABSTRACT

The analysis and characterization of the steady-state security of a bulk-power electric system is investigated in a region-wise or set-theoretic framework. The study is divided into three parts: a detailed examination of the theoretical aspects of general security regions; a formulation and analysis of the problem of characterizing a set of secure operating points by a simple, explicit function; and an investigation into the secure loadability of a power system.

Based on the results of the theoretical study, general approximate relations expressing dependent load flow variables in terms of the nodal injections are derived. Their degree of accuracy and extent of validity are investigated through analytical and simulation-based analyses.

The general problem of characterizing subsets of a security region by simple, explicit functions is formulated as an optimization problem. For the case where the subsets are expressed by ellipsoids, two algorithms are developed and tested. The problem is then extended to include embedding the largest ellipsoid of a fixed orientation inside a security region.

The application of explicit security sets to the problem of predictive security assessment is studied in detail. A number of explicit security subsets overlapping along the predicted daily trajectory is used to define a "security corridor". This predicted corridor has the property that as long as the actual trajectory stays within it, very little computation is needed to assess the system security.

The secure loadability of a power system is first studied in the demand space by considering the orthogonal projection of security sets into that space. It is then studied in the voltage space in the context of existence of a secure load flow solution to a given loading condition. Properties of the set of secure voltage solutions are explored by enclosing it with a linear set. Furthermore, it is shown that, under favorable conditions, one can easily characterize a subset of the set of secure voltage solutions by a number of linear constraints.

RESUME

L'analyse et la caractérisation de la sécurité en régime permanent pour un réseau et transmission ont été étudiées dans le contente de la théorie des ensembles. L'étude est divisée en trois parties: un examen détaillé des aspects théoriques des régions de sécurité générale; la formulation et l'analyse de problème de la caractérisation d'un ensemble de points de fonctionnement par une fonction simple, sous forme explicite, et l'étude de la capacité de charge d'un réseau.

Une analyse théorique a permis de dériver des relations approximative générales, exprimant les variables dépendantes de l'écoulement de puissance en terme des injections de noeud. Le degré de précision de ces approximations aini que leurs limites d'application sont déterminées à l'aide de simulations et d'analyses théoriques.

Le problème général de la caractérisation des sous-ensembles d'une région de sécurité par des fonctions simples et sous forme explicite est formulé comme problème d'optimisation. Dans le cas ou les sous-ensembles sont exprimés par des ellipsoides, deux algorithmes sont développés et vérifiés. Le problème est alors élargi de façon à inclure le plus grand ellipsoide d'orientation fixe à l'intérieur d'une région de sécurité.

L'application d'ensembles de sécurité au problème de l'évaluation préventive est étudiée en détail. On utilise un certain nombre d'ensembles de sécurité se recoupant long de la trajectoire journalière prévue de façon à définir un corridor de sécurité. Ce corridor prévu possède la propriété qu'aussi longtemps que la trajectoire y est confinée, un minimum de calculs est requis pour évaluer la sécurité du système.

Le chargement sécuritaire d'un réseau est en premier lieu étudié en considérant la projection orthogonale des ensembles de sécurité sur cet espace. Il est ensuite étudié dans l'espace des tensions, dans le contexte de l'existence d'une solution pour une charge donnée. Les proprietés de l'ensemble des solutions sécuritaires sont explorées en l'enchassant dans un ensemble linéaire. De plus, il est démontré que, dans les circonstances favorables, il est aisé de caractériser un sous-ensemble des solutions sécuritaires par un certain nombre de contraintes linéaires.

ACKNOWLEDGEMENTS

The author wishes to express his highest esteem, sincere appreciation and deepest gratitude to Dr. F.D. Galiana for his able guidance and invaluable advices. His constant enthusiasm, initiation of new ideas, and friendly disposition have been the sources of inspiration in the course of this research.

My warm thanks are offered to Drs. B.T. Ooi and N. Foroud for their constant encouragement and friendship.

Thanks are also due to all friends and colleagues in the Electrical Engineering Department of McGill University for their good company and support. In particular, Ms. P. Hyland deserves special mention for her excellent typing. Special thanks go to the fellows in Room 848 for being such a nice bunch.

The author is grateful to Mr. L. Fink and Drs. T. Trygar and K. Carlson of the U.S. Department of Energy for monitoring this research and providing the financial support.

Finally, let me offer my heartfelt thanks to my courageous wife, Nahid, for her compassion and sacrifices during these years of intensive effort of my graduate studies, and to my son, Arash, who missed much weekend fun because "Daddy had work to do".

TABLE OF CONTENTS

NOMENCLATURE

N_b	Number of nodes (buses) in the network.
$N_z = 2N_b - 1$	Number of specified injections.
$\underline{I}$	Vector of complex nodal currents (N_b - dimensional).
$\underline{V}$	Vector of complex bus voltages (N_b - dimensional).
S_k	Net complex power injected into bus K.
I_{ij}	Complex line current, flowing from bus i to j.
S_ℓ^L	Complex line power flow, flowing in line ℓ.
$\lvert I_\ell \rvert^2$	Square of the line current magnitude for line ℓ.
v_k^2	Square of the voltage magnitude at bus k.
P_k	Net real power injected into bus k.
q_k	Net reactive power injected into bus k.
$[Y_b]$	Complex bus admittance matrix ($N_b \times N_b$ dimensional).
$[G]$	Real part of $[Y_b]$.
$[B]$	Imaginary part of $[Y_b]$.
Y_ℓ^{ser}	Series admittance of line ℓ.
Y_ℓ^{sht}	Shunt susceptance of line ℓ.

$\underline{e}$	Real part of $\underline{V}$.
$\underline{f}$	Imaginary part of $\underline{V}$.
$V_r = e_r + j\, f_r$	Complex voltage at the reference bus.
θ_r	Phase angle at the reference bus.
θ_k	Phase angle of V_k , the kth component of $\underline{V}$.
$\underline{x}_r$	$(\underline{e}^T , \underline{f}^T)^T$.
$I_k\, (\underline{x}_r)$	kth component of $\underline{I}$.
$\underline{x}$	$\underline{x}_r$ without f_r (N_z - dimensional) .
z_k	A specified injection at bus k .
$Z_k(\underline{x}) = z_k$ *	Functional representation of z_k .
$[Z_k]$ *	A symmetric matrix representing the functional dependence of z_k with the network parameters ($N_z \times N_z$ - dimensional) .
$\underline{z} = \underline{Z}\, (\underline{x})$	Load flow equations.
$[J\, (\underline{x})] = \frac{\partial \underline{z}}{\partial \underline{x}}$	Jacobian of the load flow equations.

* Similar definitions apply to the components of $\underline{y}$, $\underline{u}$, and $\underline{d}$.

$[L\ (\underline{x})]$	Half of $[J\ (\underline{x})]$.
$[Z\ (\underline{\alpha})]$	$\sum_{k=1}^{N_z} \alpha_k\ [Z_k]$.
N_{dp}	Number of dependent variables in the system.
N_c	Number of control variables in the system.
N_d	Number of demand variables in the system.
N_ℓ	Number of transmission lines in the network.
N_g	Number of generation buses in the system.
P_1^g	Real power generation at the slack bus.
$\underline{P}^v$	Vector of real power generations at the PV buses (N_v - dimensional) .
$\underline{P}^g$	$(P_1^g\ ,\ \underline{P}^{vT})^T$: The generation vector.
$\underline{v}^2$	$(v_1^2\ ,\ v_2^2\ ,\ \ldots\ ,\ v_{N_v}^2)^T$.
$\underline{u}$	$(\underline{v}^{2T},\ \underline{P}^{vT})^T$: The control vector.
$\underline{P}^d$	Vector of real power demand.
$\underline{q}^d$	Vector of reactive power demand.
$\underline{d}$	$(-\underline{P}^{dT},\ -q^{dT})^T$: The demand vector.

$\underline{y}$	Vector of load flow dependent variables (N_{dp} - dimensional) .
$\underline{\eta}$	$[\underline{z}^T , \underline{y}^T]^T$.
$\underline{w}$	Vector of network parameters.
$\underline{\S}$	$[\underline{w}^T, \underline{u}^T, \underline{d}^T]^T$.
$\underline{h} = \underline{H} (\underline{\S}, \underline{x})$	General vector representing the constrained variables.
$\underline{h} \leq \underline{h}^{\ell}$	Operating constraints.
$S_{\S}$	General steady-state security regions.
$S_{\S}^{j}$ *	Set of normal conditions which are secure against the jth contingency.
$S_{\S}^{I}$ **	General steady-state invulnerability region.
N_{cg}	Number of probable contingencies.
$C (\underline{\S})$	Set of the probable contingencies at $\underline{\S}$.
$\underline{\rho}^{j} (\underline{\S})$	Functional representation of the jth contingency.
S_z	Set of normally secure injections.

---

* Similar definitions apply to S_z^j and S_d^j in their respective spaces.

** Similar definitions apply to S_z^I and S_d^I in their respective spaces.

$S_z\ (\underline{d} = \underline{d}_0)$	Cross-section of S_z corresponding to $\underline{d} = \underline{d}_0$.
S_d	Normal loadability set.
$\underline{E}\ (\underline{d})$	Function representing the unconstrained optimal control strategy for a given $\underline{d}$.
S_d^e	Secure-economic loadability set.
H_u	Set of admissible control strategies $\varepsilon\ R^{N_c}$.
H_y	Set of allowable ratings $\varepsilon\ R^{N_{dp}}$.
H_d	The a priori loading set $\varepsilon\ R^{N_d}$.
H_z	$H_u \cap H_d$ in the $\underline{z}$ space.
X^j	Region defined by $h_j \le h_j^\ell$ in the $\underline{x}$ space.
Z^j	Region defined by $h_j \le h_j^\ell$ in the $\underline{z}$ space.
U_x	Set of voltage vectors satisfying $\underline{u}\ \varepsilon\ H_u$.
Y_x	Set of voltage vectors satisfying $\underline{y}\ \varepsilon\ H_y$.
D_x	Set of voltage vectors satisfying $\underline{d}\ \varepsilon\ H_d$.
S_x	Normal steady-state security region in the $\underline{x}$ space.

R_z	Load flow feasibility region $\varepsilon\ R^{N_z}$.
$\underline{z}^M$ *	Upper bound on $\underline{z}$.
$\underline{z}^m$ *	Lower bound on $\underline{z}$.
$\underline{\ell}_j$	Vector whose only non-zero entry is 1 at the jth location.
$\underline{x}_0$ or $\underline{z}_0$	Taylor series expansion point ($\underline{z}_0 = \underline{Z}\ (\underline{x}_0)$) .
$T_n\ (\underline{x}_0, \Delta\ \underline{z})$	nth term of the Taylor series.
$\underline{\beta}\ (\underline{x}_0)$	Coefficient vector for the linear term in the series.
$[C\ (\underline{\beta})]$	Coefficient matrix for the quadratic term in the series.
$\underline{\beta}_i\ (\underline{x}_0)$	$\underline{\beta}\ (\underline{x}_0)$ corresponding to y_i .
$\varepsilon_1\ (\underline{x})$	Error associated with a linear approximation.
λ^{max}	Maximum eigenvalue.
λ^{min}	Minimum eigenvalue.

---

* Similar definitions apply to the lower and upper bounds on $\underline{y}$, $\underline{u}$, $\underline{d}$, and $\underline{\eta}$.

$\lVert \underline{x} \rVert$	Euclidean norm of the vector $\underline{x}$.
$\underline{Z}_i^{-1}$ ( )	Inverse transformation corresponding to the ith solution of $\underline{z} = \underline{Z}\ (\underline{x})$.
ε_j^k	Fractional change in the injection z_j representing the kth contingency in part.
P_ℓ	Total I^2R loss in the network.
P_d	Total demand.
$\underline{z}_g$	Given injection.
$\underline{x}_g$	Load flow solution to $\underline{z}_g$.
S_s (c)	Subset of S_z for a given c .
C ($\underline{z}$, $\underline{z}_g$)	Function describing S_s (c) .
L ($\underline{z}$, λ)	Lagrange function.
L ($\underline{z}$, λ, ρ)	Augmented Lagrange function.
B_x	Boundary of S_x .
E_z^k	Largest ellipsoid embedded inside S_z^k.

$\underline{z}_k^*$	Center of the ellipsoid defining E_z^k .
E^i	ith ellipsoid forming the security corridor.
$\underline{z}_i$	Center of the ith ellipsoid.
$[A_i]$	Positive-definite matrix defining E^i .
c_i	Constant describing the boundary of E^i .
E_s^i	Secure part of E^i .
E_s^c	$\bigcup_{i=1}^{n} E_s^i$: Security corridor.
I^i	Set of constraints Z^j intersecting E^i .
t_i	Time corresponding to $\underline{z}_i$ on the trajectory .
c_{ij}^{ℓ}	Smallest value of c_i for which E^i touches the boundary of the set Z^j . This boundary is defined either by $y_j = y_j^M$ $(\ell = M)$ or $y_j = y_j^m$ $(\ell = m)$.
M_x $(\underline{d})$	The set of voltage vectors satisfying the demand $\underline{d}$.
S_x $(\underline{d})$	$M_x \cap U_x \cap Y_x$: The set of secure load flow solutions corresponding to $\underline{d}$.
L_x^a $(\underline{d})$	Linear set enclosing S_x $(\underline{d})$.

$L_x^b\,(\underline{d})$	Linear set enclosed by $S_x\,(\underline{d})$.
$I_k^{re}\,(\underline{x}_r)$	Real part of $I_k\,(\underline{x}_r)$.
$I_k^{im}\,(\underline{x}_r)$	Imaginary part of $I_k\,(\underline{x}_r)$.
ψ_k	Estimate of the average value of θ_k over $S_x\,(\underline{d})$.
δ_k	Upper-bound on the deviation of ψ_k from θ_k .

ABBREVIATIONS

LFE	Load flow equations.
SSSR	Steady-state security region.
TSE	Taylor series expansion.
LP	Linear programming.
OPF	Optimal Power Flow.
BNA	Based Newton Algorithm.

CHAPTER I

INTRODUCTION

1.1 General

1.1.1 Description of a Bulk-Power System [1]

A bulk-power system is made up of a high-voltage transmission network joining the generating plants to the transmission sub-stations. Generating plants normally consist of a number of synchronous generators driven by steam, gas, or hydro turbines. A step-up transformer directly feeds the output of a generating plant into the transmission system.

The transmission system is composed of several separate successive networks which are tied together at sub-stations. Each network is distinguished by its operating voltage level. The structure of transmission system enables it to serve a variety of load points at different voltage levels over a large geographical area. Another function of the transmission network is to provide links between the underlying system and its neighbouring power systems, integrating them into a "power pool".

The distribution systems are not considered here as part of the transmission system, but rather as major loading points fed from the transmission system.

1.1.2 Background and Motivation

The main function of an electric power system is to generate electric power in sufficient quantities at the most suitable generating locality, transmit it to the load centers, and distribute it to the individual customers. Furthermore, this has to be done reliably, in proper form and quantity, and at the lowest possible ecological and economical cost, [2] . Each of these requirements poses a variety of operational constraints which are to be considered in the planning and enforced during the operation of the system. The degree of complexity associated with achieving these objectives in a power system is closely tied to the system size, or equally to its vulnerability to disturbances or equipment failure.

The present day power systems include hundreds of transmission lines, generating plants and sub-stations. The rapid expansion of power systems in North American countries is in response to the growing energy demand which, in turn, is influenced by the population growth and the consumer oriented social structure of the countries. The largest growth rate in energy consumption in the United States has been in the electric sector at a rate of 6.7% annually [3] . This amounts to doubling the total electric energy demand every 11 years. Figure 1.1 depicts the projection of Canada's energy supply / demand curve up to year 2000 [4] . Here, a basically exponential growth trend can be observed. The congestion of traditional urban areas and the imposition of more stringent pollution laws has also contributed to the expansion of power systems. During the last

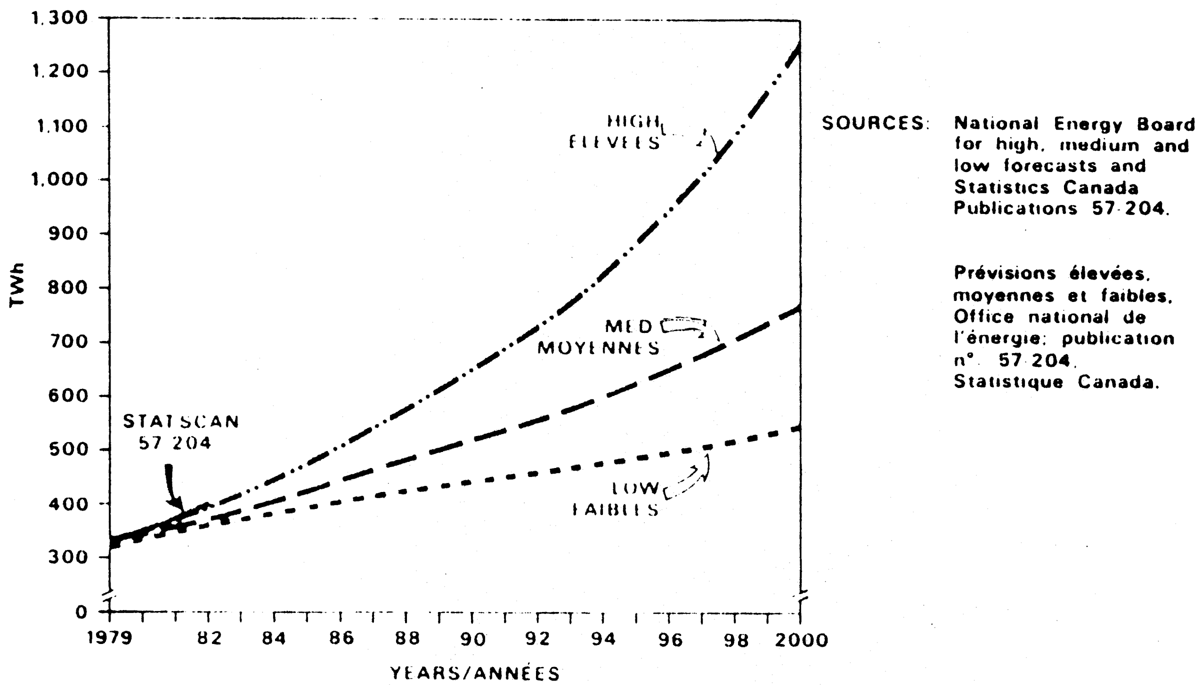

(a)

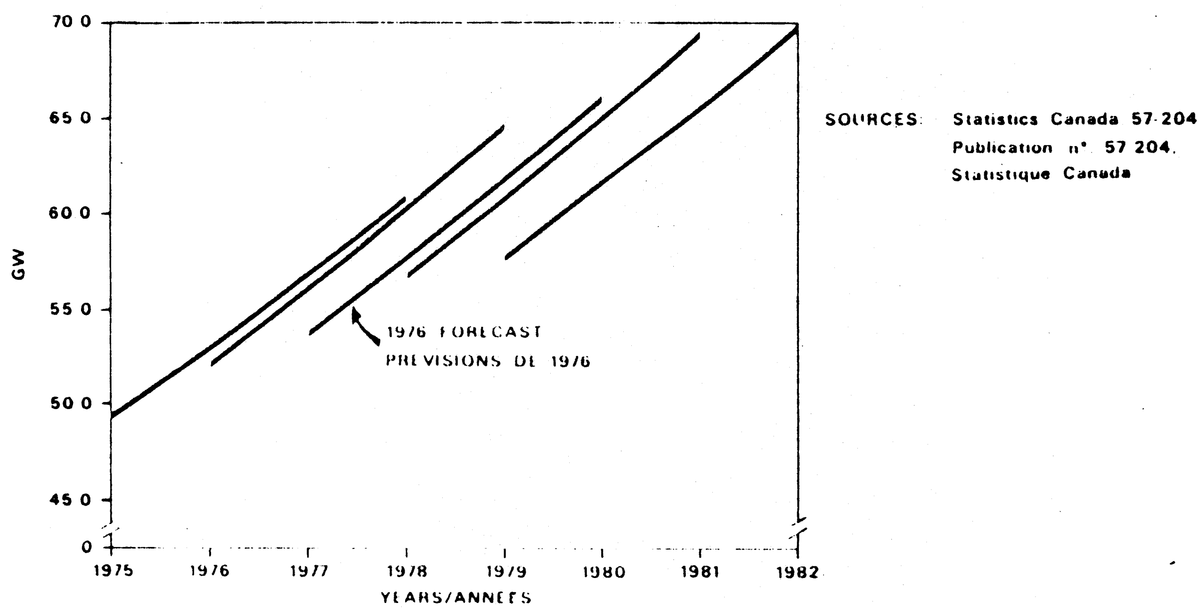

(b)

Figure 1.1. Electric energy forecasts (a), and the firm power peak load forecast (b) for Canada.

decade the residential areas and industrial units have been moving to the countryside at an increasing rate. This trend is expected to be accelerated in the future.

The degree of vulnerability of present-day power systems to disturbances (from internal or external sources) can be appreciated from the available statistics on the large and small scale blackouts during the last few years [7] . On the U.S. bulk-power system alone, an annual average of 35 interruption of at least 100 Mw for periods longer than 15 minutes is reported. Among the major blackouts, the New York blackout in 1977 is the best known [5] . Similar wide-spread blackouts were also experienced in France and Sweden in 1978 and early 1979, respectively.

The tremendously high social and economical costs of large scale blackouts [6] had been the prime factor in calls for improved system reliability and urgent need for developing security oriented operating strategies. These are operating strategies which should enable a system to absorb the impact of a wide range of disturbances easily, while the system remains faithful to its basic objectives. The widespread installation of modern control centers, equipped with high speed computers capable of coordinating the actions of various decision points in the system, has been in part the response of the power industry to this need [13] . The complex nature of the problems associated with evaluating the desired operating strategies, however, has kept, and continues to keep, the search for more efficient strategies an active field of research.

The evaluation of the degree of vulnerability of a power system to various potential disturbances and the computation of control actions which can minimize the impact of a set of disturbances is what is called "the security problem". In this thesis, different aspects of the security problem are studied and new techniques for treating some of the pertinent problems are proposed.

1.2 Power System Security

1.2.1 Basic Definitions [8]

Security of a bulk power system is considered as referring to "an instantaneous, time varying condition that is a function of the robustness of the system relative to imminent disturbances". The degree of security of an operating point is estimated by evaluating its security level based on the available reserve margins (i.e., transmission and generation capacity) on the one hand, and the likelihood of the disturbances on the other.

Being basically an operating problem, power system security is divided into two different problems: a state evaluation (detection, estimation) problem, referred to as "security assessment" [9] , and a control problem, termed the "security enhancement" [10] .

Generally, security assessment refers to the process of assessing the relative robustness of the system in its actual state through extracting the necessary information from system-derived data. This process, however, is often viewed as a combination of two primary security functions: Security monitoring and security analysis. Security monitoring refers to the function of processing the incoming data and correlating it with available data to reliably estimate the system's present or the near future operating condition. The security analysis function consist of simulating the system under various contingency conditions in order to estimate the security level of the system and supply data to the security enhancement process [9] . Obviously, the availability of a set of precisely defined system states is the prerequisite to the process of security assessment.

Security enhancement refers to any set of on-line control actions aimed at increasing the system's robustness and, thus, raising its security level. Security enhancement is viewed as a means for better utilization of installed generation and transmission capacity in an operating power system through improved controls. It involves considering alternative operating control strategies for the actual loading condition in order to attain the highest possible security level subject to the economic considerations.

1.2.2 Operating States and Related Control Actions

In 1966, with the aim of developing a framework for systematic analysis of the overall power system operating problem, Dyliacco introduced the concept of multi-state operation of electric power systems [11] . He originally decomposed system operation into three states: Normal; Emergency; and Restorative. Refinements of these definitions were later suggested [12, 13], by decomposing the normal state into two stages: Secure and Alert (or Insecure). To date, the most comprehensive classification of the operating states is due to Fink and Carlson [8] , who introduced the concept of the security levels and added an additional state, referred to as "in extremes". Their normal state is restricted to the operating conditions with an adequate security level and does not include the alert state. In this thesis, except for using the original definition of normal state, (i.e., including the alert state), the definitions of [8] are used.

The decomposition of steady-state operating states is based on two sets of algebraic relations - one comprised of equality and the other of inequality constraints - and a subjective measure, namely the security level. The equality constraints represent the system's total demand - total generation balance while the inequalities reflect various operating restrictions on the system components.

In the normal state both sets of constraints are satisfied, and it is only the security level which determines if an operating point is in the secure or alert state. As shown in Figure 1.2, a normal operating point will be in the secure state if it is accompanied by sufficient reserve margins to provide an "adequate" level of system security with respect to the stresses which the system may be subjected to. The same operating point could, however, be in the alert state if the reserve margins fall below some "threshold of adequacy" or if the probability of some disturbances increase significantly. In that case

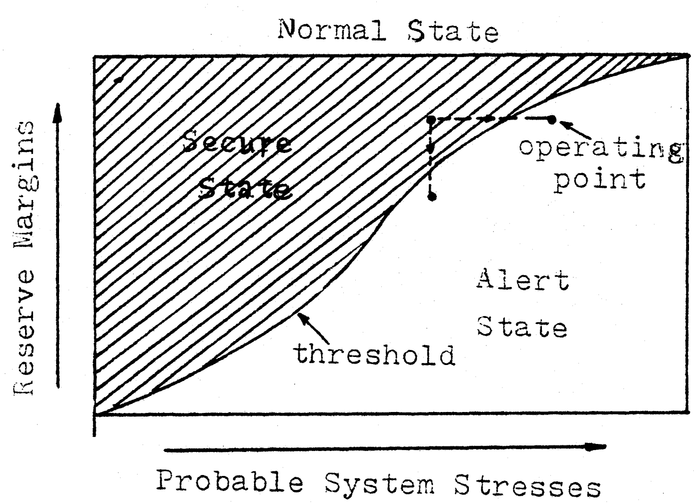

Figure 1.2. Pictorial representation of the impact of system reserve margins and probable stresses on the operating state of an operating point.

<u>preventive controls</u> are needed to increase the system security level to that of the secure state. If the required preventive measures are not taken, a sufficiently severe disturbance can take the system to an

Emergency state. In this state, inequality constraints are violated and the security level is negative. The system, however, would still be intact and should the heroic measures (or corrective controls) be taken in time, the system could be guided toward the normal state. If these measures fail to produce the desired state transition or are not taken in time, the system then begins to disintegrate and is in extremes. Here, both sets of constraints are violated; portions of the system load are rejected and the system is no longer intact. At this stage, coordinated emergency actions are needed to avert the total collapse of as many parts of the system as possible. When the collapse is averted, the system could enter the restorative state. In this state restorative control actions are directed toward reconnecting the system and picking up all the rejected loads. Once these measures are fully in effect, the system could transit to the normal state.

1.3 Review of Previous Work

1.3.1 General Classifications

A short classification of security problems is given in Figure 1.3. In this study we are primarily concerned with the steady-state security analysis in its deterministic mode.

There are two distinct classes of approaches as applied to power system security analysis. The distinction is based mainly on the

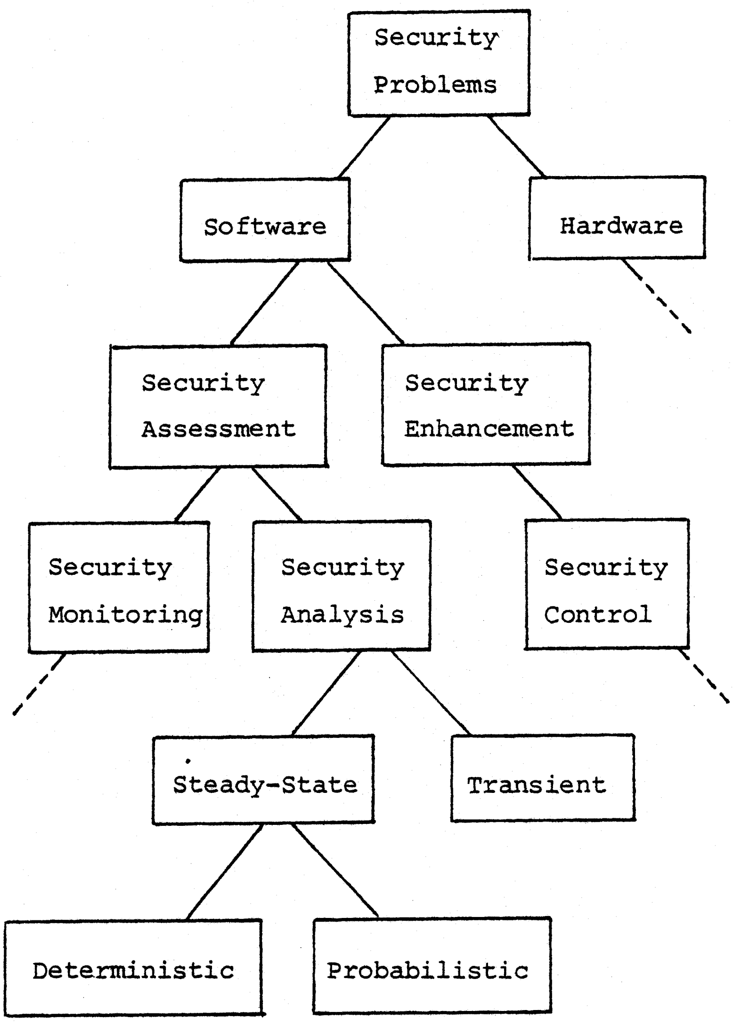

Figure 1.3. A short classification of security problems.

general philosophy behind the two. One class tries to evaluate directly every operating condition in terms of its security. This is a "point-wise" methodology and the basis of the majority of numerical techniques which are now widely employed in the power system industry for security analysis. The approaches which fall into this category require detailed on-line analysis for every operating condition from load or network changes. The other class opts for a more general view by first identifying a large set of secure operating conditions. This is a "region-wise" methodology and it is often referred to as "set-theoretic approach". The set oriented approaches try to reduce the on-line computational burden by assigning some of this effort to their initial off-line phase.

1.3.2 Numerical Based Approaches

Two numerical algorithms are the backbone of different approaches used in the point-wise security analysis. These are: The load flow [17] and the optimal load flow [41] . For a given network, loading condition, and control strategy the load flow program analyzes the steady-state interaction among real and reactive powers and voltage magnitudes in the system. In contingency evaluation, load flow programs are used to compute the impact of the potential disturbances on the system. The optimal load flow program manipulates the control variables to evaluate the best operating strategy with respect to a specific technical or economic objective. Theoretically, such algorithms can be used to compute control actions needed for the transition from an operating state to another. In practice, however, both these algorithms, when used on-line, are employed in simplified or approximate forms.

1.3.2.1 Security Analysis Calculations

A large volume of literature discussing a wide spectrum of numerical approaches exists on this subject (c.f. [14-26]). Their prime objective is to lessen the computational burden associated with the direct use of the load flow program, but without compromising the validity of the security predictions.

Since the sensitivity based analyses allow trade-off possibilities between the speed and the computational procedures, they are widely used in connection with the contingency evaluation. Assuming the load flow equations in the pre-outage case are given by

$$\underline{Z}\ (\underline{x}_0, \underline{w}_0) = \underline{z}_0 \tag{1.1}$$

where $\underline{w}_0$ is the vector of network parameters and $\underline{z}_0$ is the vector of specified injections, then the post-outage case is given by

$$\underline{Z}\ (\underline{x}_0 + \Delta\, \underline{x}\ ,\ \underline{w}_0 + \Delta\, \underline{w}) = \underline{z} + \Delta\, \underline{z} \tag{1.2}$$

For relatively small change in the state vector, $\underline{x}$, from a first order Taylor series expansion of (1.2) and implication of (1.1), it follows that

$$\Delta \underline{x} \simeq \left[\frac{\partial \underline{Z}(\underline{x}_0, \underline{w}_0)}{\partial \underline{x}_0}\right]^{-1} \left\{\Delta \underline{z} - \left[\frac{\partial \underline{Z}(\underline{x}_0, \underline{w}_0)}{\partial \underline{w}_0}\right] \Delta \underline{w}\right\} \qquad (1.3)$$

The accuracy of (1.3) depends actually on how small $\Delta \underline{w}$ and $\Delta \underline{z}$ are. If these changes cannot be assumed small, then $\Delta \underline{x}$ is calculated from:

$$\Delta \underline{x} \simeq \left[\frac{\partial \underline{Z}(\underline{x}_0, \underline{w}_0 + \Delta w)}{\partial \underline{x}_0}\right]^{-1} \left\{\underline{z}_0 + \Delta \underline{z} - \underline{Z}(\underline{x}_0, \underline{w}_0 + \Delta \underline{w})\right\} \qquad (1.4)$$

Note that when (1.3) is applicable, only the base Jacobian, $\left[\frac{\partial \underline{Z}(\underline{x}_0, \underline{w}_0)}{\partial \underline{x}_0}\right]$, is needed. This is not the case in (1.4). But, by expressing the inverse of the Jacobian in (1.4) in terms of the base Jacobian through the application of the "matrix inversion lemma" its computational efficiency can be increased significantly [14] . The base Jacobian is usually available in its triangular factors which are used within a scheme of sparse matrix computation. A brief survey of outage calculation schemes based on equations (1.3) or (1.4) is given in Appendix A.

1.3.2.2 Security Control Calculations

In theory, one should be able to compute the best control strategy, under any steady-state system condition, by solving a security-constrained optimization problem. For most systems, however, such an approach is impractical. Consider for example the case where the calculation of a preventive control strategy is desired. There maintaining or enforcing a certain level of security is sought while minimizing the adverse economic or other consequences of the required control action. This in mathematical terms is translated into the following problem:

$$\text{Minimize:} \quad C\,(\underline{x}_0\,,\,\underline{u})$$

subject to

$$\begin{aligned} \underline{D}_i\,(\underline{x}_i,\,\underline{u}) &= \underline{0} \qquad i = 0, \ldots, N_{cg} \\ \underline{H}_i\,(\underline{x}_i,\,\underline{u}) &\geq \underline{0} \qquad i = 0, \ldots, N_{cg} \end{aligned} \tag{1.5}$$

where N_{cg} is the total number of contingencies considered.
The equalities represent the load constraints while the inequalities represent the operating constraints. The subscript i counts the listed contingencies and $i = 0$ corresponds to the intact system. Note that the constraints with $i \geq 1$ represent the "security constraints". A rigorous treatment of this problem would involve introducing a state vector $\underline{x}$ such that

$$\underline{x} = [\underline{x}_0^T\,,\,\underline{x}_1^T\,,\,\ldots\,,\,\underline{x}_{N_{cg}}^T\,]^T \tag{1.6}$$

For practical systems, the excessively large dimension of $\underline{x}$ renders an on-line solution to (1.5) impossible.

Because of this basic difficulty, very little work is done on solving (1.5). The general tendency (in the existing work) is to get around the dimensionality problem by indirectly accounting for the security constraints. A brief survey on various schemes used in computing different types of control actions is also included in Appendix A.

1.3.3 Set-Theoretic Approach to Security Analysis

The numerical simulation based methods of steady-state security assessment have many conceptual and practical limitations. Though these methods are very effective when analyzing one case at a time, the required amount of computation becomes excessive when a range of operating conditions are to be predicted for a large number of network structures - as is often the case. Furthermore, in view of the uncertainties present in the input data, these methods are inadequate for reliably assessing the system security.

To overcome these shortcomings, a new technique based on the computation of an explicit description of the set of secure states was proposed by the M.I.T. group [52], in the mid 1970's . In their classical paper they suggested that the problem of security assessment should be posed as: "Given the set of postulated contingencies, what is the set of all pre-contingency injection pattern that are secure?" After characterizing such a set, then the problem of evaluating the security of an operating point is simply one of verifying the membership to the set, and the problem of security control is one of having the operating trajectory guided toward, or kept inside, the set. The impact of the uncertainties in the input data on the security assessment can be evaluated by considering the closest distance of an estimated operating point to the boundary of the set.

Prior to this work, there had been few attempts to improve upon the conventional technique of sequential contingency testing, using approaches which are conceptually related to the set-theoretic approach. For example, methods suggested in references [53 - 55] for solving the transmission interchange capability problem under various potential contingencies fall in this category. These methods, nevertheless, lack the generality of the approach in [52] .

The use of the pattern recognition techniques [56, 57] for off-line computation of <u>security functions</u> can also be regarded as an effort to characterize the boundary of the set of steady-state or transient secure operating points. This method is in fact an automated and systematized extension of the conventional techniques used in power utilities in an attempt to separate the stable and unstable conditions. The pattern recognition techniques were not initially well-received because of the prohibitively excessive computational requirements involved in finding an adequate training set for large scale power systems. Recent improvements on these methods [58, 59] , coupled with the rapid evaluation of computers however have renewed optimism in their use in power system security analysis [65] .

The problem of explicit description of a security set is one of eliminating the large number of irrelevant constraints among those defining the set. Reference [52] proposes a "bounding hyper-box method" for this problem. This method is essentially an iterative process where a hyper-box is used to screen out the irrelevant constraints. Though conceptually simple, for security sets defined in large dimensional spaces, the proposed method could involve excessively large computational requirements. De Maio and Fischel [61] , instead of using the bounding hyper-box method, suggested to use the algorithm developed by Mattheiss [60] . This algorithm starts with an LP problem which maximizes a generalized slack variable representing the margin between the points inside the set (linear) and the binding constraints. Then by systematic pivoting, it passes over all the vertices of the linear set and at each vertex identifies n binding constraints. They recognized that the initial LP solution is in fact the center of the largest sphere that can be embedded into the set, and it can be interpreted as "the most secure" point in the set. In related publications [62, 63], Fischl exploits this very concept to identify a permanently secure region in the presence of uniformly distributed uncertainties in the bus load levels.

Though so far the number of available publications concerning the application of set-theoretic techniques to power system security is quite limited, nevertheless, their capabilities and advantages over purely numerical schemes are well recognized. The advantage of having a computationally feasible characterization of a security set lies in the fact that it practically contains an infinite number of secure operating points. This makes it a "powerful tool in a variety of power system operation and planning applications" [52] .

1.4 Outline of the Problem

The set theoretic approach of reference [52] is based on the DC load flow model and therefore can define security regions only in the space of the real power injections. As a result, the impact of a significant part of the system data on the security of an operating point - namely, its associated reactive power demand and voltage level - cannot be taken into account. For practical systems, one may also expect that, even when the redundant constraints are screened out, the security set still will be defined by such a large number of constraints that it does not offer any advantage over numerical schemes.

Considering the above limitations, this study addresses itself to the following important questions:

(1) What are the analytical tools needed to expand the scope of the previous work to the extent that one

can use the steady-state security regions to evaluate the security of an operating point completely and accurately?

(2) Can a secure operating region, or part of it, be expressed by a simple, explicit function?

(3) Can one, for a given loading condition, establish simple necessary and sufficient conditions to detect the existence of secure load flow solutions, or equally, the existence of control strategies capable of producing secure operating points?

(4) What are the implications of a positive answer to any one of the above questions with regard to various security related functions of a power system?

Obviously, the scope of this study is quite large and embraces a variety of problems some of which are purely theoretical in nature.

1.5 Methodology

To provide comprehensive answers to the questions motivating this study, the following methodologies are pursued:

(1) Taylor series expansion formulae are used to derive sufficiently general and accurate relations for defining the security regions in the space of the load flow specified nodal injections.

(2) Optimization techniques are employed to solve the problem of expressing part of a security set by a simple, explicit function.

(3) Necessary and sufficient conditions for detecting the secure loadability of a system is sought by considering the orthogonal projection of its security sets into the demand space. The existence of secure load flow voltage solutions is studied through enclosing such solutions by a linear set.

(4) Numerical examples are used to demonstrate various security related potential applications of the approximate relations, explicit security sets, and the linear sets enclosing the set of secure load flow solutions.

1.6 Claim of Originality

To the author's best of knowledge, the following are the original contributions of this study to the field of power system security analysis and operation:

(1) Providing a general definition for various steady state security sets and their corresponding invulnerability set. Other significant points in connection to these definitions are:

(i) Representation of probable contingencies as general functions of the state vector;

(ii) Exploring the relations between the general steady-state security sets and the security regions in the space of specified injections.

(2) Derivation of general, accurate approximation formulae for load flow dependent variables in terms of the specified nodal injections. This also involves:

(i) Setting up a framework for comprehensive error analysis of linear approximation formulae;

(ii) Generalization of the derivation scheme to include quadratic and higher-order approximaation formulae;

(iii) Demonstrating the potential application of quadratic approximation formulae for deriving highly accurate loss formulae;

(iv) Examining various implications of using these approximate formulae in formulating the secure economic dispatch problem.

(3) Exploring the influence of the choice of the reference bus, reference angle, slack bus, and the expansion point of the approximation formulae on different aspects of security regions. It is demonstrated that:

(i) In general, the security sets, both in the voltage and in the injection space, can be disjoint;

(ii) An improper choice of the expansion point for the approximate formulae may result in an empty security set, when it actually exists.

(4) Construction of various security sets and the invulnerability set in the injection space. This also embraces:

(i) Exploring the possibility of deriving the required approximation formulae, corresponding to different network configurations, using the intact network data;

(ii) Deriving functions representing the effect of simultaneous load or generator outages on the pre-outage injection vector, shortly after the occurrence of the outages.

(5) Formulation of the problem of explicit characterization of local sub-sets of a security set as an optimization problem. Other related points are:

(i) Proposing two practical algorithms for solving the problem;

(ii) Exploring the source of convergence difficulties arising in such optimization problems.

(6) Formulation of the problem of characterizing the largest sub-set of a security set for a given function.

It is shown that this problem can be formulated as a mini-max problem, and for the special case of having linear constraints it can be reduced to a standard LP problem.

(7) Proposing a practical scheme for screening out the redundant constraints among those defining the set of secure operating conditions in the voltage space.

(8) Demonstrating potential applications of the largest sub-set of a security set in fast and efficient computation of stand-by control actions.

(9) Introducing the concept of security corridors for predictive security assessment and enhancement. This includes:

(i) Proposing solutions to the problem of orientation, overlapping, and characterization of constituting elements of a security corridor;

(ii) Exploring various applications of security corridors in security monitoring, security analysis, and security control calculations.

(10) Introducing the concept of secure loadability sets. Other related points are:

(i) Proposing a solution to the problem of characterizing sub-sets of a secure loadability set;

(ii) Presenting the concept of secure-economic loadability set;

(iii) Exploring the possibility of employing loadability sets in security assessment, planning, and load management.

(ll) Proposing techniques for enclosing the set of secure load flow voltage solutions by a linear set. This concept, originally developed in [64] , is extended to include:

(i) Embedding a linear set inside the set of secure load flow voltage solutions;

(ii) Identification and tuning of the parameters affecting the "tightness" of the enclosing set;

(iii) Demonstrating the practicality and possible applications of the linear sets in conjunction with various optimal load flow algorithms.

1.7 Outline of the Thesis

The first four chapters of this thesis are essentially analytical-theoretical studies into the basic steps of a general approach to the characterization of steady-state security regions. Chapters VI and VII examine in detail the characterization and applications of security sets defined by simple, explicit functions. The next two chapters look into the characterization of secure loading conditions in the demand and voltage spaces. A more detailed description of the chapters is provided below.

Chapter II

This chapter is devoted to derivation of some of the essential analytical properties of the load flow equations. The derivations are based on the quadratic structure of the system's basic relations in the voltage space.

Chapter III

Definitions of general steady-state security regions are provided in this chapter. The relations existing between the general regions and a number of simple but fundamental security sets are also explored.

Chapter IV

In this chapter general approximation formulae which explicitly relate any dependent load flow variable to the vector of specified nodal injections are derived. Furthermore, the analytical properties of these formulae, their extent of accuracy, and the numerical aspects of their derivations are examined.

Chapter V

Some fundamental theoretical aspects of security regions in the injection space as well as in the voltage space are investigated in this chapter. The use of the approximate relations developed in Chapter VI in constructing the security regions, and their applications in the formulation of the secure-economic dispatch problem is also discussed.

Chapter VI

In this chapter, the problem of explicit characterization of sub-sets of a security region by simple functions is formulated and efficient numerical schemes for its solution are proposed. In addition, the problem of screening out the redundant constraints from implicit description of a security region is looked into.

Chapter VII

A wide range of applications of sub-sets of a security region expressed by simple, explicit functions are studied in this chapter. Their applications to various security problems are examined in the context of a set-theoretic approach to the predictive security assessment and enhancement.

Chapter VIII

The concept of secure loadability sets is introduced in this chapter. The derivation of certain important secure loadability sets and their potential applications are also explored.

Chapter IX

This chapter deals with the characterization of the set of secure load flow solutions. Certain properties of the set of secure load flow solutions are shown to be extractive from its enclosing linear set. Moreover, it is illustrated that under favorable conditions one can characterize part of the set of secure voltage solutions by embedding a linear set inside it. Results of the numerical examples are also presented.

CHAPTER II

STEADY-STATE MODEL OF ELECTRIC POWER SYSTEMS

2.0 Introductory Remarks

In this chapter we develop the well-known mathematical model of a power system under steady-state conditions. This provides essential background material for reference and further developments in the proceeding chapters. The modelling is based on the application of circuit theory and related concepts to a power system network. The modelling of transmission lines and transformers by lumped π-network model, generators by power sources, and load areas by power sinks is assumed. The result is a set of non-linear algebraic relations in the complex nodal voltages of the network which characterizes the behaviour of the complex power flows and voltage levels throughout the network under steady-state conditions.

The characterizing relations are expressed here mainly in their rectangular form. Their polar version is not used because of poor susceptibility to analytical studies and the complexity associated with exploiting some of its basic properties. Special attention is given to variable classification in the resulting model to ensure conciseness and clarity in the future chapters.

2.1 Mathematical Model

Henceforth a balanced three-phase power system is assumed. The transmission system is represented by a positive-phase-sequence network of linear lumped series and shunt branches - Figure 2.1. No network element - such as phase shifters or non-bilateral network branches - which could give rise to asymmetric nodal admittance matrix are assumed to exist in the system. The complex quantities are distinguished here by capital letters.

2.1.1 Constitutive Relations

The basic relations governing the steady-state operation of a power system are the following:

(i) Nodal current equations:

The vector of complex nodal (bus) currents, $\underline{I}$, is related to the vector of complex bus voltages, $\underline{V}$, through

$$\underline{I} = [Y_b]\, \underline{V} \tag{2.1}$$

where $[Y_b]$ represents the nodal bus admittance matrix. The dimensions of $\underline{I}$, $\underline{V}$, and $[Y_b]$ are respectively $N_b \times 1$, $N_b \times 1$ and $N_b \times N_b$, where N_b is the number of buses in the system.

(ii) Net nodal injected power:

At the k-th bus, the net nodal injected power, S_k, is related to the net nodal current, I_k, and the bus voltage, V_k, according to

$$S_k = V_k I_k^* \tag{2.2}$$

where * stands for the complex conjugate.

(iii) Line current flow

On the ℓ-th transmission line, connecting bus i and j, the line current, I_{ij}, flowing from bus i to j, is given by

$$I_{ij} = \frac{1}{2} V_i Y_\ell^{sht} + (V_i - V_j) Y_\ell^{ser} \tag{2.3}$$

or from bus j to bus i

$$I_{ji} = \frac{1}{2} V_j Y_\ell^{sht} + (V_j - V_i) Y_\ell^{ser} \tag{2.4}$$

The line parameters Y_ℓ^{ser} and Y_ℓ^{sht} are introduced in Figure 2.1. To avoid complications, the line current magnitude is however introduced by a single subscript ℓ, that is

$$|I_\ell|^2 \triangleq \frac{1}{2} (I_{ij} I_{ij}^* + I_{ji} I_{ji}^*) \tag{2.5}$$

(iv) Line Power Flow

The power flow on the ℓ-th transmission line, S_ℓ^L, is defined here by

$$S_\ell^L = \frac{1}{2} [V_i I_{ij}^* - V_j I_{ji}^*] \tag{2.6}$$

where the direction of positive flow is assumed to be from bus i toward bus j.

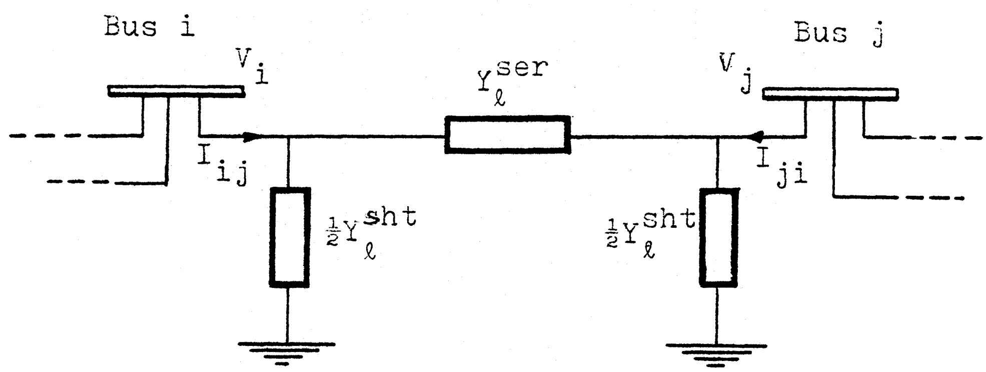

Figure 2.1. Representation of a simple transmission line.

2.1.2 State Variable Formulation

The natural choice of the state vector for a power system in steady-state is the nodal voltage vector. This is due to the fact that a knowledge of $\underline{V}$ provides one with the value of all key quantities, introduced in (2.1) - (2.6). Using the control terminology, with $\underline{V}$ as the state vector there can be no unobservable mode in the system (the transmission network is assumed to be connected).

Consider, for example, the expression for the net nodal injected power in (2.2). In matrix form,

$$S_k = \underline{V}^T [0_k] \underline{I}^* + \underline{I}^{*T} [0_k] \underline{V} \tag{2.7}$$

where T stands for transpose, and $[0_k]$ is an $N_b \times N_b$ matrix whose entries are all zero, except the (k, k) element which is 1/2. Using equation (2.1) in (2.7), it follows that:

$$S_k = \underline{V}^T [0_k] [Y_b^*] \underline{V}^* + \underline{V}^{*T} [Y_b^{*T}] [0_k] \underline{V} \tag{2.8}$$

One can easily find similar expressions for $|I_\ell|^2$ and S_ℓ^L.

Since $\underline{V}$ is a complex vector, it poses certain difficulties when considering algebraic operations which involve differentiation with respect to $\underline{V}$. This difficulty is overcome by separating the real and imaginary parts of $\underline{V}$ and other complex variables, that is:

$$\underline{V} \triangleq \underline{e} + j\,\underline{f} \tag{2.9a}$$

$$[Y_b] \triangleq [G] + j\,[B] \tag{2.9b}$$

$$S_k \triangleq p_k + j\,q_k \tag{2.9c}$$

where the definition of the rectangular components of the complex variables in (2.9) is understood. Invoking the above relations in (2.8), after some manipulation, it follows that

$$p_k = \underline{x}_r^T\,[P_k^r]\,\underline{x}_r \tag{2.10}$$

$$q_k = \underline{x}_r^T\,[Q_k^r]\,\underline{x}_r \tag{2.11}$$

where

$$\underline{x}_r^T = [\underline{e}^T,\ \underline{f}^T] \tag{2.12}$$

$$[P_k] = \left[\begin{array}{c|c} [G][0_k] + [0_k][G] & [B][0_k] - [0_k][B] \\ \hline -[B][0_k] + [0_k][B] & [G][0_k] + [0_k][G] \end{array}\right] \tag{2.13}$$

$$[Q_k] = -\left[\begin{array}{c|c} [B][0_k] + [0_k][B] & -[G][0_k] + [0_k][G] \\ \hline [G][0_k] - [0_k][G] & [B][0_k] + [0_k][B] \end{array}\right] \tag{2.14}$$

Note that the matrices $[P_k]$ and $[Q_k]$ are $2\ N_b \times 2\ N_b$ dimensional, symmetric, and highly sparse.

Similar to p_k and q_k, the square of the nodal voltage magnitudes, $v_k^2 = e_k^2 + f_k^2$, can be represented by a quadratic form in $\underline{x}_r$, i.e.,

$$v_k^2 = \underline{x}_r^T\ [V_k]\ \underline{x}_r \tag{2.15}$$

where $[V_k]$ is obtained from $[P_k]$ by setting the matrices $[G]$ and $[B]$ equal to the unity matrix. It is also easy to show that

$$|I_\ell|^2 = \underline{x}_r^T\ [I_\ell]\ \underline{x}_r \tag{2.16}$$

$$p_\ell^L = \underline{x}_r^T\ [P_\ell^L]\ \underline{x}_r \tag{2.17}$$

$$q_\ell^L = \underline{x}_r^T\ [Q_\ell^L]\ \underline{x}_r \tag{2.18}$$

where

$$p_\ell^L + j\ q_\ell^L \triangleq s_\ell^L \tag{2.19}$$

and the matrices $[I_\ell]$, $[P_\ell^L]$, and $[Q_\ell^L]$ are obtained by replacing the matrices $[G]$ and $[B]$ in $[P_k]$ and $[Q_k]$ by appropriate square matrices whose details are omitted.

2.2 Basic Analytical Formulation of Loadflow Problem

2.2.1 Loadflow Equations (LFE) and Bus Types

The steady state operation of a power system is normally characterized by specifying certain quantities at the network buses. Buses are thus classified accordingly into different types.

A PV bus is one at which the net injected active power is specified, and the voltage magnitude is maintained at a specified value by reactive power injection.

A PQ bus is one at which the net injected power is specified. The PQ buses are also referred to as "load buses".

Specifying all the real power injections in effect specifies the system I^2R losses, these being the sum of real power injections. The losses are difficult to specify in advance and quite often some voltage levels are extremely sensitive to the specified value. A few percent underestimation of losses could result in unusually high voltages at those buses. This difficulty is circumvented by letting the real power at one of the generation buses (a bus to which a generator is connected) to be free. This bus is usually referred to as the slack (or swing) bus.

The phasorial nature of the nodal voltages permits one to choose one of the voltage phase angles at will; thus, fixing a reference frame for the remaining phase angles. The bus whose phase angle is specified is called the reference bus.

The components of the reference bus voltage, V_r, are related to each other through

$$f_r = e_r \tan \theta_r \tag{2.20}$$

where θ_r is the specified reference angle. The specified injections form $N_z \triangleq 2\,N_b - 1$ non-linear equations, which when added to (2.20), form a consistent set of relations for $\underline{x}_r$, known as the <u>loadflow equations</u> (LFE). The specified quantities can be in general represented by

$$z_i = \underline{x}_r^T\,[Z_i^r]\,\underline{x}_r \qquad \begin{array}{l} i = 1, \ldots, N_z \\ (N_z \triangleq 2\,N_b - 1) \end{array} \tag{2.21}$$

where z_i is a specified nodal value whose functional relation with the network parameters is represented by $[Z_i^r]$. The linear relation (2.20) is often used in the above equations to reduce the number of unknowns by 1 and have all the equations in the quadratic form. Let $\underline{x}$ be related to $\underline{x}_r$ by

$$\underline{x}_r^T = [\underline{x}^T, f_r]$$

or

$$\underline{x}_r = [U^r]\,\underline{x} \tag{2.22}$$

where $[U^r]$ can be viewed as a unity matrix with an additional last row representing (2.20). Using the above relation in (2.21), one obtains

$$z_i = \underline{x}^T\,[Z_i]\,\underline{x} \qquad i=1, \ldots, N_z \tag{2.23}$$

where

$$[Z_i] \triangleq [U^r]^T [Z_i^r] [U^r]$$

For $\theta_r = 0$, the matrix $[Z_i]$ is obtained from $[Z_i^r]$ by deleting its last row and column.

Now from (2.23), it follows that

$$\underline{z} = \begin{bmatrix} z_1 \\ z_2 \\ \vdots \\ z_{N_z} \end{bmatrix} = \begin{bmatrix} \underline{x}^T [Z_1] \\ \underline{x}^T [Z_2] \\ \vdots \\ \underline{x}^T [Z_{N_z}] \end{bmatrix} \underline{x} \triangleq [L\ (\underline{x})]\ \underline{x} \qquad (2.24)$$

where the definition of $[L\ (\underline{x})]$ in (2.24) is understood. Note that $[L\ (\underline{x})]$ is a square $(N_z \times N_z)$ and highly sparse matrix.

2.2.2 Analytical Properties of LFE

The following properties of the rectangular version of LFE are used often in this thesis.

For constant scalars c_1 and c_2 and vectors $\underline{x}_1$ and $\underline{x}_2$:

(i) $[L\ (c_1\ \underline{x}_1 + c_2\ \underline{x}_2)] = c_1\ [L\ (\underline{x}_1)] + c_2\ [L\ (\underline{x}_2)]$ (2.25)

(ii) Since the matrices $[Z_i]$ are all symmetric,

$$[L\ (\underline{x}_1)]\ \underline{x}_2 = [L\ (\underline{x}_2)]\ \underline{x}_1 \tag{2.26}$$

For a N_z dimensional vector $\underline{\alpha}$:

(iii) $$\underline{\alpha}^T\ \underline{z} = \sum_{i=1}^{N_z} \alpha_i\ z_i = \underline{x}^T\ [Z\ (\underline{\alpha})]\ \underline{x} \tag{2.27}$$

where

$$[Z\ (\underline{\alpha})] \triangleq \sum_{i=1}^{N_z} \alpha_i\ [Z_i] \tag{2.28}$$

(iv) $$\underline{\alpha}^T\ [L\ (\underline{x})] = \underline{x}^T\ [Z\ (\underline{\alpha})] \tag{2.29}$$

which is obvious by comparing (2.27) with

$$\underline{\alpha}^T\ \underline{z} = \underline{\alpha}^T\ [L\ (\underline{x})]\ \underline{x}$$

(v) As a direct result of (2.29) and the symmetry of the matrix $[Z\ (\underline{\alpha})]$,

$$\begin{aligned} \underline{\alpha}^T \frac{\partial}{\partial\ \underline{x}} [L\ (\underline{x})] &= \frac{\partial}{\partial\ \underline{x}} \{\underline{\alpha}^T\ [L\ (\underline{x})]\} \\ &= \frac{\partial}{\partial\ \underline{x}} \{\underline{x}^T\ [Z\ (\underline{\alpha})]\} \\ &= [Z\ (\underline{\alpha})] \end{aligned} \tag{2.30}$$

(vi) For an invertable $[L\ (\underline{x})]$, the following relation is always true

$$\frac{\partial}{\partial \underline{x}} [L\ (\underline{x})]^{-1} = - [L\ (x)]^{-1} \{\frac{\partial}{\partial \underline{x}} [L\ (x)]\} [L\ (\underline{x})]^{-1}$$

where the notation $[\quad]^{-1}$ is used to denote the inverse of a matrix. The above relation is obtained by the partial differentiation of the identity

$$[L\ (\underline{x})]\ [L\ (\underline{x})]^{-1} = [I]$$

where $[I]$ represents the unit matrix. Now using equation (2.30) and the above relations, one can prove that,

$$\underline{\alpha}^T \frac{\partial}{\partial \underline{x}} [L\ (\underline{x})]^{-1} = - [Z\ (\underline{\lambda})]\ [L\ (\underline{x})]^{-1} \tag{2.31}$$

where

$$\underline{\lambda} \triangleq [L\ (\underline{x})]^{-T} \underline{\alpha}$$

($[\quad]^{-T}$ denotes the transpose and inverse of a matrix)

(vii) Noting that

$$\frac{\partial z_i}{\partial \underline{x}} = \frac{\partial}{\partial \underline{x}} \{\underline{x}^T [Z_i]\ \underline{x}\} = \{[Z_i]\ \underline{x}\}^T + \underline{x}^T [Z_i]$$

$$= 2\ \underline{x}^T [Z_i]$$

Using the definition of $[L(\underline{x})]$ in (2.24), it follows that,

$$[J(\underline{x})] \triangleq \frac{\partial \underline{z}}{\partial \underline{x}} = 2\,[L(\underline{x})] \tag{2.32}$$

Thus the matrix $[L(\underline{x})]$ is half of $[J(\underline{x})]$, the Jacobian of the LFE.

2.3 Variable Classification

2.3.1 Dependent and Independent Variables

The variables corresponding to the specified quantities in $\underline{z}$ are regarded as the independent variables. The dependent variables are the remaining ones whose value is fixed once $\underline{z}$ is specified.

Denoting the dependent variables by the vector of $\underline{y}$, the components of $\underline{y}$ are in general of the form

$$y_i = Y_i(\underline{x}) = \underline{x}^T [Y_i]\, \underline{x} \qquad i=1, \ldots, N_{dp} \tag{2.33}$$

where $[Y_i]$, a sparse symmetric matrix, specifies the functional relation of y_i with the network parameters, and N_{dp} is the number of those dependent variables which are important to power system security analysis. These include the slack bus real power generation, the reactive power generations, the voltage level at the load buses, and the line current magnitudes (or, depending on the problem, the real and reactive power flows).

2.3.2 Load Variables

Those independent variables whose values are decided primarily by the consumers are normally referred to as load or demand variables. In control theory terminology, the load variables are the disturbance variables which refer to the fact that the unpredictable changes in these variables cause the system to deviate from its nominal state.

The load variables are denoted by the vector $\underline{d}$ which consists of the vector of the real power demands, $\underline{p}^d$, and the vector of the reactive power demands, $\underline{q}^d$, that is

$$\underline{d} = - \left[\begin{array}{c} \underline{p}^d \\ \hline \underline{q}^d \end{array}\right] \tag{2.34}$$

Here, as in the conventional loadflow formulations [17] , the dependence of the load variables on the voltage levels are ignored.

2.3.3 Control and Non-Controllable Variables

The variables defining the steady-state model of a power system can also be classified according to their controllability. The load and the dependent variables, upon which the power system operator cannot exercise any direct control, are classified as the uncontrollable variables. The control variables are then those variables which can be directly manipulated to "track" and/or "control" the uncontrollable ones.

Here the control variables are denoted by the vector $\underline{u}$, which is made up of the real power generations, $\underline{p}^{v}$, and the voltage levels, $\underline{v}^{2}$, at the PV buses, i.e.

$$\underline{u} = \left[\begin{array}{c} \underline{v}^{2} \\ \hline \underline{p}^{v} \end{array}\right] \qquad (2.35)$$

Relation Between $\underline{z}$, $\underline{u}$, and $\underline{d}$

The vector of the specified injections, $\underline{z}$, is related to $\underline{u}$ and $\underline{d}$ through a linear relation of the form

$$\underline{z} = [K] \left[\begin{array}{c} \underline{u} \\ \hline \underline{d} \end{array}\right] = [K] \left[\begin{array}{c} \underline{v}^{2} \\ \hline \underline{p}^{v} \\ \hline -\underline{p}^{d} \\ \hline -\underline{q}^{d} \end{array}\right] \qquad (2.36)$$

where $[K]$ is, in general, a highly sparse, constant, rectangular matrix. Those rows of $[K]$ which correspond to real power injections, can have at most two non-zero entries $(+1, +1)$, depending on the type of bus they correspond to (i.e., simple or mixed bus). The rest, have only one non-zero entry $(+1)$. For a system with no mixed (hybrid) buses, $[K]$ is simply the unit matrix.

The mixed buses break up into simple PV and PQ buses, whenever a detailed representation of the system (including generator step-up transformers) is used. This means that, without loss of generality, one can always have

$$\underline{z} = \begin{bmatrix} \underline{u} \\ \hline \underline{d} \end{bmatrix} \tag{2.37}$$

This simplification, though not essential, permits a more elegant formulation of many security problems (see Section 3.2). It basically turns each control or load variable into a bus injection; thus, allowing them to be expressed directly in terms of $\underline{x}$, that is

$$u_i = U_i(\underline{x}) = \underline{x}^T [U_i] \underline{x} \qquad i=1, \ldots, N_c \tag{2.38}$$

$$d_j = D_j(\underline{x}) = \underline{x}^T [D_j] \underline{x} \qquad j=1, \ldots, N_d \tag{2.39}$$

where N_c and N_d are respectively the number of specified control and demand variables in the system. In this thesis, relation (2.37) is assumed to hold.

CHAPTER III

GENERAL FORMULATION OF STEADY-STATE SECURITY REGIONS

3.0 Preliminary Remarks

Our simple model of the steady state operation of a power system is far from being realistic. In this model, the range of variation of the power system variables is restricted only by the load flow equations. In reality, a mixture of practical, economical, and environmental limitations, which is equivalent to various inequality constraints on the power system variables, further restricts their range of variation. The identification of these limitations (from a technical point of view) and their incorporation into the model is a basic step toward the objectives of this thesis and is the main theme of this chapter.

A non-numerical approach of incorporating a set of inequalities into a mathematical model is basically what is called "a set-theoretic approach". The application of this approach to our model leads to the formulation of various security sets whose construction and characterization will be pursued in the proceeding chapters.

3.1 Limitations on Power System Variables

Here, a brief review on the nature and origin of the limitations on power system variables is given. They are classified into the following categories:

(i) Engineering Limitations

Like any other system, power system components have limited capabilities. For example, because its main shaft can stand up to only a certain amount of torsional torque, the real power output of a generator cannot exceed a certain amount. Alternatively, a transmission line has a restricted power handling capacity, because of its limited heat transfer capability. These types of limitations are basically of engineering nature; hence, the name "engineering limitations". They reflect the limited capabilities of the materials used in each device, as well as the compromises made in their design to accommodate conflicting design objectives.

(ii) Performance Limitations

To ensure quality and non-interruption of service, some power system variables are forced to lie within certain bands. These include, for example, the voltage levels at the load buses, whose variations are restricted to guarantee delivery of the power to the consumer at some acceptable voltage level, or the reactive power generations, which are restricted to ensure a good power factor for the generators as well as to safeguard against system instability due to over-generation of reactive power.

Normally, a performance limitation pertains to the general operation of the system, while an engineering limitation concerns the operation of a unit in the system. But in many cases, these two aspects are inter-related and cannot be separated. The distinction is thus normally avoided by referring to both types of limitations as operating constraints.

The operating constraints are further divided into the "hard" and "soft" constraints. A soft constraint being one whose slight violation can be tolerated for a limited period of time. A hard constraint, on the other hand, should be strictly respected at all times. Examples of the soft and the hard constraints are respectively the line thermal limits and the ceilings on the real power generations.

(iii) Security Constraints

Based on a preventive philosophy, power system variables are further restricted to ensure continuation of the service in the face of some postulated contingencies. In theory, these restrictions, called the "security constraints", should limit the permissible operating conditions to those which, even under certain sudden changes in the system, would not violate any of the operating constraints.

(iv) Physical Constraints [66, 67]

The load flow equations represent the physical restrictions on the power system; that is, the power demand must be met with adequate realizable power generation. The additional "realizability" condition is a direct consequence of the non-linearity of the power system and drastically affects the range of power injections that a power system could otherwise sustain. A physically non-realizable injection vector gives rise to a dynamically unstable system. Such an injection is recognized in the model as one for which there exists no real load flow solution.

3.2 The Set-Theoretic Approach

3.2.1 General Formulation

The normal operating state of a power system is defined by its physical and operational constraints. Let these constraints be defined respectively by the following general forms:

$$\underline{F}\,(\underline{\S}\,,\,\underline{x}) = \underline{0} \tag{3.1a}$$

$$\underline{h} = \underline{H}\,(\underline{\S}\,,\,\underline{x}) \leq \underline{h}^{\ell} \tag{3.1b}$$

where

$$\underline{\S}^T = [\underline{w}^T,\, \underline{u}^T,\, \underline{d}^T]$$

Here $\underline{w}$ represents the vector of network parameters while the vector $\underline{h}^{\ell}$ represents the operating limitations imposed on different power system variables, $\underline{h}$, described by the functions $\underline{H}$. Under normal operating conditions, for a given network $(\underline{w} = \underline{w}^0)$ and power demand $(\underline{d} = \underline{d}^0)$, a realizable control vector $\underline{u} = \underline{u}^0$ is available such that the resulting bus voltages, $\underline{x} = \underline{x}^0$, satisfy (3.1).

Numerical approaches for monitoring the system security are based on solving equation (3.1a) for $\underline{x}^0$ numerically, then using it in (3.1b) to check the operating constraints on the system. This has to be repeated for a large number of $\underline{w}$ and $\underline{u}$. Though very efficient algorithms are developed to perform these computations [9,17, 22] still, for large power systems, the required computing time can easily exceed a monitoring time frame.

The set-theoretic approach attempts to replace this "point-wise" approach by a "region-wise" approach. Instead of verifying the security of a single operating point it tries to characterize all the operating points $\underline{\S}$ which satisfy (3.1). Since the main part of the required computation can be carried out off-line, this approach facilitates the on-line monitoring notably.

To demonstrate the basic concepts involved in a set-theoretic approach, let there exist a vector function $\underline{X}(\underline{\S})$ such that

$$\underline{F}[\underline{\S}, \underline{X}(\underline{\S})] = \underline{0} \tag{3.3}$$

This simply means that

$$\underline{x} = \underline{X}(\underline{\S}) \tag{3.4}$$

is an explicit solution to the equations (3.1a). Now replacing relation (3.4) into (3.1b), one obtains a set of inequalities in terms of $\underline{\S}$. These inequalities define a region in the $\underline{\S}$ space with the property that its points satisfy all the physical and operational constraints. Representing this region by a set $S_{\S}$, it follows that,

$$S_{\S} = \{ \underline{\S} \,/\, H[\underline{\S}, \underline{X}(\underline{\S})] \leq \underline{h}^{\ell} \} \tag{3.5}$$

[The General Steady-State Security Region]

The set $S_{\S}$ is termed the general steady-state security region (SSSR) and any system condition $\underline{\S}^{0} \in S_{\S}$ is called a <u>normal condition</u> (or a normally secure condition).

Because of the non-linearity of $\underline{F}(\underline{\S}, \underline{x})$, the step suggested by equation (3.3) is formidable. It is, nevertheless, possible to obtain a first order approximation to $S_{\S}$ by linearizing (3.1). For a base point $(\underline{\S}_0, \underline{x}_0)$, it follows that

$$\underline{F}(\underline{\S}, \underline{x}) \simeq \underline{F}_0 + \left[\frac{\partial \underline{F}_0}{\partial \underline{\S}_0}\right](\underline{\S} - \underline{\S}_0) + \left[\frac{\partial \underline{F}_0}{\partial \underline{x}_0}\right](\underline{x} - \underline{x}_0) = \underline{0} \tag{3.6}$$

$$\underline{H}(\underline{\S}, \underline{x}) \simeq H_0 + \left[\frac{\partial \underline{H}_0}{\partial \underline{\S}_0}\right](\underline{\S} - \underline{\S}_0) + \left[\frac{\partial H_0}{\partial \underline{x}_0}\right](\underline{x} - \underline{x}_0) \leq \underline{h}^{\ell} \tag{3.7}$$

where

$$\underline{F}_0 \triangleq \underline{F}(\underline{\S}_0, \underline{x}_0) \tag{3.8}$$

$$\underline{H}_0 \triangleq \underline{H}(\underline{\S}_0, \underline{x}_0) \tag{3.9}$$

and where the partial derivatives are defined according to:

For a general function $\underline{W}(\underline{x}^1, \underline{x}^2, \ldots, \underline{x}^n)$,

$$\left[\frac{\partial \underline{W}_0}{\partial \underline{x}_0^i}\right] \triangleq \left[\frac{\partial \underline{W}(\underline{x}^1, \ldots, \underline{x}^n)}{\partial \underline{x}^i}\right]_{\substack{x^1 = \underline{x}_0^1 \\ \vdots \\ \underline{x}^n = \underline{x}_0^n}} \tag{3.10}$$

The linear expressions (3.6) and (3.7) make it possible to eliminate $\underline{x}$ and obtain a set of linear inequalities in terms of $\underline{\S}$ corresponding to (3.5). These linear inequalities can be represented in a general form by

$$[A(\underline{\S}_0, \underline{x}_0)]\, \underline{\S} \le \underline{b}(\underline{\S}_0, \underline{x}_0, \underline{h}^\ell) \tag{3.11}$$

where $[A(\underline{\S}_0, \underline{x}_0)]$ is a rectangular matrix defined by (3.6) and (3.7) and similarly for $\underline{b}(\underline{\S}_0, \underline{x}_0, \underline{h}^\ell)$. The expression (3.11) defines in effect $\hat{S}_\S$, where the super-script ^ indicates a first order approximation. Note that the system's Jacobian, $\left[\frac{\partial \underline{F}_0}{\partial \underline{x}_0}\right]$, is assumed to be non-singular at $(\underline{\S}_0, \underline{x}_0)$, while the existence of the partial derivatives with respect to $\underline{w}$ is implied.

3.2.2 Imposition of the Security Requirements

Imposing the security requirements upon a given normal condition $\underline{\S}^0$ is equivalent to demanding that in the event that the system undergoes certain sudden changes, $\Delta \underline{\S}$, the constraints (3.1) will still be respected, that is

$$\underline{F} (\underline{\S}^0 + \Delta \underline{\S} , \underline{x}) = \underline{0} \tag{3.12a}$$

$$\forall \Delta \underline{\S} \in C (\underline{\S}^0)$$

$$\underline{H} (\underline{\S}^0 + \Delta \underline{\S} , \underline{x}) \leq \underline{h}^{\ell} \tag{3.12b}$$

The set $C (\underline{\S}^0)$ contains all the probable sudden excursions (contingencies) from $\underline{\S}^0$ against which the system should remain secure, and it is defined in general, by

$$C (\underline{\S}) = \{\Delta \underline{\S} / \Delta \underline{\S} = \underline{\rho}^j (\underline{\S}) , \; j = 1, \ldots , N_{cg}\} \tag{3.13}$$

Each possible value of $\Delta \underline{\S}$, referred to as a "contingency", is specified by a function of $\underline{\S}$, $\underline{\rho}^j (\underline{\S})$. The contingencies are selected primarily based on system's past history, load predictions, weather conditions, and operator's judgement (experience) regarding the stresses developing in different parts of the system. Thus in practice N_{cg}, the number of contingencies considered, is not fixed and varies with $\underline{\S}$. However, for simplicity, we consider N_{cg} to be a constant, equal to the number of all different contingencies considered over a long period of operation. (Note that this should not affect any of our results, as long as the exclusion of a contingency from the contingency list would imply the invulnerability of the system to that contingency).

A contingency may correspond to changes in the network parameters (e.g., line or transformer outages), in the control variables (e.g., generator outages), and / or in the demand variables (e.g., loss of load).

To verify the degree of vulnerability of, say, $\underline{\S}^0$ to the postualted contingencies using numerical techniques requires running load flows for $\underline{\S}^j = \underline{\S}^0 + \underline{\rho}^j(\underline{\S}^0)$ $j = 1, \ldots, N_{cg}(\underline{\S}^0)$. On the other hand, with a knowledge of $S_{\S}$, one needs to simply check if

$$(\underline{\S}^0 + \Delta\,\underline{\S}) \in S_{\S} \qquad \forall\, \Delta\,\underline{\S} \in C\,(\underline{\S}^0)$$

Defining the pre-contingency conditions, $\underline{\S}^{pre} \triangleq \underline{\S}^0$, and the post-contingency conditions, $\underline{\S}^{post}$, then for each contingency, $\underline{\rho}^j(\underline{\S}^{pre})$, they are simply related by

$$\underline{\S}^{post} = \underline{\S}^{pre} + \rho^j(\underline{\S}^{pre})$$

Employing the above relation, one can find the set of all pre-contingency conditions which are secure to a given contingency $\underline{\rho}^j(\underline{\S}^{pre})$. Denoting this set by $S^j_{\S}$, it is simply given by (for generality the super-script "pre" has been dropped from $\underline{\S}^{pre}$):

$$S_{\S}^{j} = \{\underline{\S} \;/\; \underline{H}\,[\underline{\S} + \underline{\rho}^{j}\,(\underline{\S}),\ \underline{X}\,(\underline{\S} + \underline{\rho}^{j}\,(\underline{\S}))] \leqslant \underline{h}^{\ell}\} \tag{3.14}$$

which is obtained by replacing $\underline{\S}$ in (3.5) by $\underline{\S} + \underline{\rho}^{j}\,(\underline{\S})$. In Figure 3.1 such a transformation between the "post" and "pre" contingency states is demonstrated pictorially.

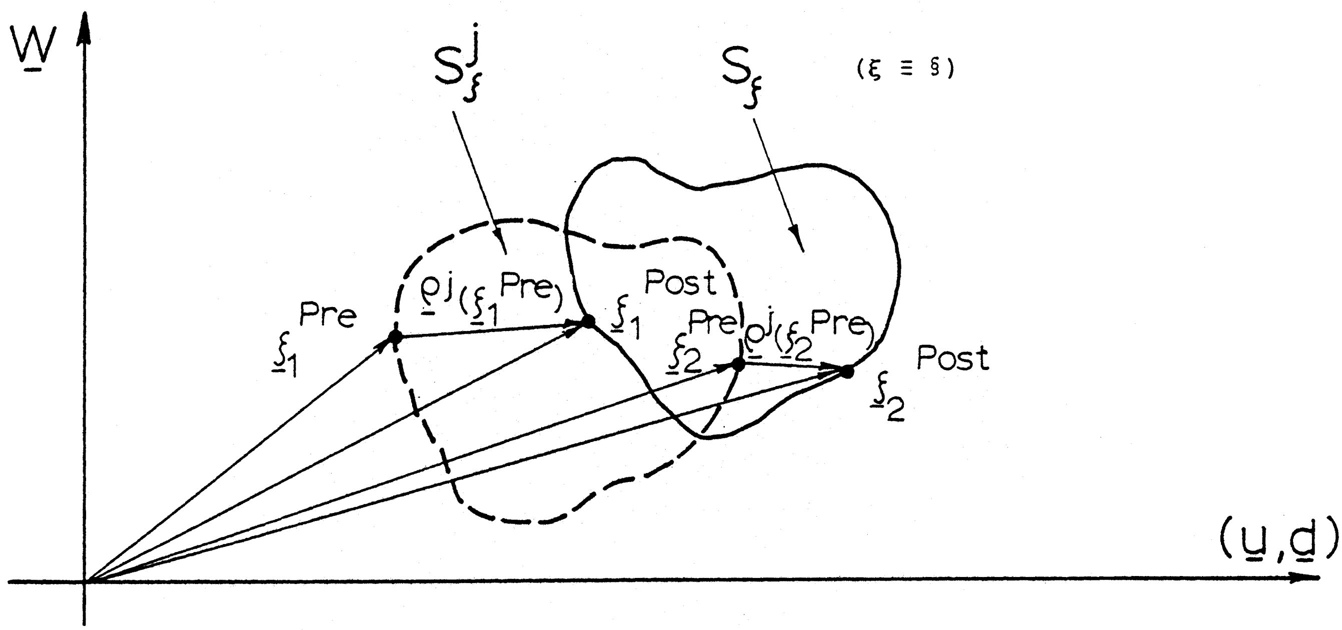

Figure. 3.1. Construction of the set $S_{\S}^{j}$ from the set $S_{\S}$ for the contingency $\Delta\,\underline{\S} = \underline{\rho}^{j}\,(\underline{\S}^{pre})$.

As can be seen in Figure 3.1, not all the points in $S_{\S}^{j}$ correspond to normal conditions. Only those points which belong to the intersection of $S_{\S}$ and $S_{\S}^{j}$ represent the pre-contingency conditions which are both normally secure and invulnerable to the jth contingency. Generalization of this property leads to the definition of $S_{\S}^{I}$, the general steady-state invulnerability set, defined by

$$S_{\S}^{I} \triangleq \bigcap_{j=0}^{N_{cg}} S_{\S}^{j} \tag{3.15}$$

[The General Steady-State Invulnerability Set]

where $S_{\S}^{0} \triangleq S_{\S}$. This set contains only those pre-contingency system conditions which are invulnerable to all the postulated contengies and are normally secure. In theory, $S_{\S}^{I}$ can be used to resolve many complex power system planning, control, and security problems. But as will be discussed in the next section, its explicit use in practice has never been exploited.

3.2.3 Cross-sections of the General SSSR

To simulate the line outages by changing $\underline{w}$, a transmission line model has to be parameterized by its admittance and shunt susceptance. For large power systems, where there are thousands of transmission lines, such parameterization results in a very large dimension for $\underline{w}$, and consequently $\underline{\S}$. This poses a major difficulty in employing the sets $S_{\S}$ and $S_{\S}^{I}$ for security and control calculations.

For security calculations, the dimensionality problem can be resolved by noting that, while performing the contingency analysis, one in fact deals with only a certain number of cross sections of $S_{\S}$ projected into the $(\underline{u}, \underline{d}) = \underline{z}$ space. Thus instead of characterizating $S_{\S}$, one can choose to characterize its projections in the $\underline{z}$ space.

Let S_z denote the cross-section of $S_{\S}$ for $\underline{w} = \underline{w}^0$, projected into the $\underline{z}$ space, i.e.,

$$S_z = \{\underline{z} \,/\, \underline{w} = \underline{w}^0, \; \underline{\S} \in S_{\S}\} \tag{3.16}$$

where $\underline{w}^0$ represents the value of the network parameters for the intact network. Clearly, S_z contains all the injections $\underline{z}$ which, under normal conditions (no contingency in effect), satisfy the operating constraints. Let us also assume (for the time being) that the contingencies simulating the sudden structural changes are not accompanied by the changes in $\underline{z}$, and there are N_w of them. In other words, the simulation of the generator and load contingencies is restricted to the intact network (consistent with the normal practice in electric power utilities). Denoting the changes in $\underline{w}^0$ due to the network contingencies by $\Delta \underline{w}^k$ $K = 1, \ldots, N_w$, projection of the cross-sections of $S_{\S}$ corresponding to $\underline{w}^0 + \Delta \underline{w}^k$ $K = 1, \ldots, N_w$ into the $\underline{z}$ space produces the following sets

$$S_z^k = \{\underline{z} \,/\, \underline{w} = \underline{w}^0 + \Delta \underline{w}^k, \; \underline{\S} \in S_{\S}\} \quad K = 1, \ldots, N_w$$

Each of the above sets contains the operating conditions which are invulnerable to a specified network contingency. Using the set S_z, the sets of the pre-contingency injections which are invulnerable to the remaining contingencies can be formed. Formulation of these sets, denoted by S_z^k $K = N_w + 1, \ldots, N_{cg}$, (as in the previous section) requires access to functions which can express the effect of a specified contingency on the pre-contingency injections.

In the case where a contingency consist of simultaneous changes in the network structure as well as in the injection vector, slight modification is needed. The operating points invulnerable to such contingency are identified by first finding the cross-section of $S_{\S}$ corresponding to the post-contingency value of $\underline{w}$, and then subjecting the resulting set to a non-linear shift relevant to the changes in the $\underline{z}$ (assumed to be given). Note that in reality, even a single structural change, because of the resulting imbalance in the reactive power and the required re-routing of the power flows, is always accompanied by changes in $\underline{z}$. These changes, which are normally small, are difficult to estimate and thus usually neglected.

Characterizing the aforementioned sets would allow characterization of the invulnerability set in the $\underline{z}$ space, defined by,

$$S_z^I \triangleq \bigcap_{k=0}^{N_{cg}} S_z^k \tag{3.17}$$

where $S_z^0 = S_z$. It is readily seen that S_z^I is the projection of $S_{\S}^I$ ($\underline{w} = \underline{w}^0$) into the $\underline{z}$ space. In Figure 3.2, for the case where there are only two network contingencies, the relations existing among $S_{\S}$, S_z, and S_z^I are shown pictorially.

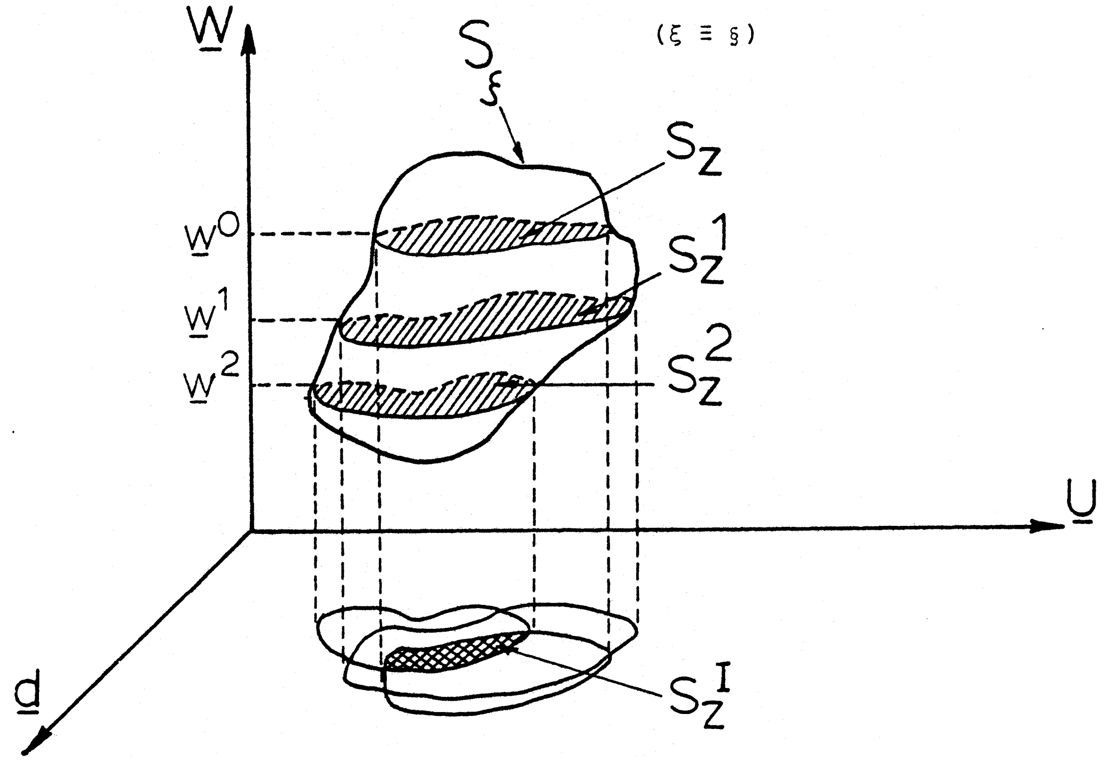

Figure 3.2. Typical relations among $S_§$, S_z, and S_z^I for a power system subjected to two postulated network contingencies.

3.3 Direct Construction of S_z

The mathematical model of a power system in the $\underline{§}$ space is highly non-linear, which makes it very unattractive to try to characterize S_z by first constructing $S_§$. The alternative would be to construct S_z directly. This requires first defining a number of simple, basic sets in their appropriate spaces. These sets can be viewed as the building blocks of S_z, whose recognition allows a better understanding of the make up of S_z . Note that, compared with the $\underline{\S}$ space, the power system relations are less non-linear in the $\underline{z}$ space.

3.3.1 Basic Sets

In the control space ($\underline{u}$-space), the operating limitations on the control variables define a hyper-box which is denoted by H_u , and represents the set of admissible control strategies, that is

$$H_u \triangleq \{\underline{u} \;/\; \underline{u}^m \leq \underline{u} \leq \underline{u}^M\} \tag{3.18}$$

where $\underline{u}^M$ and $\underline{u}^m$ are respectively the vector of upper and lower bounds on the components of $\underline{u}$. Here $\underline{u}$ includes the real power generations at PV buses and the square of the voltage magnitudes at the generation buses. This set is therefore more general than the generation set of reference [52] .

The dependent variables are similarly restricted by operating limitations. In the $\underline{y}$ space these bounds form a hyper-box, denoted by H_y, embodying all the allowable values that the dependent variables can assume. This set is called the set of allowable ratings for system components, and is defined by:

$$H_y \triangleq \{\underline{y} \;/\; \underline{y}^m \leq \underline{y} \leq \underline{y}^M\} \tag{3.19}$$

The vector $\underline{y}^M$ and $\underline{y}^m$ indicate the maximum and minimum bounds on the components of $\underline{y}$. Note that this set, in addition to thermal limits, includes bounds on the reactive generations, load bus voltage levels, and limits on the real power generation at the slack bus.

One can equally define a hyper-box in the load space by setting bounds on the load variables. This set is called <u>the a priori loading set</u> and is denoted by H_d that is

$$H_d \triangleq \{\underline{d} \ / \ \underline{d}^m \leq \underline{d} \leq \underline{d}^M\} \tag{3.20}$$

The vectors $\underline{d}^M$ and $\underline{d}^m$ represent respectively conservative bounds on components of $\underline{d}$. The value of $\underline{d}^M$ could correspond to the original long-term demand forecasts on whose basis the system is designed (expanded), or to the power interruption capacity of the major circuit breakers in the system. The lower bound, $\underline{d}^m$, may be taken as zero or some value well below the lowest point of the daily load trajectory.

3.3.2 Maps into the Voltage Space

Consider the ith operating constraint in (3.1b), i.e.,

$$h_i \leq h_i^{\ell}$$

where the variable h_i is expressed in $\underline{x}$ through the relation $h_i = H_i(\underline{\S}, \underline{x}) = \underline{x}^T [H_i] \underline{x}$. At the limit, the quadratic surface

$\underline{x}^T [H_i] \underline{x} = h_i^\ell$ divides the voltage space into two parts, of which the feasible one can be defined by a set X^i, where

$$X^i \triangleq \{\underline{x} \,/\, \underline{x}^T [H_i] \underline{x} \le h_i^\ell \,;\, \underline{x} \in R^{N_z}\} \tag{3.21}$$

We would like to describe that part of the voltage space which is common to the feasible regions of all the operating constraints. It will be advantageous to do this in terms of the following sets

(i) <u>The Secure Control Set:</u>

$$U_x \triangleq \{\underline{x} \,/\, \underline{U}(\underline{x}) = \underline{u} \in H_u \,;\, \underline{x} \in R^{N_z}\} \tag{3.22}$$

(ii) <u>The Secure Rating Set:</u>

$$Y_x \triangleq \{\underline{x} \,/\, \underline{Y}(\underline{x}) = \underline{y} \in H_y \,;\, \underline{x} \in R^{N_z}\} \tag{3.23}$$

(iii) <u>The Secure A priori Loading Set:</u>

$$D_x \triangleq \{\underline{x} \,/\, \underline{D}(\underline{X}) = \underline{d} \in H_d \,;\, \underline{x} \in R^{N_z}\} \tag{3.24}$$

where the components of the vector $\underline{Y}(\underline{x})$, $\underline{U}(\underline{x})$, and $\underline{D}(\underline{x})$ are defined respectively in equations (2.38), (2.33) and (2.39). That part of the voltage space whose points satisfy all the operating conditions on the intact system form a set, called <u>the secure voltage</u> set and is denoted by S_x. It is clear that

$$S_x = U_x \cap Y_x \cap D_x \tag{3.25}$$

or equivalently

$$S_x = \bigcap_{i=1}^{N_s} X^i \tag{3.26}$$

where i runs over __all__ the operating constraints, and $N_s \triangleq 2(N_c + N_d + N_{dp})$.

The bounds on $\underline{d}$ should be normally non-binding, thus one often expects to have

$$S_x \subset D_x \tag{3.27}$$

i.e., all possible loads should be satisfiable. This permits one to concentrate primarily on the other two sets.

3.3.3 Maps onto the $\underline{z}$ Space

Any point $\underline{x}$ in the voltage space can be mapped into the $\underline{z}$ space via the LFE, i.e., $\underline{z} = [L(\underline{x})]\,\underline{x}$. Under this transfromation, the following important sets are produced:

(i) __The Set of Realizable $\underline{z}$ [66, 68, 69]__

Since the transformation $\underline{z} = [L(\underline{x})]\,\underline{x}$ is non-linear in $\underline{x}$, the voltage space does not transform __onto__ the whole $\underline{z}$ space. In fact the image of the $\underline{x}$ space is jammed __into__ a solid conical structure in the $\underline{z}$ space, called the steady-state feasibility region.

This region, the range space of the operator $[L(\underline{x})]\ \underline{x}$, is denoted by R_z and is simply defined by

$$R_z \triangleq \{\underline{z} / \underline{z} = L(\underline{x})\ \underline{x} \quad ; \quad \underline{x} \in R^{N_z}\} \tag{3.28}$$

Any point $\underline{z}$ outside this conical region is not physically realizable and consequently there cannot exist a load flow solution corresponding to it.

(ii) The Set of Normally Secure Injections

By transforming S_x into the $\underline{z}$ space, the set of all injections $\underline{z}$ which do not violate the operating constraints on the intact network, that is S_z, is produced. It then follows that

$$S_z = \{\underline{z} / \underline{z} = [L(\underline{x})]\ \underline{x} \quad ; \quad \underline{x} \in S_x\} \tag{3.29}$$

A more useful definition of S_z can be formulated in terms of the feasible portions of the $\underline{x}$ space, i.e., X^i, $i=1, \ldots, N_s$, defined by the individual operating constraints. Denoting the transformation of X^i into the $\underline{z}$ space by the set Z^i, that is

$$Z^i \triangleq \{\underline{z} / \underline{z} = [L(\underline{x})]\ \underline{x} \quad ; \quad \underline{x} \in X^i\} \tag{3.30}$$

The set S_z is then simply given by

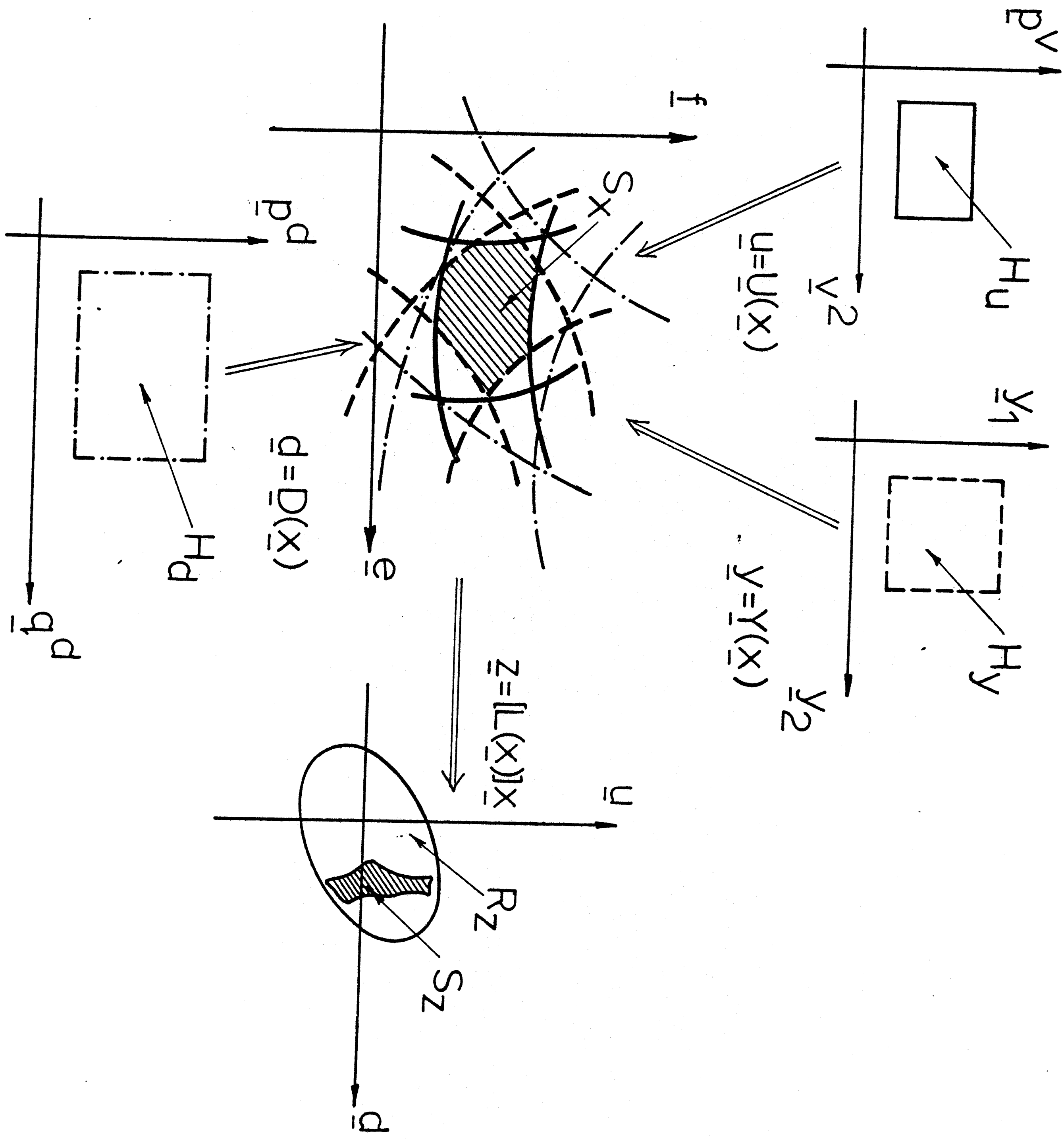

Figure 3.3. A pictorial illustration of different transformations on the basic sets producing the set S_z .

$$S_z = \bigcap_{i=1}^{N_s} Z^i \tag{3.31}$$

From the definition of R_z and S_z, it follows that,

$$S_z \subset R_z \tag{3.32}$$

which implies that all points belonging to S_z are physically realizable and have at least one load flow solution. In Figure 3.3 the different sets and transformations which produce S_z are indicated. One should take notice that once a practical scheme for characterizing S_z is established, it would be rather easy to characterize S_z^I .

3.4 Example

To shed more light on some of the ideas expressed in this chapter, a simple example is worked out here. A two bus system (Figure 3.4) is chosen for this purpose.

Choosing bus 1 as the reference bus with $\theta_1 = 0$, it follows that

$$\underline{x} = \begin{bmatrix} e_1 \\ e_2 \\ f_2 \end{bmatrix} \quad ; \quad \underline{z} = \begin{bmatrix} v_1^2 \\ -p_2 \\ -q_2 \end{bmatrix} = \begin{bmatrix} \underline{u} \\ \hline \underline{d} \end{bmatrix}$$

where

$$z_1 = v_1^2 = \underline{x}^T [V_1] \underline{x} = e_1^2 \tag{3.33a}$$

$$-z_2 = p_2 = \underline{x}^T [P_2] \underline{x} = g_{22} (e_2^2 + f_2^2) + e_1 (g_{21} e_2 + b_{21} f_2) \tag{3.33b}$$

$$-z_3 = q_2 = \underline{x}^T [Q_2] \underline{x} = - b_{22} (e_2^2 + f_2^2) + e_1 (g_{21} f_2 - b_{21} e_2) \tag{3.33c}$$

and the matrices $\{g_{ij}\} = [G]$ and $\{b_{ij}\} = [B]$ are obtained from $[Y_b]$, given by

$$[Y_b] = \begin{bmatrix} Y^{ser} + \frac{1}{2} Y^{sht} & - Y^{ser} \\ -Y^{ser} & Y^{ser} + \frac{1}{2} Y^{sht} \end{bmatrix}$$

Important dependent variables for this example are:

$$y_1 = p_1 = \underline{x}^T [P_1] \underline{x} = g_{11} e_1^2 + g_{12} e_1 e_2 - b_{12} e_1 f_2 \tag{3.34a}$$

$$y_2 = q_1 = \underline{x}^T [Q_1] \underline{x} = - b_{11} e_1^2 - g_{12} e_1 f_2 - b_{12} e_1 e_2 \tag{3.34b}$$

$$y_3 = v_2^2 = \underline{x}^T [V_2] \underline{x} = e_2^2 + f_2^2 \tag{3.34c}$$

$$y_4 = |I_1|^2 = \underline{x}^T [I_1] \underline{x} = \frac{1}{2} (b_{11}^2 + 2g_{11}^2 + b_{12}^2)[(e_1 - e_2)^2 + f_2^2]$$
$$+ (b_{22} + b_{12})^2 e_1 e_2 \qquad (3.34d)$$

Assuming the line parameters and the engineering limitations to be those given in Table 3.1, the following basic sets are defined.

TABLE 3.1.

DATA FOR THE SYSTEM OF FIGURE 3.3

y	p_1	q_1	v_2	$\|I_1\|$	μ	v_1	d	$-p_2$	$-q_2$
y^M	0.75	0.2	1.04	0.67	μ^M	1.1	d^M	1.2	0.9
y^m	0.0	-0.05	0.94	0.0	μ^m	1.0	d^m	-1.2	-0.9
$Z^{ser} = 0.2 + j\,0.5$; $Y^{sht} = 0.0 + j\,0.2$; $\theta_1 = 0$									

$$H_u = \{\underline{u} \,/\, [1.0] \le \underline{u} \le [1.1]\} \qquad (3.35a)$$

$$H_y = \left\{\underline{y} \,/\, \begin{bmatrix} 0.0 \\ -0.05 \\ 0.94 \\ 0.0 \end{bmatrix} \le \underline{y} \le \begin{bmatrix} 0.75 \\ 0.2 \\ 1.04 \\ 0.67 \end{bmatrix} \right\} \qquad (3.35b)$$

$$H_d = \left\{\underline{d} \,/\, \begin{bmatrix} -1.2 \\ \\ -0.9 \end{bmatrix} \le \underline{d} \le \begin{bmatrix} 1.2 \\ \\ 0.9 \end{bmatrix} \right\} \qquad (3.35c)$$

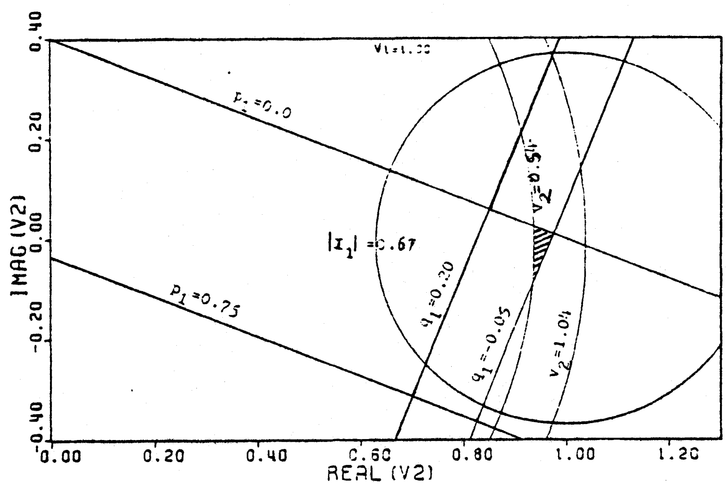

(a)

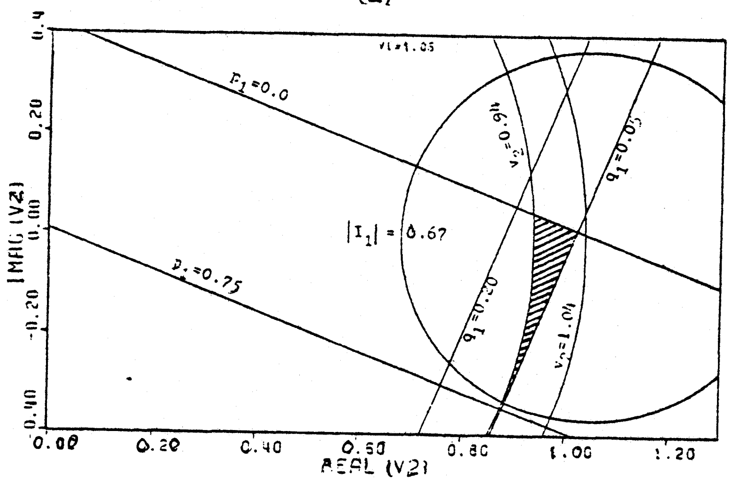

(b)

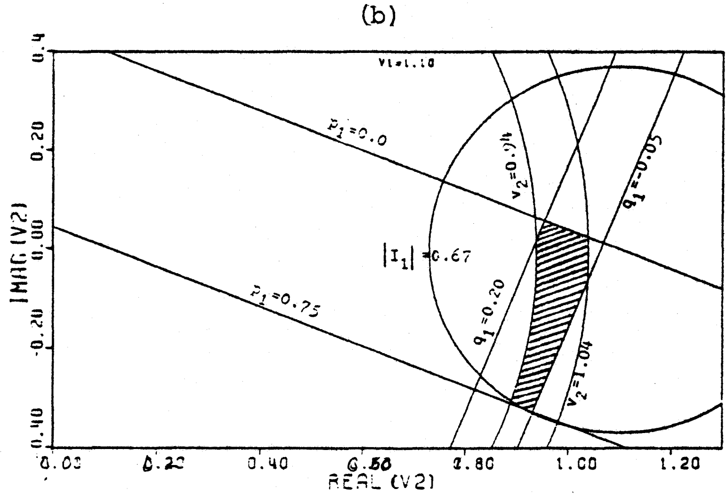

(c)

Figure 3.5. Three cross-sections of S_x corresponding to: (a) $v_1 = 1.0$; (b) $v_1 = 1.05$; (c) $v_1 = 1.1$.

The sets U_x, Y_x, and D_x are then readily obtained by using the expressions in (3.33) and (3.34) to represent their corresponding variables in (3.35). The inter-section of these sets in the voltage space defines S_x. Three cross-sections of S_x are shown in Figure 3.5.

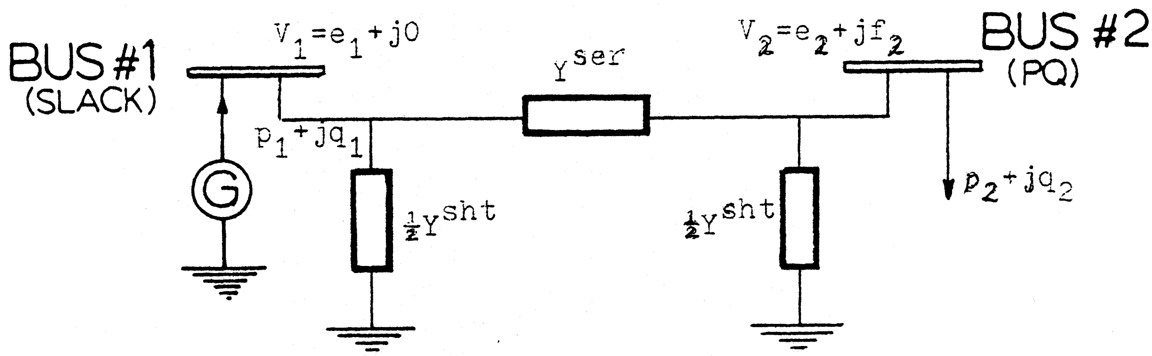

Figure 3.4. The two bus system used in the example.

For this simple example, it is possible to obtain an explicit solution to the voltage vector $\underline{x}$ in terms of $\underline{z}$. A second order equation of the form

$$e_2^2 + 2\,\alpha\,(\underline{z})\;e_2 + \beta\,(\underline{z}) \;=\; 0 \tag{3.36}$$

has to be solved for e_2. A relation of the form

$$f_2 = \gamma(\underline{z}) - \lambda(\underline{z})\, e_2 \tag{3.37}$$

then allows one to calculate f_2. Equation (3.36) restricts the range of the specified injections to those for which

$$r(\underline{z}) \triangleq \alpha^2(\underline{z}) - \beta(\underline{z}) \geq 0$$

It can be easily shown that

$$r(\underline{z}) = (b_{22} z_2 - g_{22} z_3)^2 + \Gamma_0 (b_{22} z_2 + g_{22} z_3) - \Gamma_1 z_1 z_2 - \Gamma_2 z_1^2 \tag{3.37}$$

where

$$\Gamma_0 \triangleq b_{22} (b_{21}^2 + g_{21}^2) / g_{22}$$

$$\Gamma_1 \triangleq \Gamma_0 (b_{22}^2 + g_{22}^2) / b_{22}$$

$$\Gamma_2 \triangleq (b_{21}^2 + g_{21}^2)^2 / 4$$

It follows that

$$R_z = \{\underline{z} \,/\, r(\underline{z}) \geq 0\}$$

Equations (3.36), (3.37), and (3.33a) thus can be used to express all the dependent variables in (3.34) in terms of $\underline{z}$. An

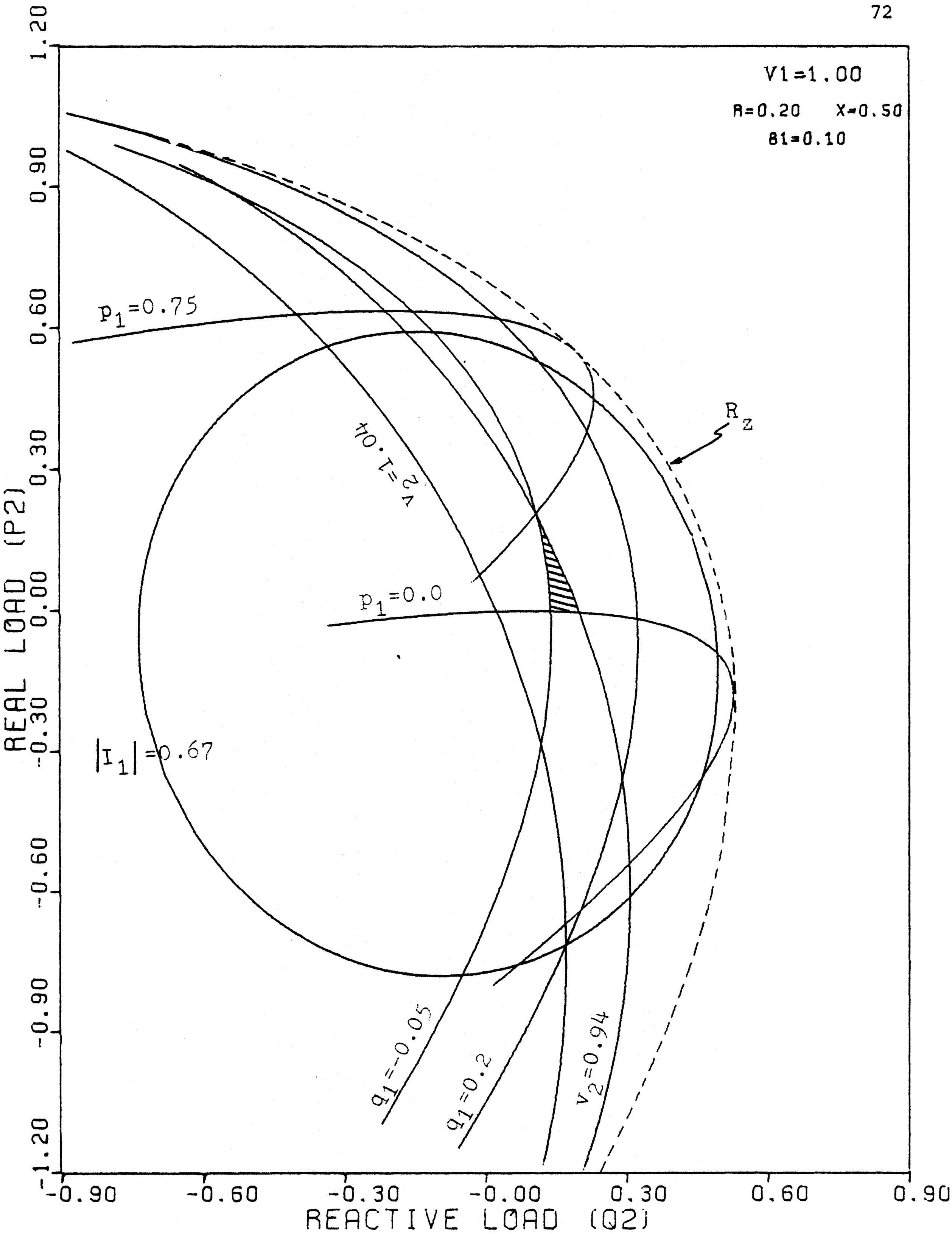

Figure 3.6a. Cross-sections of R_z and S_z corresponding to v_1 = 1.0.

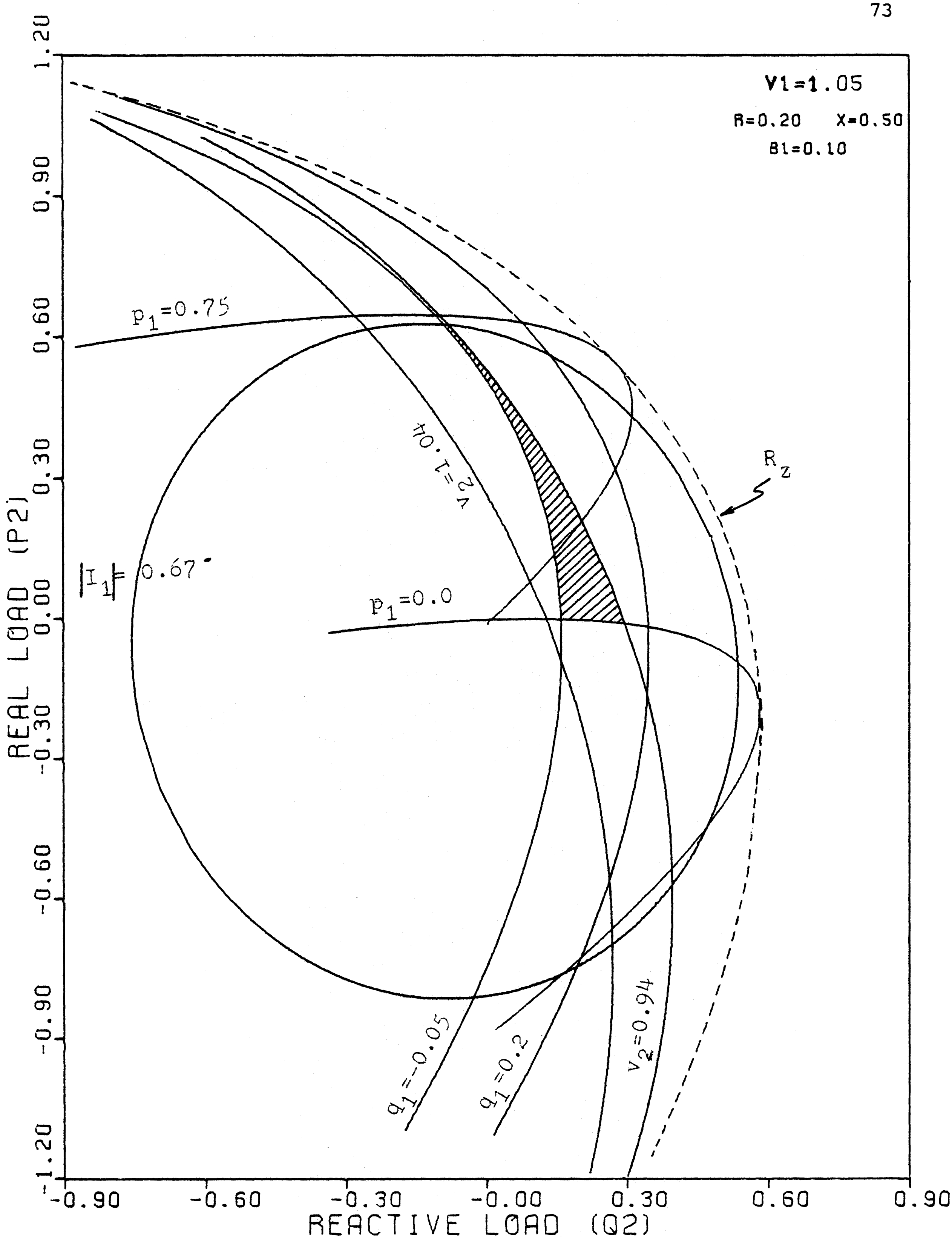

Figure 3.6b. Cross-sections of R_z and S_z corresponding to v_1 = 1.05.

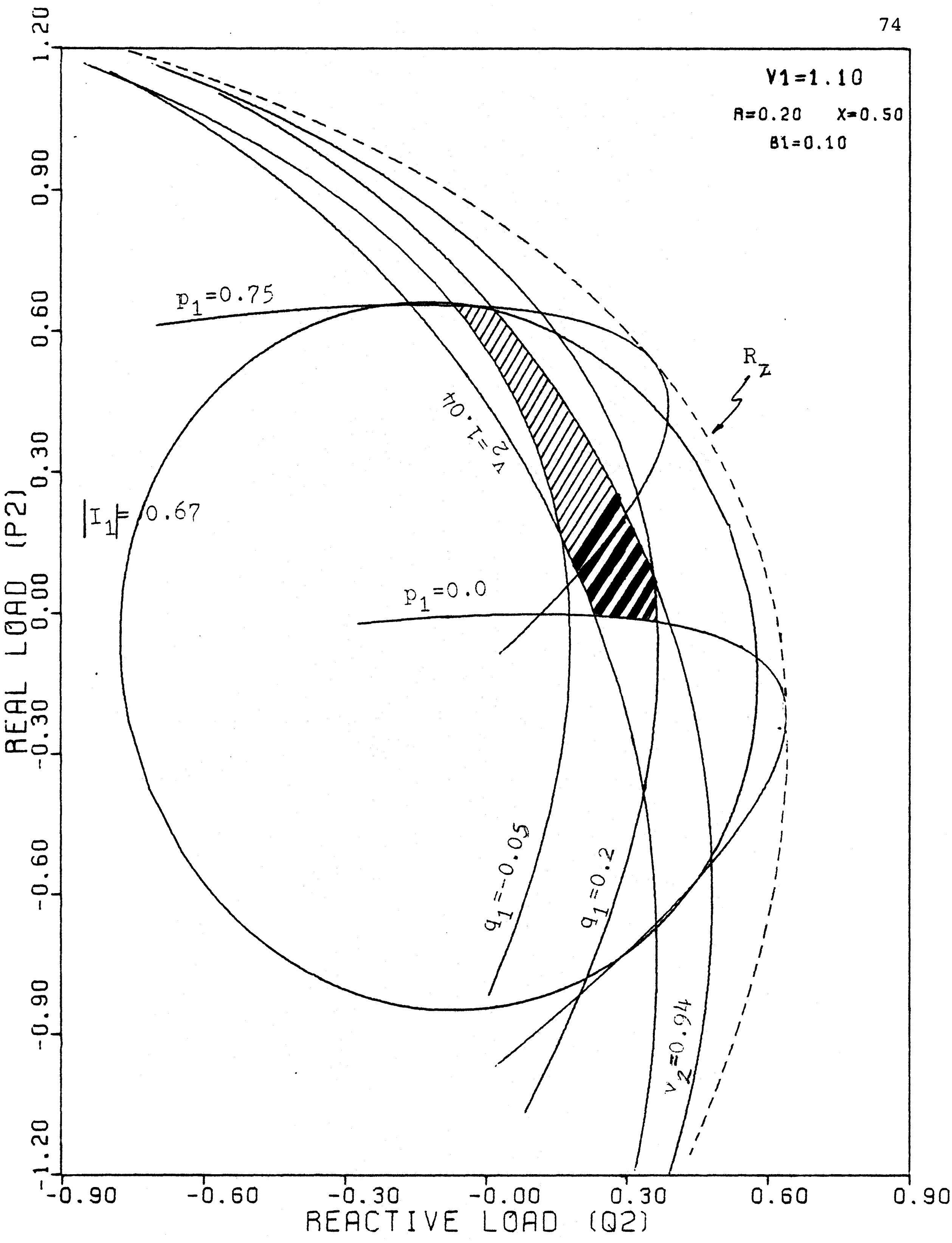

Figure 3.6c. Cross-sections of R_z and S_z corresponding to v_1 = 1.1.

exact description of S_z in this case is therefore possible. In Figure 3.6 three cross-sections of R_z and S_z, corresponding to those of Figure 3.5, are shown. A number of cross-sections of S_z are also super-imposed in Figure 3.7 to produce a 3-dimensional impression of S_z.

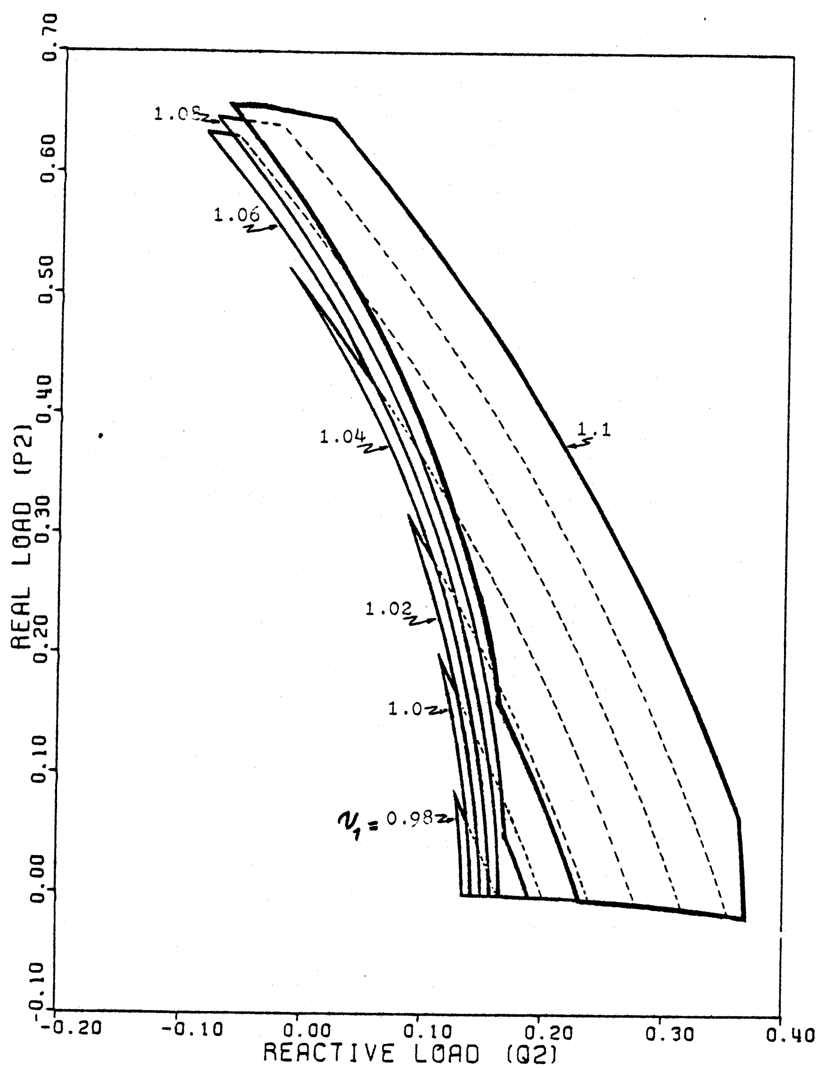

Figure 3.7. Super-imposition of a number of cross-sections of S_z.

CHAPTER IV

GENERAL APPROXIMATION FORMULAE FOR LOAD FLOW DEPENDENT VARIABLES

4.0 Introductory Remarks

Explicit formulae relating the load flow dependent variables to certain independent injections have been extensively used in the analysis of power system problems. The distribution factors [15 , 16], DC load flow [17, 18] and the decoupled load flow schemes [20, 21] each can provide such formulae. The resulting formulae are, nevertheless, limited in their accuracy and generality.

In this chapter, general approximation formulae are derived which explicitly relate any dependent load flow variable to the vector of specified nodal injections. The approach introduced here is novel because: first, it involves all the specified nodal injections; second, it can theoretically yield approximation formulae of any order or degree of accuracy, and third, it is highly systematic requiring only the normal load flow assumptions.

Since these approximation formulae are central to the application of the set-theoretic approach to the security problems, their various aspects are studied in some depth here.

4.1 Transformation of Dependent Variables into the $\underline{z}$ Space

4.1.1 Motivation

Relations (3.30) and (3.31) simply state that the set of all normal operating conditions, S_z, can be constructed by transforming each constrained variable from the $\underline{x}$ space into the $\underline{z}$ space separately. Since the $\underline{u}$ and the $\underline{d}$ spaces are the orthogonal subspaces of the $\underline{z}$ space, constrained control or load variables are transformed into the $\underline{z}$ space trivially, e.g.

$$u_i = U_i(\underline{x}) = \underline{\ell}_i^T \underline{z} \tag{4.1}$$

where all the entries of $\underline{\ell}_i$ are zero except its ith one which is 1. On the other hand, the constrained variables belonging to Y_x are complicated functions of $\underline{z}$ which in general cannot be computed as closed form relations. Thus any relation expressing the dependent variables explicitly in $\underline{z}$ will be approximate in nature. The proceeding sections examine the schemes for computing such approximate relations.

4.1.2 General Formulation

Let the set of the LFE be expressed generally by

$$\underline{z} = \underline{Z}(\underline{x}) \tag{4.2}$$

and a typical dependent variable by

$$y = Y(\underline{x}) \tag{4.3}$$

Theoretically, the existence of a solution to (4.2) is equivalent to the existence of an inverse operator, $\underline{Z}^{-1}$, mapping $\underline{z}$ back into the $\underline{x}$ space, namely

$$\underline{x} = \underline{Z}^{-1}(\underline{z}) \tag{4.4}$$

Disregarding the existence and uniqueness problems associated with this inverse transformation, any variable y can be expressed in terms of $\underline{z}$, that is

$$y = Y[\underline{Z}^{-1}(\underline{z})] \tag{4.5}$$

The problem of establishing explicit relation between y and $\underline{z}$ is then basically that of obtaining an explicit representation for either $\underline{Z}^{-1}(\underline{z})$ or $Y[\underline{Z}^{-1}(\underline{z})]$.

4.2 Approximation Techniques

In this section the emphasis is mainly on the approximation techniques which allow full exploitation of the quadratic formulation of the LFE. Alternative formulations with no significant advantage over these formulations are not presented here.

4.2.1 Parametric Approach

The essence of this approach is to assume a certain type of approximate relation between y and $\underline{z}$ and then try to adjust the unknown parameters in the assumed relation to ensure tracking of the exact relation by the assumed one as closely as possible.

Since a linear relation involves the smallest possible number of parameters, it is of particular interest here. Assuming a relation of the form

$$\hat{y}_p = \alpha_0 + \underline{\alpha}^T \underline{z} \tag{4.6}$$

for y, there are $1 + N_z = 2\ N_b$ parameters (α_0 and $\underline{\alpha}$) to determine. Invoking relation (2.27), it follows that

$$\hat{y}_p = \alpha_0 + \underline{x}^T\ [Z\ (\underline{\alpha})]\ \underline{x} \tag{4.7}$$

The exact relation for y, as introduced in (2.33), is however of the form

$$y = \underline{x}^T\ [Y]\ \underline{x} \tag{4.8}$$

comparing the last two relations, the temptation is to set α_0 to zero and have an $\underline{\alpha}$ such that

$$[Z\ (\underline{\alpha})] \rightarrow [Y] \tag{4.9}$$

Different formulation of the problem suggested in (4.9) are possible. The most obvious one is to equate corresponding entries of the matrices $[Z\ (\underline{\alpha})]$ and $[Y]$ and, after eliminating identical equations, solve an over-determined set of linear equations for $\underline{\alpha}$.

4.2.2 Linearization Based Approach

Because of the non-linear nature of the LFE in $\underline{x}$, an inverse operator, $\underline{Z}^{-1}$, as suggested in equation (4.4), cannot in general be computed. It is, nevertheless, possible to remove the non-linearities by linearization and obtain an approximate inverse operator. Linearizing equation (2.24) about $\underline{x}_0$, yields after some manipulations,

$$\underline{z} \simeq 2\ [L\ (\underline{x}_0)]\ \underline{x} - [L\ (\underline{x}_0)]\ \underline{x}_0 \tag{4.10}$$

This allows us to obtain an expression corresponding to (4.4), that is

$$\underline{x} \simeq \hat{\underline{Z}}^{-1}\ (\underline{z}) = \frac{1}{2}\,\underline{x}_0 + \frac{1}{2}\ [L\ (\underline{x}_0)]^{-1}\ \underline{z} \tag{4.11}$$

where it is assumed that $[L\ (\underline{x}_0)]$ is non-singular. Now substituting this relation into (4.8), it follows that,

$$\tilde{Y}_L = \frac{1}{4}\, Y_0 + \frac{1}{2}\,\underline{\beta}^T\ (\underline{x}_0)\ \underline{z} + \frac{1}{4}\ \underline{z}^T\ [D\ (\underline{x}_0)]\ \underline{z} \tag{4.12}$$

where the super-script $\sim$ denotes a second-order approximation and

$$y_0 \triangleq Y(\underline{x}_0) = \underline{x}_0^T [Y] \underline{x}_0 \tag{4.13}$$

$$\underline{\beta}(\underline{x}_0) \triangleq [L(\underline{x}_0)]^{-T} [Y] \underline{x}_0 \tag{4.14}$$

$$[D(\underline{x}_0)] \triangleq [L(\underline{x}_0)]^{-T} [Y] [L(\underline{x}_0)]^{-1} \tag{4.15}$$

Equation (4.11) is basically the iteration rule of the Newton-Raphson (NR) algorithm and equation (4.12) in fact corresponds to the value of y evaluated after the first NR iteration. This suggests that higher order formulae can be obtained by explicitly carrying out the NR steps. Considering a constant gradient Newton algorithm (BNA), for the second iteration one obtains

$$\underline{x} \simeq \frac{3}{8}\underline{x}_0 + \frac{3}{4}\underline{\gamma} - \frac{1}{8}[L(\underline{x}_0)]^{-1} \underline{z}(\underline{\gamma})$$

where

$$\underline{\gamma} \triangleq [L(\underline{x}_0)]^{-1} \underline{z}$$

Inserting the above relation in $y = Y(\underline{x})$, a fourth order relation results. Further NR steps produce expressions which are of the order 8, 16, 32, and so on.

4.2.3 Taylor Series Expansion (TSE) Formulae

Approximation formulae can be systematically derived based on a Taylor series expansion of y in $\underline{z}$. Denoting such a series by y_T, it follows that,

$$y_T = y_0 + \frac{1}{1\,!} [\frac{\partial\, y_0}{\partial\, \underline{z}_0}]\, \Delta\, \underline{z} + \frac{1}{2\,!}\, \Delta\, \underline{z}^T\, [\frac{\partial^2\, y_0}{\partial\, \underline{z}_0^2}]\, \Delta\, \underline{z} + \ldots \tag{4.16}$$

where $\Delta\, \underline{z} \triangleq \underline{z} - \underline{z}_0$ and

$$\underline{z}_0 \triangleq L\, (\underline{x}_0)\, \underline{x}_0 \tag{4.17}$$

Based on (4.16), and by different truncation of the series, various approximation formulae can be derived.

4.2.4 Comparison of Approximate Formulae

We initially started experimenting with all the three schemes introduced above, testing them under similar situations. It soon became evident that the linear TSE formulae are distinctly superior to those of the parametric approach, no matter what technique is used in solving (4.9). Furthermore, the second-order TSE formulae proved to be consistently more accurate than those based on linearization of the LFE. Such a trend is exhibited in Figure 4.1, where the three schemes are applied to the 2-bus system of Section 3.4.

The parametric approach is not successful because, as seen in Figure 4.1, it tries to follow the exact value of a dependent variable all over the $\underline{x}$ space. There is no simple way of introducing in that approach the fact that in practice, under the steady-state condition, one is primarily interested in that part of the voltage space where the realis-

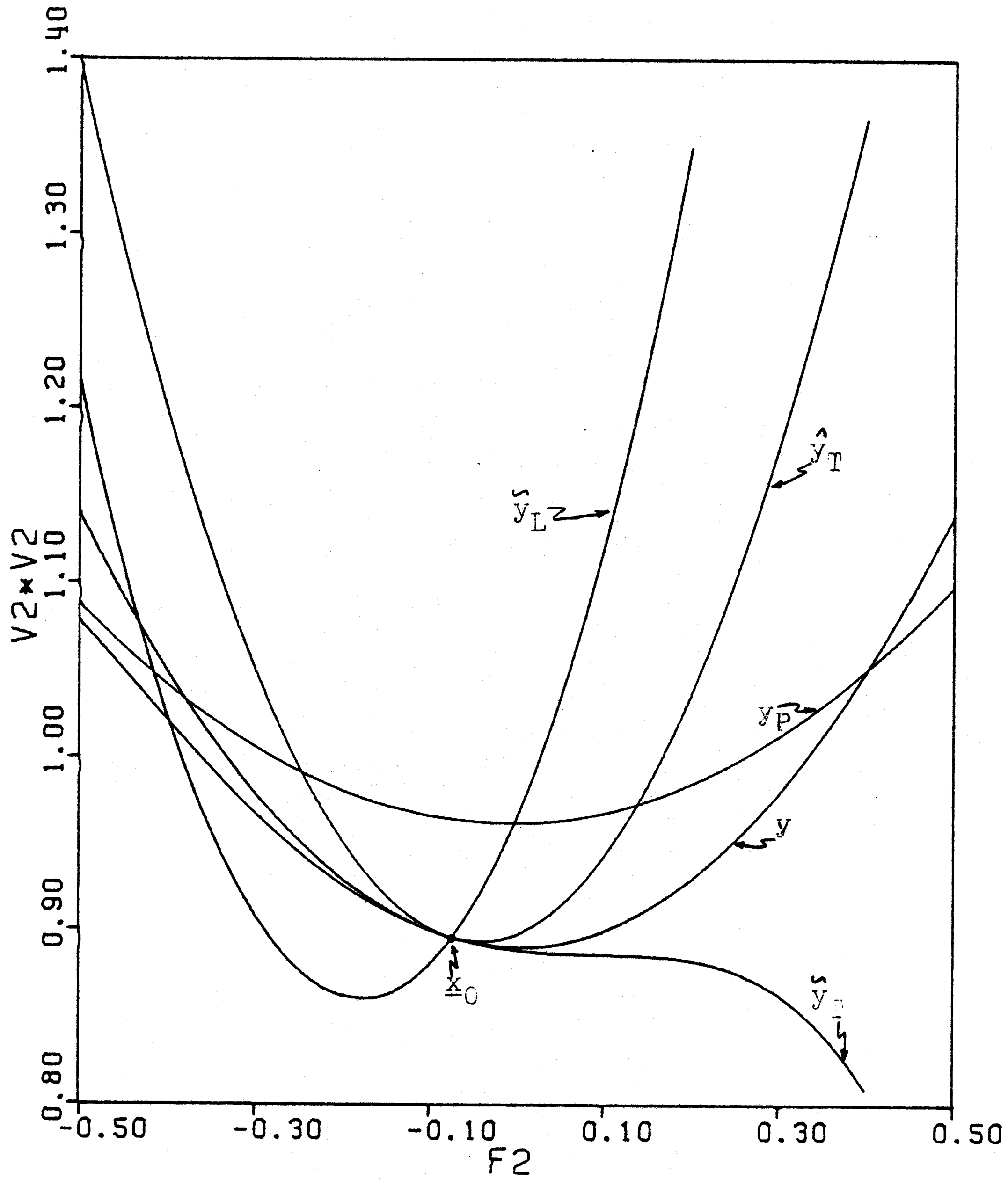

Figure 4.1. Comparison of the results of different schemes in approximating v_2^2 for the 2-bus system of Section 3.4. (Expansion point $\underline{x}_0^T$ = [1.05, 0.9432, - 0.0742] .

tic solutions lie. That part of the voltage space is shown shaded in Figure 4.2.

The linearization based approach is not competitive with the second-order TSE formulae because, in addition to a lesser degree of accuracy, it lacks the flexibility offered by the latter. In the TSE approach, the first-order term in the series normally carries the largest weight. This is due to the fact that $\hat{y}_T = \underline{\beta}^T (\underline{x}_0)\ \underline{z}$ is of the same order as $y = Y(\underline{x})$ in terms of $\underline{x}$. The higher order terms therefore are basically of refining or corrective nature. This property allows one, for example, to drop the quadratic terms from the second order expansion formulae and still represent the approximated variables with fair accuracy. This is not the case in the other approach where all the three terms in (4.12) contribute significantly to the value of $\tilde{y}_L$.

In Figure 4.3, the accuracy of the approximation formulae derived based on the iterations of the BNA is compared with those of the TSE. The graphs indicate that, comparing the formulae of the same order, the TSE formulae have higher accuracies than those of the linearization based approach. However, from a computational point of view, the formulae based on the latter can be evaluated with higher efficiency. These graphs are obtained for the 8-bus system of reference [3] and although given for a particular variable (the system losses) are typical for other dependent variables in that system.

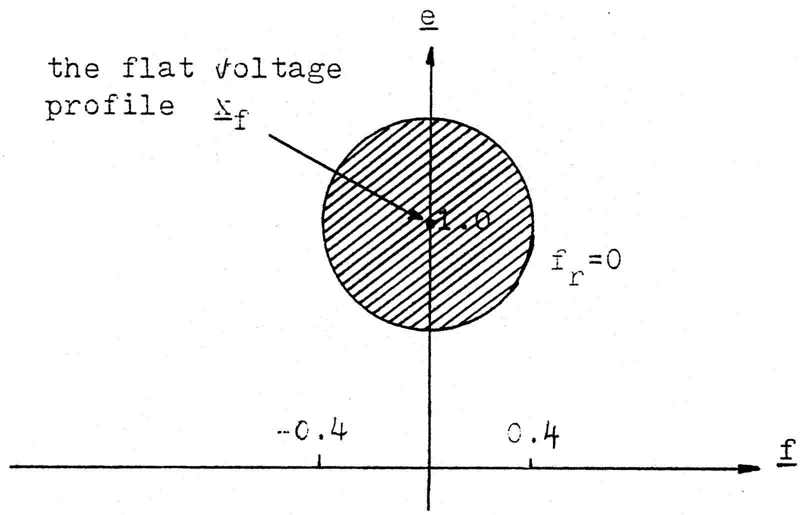

Figure 4.2. Location of the realistic voltage solutions.

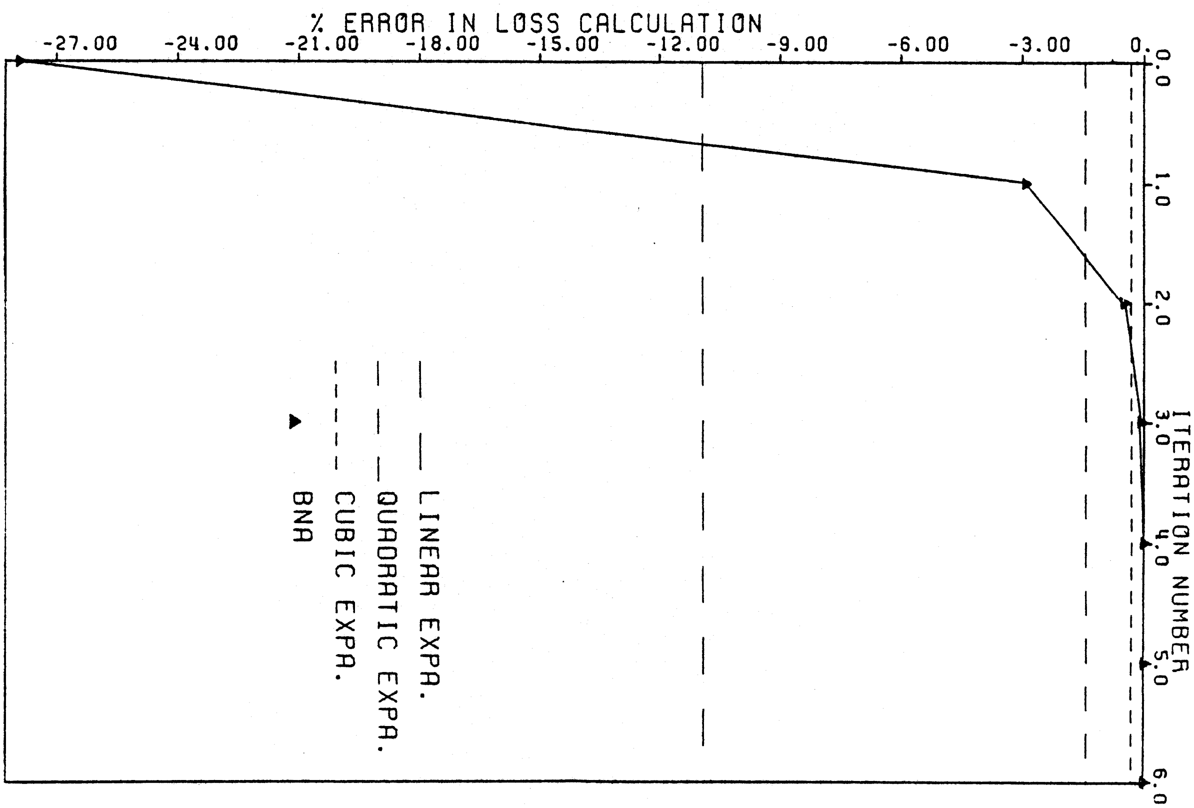

Figure 4.3. Comparison of the accuracy of the approximation formulae derived based on the iterations of BNA with those of TSE.

The rest of this and the next two chapters examine different aspects of applying the TSE formulae in forming the security sets in the injection space. The subscript T, used to distinguish the TSE approach, is dropped hereafter.

4.3 Derivation of TSE Formulae

Due to the vectorial nature of the differentiations involved in (4.16), it is obvious that after the third term one has to reckon with the increasing dimensionality of the partial derivative tensors produced. By concentrating on the evaluation of the terms in the series, as opposed to performing the differentiations separately, one can avoid such difficulties.

Denoting the nth term of the Taylor series by $T_n\ (\underline{x}_0,\ \Delta\ \underline{z})$, then

$$y = \sum_{n=0}^{\infty} T_n\ (\underline{x}_0,\ \Delta\ \underline{z})$$

where by definition

$$T_n\ (\underline{x}_0,\ \Delta\ \underline{z}) = \frac{1}{n\ !} \sum_{\substack{i=1\\ j=1\\ \vdots\\ k=1}} \left[\frac{\partial^n y_0}{\partial z_{0_i}\ \partial z_{0_j}\ \cdots\ \partial z_{0_k}}\right] \Delta z_i\ \Delta z_j\ \cdots\ \Delta z_k \tag{4.18}$$

The summation sign here, indexed with $(i, j, \ldots, k)$, represents n different summations. From above, it can be easily verified that,

$$T_n(\underline{x}_0, \Delta \underline{z}) = \frac{1}{n} \sum_{i=1}^{N_z} \frac{\partial}{\partial z_{0_i}} \{T_{n-1}(\underline{x}_0, \Delta \underline{z})\} \Delta z_i$$

$$= \frac{1}{n} \left[\frac{\partial T_{n-1}(\underline{x}_0, \Delta \underline{z})}{\partial \underline{z}_0} \right] \Delta \underline{z}$$

Applying the chain rule,

$$T_n(\underline{x}_0, \Delta \underline{z}) = \frac{1}{n} \left[\frac{\partial T_{n-1}(\underline{x}_0, \Delta \underline{z})}{\partial \underline{x}_0} \right] \left[\frac{\partial \underline{z}_0}{\partial \underline{x}_0} \right]^{-1} \Delta \underline{z}$$

$$= \frac{1}{n} \left[\frac{\partial T_{n-1}(\underline{x}_0, \Delta \underline{z})}{\partial \underline{x}_0} \right] [J(\underline{x}_0)]^{-1} \Delta \underline{z} \tag{4.19}$$

where in the last step computation (2.32) is used. Note that (4.19) involves only the differentiation of a scalar with respect to a vector.

4.3.1 Linear Relations

Since $T_0(\underline{x}_0, \Delta \underline{z}) = y_0$, from (4.19) it follows that,

$$T_1(\underline{x}_0, \Delta \underline{z}) = \left[\frac{\partial T_0(\underline{x}_0, \Delta \underline{z})}{\partial \underline{x}_0} \right] [J(\underline{x}_0)]^{-1} \Delta \underline{z}$$

$$= \left\{ \frac{\partial}{\partial \underline{x}_0} (\underline{x}_0^T [Y] \underline{x}_0) \right\} [J(\underline{x}_0)]^{-1} \Delta \underline{z}$$

$$= \{2 \underline{x}_0^T [Y]\} [J(\underline{x}_0)]^{-1} \Delta \underline{z} = \underline{\beta}^T(\underline{x}_0) \Delta \underline{z} \tag{4.20}$$

where $\underline{\beta}\ (\underline{x}_0)$ is defined in (4.13). A linear TSE formula is thus given by

$$\hat{y} = y_0 + \underline{\beta}^T(\underline{x}_0)\ \Delta\ \underline{z} \tag{4.21}$$

4.3.2 Quadratic Relations

Again based on (4.19),

$$\begin{aligned} T_2\ (\underline{x}_0,\ \Delta\ \underline{z}) &= \frac{1}{2}\left[\frac{\partial\ T_1\ (\underline{x}_0,\ \Delta\ \underline{z})}{\partial\ \underline{x}_0}\right]\ [J\ (\underline{x}_0)]^{-1}\ \Delta\ \underline{z} \\ &= \frac{1}{2}\left\{\frac{\partial}{\partial\ \underline{x}_0}\ [\underline{\beta}^T\ (\underline{x}_0)\ \Delta\ \underline{z}]\right\}\ [J\ (\underline{x}_0)]^{-1}\ \Delta\ \underline{z} \\ &= \frac{1}{2}\ \Delta\ \underline{z}^T\ \left[\frac{\partial\ \underline{\beta}\ (\underline{x}_0)}{\partial\ \underline{x}_0}\right]\ [J\ (\underline{x}_0)]^{-1}\ \Delta\ \underline{z} \end{aligned} \tag{4.22}$$

Using the definition of $\underline{\beta}\ (\underline{x}_0)$ and the computations in (2.31) and (2.32)

$$\begin{aligned} \frac{\partial\ \underline{\beta}\ (\underline{x}_0)}{\partial\ \underline{x}_0} &= [L\ (\underline{x}_0)]^{-T}\ [Y] + \left\{\underline{x}_0^T\ [Y]\ \frac{\partial}{\partial\ \underline{x}_0}\ [L\ (\underline{x}_0)]^{-1}\right\}^T \\ &= [L\ (\underline{x}_0)]^{-T}\ [Y] + \left\{-\ [Z\ (\underline{\beta})]\ [L\ (\underline{x}_0)]^{-1}\right\}^T \\ &= 2\ [J\ (\underline{x}_0)]^{-T}\ \{[Y] - [Z\ (\underline{\beta})]\} \end{aligned} \tag{4.23}$$

A quadratic TSE formulae is then of the form

$$\tilde{y} = y_0 + \underline{\beta}^T (\underline{x}_0) \, \Delta \underline{z} + \Delta \underline{z}^T [C(\underline{\beta})] \, \Delta \underline{z} \tag{4.24}$$

where

$$[C(\underline{\beta})] \triangleq [J(\underline{x}_0]^{-T} \{[Y] - [Z(\underline{\beta})]\} [J(\underline{x}_0)]^{-1} \tag{4.25}$$

4.3.3 Higher Order Relations

Similarly to the way in which the first and second order TSE formulae are derived, the third and higher order relations can be obtained. As one embarks on deriving the higher order relations, the computations get, nevertheless, more messy. This necessitates a more organized approach in manipulating the results, as demonstrated in ref. [70] where a third order TSE formula is derived.

4.4 Error Analysis

4.4.1 Analytical Properties of the Linear Expansion Error

By noting that

$$\underline{\beta}^T (\underline{x}_0) \, \underline{z}_0 = \{\underline{x}_0^T [Y] [L(\underline{x}_0)]^{-1}\} [L(\underline{x}_0] \, \underline{x}_0 = y_0$$

one is able to simplify relation (4.21) to

$$\hat{y} = \underline{\beta}^T (\underline{x}_0) \, \underline{z} \tag{4.26}$$

Now let us denote the error associated with the linear approximation by $\varepsilon_1(\underline{x})$, that is

$$y = \underline{\beta}^T(\underline{x}_0)\,\underline{z} + \varepsilon_1(x) \tag{4.27}$$

Using equations (2.27) and (4.8), the error $\varepsilon_1(\underline{x})$ then can be simply expressed by

$$\begin{aligned}\varepsilon_1(\underline{x}) &= \underline{x}^T[Y]\,\underline{x} - \underline{x}^T[Z(\underline{\beta})]\,\underline{x} \\ &= \underline{x}^T[E(\underline{x}_0)]\,\underline{x}\end{aligned} \tag{4.28}$$

where

$$[E(\underline{x}_0)] \triangleq \{[Y] - [Z(\underline{\beta})]\}$$

The matrix $[E(\underline{x}_0)]$ has a central role in the expansion formulae. It appears in all the higher order expansion formulae (see equation (4.25) and (4.24)), emphasizing their secondary or corrective nature compared to the first order formulae. Since at $\underline{x}_0$ the error is zero, (i.e., $\varepsilon_1(\underline{x}_0) = 0$), it follows that,

$$[E(\underline{x}_0)]\,\underline{x}_0 = \underline{0} \tag{4.29}$$

Exploiting (4.29), the error can also be expressed as a quadratic function of $\Delta\,\underline{x} \triangleq \underline{x} - \underline{x}_0$, that is

$$\varepsilon_1(\underline{x}) = \Delta\,\underline{x}^T[E(\underline{x}_0)]\,\Delta\,\underline{x} \tag{4.30}$$

Since the matrix $[E\ (\underline{x}_0)]$ appears in all higher order relations, relation (4.29) can be used to simplify them. The quadratic expansion formulae in (4.24), for example, reduces to

$$\tilde{y} = \underline{\beta}^T\ (\underline{x}_0)\ \underline{z} + \underline{z}^T\ [C\ (\underline{\beta})]\ \underline{z} \tag{4.31}$$

4.4.2 Bounds on the Linear Expansion Error

Various properties of quadratic forms can be used to analyze the nature of $\varepsilon_1\ (\underline{x})$ in order to better understand the validity of the linear approximation formulae. Numerical results, for example, indicate that for some variables (those that are always non-negative), such as the voltage magnitude squared, magnitude squared of line currents or the line losses, the linear expansion error is always positive or zero when the expansion point is near the flat voltage profile (condition for zero transmission losses). This implies that the matrix $[E\ (\underline{x}_0)]$ is positive semi-definite for these variables. A rigorous proof of this result for the system losses is presented in Appendix H .

A more quantitative relation on the error $\varepsilon_1\ (\underline{x})$ can be derived from the minimum $(\lambda_\varepsilon^{min})$ and maximum $(\lambda_\varepsilon^{max})$ eigen-values of $[E\ (\underline{x}_0)]$. From (4.28), it follows [71] ,

$$\lambda_\varepsilon^{min}\ \|\underline{x}\|^2 \le \varepsilon_1\ (\underline{x}) = \underline{x}^T\ [E\ (\underline{x}_0)]\ \underline{x} \le \lambda_\varepsilon^{max}\ \|\underline{x}\|^2 \tag{4.32}$$

Similarly, for each entry of $\underline{z}$, one can write

$$\lambda_j^{min} \|\underline{x}\|^2 \leq z_j = \underline{x}^T [Z_j] \underline{x} \leq \lambda_j^{max} \|\underline{x}\|^2$$

$$j = 1, \ldots, N_z \tag{4.33}$$

where λ_j^{min} and λ_j^{max} are respectively the largest and the smallest eigen-values of the matrix $[Z_j]$. Relation (4.33) can be used to establish bounds on the magnitude of $\underline{z}$ in terms of $\|\underline{x}\|^2$, that is

$$\gamma^{min} \|\underline{x}\|^2 \leq \|\underline{z}\| \leq \gamma^{max} \|\underline{x}\|^2 \tag{4.34}$$

where γ^{min} and γ^{max} are simple, positive functions of λ_j^{min} and λ_j^{max}, $j = 1, \ldots, N_z$. As shown in reference [72] , the special structure of the matrices $[Z_j]$ $j = 1, \ldots, N_z$, can be exploited to obtain explicit relations for their eigen-values in terms of the network parameters. Combining the last few expressions, it is easy to verify:

$$(\lambda_\varepsilon^{min} / \gamma^{max}) \|\underline{z}\|^2 \leq \varepsilon_1 (\underline{x}) \leq (\lambda_\varepsilon^{max} / \gamma^{min}) \|\underline{z}\|^2 \tag{4.35}$$

This relation provides the absolute bounds on $\varepsilon_1 (\underline{x})$ for any injection vector $\underline{z}$.

4.4.3 Short Cut to the Derivation of TSE Formulae

While seeking for a relationship between the TSE formulae and the Newton-Raphson (NR) load flow algorithms, we noticed that the tedious derivations of the expansion formulae can be avoided by using equation (4.11), which is the essence of all NR algorithms.

Since $\hat{y}$ is in fact the first order sensitivity of y to $\underline{z}$, it is not surprising to see that equation (4.26) can be derived simply by linearizing y and using equation (4.11), that is

$$\hat{y} = -\underline{x}_0^T [Y] \underline{x}_0 + 2 \underline{x}_0^T [Y] \underline{x}$$

$$= -\underline{x}_0^T [Y] \underline{x}_0 + 2 \underline{x}_0^T [Y] \{\tfrac{1}{2} \underline{x}_0 + \tfrac{1}{2} [L (\underline{x}_0]^{-1} \underline{z}\} = \underline{\beta}^T (\underline{x}_0) \underline{z} \tag{4.36}$$

Now consider equation (4.27), that is

$$y = \underline{\beta}^T (\underline{x}_0) \underline{z} + \underline{x}^T [E (\underline{x}_0)] \underline{x} \tag{4.37}$$

It is not possible to improve over the first order expansion formulae by expressing $\varepsilon_1 (\underline{x})$ linearly in terms of $\underline{z}$. This is due to the existence of relation (4.29), making the corresponding $\underline{\beta}$ identically zero. One can, however, use equation (4.11) to approximate $\varepsilon_1 (\underline{x})$ by a quadratic function of $\underline{z}$, namely

$$\tilde{\varepsilon}_1 (\underline{x}) = \{\tfrac{1}{2} \underline{x}_0 + \tfrac{1}{2} [L (\underline{x}_0]^{-1} \underline{z}\}^T [E (\underline{x}_0)] \{\tfrac{1}{2} \underline{x}_0 + \tfrac{1}{2} [L (\underline{x}_0)]^{-1} \underline{z}\}$$

$$= \underline{z}^T [C (\underline{\beta})] \underline{z} \tag{4.38}$$

where we have made use of the computation (4.29) and the definitions (2.32) and (4.26). It is interesting to note that now by replacing $\varepsilon_1 (x)$ in (4.37) by $\tilde{\varepsilon}_1 (\underline{x})$ the same expression for $\tilde{y}$, as given in (4.31), results.

With slight modifications, the same scheme can be followed to obtain the expansion formulae for higher order terms. A third order formulae, for example, can be derived by first defining a vector $\underline{\gamma} (\underline{x}_0, \underline{z})$ such that

$$\tilde{y} = \underline{\gamma}^T (\underline{x}_0, \underline{z})\ \underline{z} \tag{4.39}$$

From (4.31), it follows that,

$$\underline{\gamma} (\underline{x}_0, \underline{z}) = \underline{\beta} (\underline{x}_0) + [C (\underline{\beta})]\ \underline{z} \tag{4.40}$$

then adding an approximate error function $\varepsilon_2 (\underline{x})$ to $\tilde{y}$ and repeating the previous steps, one can readily arrive at,

$$y^{(3)} = \underline{\beta}^T (\underline{x}_0)\ \underline{z} + \underline{z}^T [C (\underline{\beta})]\ \underline{z} + \underline{z}^T [C (\underline{\gamma})]\ \underline{z} \tag{4.41}$$

where the super-script (3) indicates a third order TSE formula.

4.5 Numerical Results

4.5.1 Error Propagation Maps for a Two Bus System

A two bus system is examined here primarily because its mathematical model, as opposed to larger systems, involves only a few variables, enabling us to show some of the results graphically.

The system here is that of Section 3.4, Figure 3.4. The first four graphs show how the equi - % error contours propagate in the $P_2 - Q_2$ plane for the first order expansion of the indicated dependent variables. Figures 4.5a through 4.5d show the propagation of equi - % error contours, when the second order expansions are used. The following points in relation to these graphs are of importance:

(i) A large area around the expansion point can be identified as a very low error region.

(ii) Among the variables examined, the expansion formula for the reactive power injection seem to be more susceptible to large errors as $\underline{z}$ moves away from $\underline{z}_0$. It is, nevertheless, important to note that the $\pm \infty$ % error contour present in Figure 4.4b corresponds to the zero reactive power injection contour and the <u>error</u> (not the % error) is indeed numerically quite small along this contour.

Figure 4.4. Equi - % error contours for linear approximation of (a) p_1 ; (b) q_1 ; (c) v_2^2 ; (d) $|I_1|^2$ for $v_1 = 1.0$. (Expansion point $\underline{z}_0^T = [1.0,\ 0.0,\ -0.25]$).

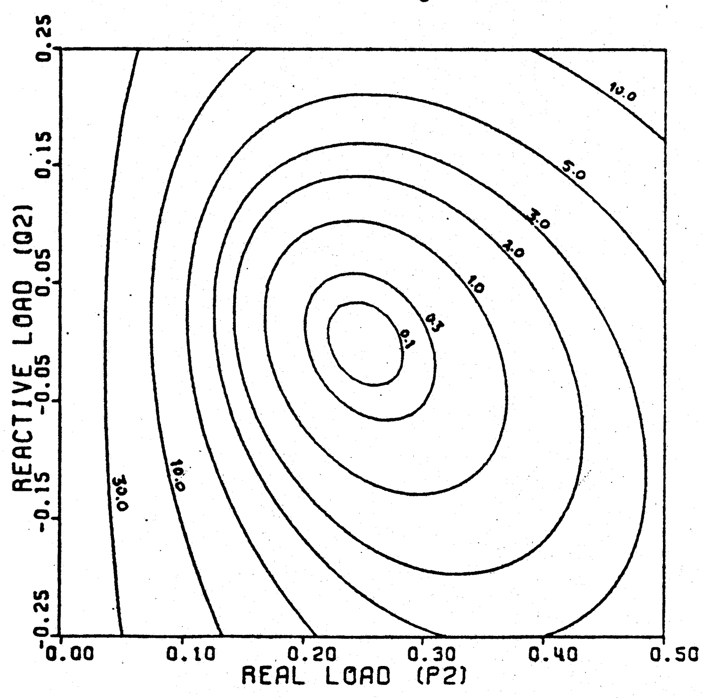

(a)

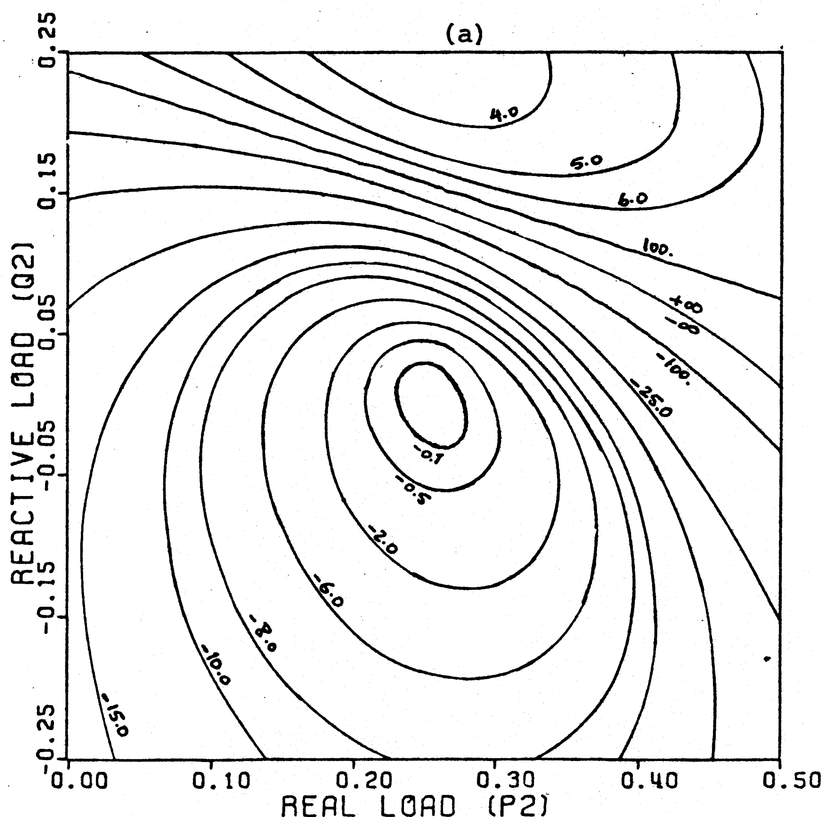

(b)

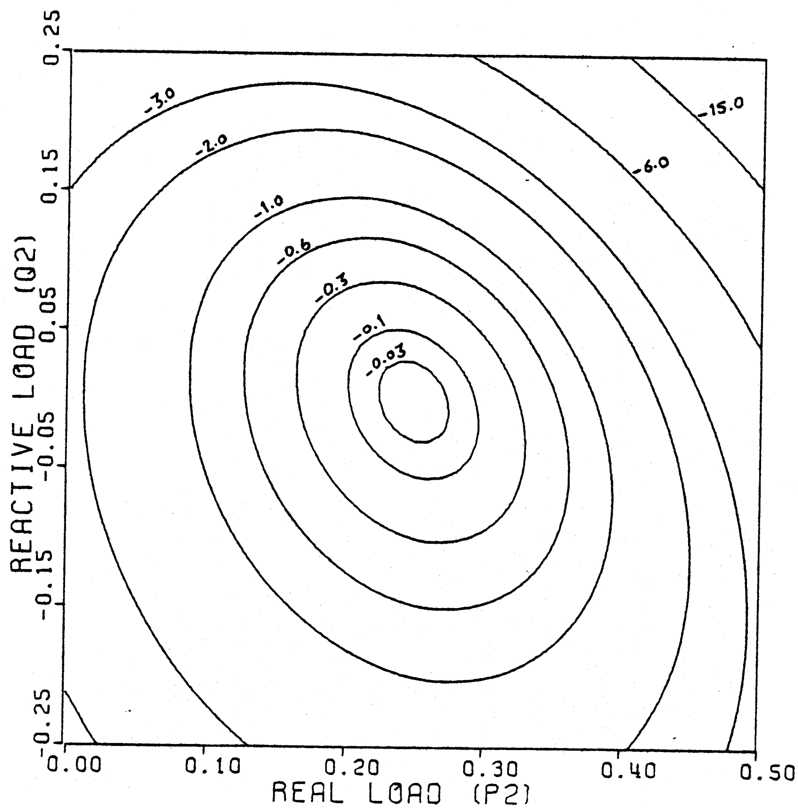
-3.0
-2.0
-1.0
-0.6
-0.3
-0.1
-0.03
-15.0
-6.0
REACTIVE LOAD (Q2)
0.25
0.15
0.05
-0.05
-0.15
-0.25
0.00
0.10
0.20
0.30
0.40
0.50
REAL LOAD (P2)

(c)

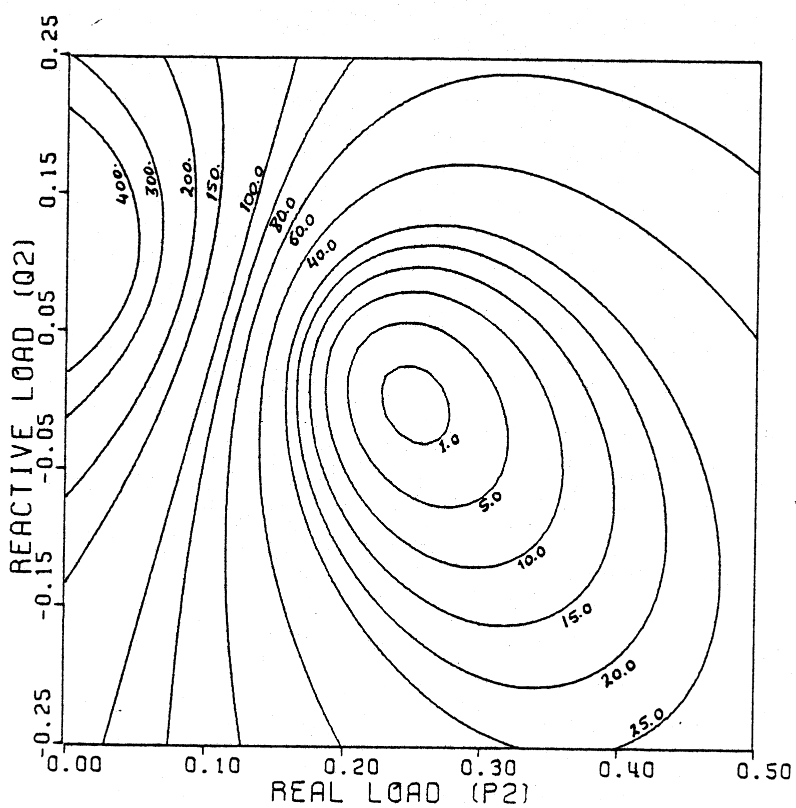
400.
300.
200.
150.
100.0
80.0
60.0
40.0
1.0
5.0
10.0
15.0
20.0
25.0
REACTIVE LOAD (Q2)
0.25
0.15
0.05
-0.05
-0.15
-0.25
0.00
0.10
0.20
0.30
0.40
0.50
REAL LOAD (P2)

(d)

Figure 4.5. Equi - % error contours for quadratic approximation of: (a) p_1 ; (b) q_1 ; (c) v_2^2 ; (d) $|I_1|^2$, for $v_1 = 1.0$. (Expansion point $\underline{z}_0^T = [1.0, 0.0, -0.25]$).

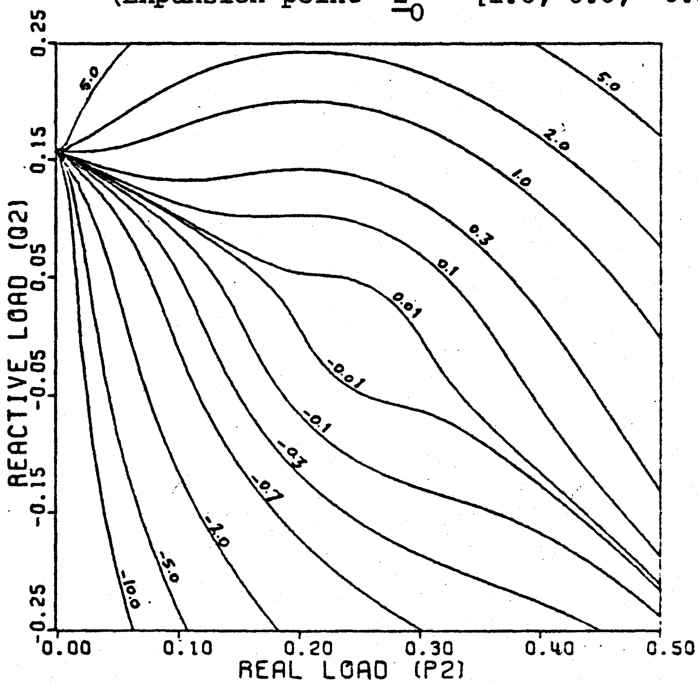

(a)

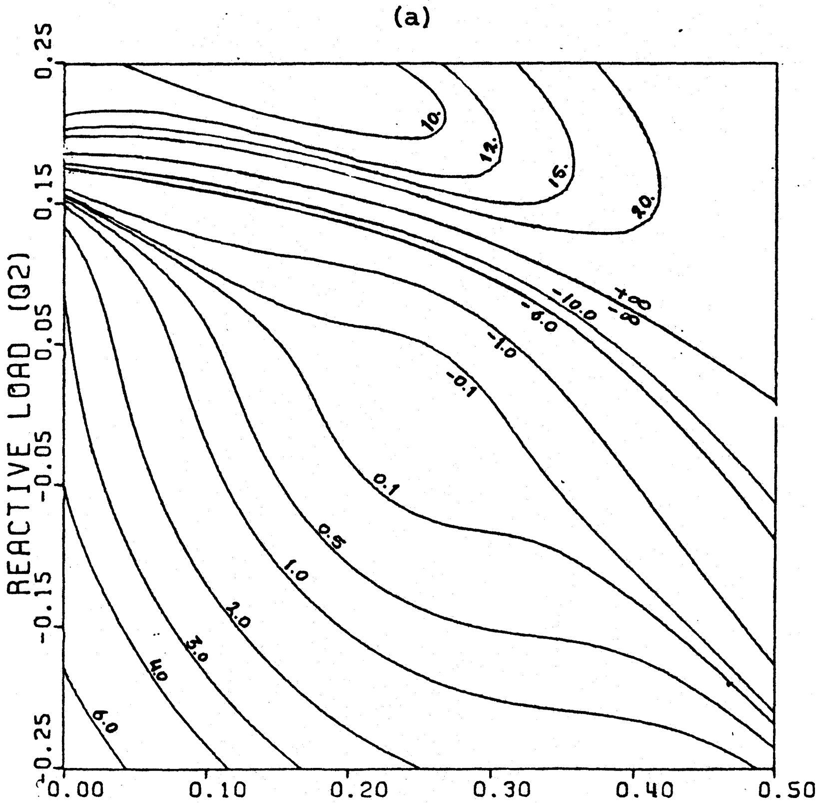

(b)

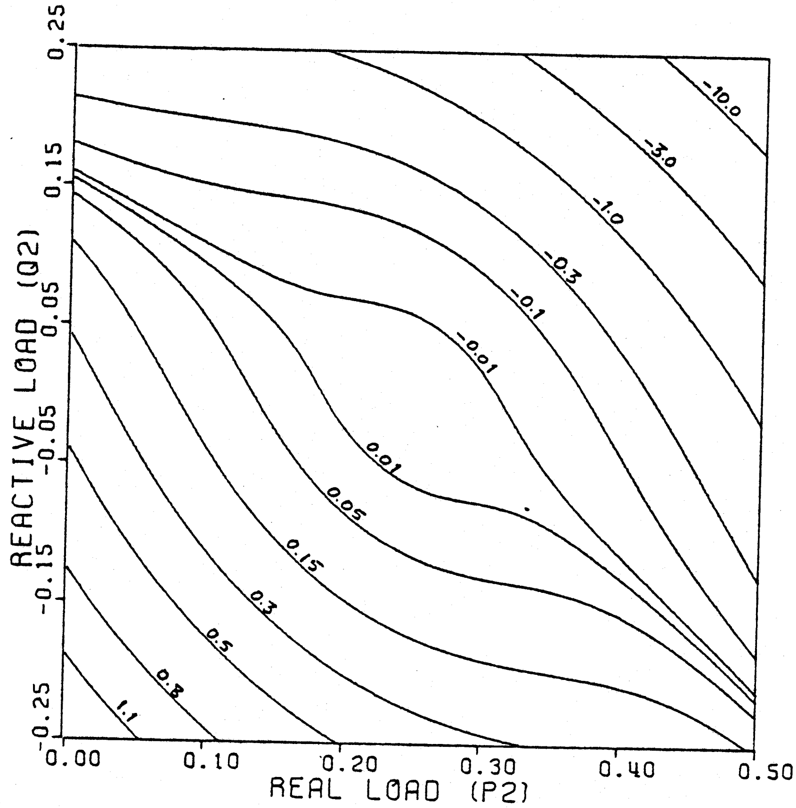

REACTIVE LOAD (Q2)
REAL LOAD (P2)
0.25
0.15
0.05
-0.05
-0.15
-0.25
0.00
0.10
0.20
0.30
0.40
0.50
-10.0
-3.0
-1.0
-0.3
-0.1
-0.01
0.01
0.05
0.15
0.3
0.5
0.8
1.1

(c)

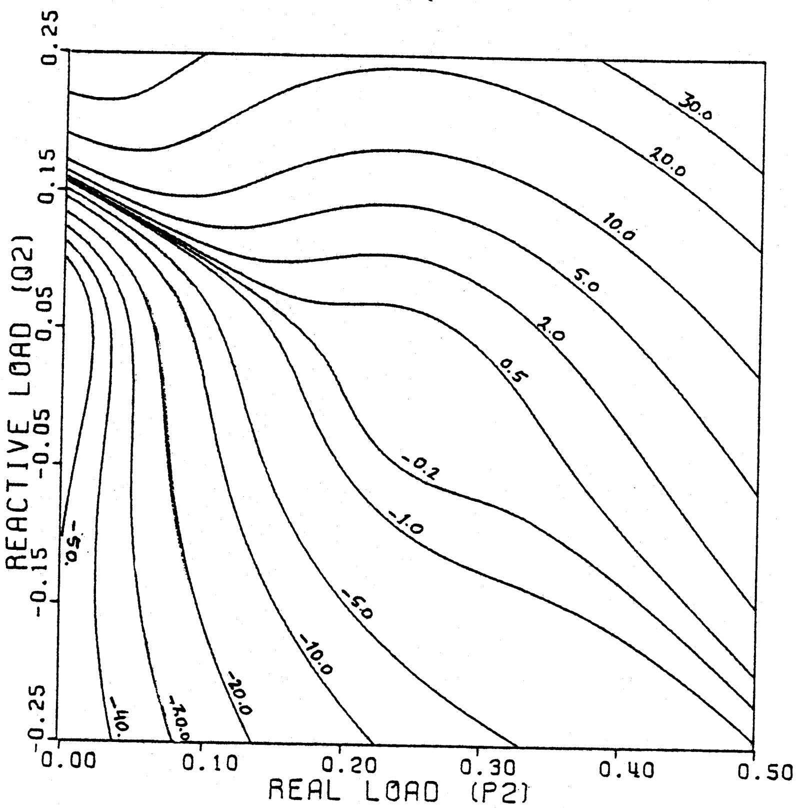

REACTIVE LOAD (Q2)
REAL LOAD (P2)
0.25
0.15
0.05
-0.05
-0.15
-0.25
0.00
0.10
0.20
0.30
0.40
0.50
30.0
20.0
10.0
5.0
2.0
0.5
-0.2
-1.0
-5.0
-10.0
-20.0
-30.0
-40.
-50.

(d)

4.5.2 Numerical Simulations

The eight bus system of reference [3] is chosen to study the errors involved in approximating unknown variables in the system. The error analysis here is based on a random simulation approach. Random numbers are generated within a hyper-box in the $\underline{x}$ space. The sides of the hyper-box are 0.2 p.u. long and the expansion point, $\underline{x}_0$, is at its center.

These variations of $\underline{x}$ around $\underline{x}_0$ generate a wide spectrum of operating points covering and going beyond their normal expected range. The generated numbers are substituted into the system equations to obtain generations, loads, voltage levels, and power transfers. Those numbers which do not correspond to realistic load flows (i.e., positive real power generations, negative real loads) are discarded. After forming $\underline{z}$ from these data, the expansion formulae are used to calculate the value of the unspecified variables in the system. The results are then compared with their calculated exact value. A few typical results for some of the dependent variables, y, are shown in Figures 4.6a through 4.6d. Note that y_1 and y_2 in these graphs are representing the linear and quadratic approximations respectively. Table 4.1 below summarizes these errors. Note that in accord with the previous observation, the error associated with approximating the reactive power generations is relatively larger than in other variables in the system.

To reduce the volume of this thesis the results of similar comparisons, between the linear TSE formulae and those linear formulae

Figure 4.6. Typical error spread of linear (y_1) and quadratic (y_2) approximations to : (a) real power injection at the slack bus ; (b) reactive power injections at generator buses; (c) voltage squared at load buses; (d) real line flows, for random operating points.

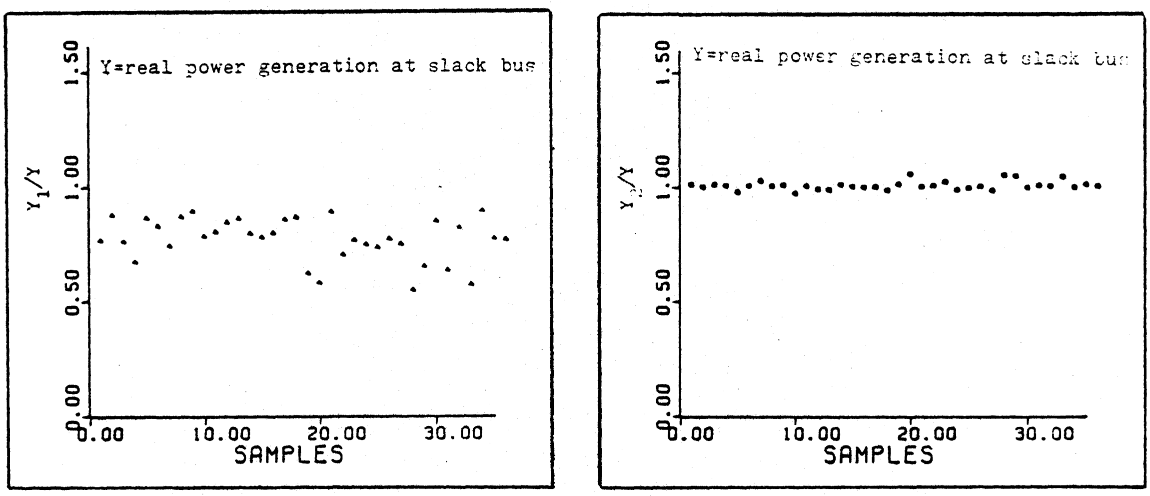

(a)

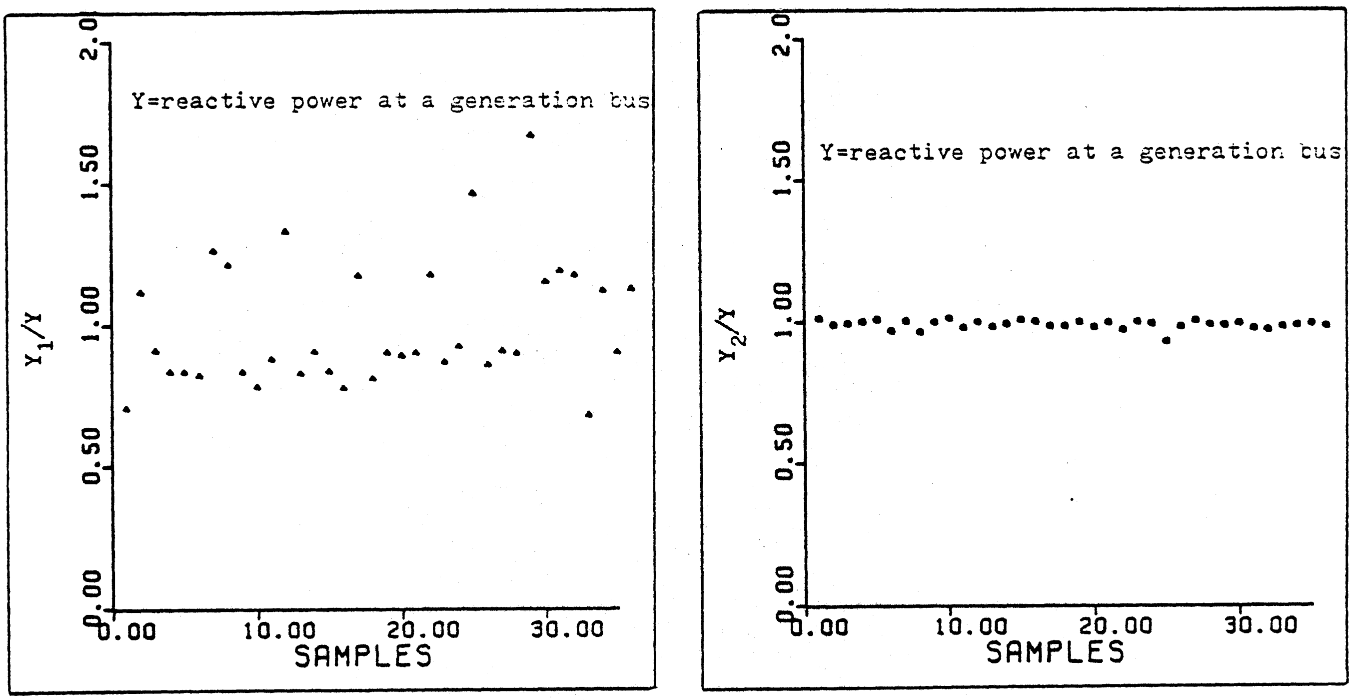

(b)

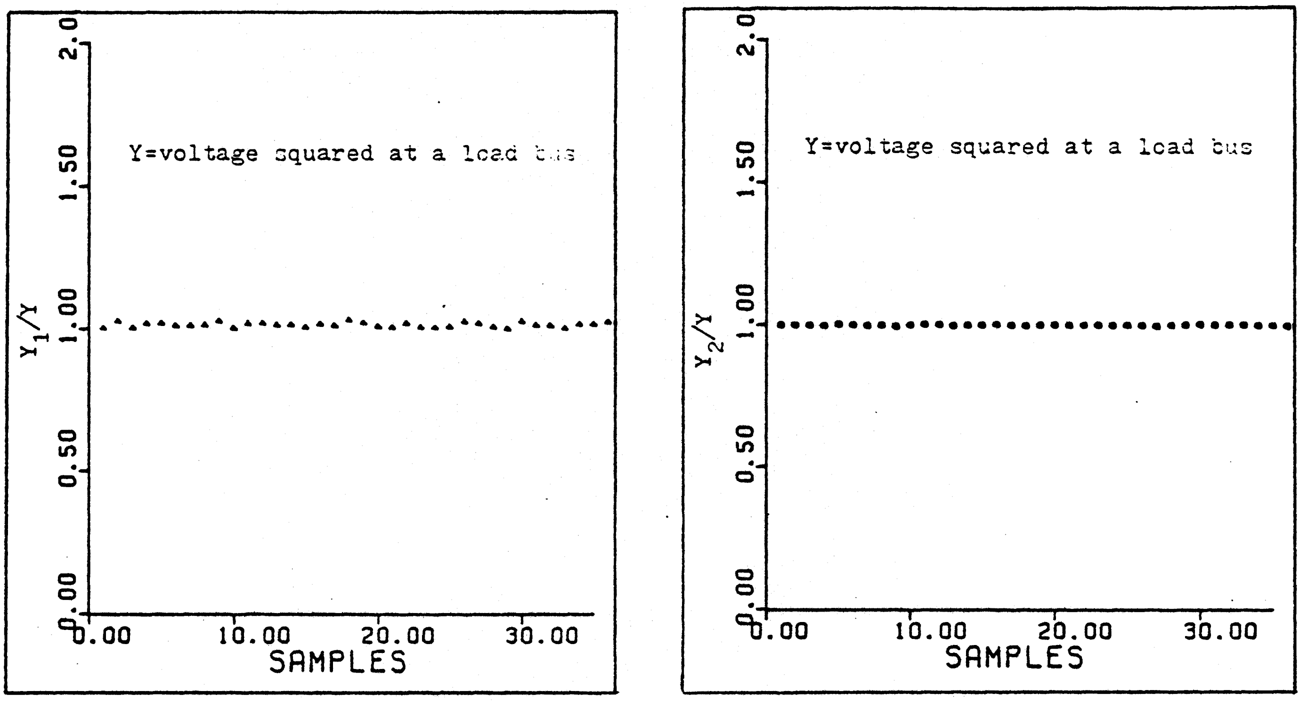
Y=voltage squared at a load bus
Y_1/Y
0.00
0.50
1.00
1.50
2.0
0.00
10.00
20.00
30.00
SAMPLES
Y=voltage squared at a load bus
Y_2/Y
0.00
0.50
1.00
1.50
2.0
0.00
10.00
20.00
30.00
SAMPLES

(c)

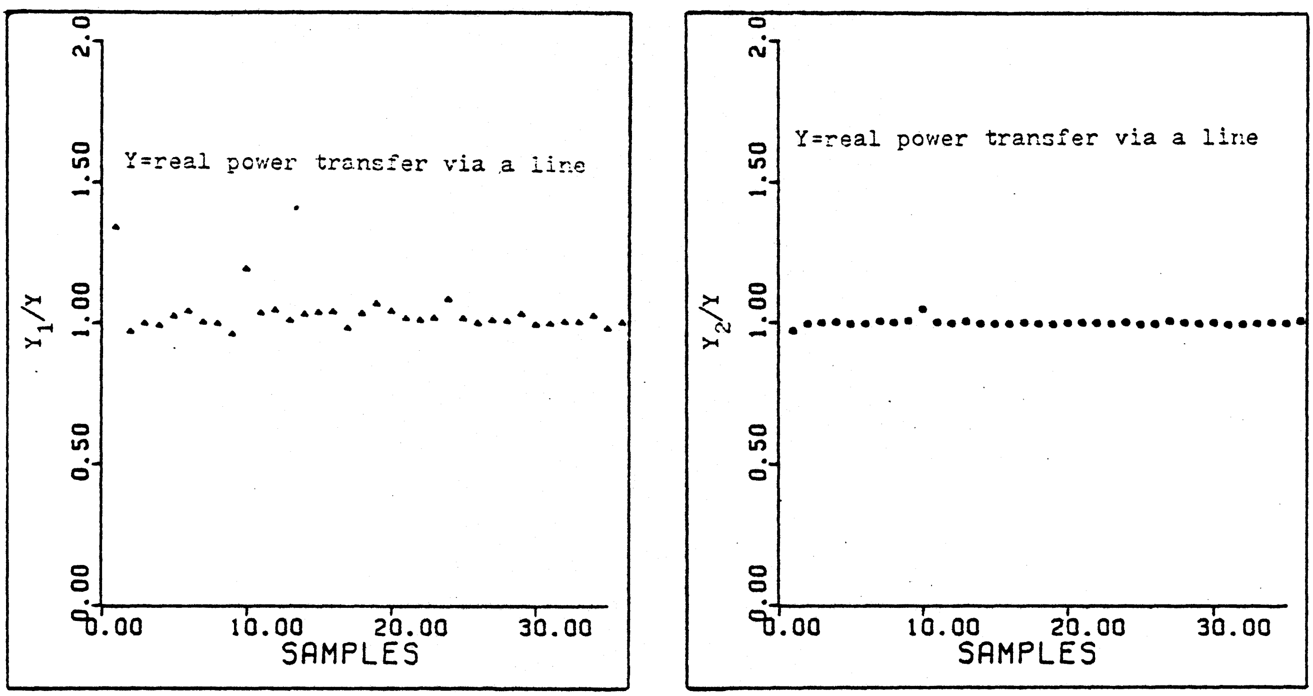
Y=real power transfer via a line
Y_1/Y
0.00
0.50
1.00
1.50
2.0
0.00
10.00
20.00
30.00
SAMPLES
Y=real power transfer via a line
Y_2/Y
0.00
0.50
1.00
1.50
2.0
0.00
10.00
20.00
30.00
SAMPLES

(d)

which are currently in use, are not presented here. One should recognize, however, that since these formulae usually do not carry any information on the voltage levels or reactive generations, a meaningful comparison between them and the TSE formulae is difficult to make. In those cases where a comparison is possible (e.g., with real line flows) the TSE formulae produce more accurate and more general results.

TABLE 4.1.

AVERAGE OF THE % ERRORS

FOR SOME TYPICAL DEPENDENT VARIABLES

	V^2_{Load}	P_{Slack}	Q_{Slack}	P_{Line}
$100 \times \left\| \frac{\varepsilon_1}{y} \right\|$	2	20	25	8
$100 \times \left\| \frac{\varepsilon_2}{y} \right\|$	0.2	3	3.5	1

CHAPTER V

APPLICATION OF THE TSE FORMULAE TO SECURITY RELATED PROBLEMS

5.0 Preliminary Remarks

The general approximation formulae developed in the previous chapter are strong analytical tools for the in depth study of a number of power system problems. With their aid, many of the problems which are historically formulated based on approximation formulae, can be reformulated with a wider scope and more encompassing objectives. Moreover, since these approximation formulae are general, they can potentially constitute the basis of fresh approaches to a number of problems whose conventional formulation does not call for the use of such formulae.

In this chapter, initially, some mathematical properties of security sets are summarized. This is to provide a clear picture of various security sets in different spaces, and to pin-point possible pitfalls which are historically overlooked in their analysis. The employment of the TSE formulae in constructing the security sets in the $\underline{z}$ space is then studied. Next, the role of the approximation formulae in various formulations of the secure-economic dispatch is high-lighted.

5.1 Some Mathematical Properties of Security Sets

The objective of this section, is to clearly show how, under the transformation $\underline{z} = \underline{Z}(\underline{x})$, various security sets are related. The pertaining concepts are presented primarily pictorially, without going into lenghty proofs.

5.1.1 Structure of S_z

The set S_z is the intersection of a hyper-box H_z, with a non-linear set Y_z, i.e.

$$S_z = H_z \cap Y_z \tag{5.1}$$

where

$$H_z = \{\underline{z} \,/\, \underline{z}^m \le \underline{z} \le \underline{z}^M\} \qquad (\underline{z}^\ell = \begin{bmatrix} \underline{u}^\ell \\ \underline{d}^\ell \end{bmatrix} ; \quad \ell = M \text{ or } m) \tag{5.2}$$

and

$$Y_z = \{\underline{z} \,/\, \underline{z} = [L\ (\underline{x})]\ \underline{x} \quad ; \quad \underline{x} \in Y_x\} \tag{5.3}$$

The set Y_x is defined in equation (3.23).

To demonstrate this, consider the following maps:

$$U_x \xrightarrow{\underline{z} \;=\; \underline{Z}\;(\underline{x})} H_u \tag{5.4}$$

$$D_x \xrightarrow{\underline{z} \;=\; \underline{Z}\;(\underline{x})} H_d \tag{5.5}$$

$$Y_x \xrightarrow{\underline{z} \;=\; \underline{Z}\;(\underline{x})} Y_z \tag{5.6}$$

The sets H_u and H_d in the $\underline{z}$ space represent two open-ended parallelograms, whose intersection defines H_z, i.e.

$$U_x \cap D_x \xrightarrow{\underline{z} = \underline{Z}(\underline{x})} H_u \cap H_d \triangleq H_z \tag{5.7}$$

Now since $S_x = (U_x \cap D_x) \cap Y_x$, using (5.6) and (5.7), one can write

$$S_x \xrightarrow{\underline{z} = \underline{Z}(x)} H_z \cap Y_z = S_z \tag{5.8}$$

Hence, to describe S_z, one basically needs to describe Y_z.

5.1.2 Properties of $U_x \cap D_x$

Consider the set $U_x \cap D_x$. This set, in theory, can be disjoint. This is demonstrated in Figure 5.1, where U_x and D_x are defined by

$$U_x = \{\underline{x} \,/\, 4 \le u_1 = \underline{x}^T \begin{bmatrix} 1.0 & 0 \\ 0 & 1.0 \end{bmatrix} \underline{x} \le 9\}$$

$$D_x = \{\underline{x} \,/ 0.5 \le d_1 = \underline{x}^T \begin{bmatrix} 0 & 0.5 \\ 0.5 & 0 \end{bmatrix} \underline{x} \le 2\}$$

Since $\underline{z} = \begin{bmatrix} u_1 \\ d_1 \end{bmatrix}$, the disjoint parts of the set $U_x \cap D_x$ all map into a single region in the $\underline{z}$ space, i.e., into the hyper-box H_z. Here

$$H_z = \{\underline{z} / \begin{bmatrix} 4 \\ 0.5 \end{bmatrix} \leq \underline{z} \leq \begin{bmatrix} 9 \\ 2 \end{bmatrix}\}$$

Now, considering the inverse map (i.e., from the $\underline{z}$ space into the $\underline{x}$ space), each $\underline{z} \in H_z$ maps into various disjoint parts of $U_x \cap D_x$. In other words, the disjoint parts of $U_x \cap D_x$ are the locii of load flow solutions to injections $\underline{z} \in H_z$. The solutions to $\underline{z}_0^T = [5,8, 0.9]$ for example, are the intersections of the surfaces $u_1 = 5.8$ and $d_1 = 0.9$, shown by dotted lines in the picture. Thus one can associate an inverse transformation, $\underline{x} = \underline{Z}_i^{-1}(\underline{z})$, with the ith disjoint part.

5.1.3 Map of S_x into the $\underline{z}$ Space

From above, it is clear that

$$S_x \subseteq U_x \cap D_x \Leftrightarrow S_z \subseteq H_z \tag{5.9}$$

Hence, when S_x is disjoint, S_z can be either connected or disjoint, depending on how the disjoint parts of S_x are located relative to those of $U_x \cap D_x$. If each disjoint part of S_x lies in a different disjoint part of $U_x \cap D_x$, S_z will be connected. This is demonstrated in Figure 5.2(a), where Y_x is defined by

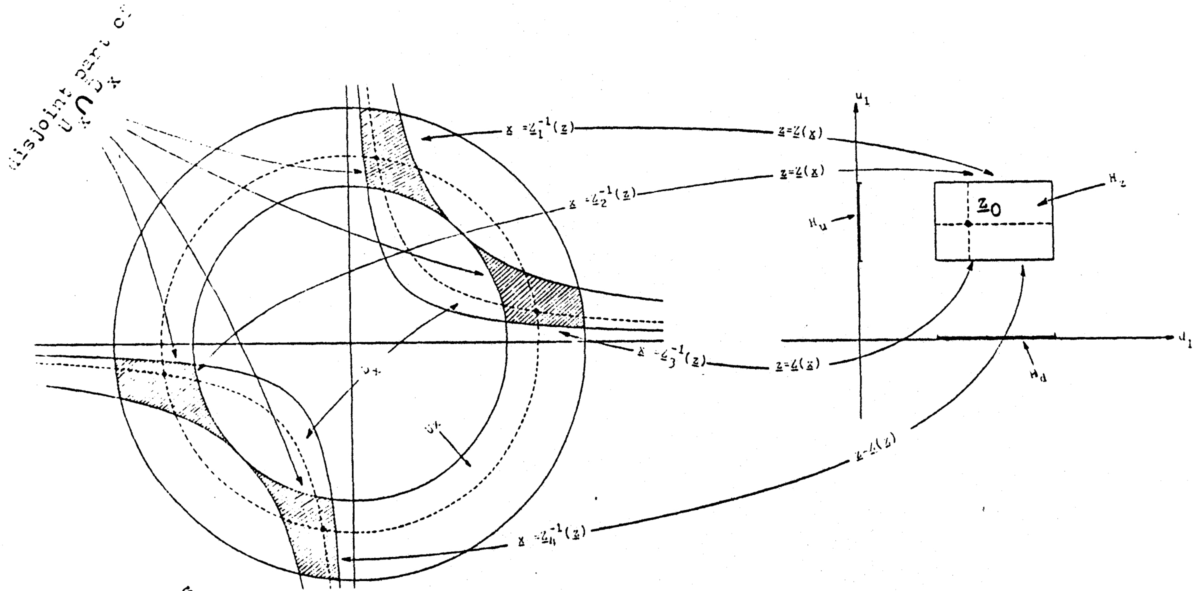

Figure 5.1. Illustration of possible disjointness of S_x .

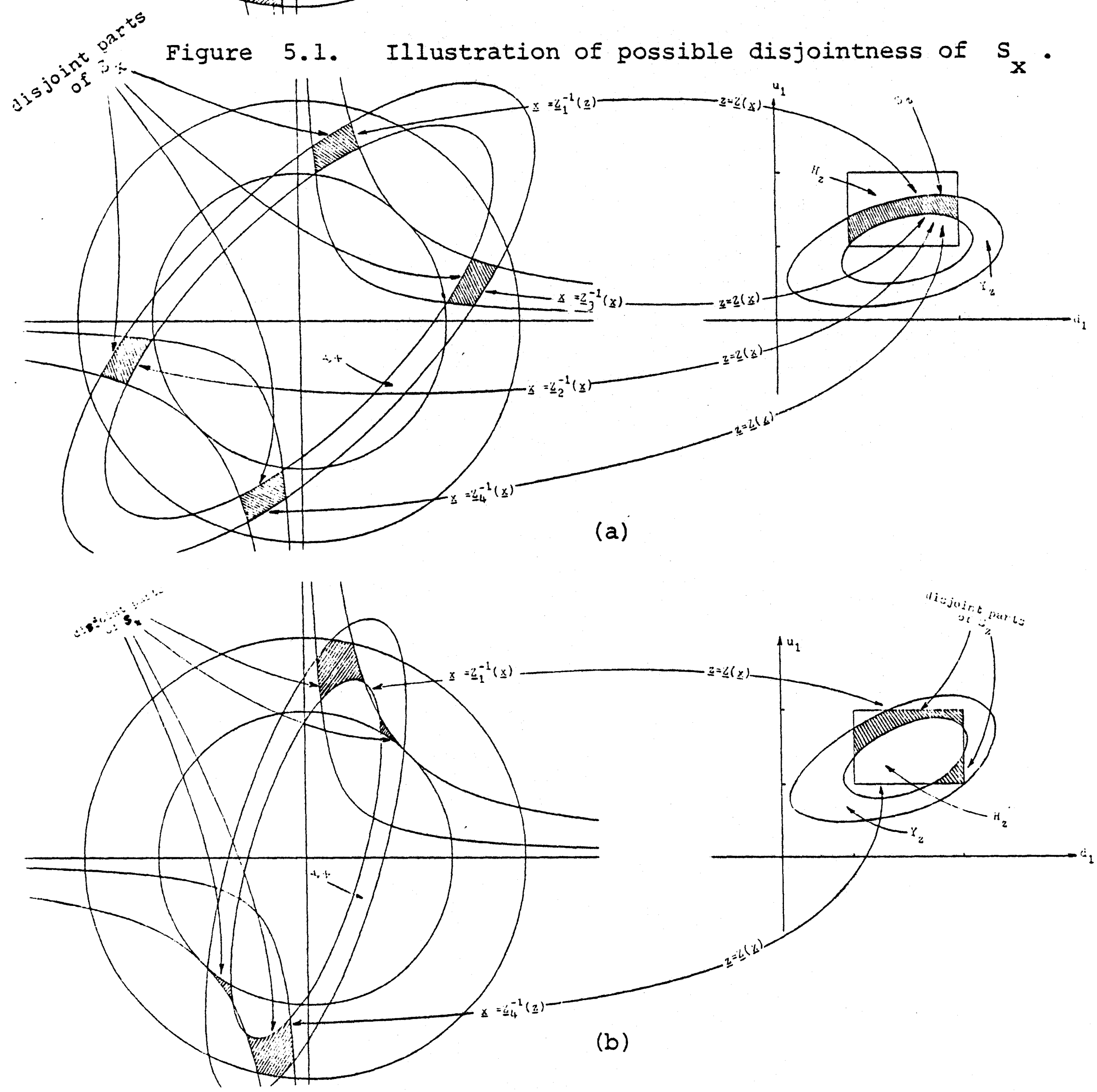

Figure 5.2. Illustration of conditions which give rise to: (a) a connected S_z ; (b) a disjoint S_z .

$$Y_x = \{\underline{x} \;/\; 2.5 \le y_1 = \underline{x}^T \begin{bmatrix} 1 & -0.875 \\ -0.875 & 1 \end{bmatrix} \underline{x} \le 5.0\}$$

When more than one disjoint part of S_x lie inside one of the disjoint parts of $U_x \cap D_x$, S_z will be disjoint. That is demonstrated in Figure 5.2(b) for

$$Y_x = \{\underline{x} \;/\; 4 \le y_1 = \underline{x}^T \begin{bmatrix} 1 & -1.75 \\ -1.75 & 7 \end{bmatrix} \underline{x} \le 8\}$$

This is, however, a very unusual case and there is no evidence that it could actually happen in practice.

5.1.4 Choice of the Inverse Transformation

In Section 4.2, it was demonstrated that in transforming a dependent variable into the $\underline{z}$ space via a TSE formula, a first order approximation to $\underline{x} = \underline{Z}^{-1}(\underline{z})$ is needed. From Figure 5.2, it is clear that not all the possible inverse transformations are suitable for this purpose. To have a non-empty S_z, the choice has to be restricted to those inverse transformations which correspond to the disjoint parts of S_x (here $\underline{Z}_1^{-1}(\underline{z})$ and $\underline{Z}_4^{-1}(\underline{z})$). Now the key question is how one should know à priori which inverse transformation(s) fall(s) in this category.

Apparently, there is no simple answer to this question. Traditionally, it is assumed that whenever S_x is non-empty, it has a disjoint part corresponding to the realistic voltage solutions. There seems to be no rigorous proof to support this assumption, but it can be loosely related to the conventional choice of the reference angle (i.e., $\theta_r = 0$; $f_r = 0$; $v_r^m \leqslant e_r \leqslant v_r^M$) .

By accepting this assumption, the inverse transformation corresponding to the realistic voltage solutions is always among the "right" ones. Note that by choosing $\underline{x}_0$ to be a realistic voltage solution, then

$$\underline{x} = \underline{Z}^{-1} (\underline{z}) \approx \frac{1}{2} \underline{x}_0 + \frac{1}{2} [L (\underline{x}_0)]^{-1} \underline{z}$$

is an approximation to the inverse transformation corresponding to that particular type of voltage solutions. Other inverse transformations can be approximated by using their proper $\underline{x}_0$.

5.1.5 <u>Influence of the Reference and Slack Buses on Security Sets</u>

To study the impact of the location of the reference bus or the choice of the slack bus on various aspects of security sets, one has to look for more general operating spaces.

Let us denote all the dependent and independent variables by the vector $\underline{\eta}$. The system's physical and operating constraints then can be expressed, in general, by,

$$\eta_i - \underline{x}_r^T [\eta_i] \underline{x}_r = 0 \qquad (5.10)$$

$$i = 1, \ldots, N_{dp} + N_z$$

$$\eta_i^m \leq \eta_i \leq \eta_i^M \qquad (5.11)$$

By substituting for η_i in (5.11), using (5.10), one obtains a security set, denoted by S_r, in the $\underline{x}_r$ space. That is

$$S_r \triangleq \{\underline{x}_r / \eta_i^m \leq \underline{x}_r^T [\eta_i] \underline{x}_r \leq \eta_i^M, i = 1, \ldots, N_{dp} + N_z\} \qquad (5.12)$$

This set is obviously invariant with the location of the reference bus. The intersection of S_r with the hyper-plane

$$\underline{\alpha}_r^T \underline{x}_r = 0$$

defines the set S_x, where the entries of $\underline{\alpha}_r$ are all zero, except its rth and $(r + N_b)$-th entries which are $-\tan \theta_r$ and $+1$, respectively (equation (2.20)). For different values of θ_r and different locations of the reference bus, different $\underline{\alpha}_r$ and, consequently, different S_x result. However, for a fixed location of the reference bus, variation of θ_r does not change the size or the shape of S_x, but affects only its location in the $\underline{x}$ space. Therefore, the set S_x, while it fails to be invariant with the location of the reference bus, can be regarded as invariant under θ_r variations.

To define an invariant set corresponding to S_z , one has to work in the $\underline{\eta}$ space. The set of points $(\underline{\eta}\ ,\ \underline{x})$ satisfying equation (5.10) define a non-linear manifold in the $(\underline{\eta}\ ,\ \underline{x})$ space. The projection of this manifold into the $\underline{\eta}$-space when intersected with the hyper-box defined in (5.11), defines a set, S_η , which is invariant under the choice of the slack bus. As shown in Figure 5.3, S_z is then the projection of S_η into some N_z dimensional sub-space of the $\underline{\eta}$-space, specified by the choice of the independent variables.

By choosing different slack buses, one is in fact specifying different sets of independent variables, or is equivalently choosing different sub-spaces of $\underline{\eta}$. The projection of S_η is not, in general, the same in these different sub-spaces and different S_z could result.

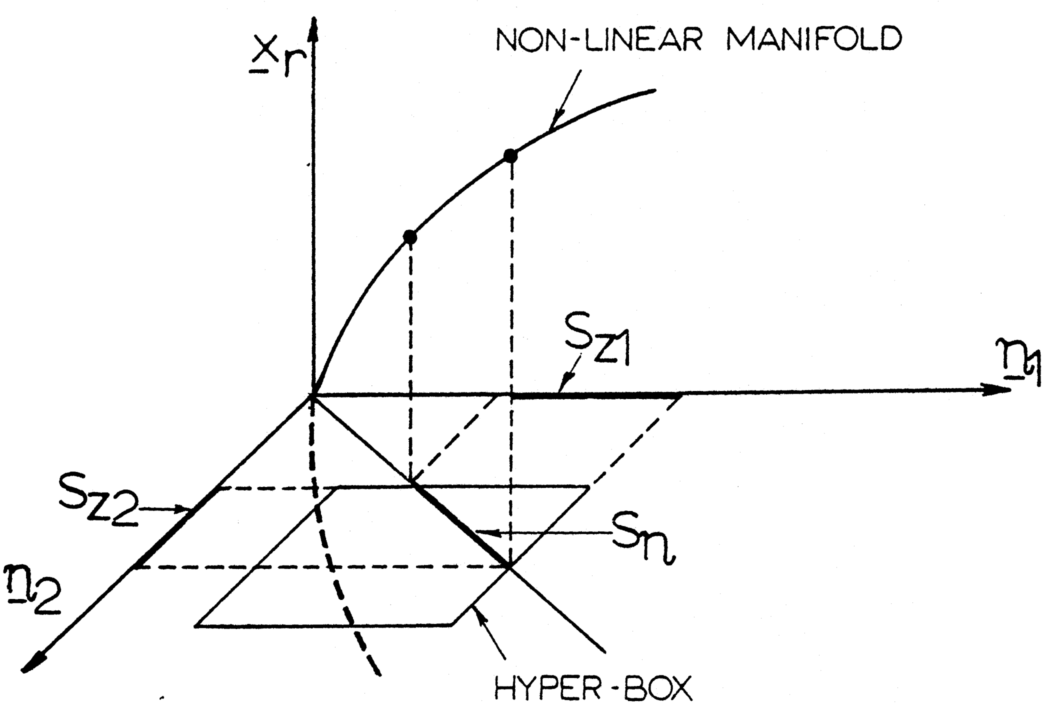

Figure 5.3. An illustration of the relationship between S_η and S_z .

An important conclusion here is that, a security margin computed based on the distance of the operating point to the boundary of a set, as suggested in [62], is meaningful only when the set is an invariant security set. For S_x or S_z, such a security margin will have different values depending on the location of the reference bus or choice of the slack bus.

5.2 Construction of S_z and S_z^I

Henceforth, the following assumptions are made:

(i) The set S_x, if non-void, contains realistic voltage solutions.

(ii) The set S_z is a connected one.

5.2.1 Implicit Description of S_z

Based on the above discussions and the use of (5.1), S_z can be described approximately by representing each constraint defining Y_z by a single TSE formula. When a first order TSE formulae is used for this purpose, a linear set, denoted by $\hat{S}_z$, results. That is,

$$\hat{S}_z = H_z \cap \{\underline{z} \;/\; y_i^m \leq \underline{\beta}_i^T (\underline{x}_0)\, \underline{z} \leq y_i^M \;;\; i=1, \ldots , N_{dp}\} \tag{5.10}$$

The set $\hat{S}_z$ is a convex polyhedron which tries to approximate the non-linear set S_z. The above description of $\hat{S}_z$ is an "implicit" one, because a good many of the constraints defining it are redundant, i.e., their deletion does not alter $\hat{S}_z$. The minimal representation [52] of $\hat{S}_z$, then will be its "explicit" description.

For the example of Section 3.4, three cross-sections of $\hat{S}_z$ are given in Figure 5.4. Comparing these cross-sections with those of Figure 3.6 indicate that $\hat{S}_z$ is approximating S_z with reasonable accuracy.

A second order approximation to the constraints defining Y_z produces a closer approximation to S_z. Denoting the resulting set by $\tilde{S}_z$, it can be expressed by

$$\tilde{S}_z = H_z \cap \{\underline{z} \;/\; y_i^m \leq \underline{\beta}_i^T \underline{z} + \underline{z}^T [C\, (\underline{\beta}_i)]\, \underline{z} \leq y_i^M \;;i=1, \ldots , N_{dp}\} \tag{5.11}$$

A comparison of the cross-sections of $\tilde{S}_z$, given in Figure 5.5, with those of S_z, for the same example, confirms that $\tilde{S}_z$ is indeed representing S_z fairly accurately. Note that since the TSE formulae are accurate only locally, the accuracy of $\hat{S}_z$ and $\tilde{S}_z$ will be enhanced when $\underline{x}_0$ is chosen from S_x (i.e., $\underline{x}_0 \in S_x$).

Figure 5.4. Cross-sections of $\hat{S}_z$, corresponding to Figure 3.6, for: (a) $v_1 = 1.0$; (b) $v_1 = 1.05$; (c) $v_1 = 1.10$. (Expansion point : $\underline{z}_0^T = [1.1025, -0.2, -0.2]$).

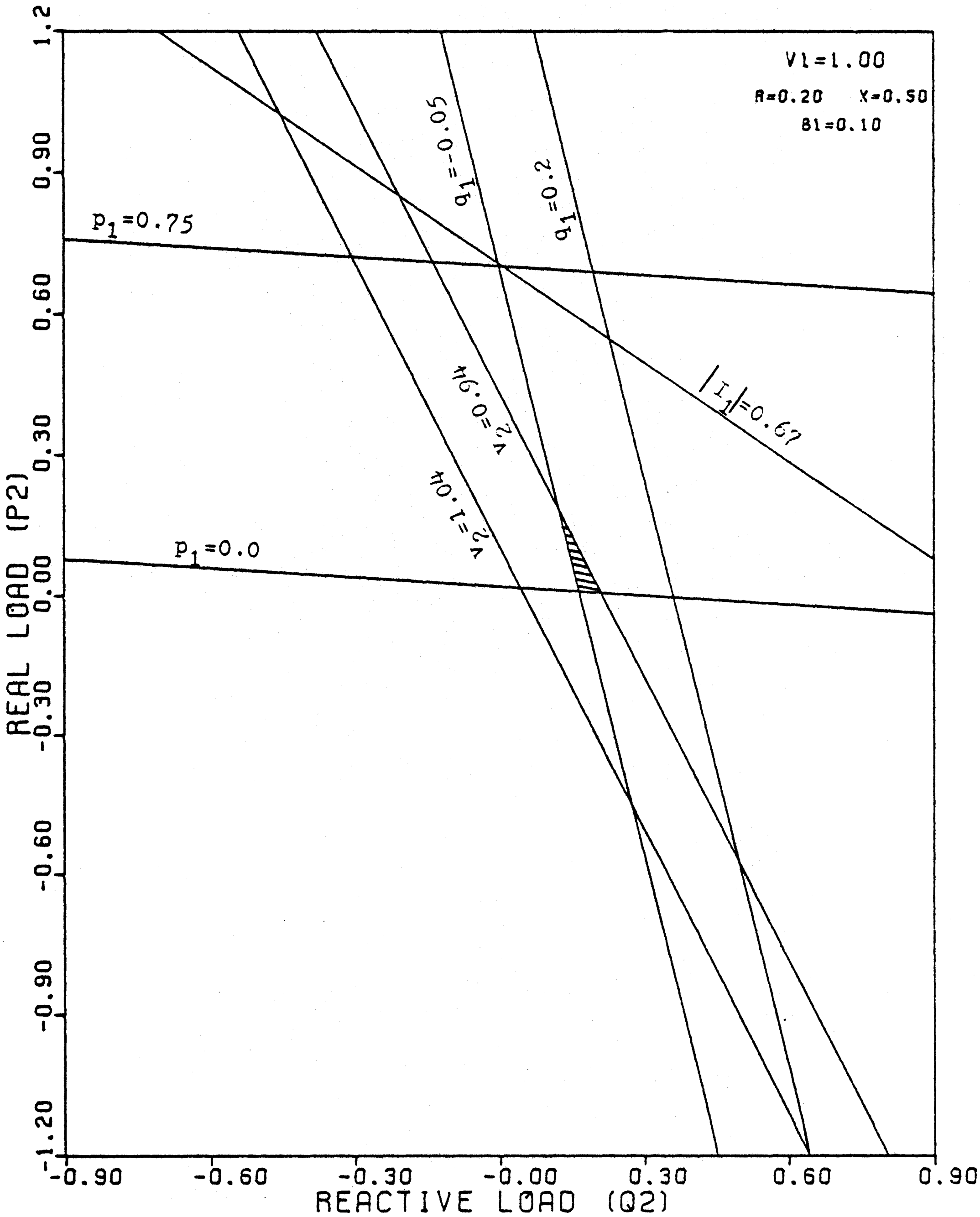

(a)

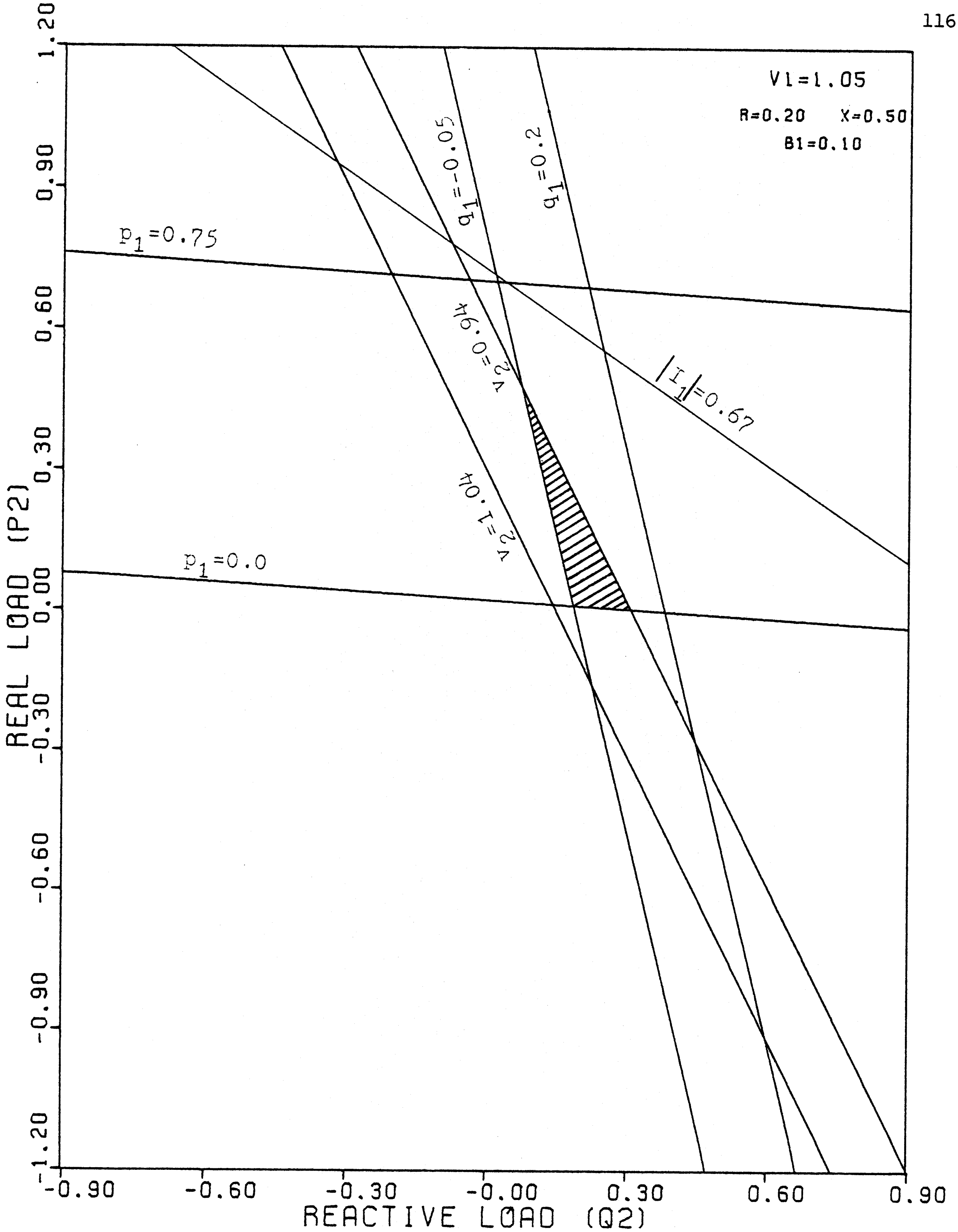
V1=1.05
R=0.20 X=0.50
B1=0.10
q_1=-0.05
q_1=0.2
p_1=0.75
p_1=0.0
v_2=0.94
v_2=1.04
$|I_1|$=0.67
REAL LOAD (P2)
REACTIVE LOAD (Q2)
1.20
0.90
0.60
0.30
0.00
-0.30
-0.60
-0.90
-1.20
-0.90
-0.60
-0.30
-0.00
0.30
0.60
0.90

(b)

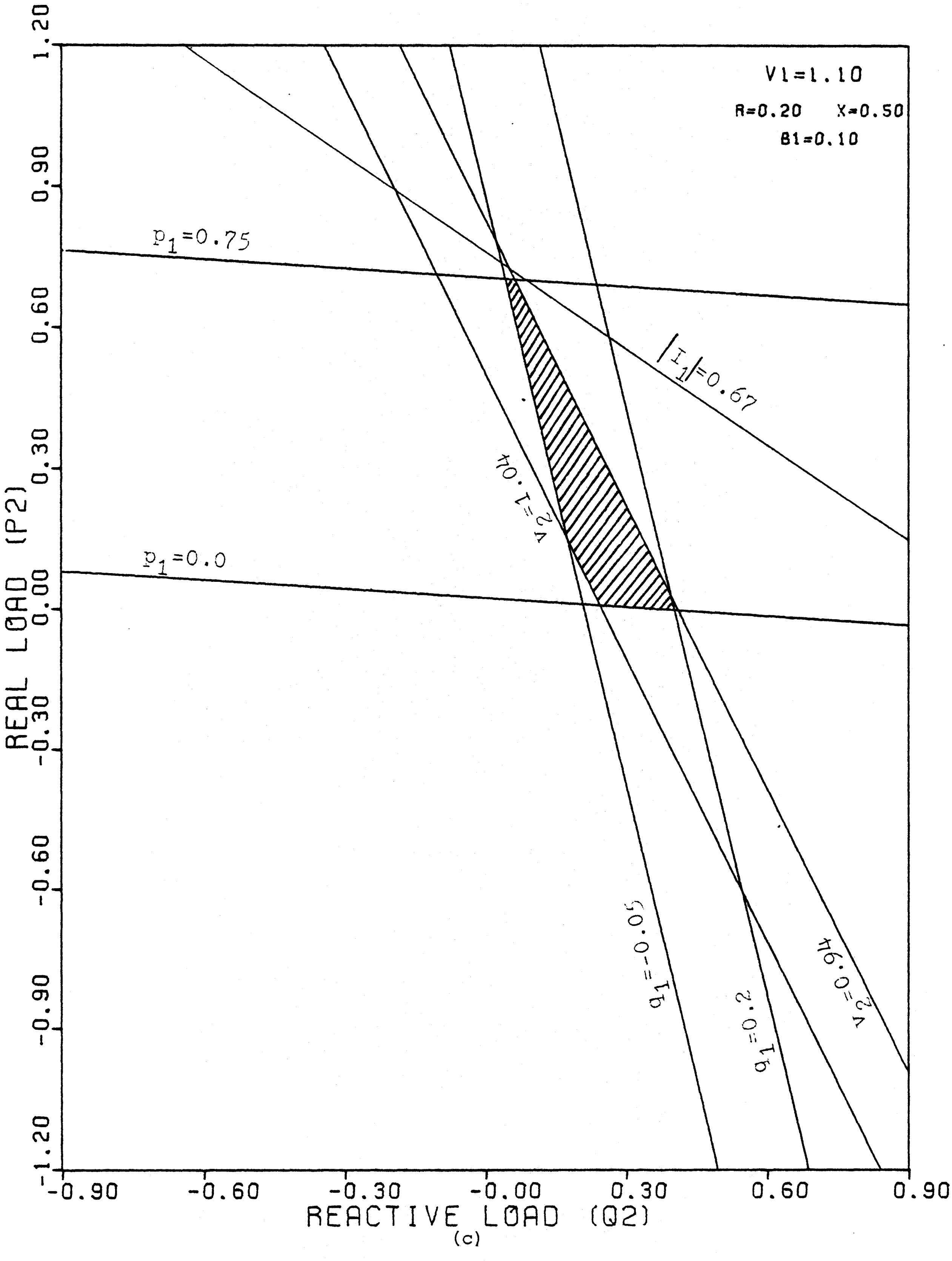
V1=1.10
R=0.20 X=0.50
B1=0.10
p_1=0.75
p_1=0.0
$|I_1|$=0.67
v_2=1.04
q_1=-0.05
q_1=0.2
v_2=0.94
REAL LOAD (P2)
REACTIVE LOAD (Q2)
1.20
0.90
0.60
0.30
0.00
-0.30
-0.60
-0.90
-1.20
-0.90
-0.60
-0.30
-0.00
0.30
0.60
0.90

(c)

Figure 5.5. Cross-sections of $\tilde{S}_z$, corresponding to Figure 3.6, for: (a) $v_1 = 1.0$; (b) $v_1 = 1.05$; (c) $v_1 = 1.1$. (Expansion point : $\underline{z}_0^T = [1.1025, -0.2, -0.2]$) .

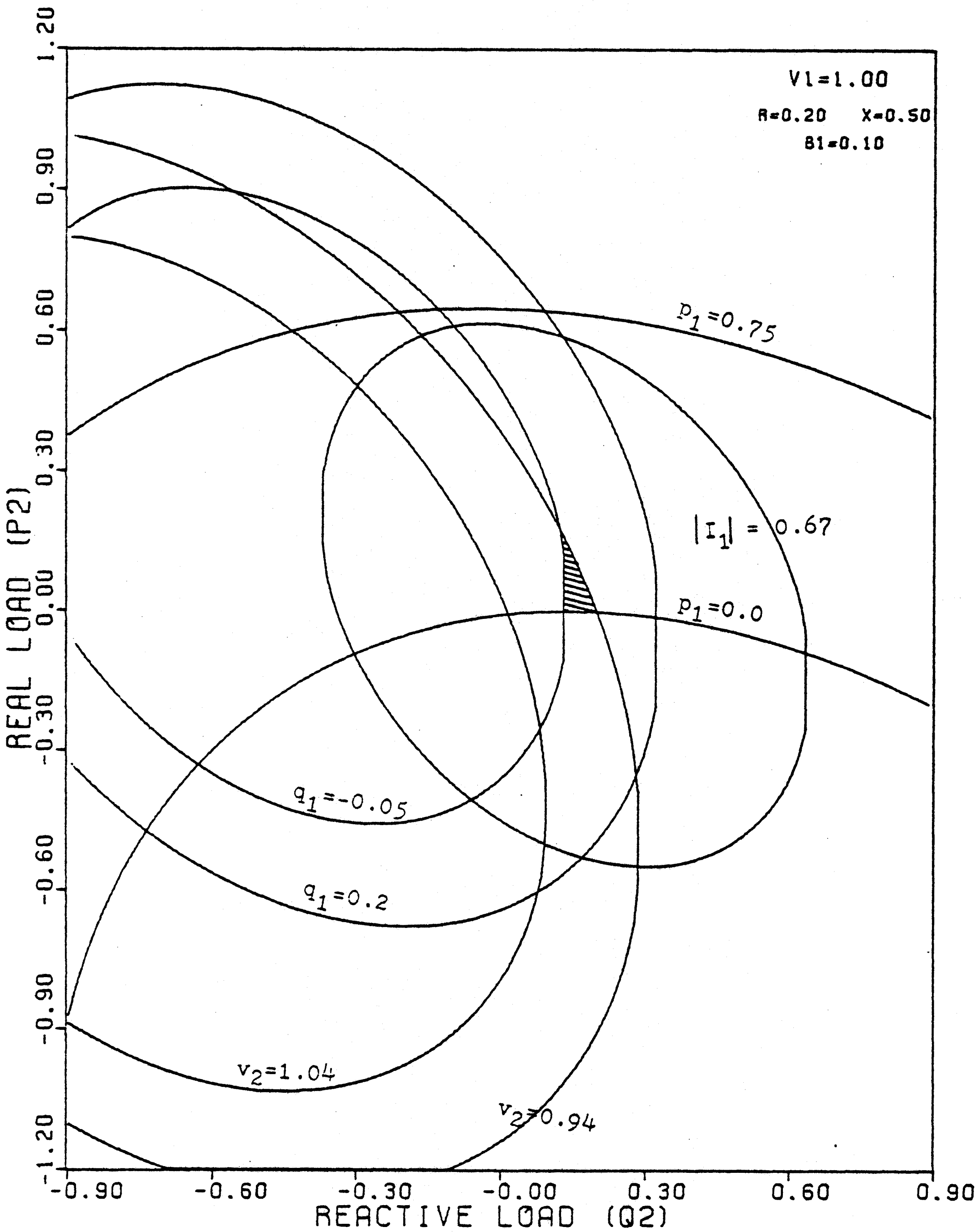

(a)

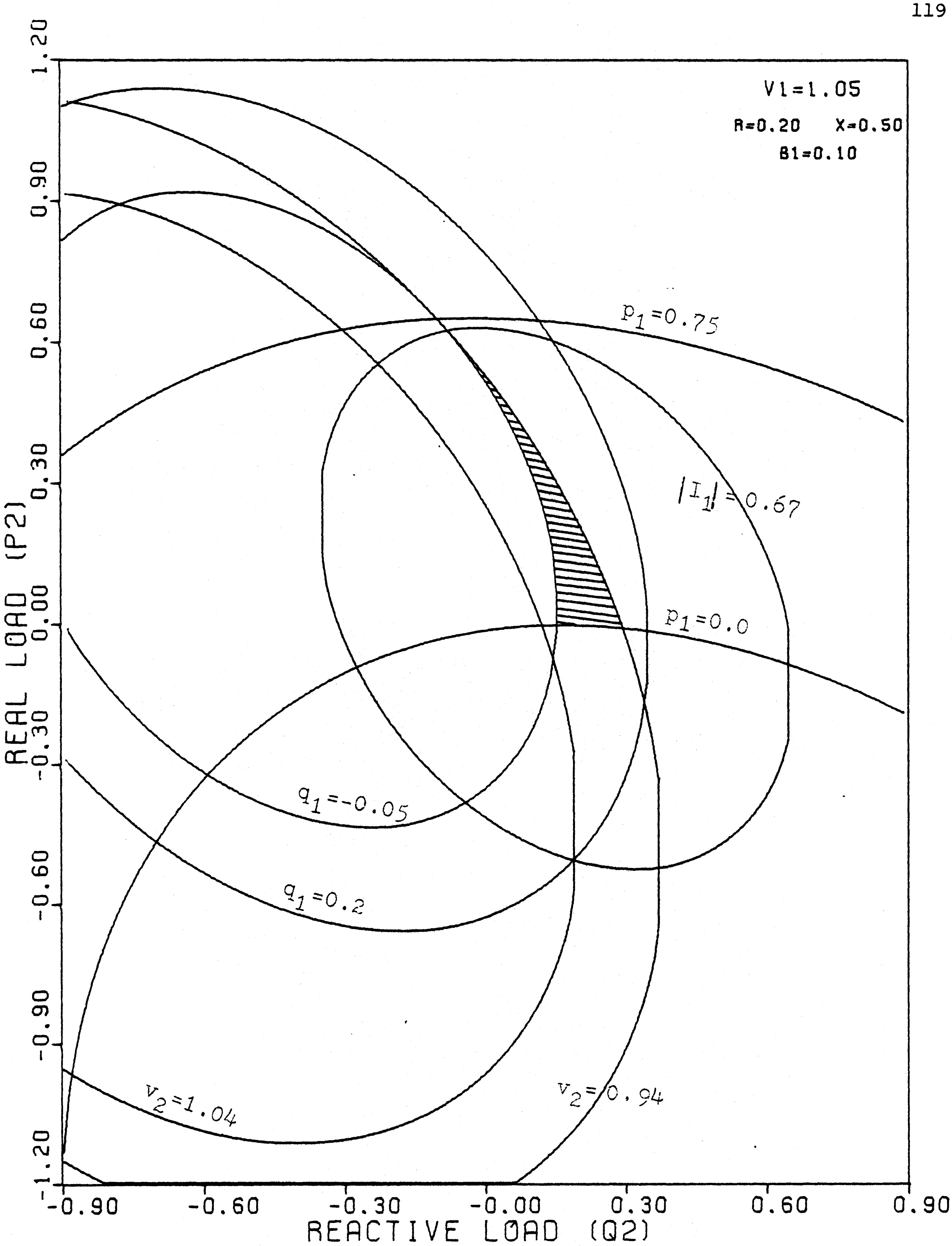
V1=1.05
R=0.20 X=0.50
B1=0.10
$p_1=0.75$
$|I_1|=0.67$
$p_1=0.0$
$q_1=-0.05$
$q_1=0.2$
$v_2=1.04$
$v_2=0.94$
REAL LOAD (P2)
REACTIVE LOAD (Q2)
1.20
0.90
0.60
0.30
0.00
-0.30
-0.60
-0.90
-1.20
-0.90
-0.60
-0.30
-0.00
0.30
0.60
0.90

(b)

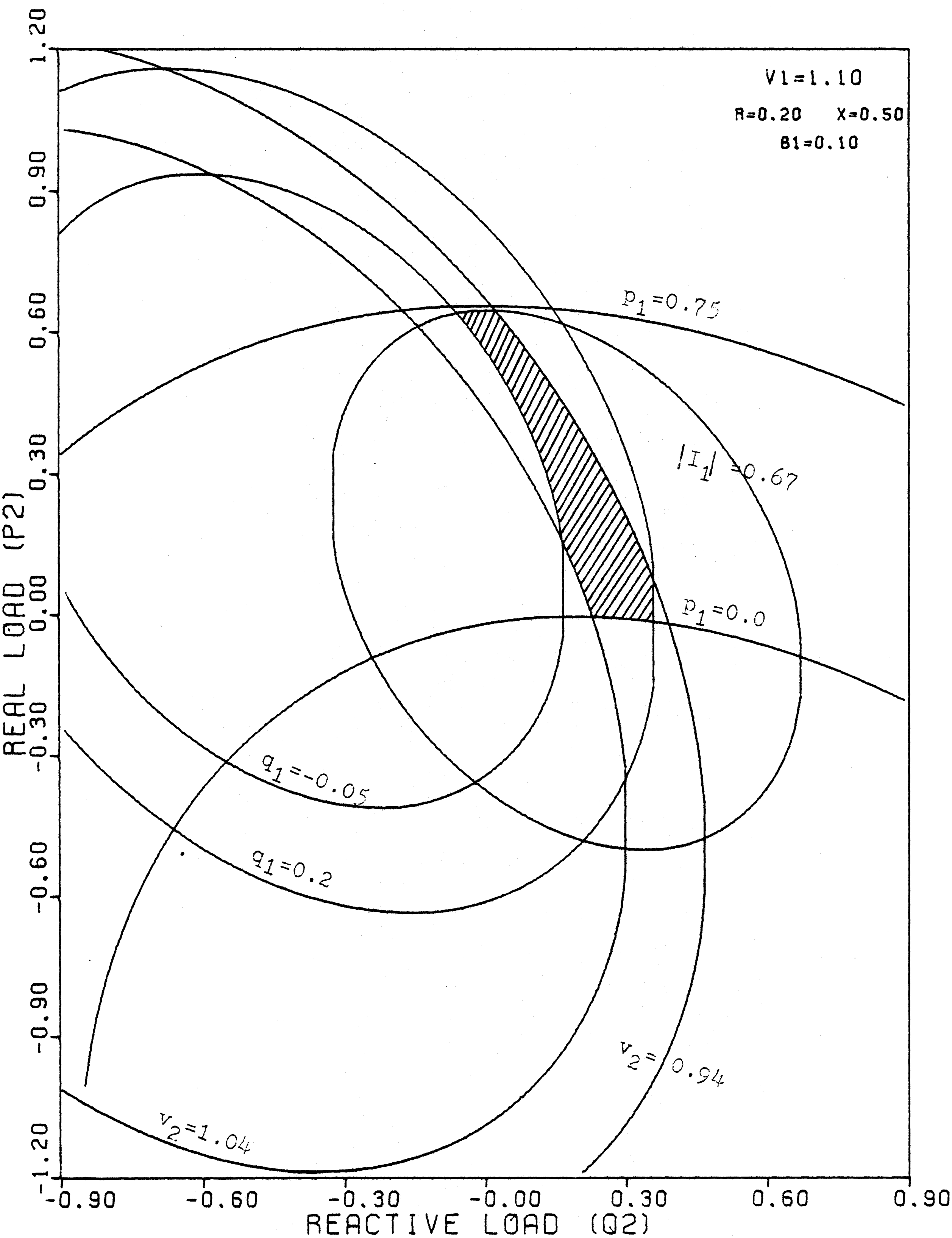
V1=1.10
R=0.20 X=0.50
B1=0.10
p_1=0.75
$|I_1|$ =0.67
p_1=0.0
q_1=-0.05
q_1=0.2
v_2= 0.94
v_2=1.04
REAL LOAD (P2)
REACTIVE LOAD (Q2)
1.20
0.90
0.60
0.30
0.00
-0.30
-0.60
-0.90
-1.20
-0.90
-0.60
-0.30
-0.00
0.30
0.60
0.90

(c)

Now by comparing the surface $P_1^g = 0.75$ in Figure 5.5 with its exact counter-part in Figure 3.6, it becomes clear that the exact map is the result of two inverse transformations $\underline{Z}_1^{-1}(\underline{z})$ and $\underline{Z}_2^{-1}(\underline{z})$ (solutions to equation (3.21)). The upper-half of the surface is produced by the inverse transformation corresponding to the realistic voltage solutions, $\underline{Z}_1^{-1}(\underline{z})$, while the lower-half is produced by $\underline{Z}_2^{-1}(\underline{z})$. The two emerge into one on the boundary of R_z.

The expansion point used here to derive various TSE formulae is a realistic voltage solution. Hence, in Figure 5.5, only the upper-half of the surface $P_1^g = 0.75$ is approximated. Had we used an expansion point corresponding to $\underline{Z}_2^{-1}(\underline{z})$, the resulting TSE formulae would have, instead, approximated the lower-half of that surface.

An important point here is that, unlike the surfaces in Figure 3.6, parts of the surfaces defining $\hat{S}_z$ or $\tilde{S}_z$ lie outside R_z. This is due to the fact that an approximate relation for $\underline{x} = \underline{Z}^{-1}(\underline{z})$, and consequently the TSE formulae based on that, do not contain the inherent restrictions which limit the range of their exact counterparts to R_z. In the next chapter, we discuss cases where this aspect of the approximation formulae could cause certain difficulties.

5.2.2 Implicit Description of S_z^I

In Section 3.1.2 we introduced the functions $\Delta \underline{\S}^j \triangleq \underline{\rho}^j(\underline{\S})$, $j=1, \ldots, N_{cg}$ to represent the changes in the system condition after the occurrence of any one of the listed contingencies. On the assumption that these functions are available, we were able to formulate $S_{\S}^I$ in the $\underline{\S}$ space.

To characterize $S_z^I = \bigcap_{j=0}^{N_{cg}} S_z^j$, as a first step, one needs to have similar functions to systematically derive conditions under which a pre-contingency injection remains secure to the listed contingencies.

Since the network parameters cannot be manipulated directly in the $\underline{z}$ space, the contingencies involving changes in $\underline{w}$ have to be treated separately.

(i) Generator or Load Outages

We emphasize again that here only those contingencies are considered which do not change the topological structure of the power network. This implies that we are considering only the type of generator (or load) outages that lead to partial shut-down of a generating plant (or load point). This is to avoid conversion of a PV bus to PQ due to the outage.

Let the kth outage be represented in general by a sudden change of every z_i by $\varepsilon_i^k z_i$ (ε_i^k, i=1, ... , N_z are mostly zero). As a result of the outage, the operating state changes from $\underline{z}^{pre}$ to $\underline{z}^{post} = \underline{z}^{pre} + \Delta \underline{z}^k$. We would like to obtain an explicit expression for $\Delta \underline{z}^k$ in terms of $\underline{z}^{pre}$.

Shortly after the outage the inertial response of the generators causes a shift in the system frequency. This frequency shift activates the automatic controls local to each substation, causing the internal reserve of the system to pick up the loss of generation (or sudden load increase). Next the generators are rescheduled by central control, allocating the existing demand between the generators based on an economic dispatch.

In Appendix B, it is shown that a first order approximation to the function describing $\Delta \underline{z}^k$ is possible, and it has the general form

$$\Delta \underline{z}^k = [N(\underline{\varepsilon}^k)]\, \underline{z} \tag{5.12}$$

For the time frames considered above, the matrix $[N(\underline{\varepsilon}^k)]$ has different forms and leads to different vulnerability sets.

Using (5.12), the post-contingency injections for the kth contingency are related to the pre-contingency ones through:

$$\underline{z}^{post} = \underline{z}^{pre} + \Delta\,\underline{z}^{k} = [IN\ (\underline{\varepsilon}^{k})]\ \underline{z}^{pre} \tag{5.13}$$

where

$$[IN\ (\underline{\varepsilon}^{k})] \triangleq \{[I] + [N\ (\underline{\varepsilon}^{k})]\} \tag{5.14}$$

The set of those pre-contingency injections which are secure to the kth contingency is then obtained easily by replacing $\underline{z}$ by $[IN\ (\underline{\varepsilon}^{k})]\ \underline{z}$ in all the constraints defining S_z. In particular, for the first order approximation:

$$\hat{S}_z^k \triangleq \hat{S}_z\ (\underline{z} \Rightarrow [IN\ (\underline{\varepsilon}^{k})]\ \underline{z}) \qquad k=1 \ldots N_{cg} - N_w \tag{5.15}$$

or for the second order,

$$\tilde{S}_z^k \triangleq \tilde{S}_z\ (\underline{z} \Rightarrow [IN\ (\underline{\varepsilon}^{k})]\ \underline{z}) \qquad k=1 \ldots N_{cg} - N_w \tag{5.16}$$

(ii) Line or Transformer Outage

A line or transformer outage alters the network admittance matrix, $[Y_b]$. As a result, all $\underline{\beta}_i\ (\underline{x}_0)$ and $[C\ (\underline{\beta}_i)]$ computed for the intact network change. Since $[L\ (\underline{x}_0)]^{-1}$ enters into the definition of $\underline{\beta}_i\ (\underline{x}_0)$ and $[C\ (\underline{\beta}_i)]$, $i=1, \ldots, N_{dp}$, there is no simple way to modify them to account for the changes in $[Y_b]$. To form the set of pre-contingency injections which are secure to the jth contingency (involving line or transformer outages), one has to calculate $\underline{\beta}_i^j\ (\underline{x}_0)$ and $[C^j\ (\underline{\beta}_i)]$, $i=1, \ldots, N_{dp}$ directly, i.e., as in the case of the intact network. The superscript "j" indicates the jth contingency.

5.2.3 Numerical Considerations

From (4.14), $\underline{\beta}_i^j\ (\underline{x}_0)$, i=1, ... , N_{dp} are the solutions to

$$[L^j\ (\underline{x}_0)]^T\ \underline{\beta}_i^j\ (\underline{x}_0) = [Y_i^j]\ \underline{x}_0 \quad i=1,\ \ldots\ ,\ N_{dp} \tag{5.17}$$

where $[L^j\ (\underline{x}_0)]$ and $[Y_i^j]$ are the counterparts of $[L\ (\underline{x}_0]$ and $[Y_i]$, for the outaged network. The above equations can be solved by one of the following schemes:

(a) Inverting $[L^j\ (\underline{x}_0)]$;

(b) Decomposing $[L^j\ (\underline{x}_0)]$ into a triangular form ;

(c) Using only $[L\ (\underline{x}_0)]$.

For a large power system, inverting $[L^j\ (\underline{x}_0)]$ is very expensive and time consuming. Decomposing $[L^j\ (\underline{x}_0)]$ is often a more realistic approach. In cases where $[L\ (\underline{x}_0)]$ is already in a decomposed form and storage limitations do not permit compiling a new Jacobian, it is possible to formulate (5.17) in terms of $[L\ (\underline{x}_0)]$. Defining:

$$[\Delta L^j(\underline{x}_0)] \triangleq [L^j(\underline{x}_0)] - [L(\underline{x}_0)] \tag{5.18a}$$

$$[\Delta Y_i^j] \triangleq [Y_i^j] - [Y_i] \tag{5.18b}$$

$$\Delta \underline{\beta}_i^j \triangleq \underline{\beta}_i^j(\underline{x}_0) - \underline{\beta}_i(\underline{x}_0) \tag{5.18c}$$

$$\underline{b}_i^j \triangleq [\Delta Y_i^j]\,\underline{x}_0 - [\Delta L^j(\underline{x}_0)]^T \underline{\beta}_i(\underline{x}_0) \tag{5.18d}$$

and recalling that $\underline{\beta}_i(\underline{x}_0)$ is the solution to

$$[L(\underline{x}_0)]^T \underline{\beta}_i(\underline{x}_0) = [Y_i]\,\underline{x}_0$$

after some manipulation, one can rewrite equation (5.17) in the form:

$$[L(\underline{x}_0)]^T \Delta \underline{\beta}_i^j = \underline{b}_i^j - [\Delta L^j(\underline{x}_0)]\,\Delta \underline{\beta}_i^j \tag{5.19}$$

The above equations can be solved iteratively for $\Delta \underline{\beta}_i^j$. Normally after two to three iterations sufficient convergence is achieved. As shown in ref. [14], for a single line outage, the matrix $[\Delta L^j(\underline{x}_0]$ can have at most 16 non-zero elements, thus no significant memory is normally needed to store $[\Delta L^j(\underline{x}_0)]$.

Computing the Jacobian inverse seems to be the most efficient way of calculating $[C(\underline{\beta}_i)]$ $i=1, \ldots, N_{dp}$, for the intact or the outaged network. In this case the matrix inversion lemma (c.f. [73]) can be employed to compute $[L^j(\underline{x}_0)]^{-1}$ using $[L(\underline{x}_0)]^{-1}$.

5.3 Secure-Economic Dispatch

The economical allocation of the total real power demand among the generating units without violating any one of the operating limits is called the "secure-economic dispatch" [43, 44, 74, 75]. The approximation formulae have historically played a significant part in the analysis of this problem [76, 77, 78, 79]. In this section, we highlight the potential gains in using the TSE formula over other approximate relations presently in use.

5.3.1 Problem Formulation

Using the notation of Section 5.1.5, the secure-economic dispatch problem can be formulated as a constrained optimization problem of the general form

Minimize: $f(\underline{\eta})$

subject to

$$\eta_i - \underline{x}_r^T [\eta_i] \underline{x}_r = 0 \qquad i = 1, \ldots, N_{dp} + N_z \tag{5.20}$$

$$\eta^m \leqslant \eta_i \leqslant \eta_i^M$$

where $f(\underline{\eta})$ describes the way the total generation cost varies with $\underline{\eta}$. Those η_i which correspond to the load variables are fixed, i.e.,

$\eta_j^m = \eta_j^M = d_j^0$, $j = 1, \ldots, N_d$, where $\underline{d}^0$ is a given demand vector. The dimension of the above problem is excessively large and its solution is in general quite time consuming. Since one is searching for an optimum control strategy, the dimension of the problem would be reduced drastically, if $f(\underline{\eta})$ can be expressed in terms of $\underline{u}$. The problem then becomes:

$$\text{Minimize:} \quad f(\underline{\eta}) = g(\underline{u})$$

$$\underline{u} \in S_z \, (\underline{d} = \underline{d}^0) \tag{5.21}$$

As shown in Figure 5.6, the set $S_z \, (\underline{d} = \underline{d}^0)$ is the projection of the cross-section of S_z , corresponding to $\underline{d} = \underline{d}^0$, into the $\underline{u}$ space. The cost function, is often expressed by

$$f(\underline{\eta}) = \sum_{i=1}^{N_g} f_i \, (p_i^g) \tag{5.22}$$

where $f_i \, (p_i^g)$ represents the generation cost of the ith generator. The total number of generation units is N_g which includes the slack bus (p_1^g) . For simplicity, we assume that there is only one generator per bus, thus allowing the generation vector, $\underline{p}^g$, to be expressed by

$$\underline{p}^g = \begin{bmatrix} p_1^g \\ \underline{p}^v \end{bmatrix} \tag{5.23}$$

Unlike p_i^g , i=2, ... , N_g, the dependent variable p_1^g is not part of the control vector, $\underline{u}$, and its relation with $\underline{u}$ is not known.

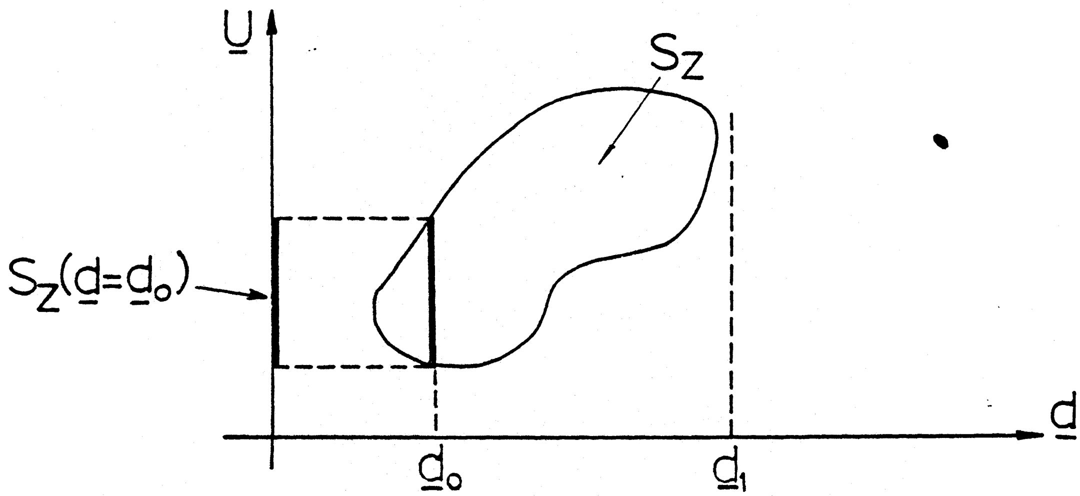

Figure 5.6. An illustration of the relation between S_z and S_z $(\underline{d} = \underline{d}_0)$.

5.3.2 The Loss Formula

To simplify the problem, the set S_z $(\underline{d} = \underline{d}^0)$ is often approximated by the hyper-box $(P_i^g)^m \le P_i^g \le (P_i^g)^M$, i= 1, ... , N_g . The resulting problem is called the generation constrained economic dispatch. Here, p_1^g is the only variable which has to be expressed in terms of $\underline{u}$.

Traditionally, variations of p_1^g with $\underline{u}$ is approximated indirectly. First p_ℓ , the total I^2R loss in the system, is approximated by a quadratic function of the form

$$p_\ell = \underline{B}_0^T \, \underline{p}^v + \underline{p}^{vT} \, [B] \, \underline{p}^v \qquad (5.24)$$

Then, by substituting p_ℓ from above into the real power balance equation, that is

$$\sum_{i=1}^{N_g} p_i^g = p_\ell - p_d \qquad (5.25)$$

an expression for p_1^g is found (p_d is the total real power demand) .

The expression in (5.24) is often referred to as the "loss formula" [76, 80, 81, 82] , and the constants $\underline{B}_0$ and [B] as the "B- coefficients". Because of the basic role of the loss formula in economic dispatch, during the last three decades, it has been the subject of extensive research [76, 81, 83, 84] . As a result, a large volume of literature, discussing various techniques of computing the B-coefficients, is available. Many of these techniques involve complicated transformations based on restrictive assumptions [3 , 76, 85] or premises incompatible with the mathematical model of the system [110] . The use of the TSE formulae [70] in deriving a loss formula, seems to have been overlooked by other authors.

Using the expressions for the net real power injections in (5.25), it readily follows that

$$p_{\ell} = \underline{x}_r^T \; [P_{\ell}] \; \underline{x}_r \tag{5.26}$$

where

$$[P_{\ell}] = \left[\begin{array}{c|c} [G] & 0 \\ \hline 0 & [G] \end{array}\right] \tag{5.27}$$

A quadratic expansion for p_{ℓ} in terms of $\underline{z}$, that is

$$\tilde{p}_{\ell} = \underline{\beta}_{\ell}^T \underline{z} + \underline{z}^T [C\;(\underline{\beta}_{\ell})] \; \underline{z} \tag{5.28}$$

produces a loss formula which has the same form as (5.24). The advantage of this formula, over those presently in use, is that:

(a) It is quite general and includes the effect of all injection variables on the losses;

(b) its derivation is very systematic and involves only the usual load flow assumptions;

(c) under unbiased conditions, it offers a much higher accuracy.

A simple comparison of the derivation of various loss formulae with that suggested in (5.28) confirms the validity of the first two statements. The last statement is verified by a simulation-based accuracy test.

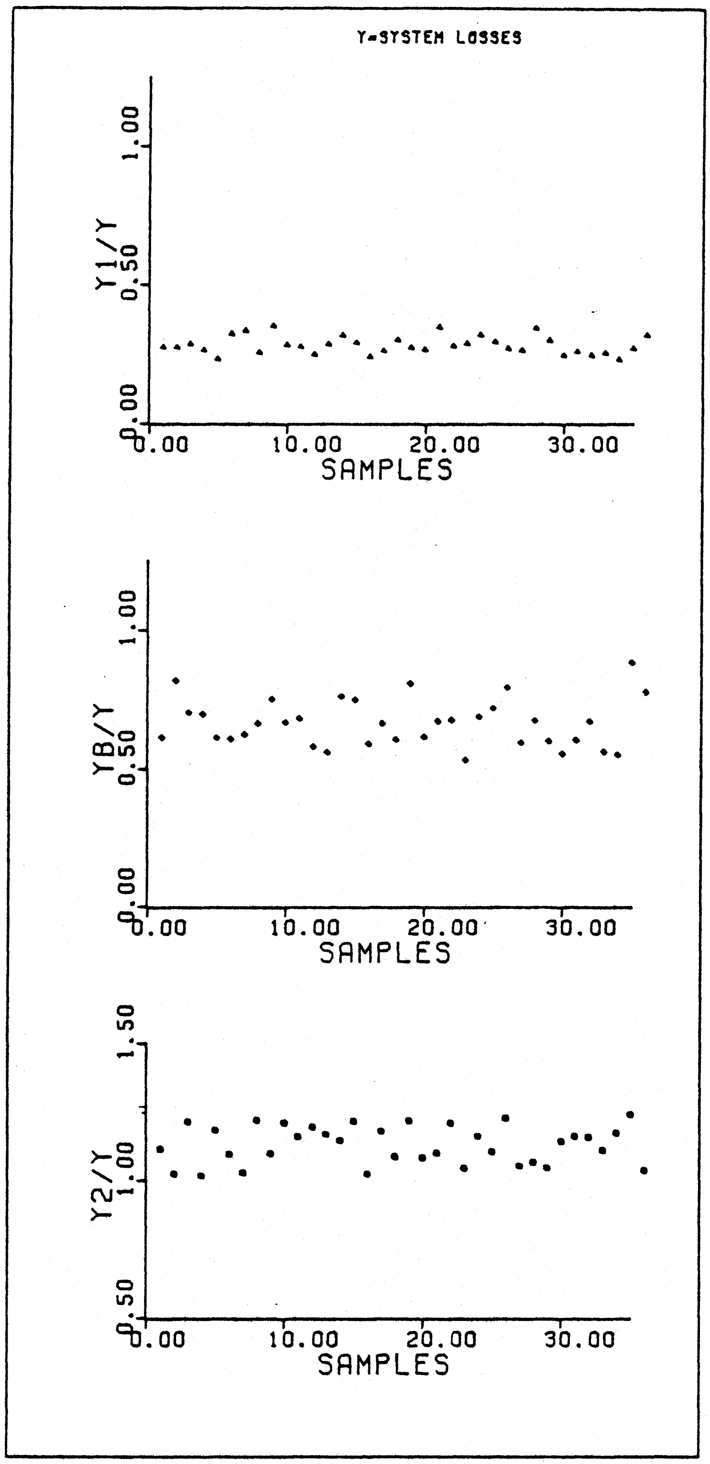

Figure 5.7. Comparison of the simulation results for the loss formula of ref. [109] and those derived based on the TSE formula.

In Figure 5.7, the relative accuracy of the expansion formulae in calculating the total I^2R loss is compared with a B-coefficient loss-formula. The expansion formulae are derived for the eleven bus system of reference [109], where the corresponding B-coefficients are supplied. We have subjected the three loss-formulae to an error analysis similar to that explained in Section 4.5.2. The expansion point of the TSE formulae corresponds to one of the base points upon which the B-coefficients are calculated. As the results show, the quadratic TSE loss-formula estimates the system losses consistently more accurately than the B-coefficient loss-formula. The average of the errors for the linear expansion was 65% . The average for B-coefficients loss-formula was 30% while that for the second order Taylor was 7% .

Unlike $[P_\ell]$, the matrix $[P_1^g]$ $(P_1^g = \underline{x}^T [P_1^g] \underline{x})$ is highly sparse. This makes direct expansion of p_1^g in terms of $\underline{z}$ computationally more efficient than calculating $\tilde{p}_\ell$ and using (5.25). It can be proved, however, that when the loss formula is given by (5.28), both schemes produce the same expression for p_1^g .

Consider a quadratic expansion of p_1^g . By partitioning it, one can express $\tilde{P}_1^g$ in terms of $\underline{u}$, namely

$$P_1^g \simeq \underline{\beta}_{01} + \underline{\beta}_{u1}^T \underline{u} + \underline{u}^T [C_{u1}] \underline{u} \tag{5.29}$$

The generation constrained problem is then

$$\text{Minimize:} \quad f(\underline{u}, P_1^g) = \sum_{i=1}^{N_g} f_i(P_i^g) \tag{5.30}$$

subject to

$$(\underline{P}^g)^m \leq \underline{P}^g \leq (\underline{P}^g)^M$$

and (5.29). Rather than being used to express $f_1(P_1^g)$ and $(P_1^g)^m \leq P_1^g \leq (P_1^g)^M$ in terms of $\underline{u}$, expression (5.29) is normally treated as an equality constraint. The dependent variable P_1^g then plays the role of a decision variable. The resulting simplicity can be readily appreciated.

5.3.3 The General Secure-Economic Dispatch Problem

As mentioned in Chapter I, based on replacing each cost function by a number of piece-wise linear segments and the use of LP techniques, Stott [48] has proposed a very efficient approach for solving (5.21). Central to his approach is the assumption that power systems, in general, even under stress, can be operated with only a few dependent variables at their limits. As a result, only few constraints in Y_z need to be considered. He formulates the problem in terms of $\underline{p}^v$; consequently, the constraints defining Y_z are limited to real line flows.

By adopting Stott's approach, but using the TSE formulae to express dependent variables, a comprehensive formulation of the problem results. The significant improvements will be:

(i) All the operating constraints can be considered;

(ii) the control vector here includes the voltage levels, allowing to:

(a) Add the system losses ($\hat{p}_\ell = \underline{\beta}_\ell^T \underline{z}$) to the objective function to minimize the total loss;

(b) alleviate violations of bounds on dependent variables which are relatively insensitive to real power variations;

(iii) since at each LP iteration, all components of $\underline{u}$ (and thus $\underline{z}$) are shifted optimally, the scheme can potentially converge to the exact solution (i.e., by up-dating $\underline{\beta}_i(\underline{x}_0)$ for the dependent variables involved).

Since the scheme uses a reduced "basis" (tableau) [86] method, the inclusion of the voltage levels as control variables does not have any significant effect on the amount of computation required. Note that, instead of running a DC load flow to check the constraints after each generation reschedual (as suggested in [48]) one iteration of a BNA type load flow can be used.

CHAPTER VI

CHARACTERIZATION OF LOCAL AND GLOBAL SUBSETS OF SECURITY SETS

6.0 Preliminary Remarks

The security sets, in their implicit form, suffer from the following limitations:

(i) Their inside points are not easily accessible.

(ii) Since they are described by a large number of constraints, their direct use in the analysis of security related problems is not computationally desirable.

In this chapter, we have addressed these difficulties by investigating the possibility of describing a subset of a security set by a simple, easy to evaluate function. Furthermore, we have looked into the problem of filtering out redundant constraints from implicit description of a security set.

6.1 Characterizing a Local Subset

In this section, the problem of expressing part of a security region by a simple, explicit, and easy to evaluate function is examined. The application of such subsets are discussed in the next chapter.

6.1.1 Problem Statement

Consider the following problem. Find a large subset of S_z such that it contains a given point and can be described by an explicit function.

Let $\underline{z}_g$ be the given point and $C(\underline{z}, \underline{z}_g)$ represent the function. We are actually searching for a set $S_s(c)$, which can be defined by:

$$S_s(c) \triangleq \{\underline{z} \,/\, 0 \leq C(\underline{z}, \underline{z}_g) \leq c\} \tag{6.1}$$

The constant c has to be chosen such that

$$S_s(c) \subseteq S_z$$

With a little thought, one can conclude that the function $C(\underline{z}, \underline{z}_g)$ should necessarily have the following properties:

(i) Since S_z is normally a closed set, the contours of $C(\underline{z}, \underline{z}_g)$ must define closed surfaces;

(ii) For $c_1 > c_2$,

$$S_s(c_1) \supset S_s(c_2)$$

(iii) To have $\underline{z}_g$ always inside $S_s(c)$ (irrespective of the value of $c > 0$), the function $C(\underline{z}, \underline{z}_g)$ must have a single minimum at $\underline{z} = \underline{z}_g$ and $C(\underline{z}_g, \underline{z}_g) = 0$.

Note that the last property ensures the automatic satisfaction of the lower bound on $C(\underline{z}, \underline{z}_g)$.

Because of the second property, to have $S_s(c) \subseteq S_z$, the value of c has to be bounded from above. Denoting this bound by c^*, the set $S_c(c^*)$ is the largest subset that $C(\underline{z}, \underline{z}_g)$ can define. As shown in Figure 6.1, the boundary of $S_s(c^*)$, defined by $C(\underline{z}, \underline{z}_g) = c^*$, touches the boundary of S_z, at least, at one point. Clearly, c^* is the solution to the following problem:

$$\underset{\underline{z}\, \epsilon\, \mathrm{Ext}\,(S_z)}{\text{Minimize}} \quad c = C(\underline{z}, \underline{z}_g) \tag{6.2}$$

Because of the properties of $C(\underline{z}, \underline{z}_g)$, this very difficult problem, breaks down into a series of relatively simple and manageable sub-problems. Examining Figure 6.1, it is easily understood that the solution to (6.2) is simply the smallest value that $C(\underline{z}, \underline{z}_g)$ assumes

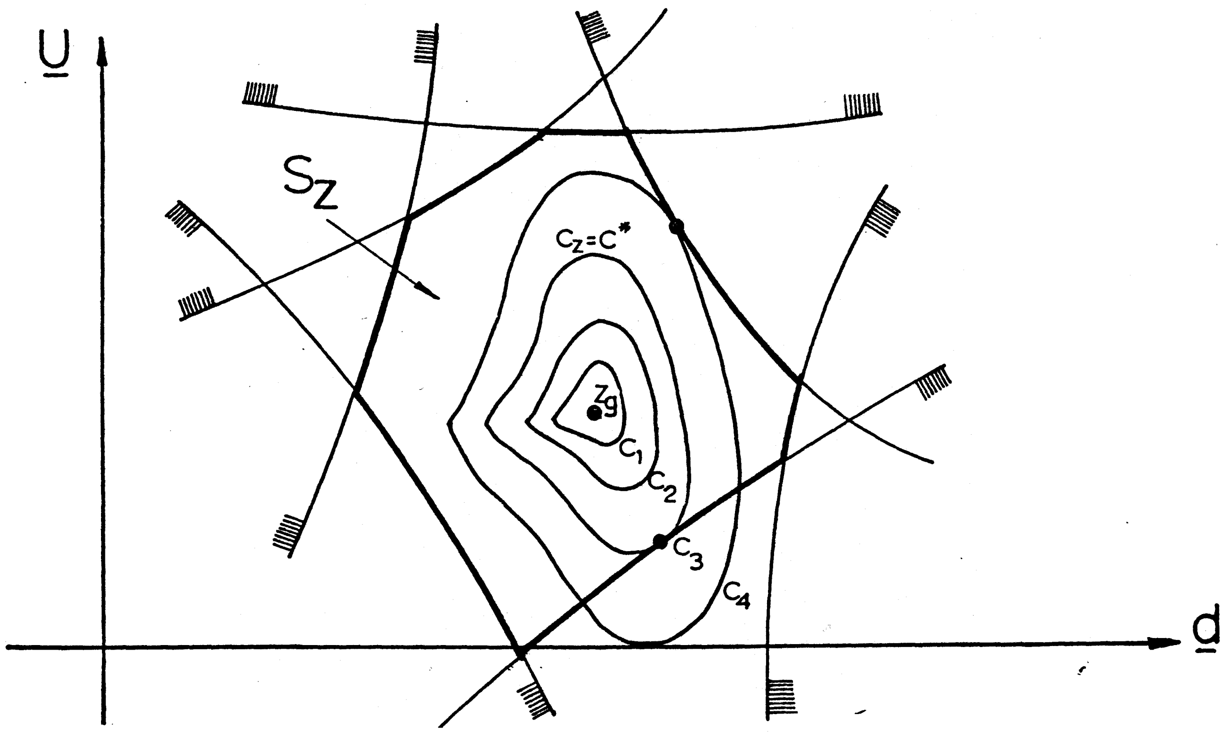

Figure 6.1. Contours of $C(\underline{z}, \underline{z}_g)$ and the boundary of S_z .

when it is maximized subject to the operating constraints <u>one at a time.</u> In other words:

$$c^* = \underset{j}{\text{Min}}\ [c_j^*] \tag{6.3}$$

where

$$c_j^* = \underset{\underline{z}\varepsilon\ \text{Ext}\ (Z^j)}{\text{Min}}\ [C(\underline{z}, \underline{z}_g)] \tag{6.4}$$

The set Z^j is defined in (3.30) . Note that in this chapter the superscript * identifies optimum and sub-optimum values.

6.1.2 Choice of the Function $C(\underline{z}, \underline{z}_g)$

Among various possibilities, we opt to describe $C(\underline{z}, \underline{z}_g)$ by a hyper-ellipsoid of the form:

$$C(\underline{z}, \underline{z}_g) \triangleq (\underline{z} - \underline{z}_g)^T [A] (\underline{z} - \underline{z}_g)$$

The positive definite matrix [A], which defines the shape and the orientation of the hyper-ellipsoid, offers adequate flexibility to S_s (c). Note that the suggested function possesses all the listed properties for $C(\underline{z}, \underline{z}_g)$.

With this choice of $C(\underline{z}, \underline{z}_g)$, the problem in (6.4) when involving an independent variable is simply

$$\text{Minimize} \quad c_i = (\underline{z} - \underline{z}_g)^T [A] (\underline{z} - \underline{z}_g) \tag{6.5}$$

subject to

$$\underline{\ell}_i^T \underline{z} = z_i^{\ell} \qquad (z_i^{\ell} = z_i^M \text{ or } z_i^m)$$

where $\underline{\ell}_i$ is defined in (4.1). The Ext (Z^i) is represented by the boundary hyper-surface $(\underline{\ell}_i^T \underline{z} = z_i^{\ell})$.

For a constrained dependent variable, using $\underline{z} = [L(\underline{x})]\,\underline{x}$, the problem takes the form:

$$\text{Minimize } c_j = \{[L(\underline{x})]\,\underline{x} - \underline{z}_g\}^T [A] \{[L(\underline{x})]\,\underline{x} - \underline{z}_g\}$$

subject to (6.6)

$$\underline{x}^T [Y_j]\,\underline{x} = y_j^{\ell}$$

The relative complexity of this problem can be appreciated by recognizing that solving a much simpler problem of this type, that is

$$\underset{\underline{x}}{\text{Minimize:}} \; \{[L(\underline{x})]\,\underline{x} - \underline{z}^{spec}\}^T \{[L(\underline{x})]\,\underline{x} - \underline{z}^{spec}\} \qquad (6.7)$$

has been the subject of extensive research during the last decade [87, 88, 89] .

6.1.3 Solution Techniques

The solution to the problem (6.5) is straight forward. The stationary point of the Lagrange function, $L(\underline{z}, \lambda)$, defined by

$$L(\underline{z}, \lambda) \triangleq (\underline{z} - \underline{z}_g)^T [A] [\underline{z} - \underline{z}_g) - \lambda (\underline{\ell}_i^T \underline{z} - \underline{z}_i^{\ell}) \qquad (6.8)$$

coincides with the solution point. Thus, one needs to solve

$$\left[\frac{\partial L(\underline{z}, \lambda)}{\partial \underline{z}}\right]^T = 2[A](\underline{z} - \underline{z}_g) - \lambda\,\underline{\ell}_i = \underline{0} \qquad (6.9)$$

for $\underline{z}^*$. Here an analytical solution is possible, namely

$$\underline{z}^* = \underline{z}_g + \frac{\lambda^*}{2} [A]^{-1} \underline{\ell}_i \tag{6.10}$$

This gives

$$c_i^* = (\frac{\lambda^*}{2})^2 \underline{\ell}_i^T [A]^{-1} \underline{\ell}_i \tag{6.11}$$

The value of λ^* is obtained by insisting that $\underline{z}^*$ should lie on $\underline{\ell}_i^T \underline{z} = z_i^\ell$, giving

$$\frac{\lambda^*}{2} = \frac{[z_i^\ell - \underline{\ell}_i^T \underline{z}_g]}{\underline{\ell}_i^T [A]^{-1} \underline{\ell}_i} > 0 \tag{6.12}$$

A widely accepted approach for solving problems such as (6.6) is to solve a sequence of unconstrained problems [90, 91, 92] of the form

$$\begin{aligned} \underset{\underline{x},\lambda}{\text{Min}} : \quad L(\underline{x}, \lambda, \rho) = & \{[L(\underline{x})] \underline{x} - \underline{z}_g\}^T [A] \{[L(\underline{x})] \underline{x} - \underline{z}_g\} \\ & - \lambda \{\underline{x}^T [Y_j] \underline{x} - y_j^\ell\} + {}^\rho/2 \{\underline{x}^T [Y_j] \underline{x} - y_j^\ell\}^2 \end{aligned} \tag{6.13}$$

The role of the parameter ρ in the augmented Lagrange function, $L(\underline{x}, \lambda, \rho)$, is to make sure that $L(\underline{x}, \lambda, \rho)$ has a minimum. This will be the case if ρ is chosen larger than a certain value [90] . Here, one starts with some value for ρ and an initial guess to λ , and solves the resulting problem in (6.13). Next, the solution is used to update λ (and possibly ρ). The problem is then resolved using the updated λ. This process is repeated till certain convergence requirements are satisfied.

Sasson [87, 88], after experimenting with various optimization algorithms, chooses a Fletcher-Powell scheme [93, 94] for solving (6.7). This algorithm is highly reliable but converges in more than N_z iterations, making it unsuitable for large dimensional systems. Since (6.6) has to be solved for all the constrained dependent variables, and each solution could involve solving (6.13) a few times, the adaptation of that scheme is not justified here. In the following, we discuss two schemes which proved to be quite efficient in solving (6.6).

<u>Proposed Algorithm:</u>

The gradient of $L(\underline{x}, \lambda, \rho)$ is simply

$$\left[\frac{\partial L(\underline{x}, \lambda, \rho)}{\partial \underline{x}}\right]^T = 4\,[L(\underline{x})]^T [A] \{[L(\underline{x})]\,\underline{x} - \underline{z}_g\} - 2\lambda\,[Y_j]\,\underline{x}$$
$$+ \rho\,\{\underline{x}^T [Y_j]\,\underline{x} - y_j^{\ell}\}\,[Y_j]\,\underline{x} \qquad (6.14)$$

At the solution point, $\underline{x}^*$, the gradient vanishes and $Y_j(\underline{x}^*) = y_j^{\ell}$. Hence, $\underline{x} = \underline{x}^*$ satisfies:

$$4\,[L(\underline{x})]^T [A] \{[L(\underline{x})]\,\underline{x} - z_g\} = 2\lambda\,[Y_j]\,\underline{x} \qquad (6.15)$$

or

$$[L(\underline{x})]\,\underline{x} = \underline{z}_g + \lambda\,[A]^{-1}\,[L(\underline{x})]^{-T}\,[Y_j]\,\underline{x} \tag{6.16}$$

To solve this system of non-linear equations, we propose the following iterative scheme

$$[L(\underline{x}^{k+1})]\,\underline{x}^{k+1} = \underline{z}^{k} \tag{6.17}$$

where

$$\underline{z}^{k} \triangleq \underline{z}_g + \lambda^{k}\,[A]^{-1}\,[L(\underline{x}^{k})]^{-T}\,[Y_j]\,\underline{x}^{k} \tag{6.18}$$

Note (6.17) represents a load flow problem. For enforcing $Y_j(\underline{x}) = y_j^{\ell}$, λ^k is updated in analogy to equation (6.12), namely

$$\lambda^{k} = 2\,\frac{[y_j^{\ell} - \underline{\beta}_j^{T}(\underline{x}^{k})\,\underline{z}_g]}{\underline{\beta}_j^{T}(\underline{x}^{k})\,[A]^{-1}\,\underline{\beta}_j(\underline{x}^{k})} \tag{6.19}$$

where $\underline{\beta}_j(\underline{x}^k) = [L(\underline{x}^k)]^{-T}\,[Y_j]\,\underline{x}^k$. This is based on the recognition that $\underline{z}^k$ can be viewed as the solution to the following problem:

$$\underset{\underline{z}}{\text{Min}}:\quad (\underline{z} - \underline{z}_g)^{T}\,[A]\,(\underline{z} - \underline{z}_g)$$

subject to (6.20)

$$\underline{\beta}_j^{T}(\underline{x}^{k})\,\underline{z} = y_j^{\ell}$$

In other words, for each iteration, by replacing $Y_j(\underline{x})$ with its linear TSE formulae, problem (6.6) is solved approximately. Then by running a load flow (i.e., solving equation (6.17)) $\underline{\beta}_j(\underline{x}^k)$ and λ^k

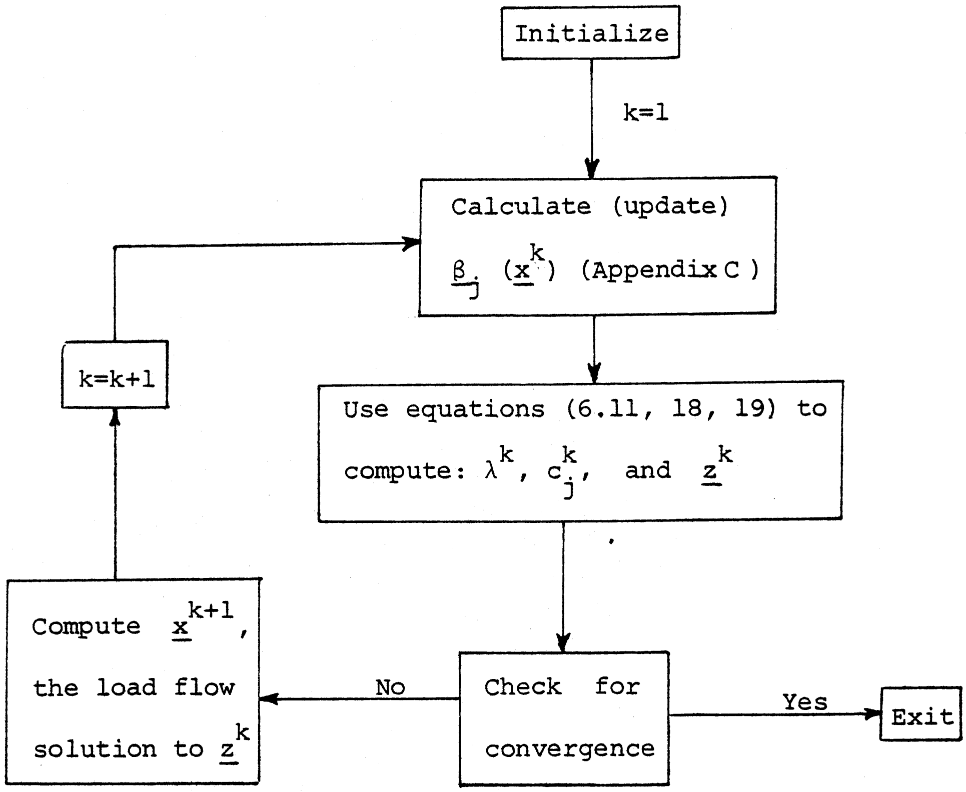

Figure 6.2. Flow diagram for computation of C_j^*.

are updated. This view of the proposed iterative scheme provides valuable insight into the behaviour of the algorithm.

The major steps of the algorithm are summarized in the flow diagram of Figure 6.2. To calculate $\underline{\beta}_j(\underline{x}^k) = [L(\underline{x}^k)]^{-T}[Y_j]\underline{x}^k$, it is not necessary to compute $[L(\underline{x}^k)]$. This is documented in Appendix C where it is shown that the problem of computing $\underline{\beta}_j(\underline{x}^k)$ can be formulated in terms of any available base Jacobian.

From the interpretation given to the algorithm in (6.20), it is clear that the sequence of the solutions, obtained during the iterations, satisfy all the optimality conditions, except $Y_j(\underline{x}) = y_j^\ell$ which is satisfied approximately. The iterations are thus aimed at enforcing this condition. At the solution, however,

$$y_j^\ell = \underline{\beta}_j^T(x^*)\,\underline{z} = \underline{x}^{*T}[Y_j]\,[L(x^*)]^{-1}\{[L(\underline{x}^*)]\,\underline{x}^*\}$$

$$= \underline{x}^{*T}[Y_j]\,\underline{x}^* = y_j(\underline{x}^*) \qquad (6.21)$$

The optimality conditions for this problem are listed in Appendix D.

Modified Algorithm:

In the proposed algorithm, during the load flow iterations the injection vector $\underline{z}^k$, or equivalently $\underline{\beta}_j(\underline{x}^k)$ and λ^k, are fixed. These quantities are updated only after the load flow converges. One may logically expect that updating λ^k and $\underline{\beta}(\underline{x}^k)$ during the load-flow iterations could improve the algorithm's overall rate of convergence.

To study this possibility, we chose to look into the iterations of a BNA type algorithm [17]. This choice was made to capitalize on the computational efficiency offered by the existing load flow routines.

Consider a general load flow problem:

$$[L\ (x)]\ \underline{x} = \underline{z}$$

By setting $\underline{x} = \underline{x}_b + \Delta\ \underline{x}$ ($\underline{x}_b$ corresponds to a base operating point) in this relation, the following iterative rule results:

$$\underline{x}^{k+1} = \frac{1}{2}\underline{x}_b + \frac{1}{2}[L\ (\underline{x}_b)]^{-1}\{\underline{z} - \Delta\ \underline{z}^k\} \tag{6.22}$$

where $\Delta\ \underline{z}^k \triangleq [L\ (\Delta\ \underline{x}^k)]\ \Delta\ \underline{x}^k$. Now by replacing $\underline{z}$ by $\underline{z}^k$ in (6.22), after some manipulation, it follows that,

$$\underline{x}^{k+1} = \underline{x}_d^k + \lambda^k\ \underline{b}^k \tag{6.23}$$

where

$$\underline{x}_d^k \triangleq \frac{1}{2}\underline{x}_b + \frac{1}{2}\ [L\ (\underline{x}_b)]^{-1}\{\underline{z}_g - \Delta\ \underline{z}^k\} \tag{6.24}$$

$$\underline{b}^k \triangleq \frac{1}{4}[L\ (\underline{x}_b)]^{-1}\ [A]^{-1}\ \underline{\beta}_j\ (\underline{x}^k) \tag{6.25}$$

Here λ^k is determined by demanding that $\underline{x}^{k+1}$ must satisfy $Y_j\ (\underline{x}) = y_j^\ell$, i.e., by solving

$$(\underline{x}_d^k + \lambda^k\ \underline{b}^k)\ [Y_j]\ (\underline{x}_d^k + \lambda^k\ \underline{b}^k) = y_j^\ell$$

or equivalently,

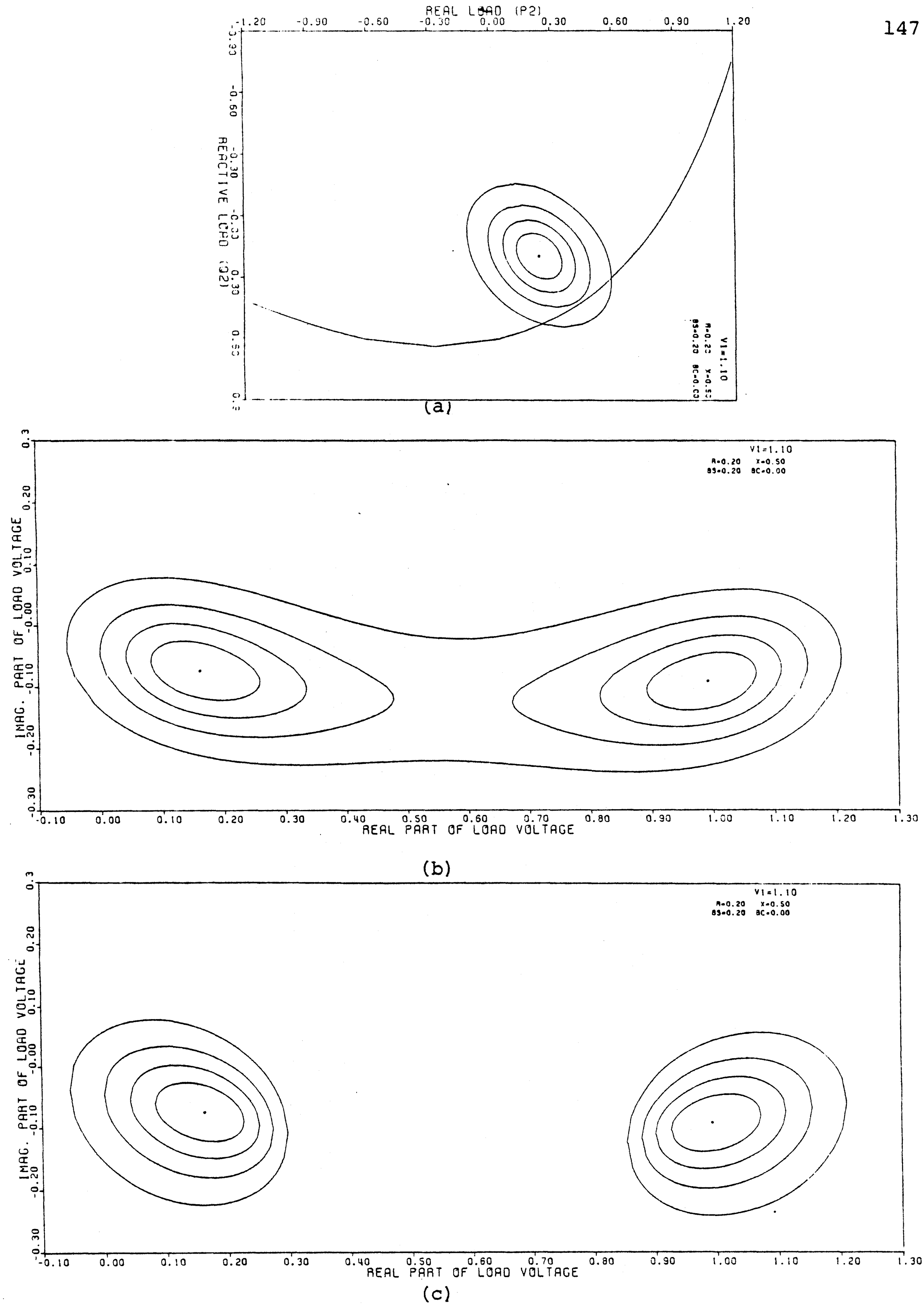

Figure 6.3. For the 2-bus system of Section 3.4: (a) Contours of an ellipse in the $\underline{z}$ space; (b) Image of the contours in the $\underline{x}$ space; (c) Quadratic approximation to the images.

$$Y_j\ (\underline{b}^k)\ \lambda^{k^2} + 2\ \{\underline{b}^{k^T}\ [Y_j]\ \underline{x}_d^k\}\ \lambda^k + Y_j\ (\underline{x}_d^k) - y_j^\ell = 0 \tag{6.26}$$

With the matrices $[A]$ and $[L\ (\underline{x}_b)]$ available in appropriate forms, the major part of the required computation per-iteration goes into the the updating of $\beta_j\ (\underline{x}^k)$. This computation, as explained in Appendix C can also be carried out using $[L\ (\underline{x}_b)]$, instead of $[L\ (\underline{x}^k)]$.

A good base point for this algorithm is $\underline{x}_g$ (i.e., $\underline{x}_b = \underline{x}_g$), the load flow solution to $\underline{z}_g$. This choice of $\underline{x}_b$ changes $\underline{x}_d^k$ to

$$\underline{x}_d^k = \underline{x}_g - \frac{1}{2}\ [L\ (\underline{x}_g)]^{-1}\ \Delta\ \underline{z}^k \tag{6.27}$$

It can be readily shown that in each iteration of this algorithm, one is almost solving the following problem

$$\begin{aligned} \text{Minimize}\quad C^k &= (\underline{x} - \underline{x}_d^k)^T\ [D^k]\ (\underline{x} - x_d^k) \\ \underline{x}^T\ [Y_j]\ \underline{x} &= y_j^\ell \end{aligned} \tag{6.28}$$

where $[D^k]^{-1} \triangleq \frac{1}{4}[L\ (\underline{x}_b)]^{-1}\ [A]^{-1}\ [L\ (x^k)]^{-T}$. In Figure 6.3, it is shown that the objective function in (6.28) is locally a good approximation to the original one in (6.6).

In Appendix D, the optimality conditions for a solution to (6.6) are discussed. It seems that, because of the special form of the objective function and the constraints, by choosing $\underline{x}_g$ as the initial point, the resulting solutions should satisfy all the optimality conditions.

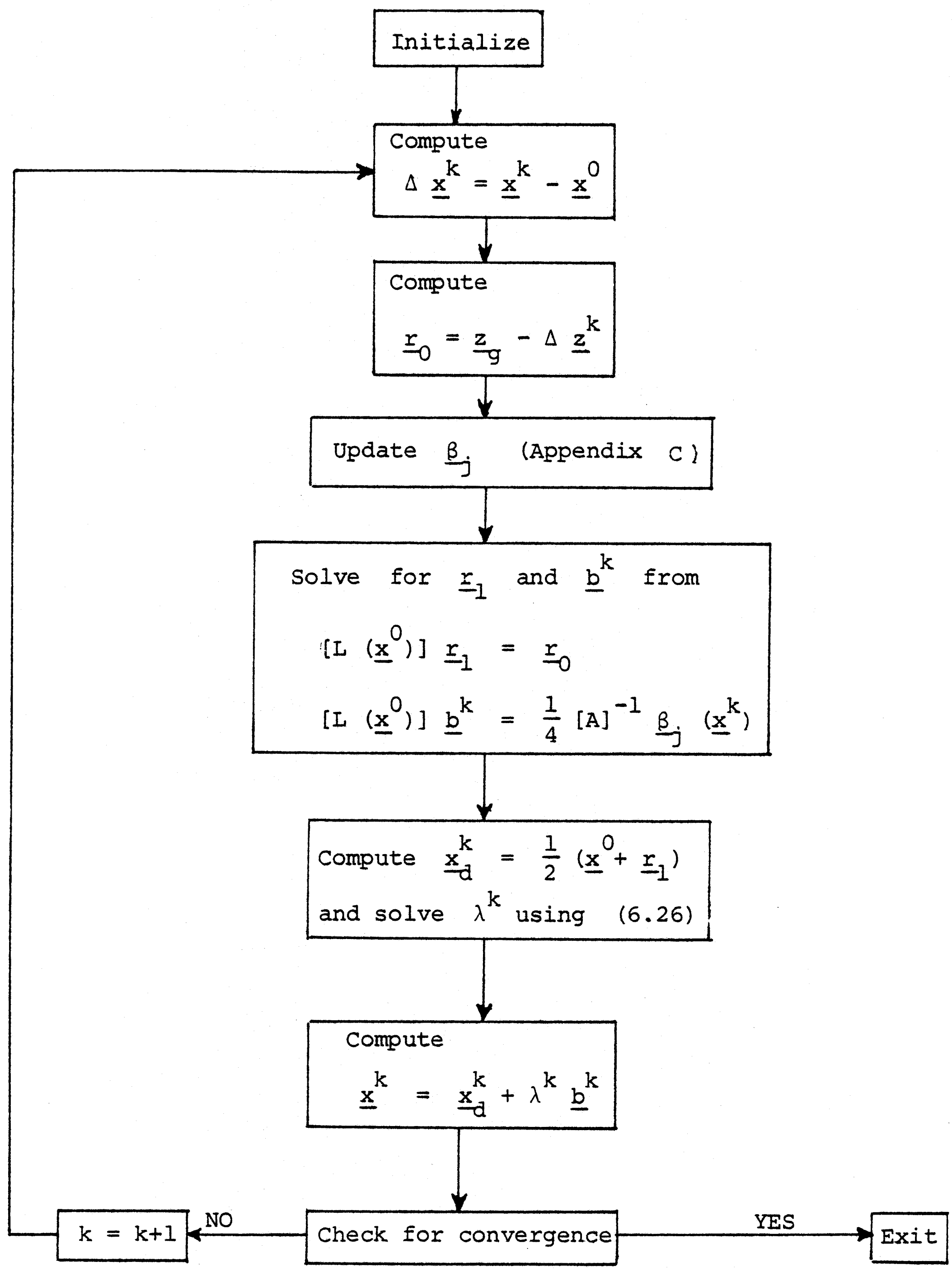

Figure 6.4. The flow diagram for the modified algorithm.

The major steps of the resulting algorithm are summarized by the flow chart in Figure 6.4.

6.1.4 Features of the Proposed Algorithms

The first algorithm is conceptually simple and straight forward. Its main feature is that a substantial part of its required computation can be carried out in the form of load flow runs, for which highly sophisticated routines are already available.

Its major drawback is its susceptibility to divergence. In few cases, where the value of y_j^ℓ was relatively high (or low, depending on the variable) the algorithm failed to converge to a solution. To understand the circumstances which give rise to such situations, the interpretation of the iterative scheme, as given in (6.20), can be used. As shown in Figure 6.5, for large values of y_j^ℓ (or small), the contours of $Y_j(\underline{x}) = y_j^\ell$ in the $\underline{z}$ space approach partially the boundary of R_z. As a result, only a small portion of the hyper-plane $\underline{\beta}_j^T(\underline{x}^k)\,\underline{z} = y_j^\ell$ will be inside R_z. This, as indicated in Figure 6.6, increases the chances that $\underline{z}^k$, k=1, ... , fall outside R_z; causing (6.17) to diverge.

An obvious remedy here is to use initially a smaller value for y_j^ℓ. If the resulting c_j^* was larger than any of the previously calculated c_j^*'s, no more computation is needed. Otherwise, y_j^ℓ can

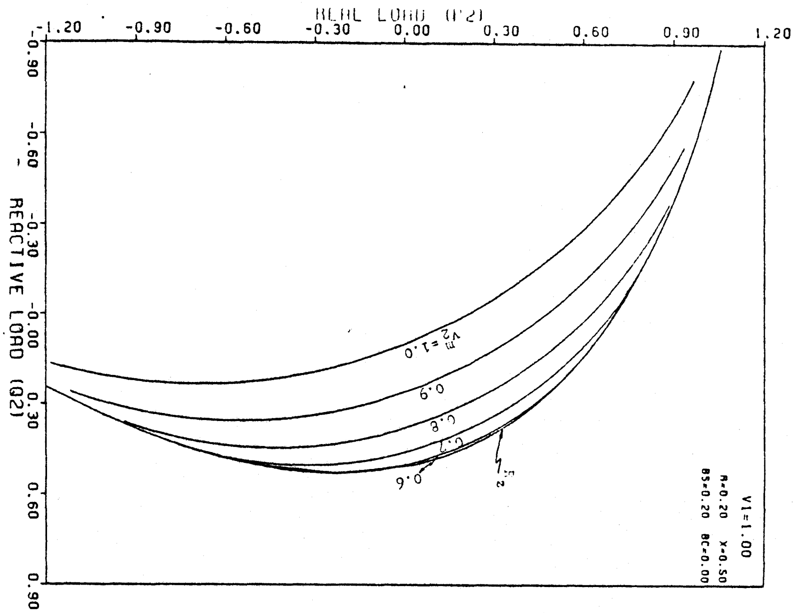

Figure 6.5. Relative position of the boundary of R_z and hyper-surface $v_2^2(\underline{x}) = (v_2^m)^2$ for various values of v_2^m.

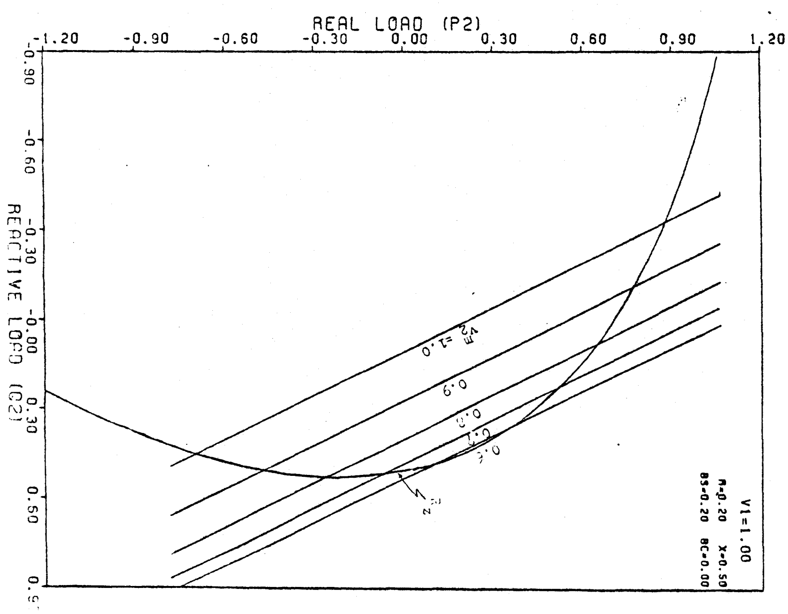

Figure 6.6. Relative position of the boundary of R_z and hyper-planes approximating $v_2^2(\underline{x}) = (v_2^m)^2$ in the $\underline{z}$ space.

be increased to its full value in steps; using the solution of one step as the starting point to its proceeding one. This is an effective, but computationally expensive process.

The modified algorithm enables one to stay on the hyper-surface $Y_j(\underline{x}) = y_j^{\ell}$ all the time. Since the map of $Y_j(\underline{x}) = y_j^{\ell}$ lies completely inside R_z, this algorithm is not susceptible to the type of divergence discussed above. For the few non-convergent cases witnessed before, the modified algorithm converges, but rather slowly. It exhibits a "zig-zagging" convergence pattern, which we could only attribute to the ill-conditioning of the matrix $[D^k]$ in (6.28).

The second order equation for λ^k, in rare cases, may have no real solution. This situation is shown in Figure 6.7. In such cases, λ^k is computed from:

$$\lambda^k = - \frac{\underline{b}^{kT} \, [Y_j] \, \underline{x}_d^k}{Y_j \, (\underline{b}^k)} \tag{6.31}$$

which is the only solution to

$$\underset{\lambda^k}{\mathrm{Min}} : \; \{ (\underline{x}_d^k + \lambda^k \, \underline{b}^k)^T \, [Y_j] \, (\underline{x}_d^k + \lambda^k \, \underline{b}^k) - y_j^{\ell} \}^2$$

The modified algorithm normally converges in 3 iterations. Allowing two BNA iterations for updating $\underline{\beta}_j (\underline{x}^k)$, each iteration is

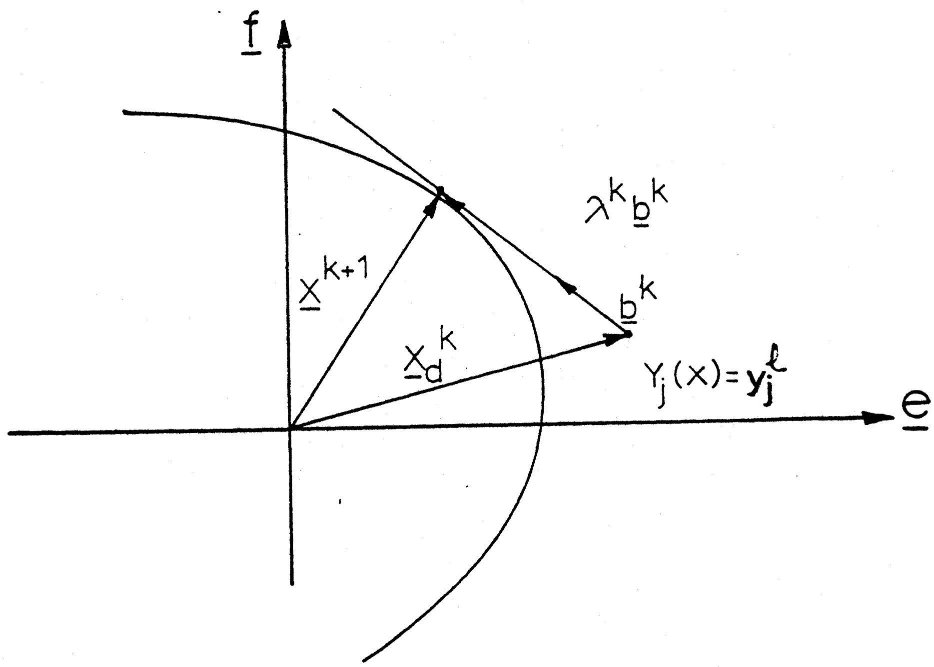

Figure 6.7. Geometrical representation of a case where (6.26) has no solution.

computationally equivalent to $4\frac{1}{2}$ BNA iterations; thus, requiring a total of $13\frac{1}{2}$ BNA iterations per problem. For the same problems, the first algorithm often converges in less than 4 iterations (i.e., 3 load flow runs are needed, at most). Assuming an average of 4 iterations per load flow, it takes a total of 19 BNA iterations to converge, i.e., $5\frac{1}{2}$ BNA iterations more than what is required by the modified algorithm (the above estimates are based on the cases where [A] has been a diagonal matrix or $[A]^{-1}$ has been supplied).

6.2 Characterization of a Global Subset

6.2.1 Problem Statement

We would like to solve the following problem. What is the largest possible subset of S_z which is expressible by a given function?

Again we use $C(\underline{z}, \underline{z}_g)$ to represent the function, implying that it satisfies all the previously stated conditions. The above problem then can be formulated as:

$$\text{Maximize } c = C(\underline{z}, \underline{z}_g) \qquad (6.32)$$
$$\underline{z}, \underline{z}_g \in S_z$$

The main difference between this problem and the one in (6.2) is that, unlike the latter, here $\underline{z}_g$ can vary over the whole S_z. Upon varying $\underline{z}_g$ over S_z we wish to find a $\underline{z}_g = \underline{z}_g^*$ such that $C(\underline{z}, \underline{z}_g^*)$ could describe <u>the largest local subset</u> of S_z. The solution to (6.32) will be a set, similar to (6.1), representing in effect a crude approximation to S_z.

6.2.2 Problem Formulation

Using relations (6.3) and (6.4), problem (6.32) can be restated as

$$c^* = \underset{\underline{z}_g \varepsilon S_z}{\text{Max}} : \underset{j}{\text{Min}} \{ \underset{\text{Ext}(Z^j)}{\text{Min}} [c(\underline{z}, \underline{z}_g)]\} \tag{6.33}$$

In words, to find the solution, a "maxi-min" problem has to be solved.

The mini-max or maxi-min problems are encountered frequently in various engineering and economic areas [95, 96, 97] . As a result, there is a good deal of literature, discussing various solution algorithms, available on this subject [98, 99,100,101] . The proposed approaches are, however, very specialized, tailored for certain applications (c.f. [98]) .

In the next section, it is shown that, when $C(\underline{z}, z_g)$ is represented by a hyper-ellipsoid and S_z is approximated by $\hat{S}_z$, a unique solution to (6.33) can be found easily.

6.2.3 Solution in $\underline{z}$-space

Consider the case where Z^j is described approximately by $\underline{\beta}_j^T(\underline{x}^0)\,\underline{z} \le y_j^\ell$. Using relations (6.11) and (6.12), the solution to the problem : $\underset{Z^j}{\text{Max}}\ [C(\underline{z}, \underline{z}_g)]$ is simply :

$$c_j^* = [\underline{\beta}_j^T(\underline{x}^0)\,\underline{z}_g - y_j^\ell]^2 / \eta_j^2 \qquad j=1, \ldots , N_s \tag{6.34}$$

where $\eta_j^2 = \underline{\beta}_j^T(\underline{x}_0)\,[A]^{-1}\,\underline{\beta}_j(\underline{x}_0)$. We would like to find a $\underline{z}_g$ such that

$$c^* = \underset{\underline{z}_g \varepsilon S_z}{\text{Max}} \; \underset{j}{\text{Min}} \{ [\frac{\underline{\beta}_j^T (\underline{x}_0) \, \underline{z}_g - y_j^\ell}{\eta_j}]^2 \} \tag{6.35}$$

Let c represent the smallest of c_j^*, $j=1, \ldots, N_s$ (i.e., $c_j^* \geq c > 0$ $j=1, \ldots, N_s$) . This obviously implies

$$(c_j^*)^{1/2} \geq c^{1/2} \qquad j=1, \ldots, N_s \tag{6.36}$$

Inserting equations (6.34) into the above expression, one obtains,

$$- [\frac{\underline{\beta}_j^T (\underline{x}^0) \, \underline{z}_g - y_j^\ell}{\eta_j}] \geq c^{1/2} \qquad j=1, \ldots, N_s \tag{6.37}$$

where the minus sign indicates that the original inequalities are of the form $\underline{\beta}_j^T (\underline{x}^0) \, \underline{z} \leq y_j^\ell$. The inequalities in (6.37) can be used to reformulate the problem in (6.35) as an LP problem, namely:

$$\text{Maximize:} \quad c^{1/2} \tag{6.38}$$

subject to

$$\underline{\beta}_j^T (\underline{x}_0) \, \underline{z}_g + \eta_j \, c^{1/2} \leq y_j^\ell \qquad j=1, \ldots, N_s$$

Here $c^{1/2}$ is treated as a simple variable. By solving this standard LP problem, one obtains $\underline{z}_g^*$ and $c^{*1/2}$. The following points are worth mentioning here:

(1) Since both $c^{*1/2}$ and η_j are positive, it is obvious that the set

$$\underline{\beta}_j^T \underline{z} \le y_j^{\ell} - \eta_j c^{*1/2} \qquad j=1, \ldots, N_s$$

is a sub-set of $\hat{S}_z$ and thus $\underline{z}_g^* \in \hat{S}_z$.

(2) At the solution, $N_z + 1 = 2 N_b$ of the constraints are satisfied at their bounds. Therefore, the embedded hyper-ellipsoid touches (at least) that many active constraints.

(3) The presence of the redundant constraints do not hamper the algorithm.

To improve the solution accuracy, one needs to run at least $2 N_b$ load flows, in order to update the $\underline{\beta}$s of the "touching" constraints and repeat the solution. One may, instead, argue that the solution point computed here should not be too far from the true $\underline{z}_g^*$, and thus it can be employed to calculate an exact local subset of S_z (using the modified algorithm). In this case only the touching constraints and those close to being touched need to be considered.

6.2.4 Solution in $\underline{x}$-Space

It is not easy to solve problem (6.33) in the $\underline{x}$-space with acceptable accuracy. Instead, we try to solve the following problem:

$$\underset{\underline{x}_g \, \varepsilon \, S_x}{\text{Maximize}} \quad \underset{\underline{x} \, \varepsilon \, \text{Ext}\,(S_x)}{\text{Minimize}} \quad r = R\,(\underline{x}, \underline{x}_g) \tag{6.39}$$

where

$$R\,(\underline{x}, \underline{x}_g) \triangleq (\underline{x} - \underline{x}_g)^T\,[A]\,(\underline{x} - \underline{x}_g) \tag{6.40}$$

Here, an exact solution is possible.

Consider the set of operating constraints, defining S_x, namely

$$h_i = \underline{x}^T\,[H_i]\,\underline{x} \leq h_i^{\ell} \qquad i=1, \ldots, N_s \tag{6.41}$$

Assume a point $\underline{x}^0 \, \varepsilon \, S_x$ is available. Linearizing the above constraints around $\underline{x}^0$, one obtains

$$\underline{\alpha}_i^T\,(\underline{x}^0)\,\underline{x} \leq k_i \qquad i=1, \ldots, N_s \tag{6.42}$$

where

$$\alpha_i\,(\underline{x}^0) \triangleq [H_i]\,\underline{x}^0 \tag{6.43}$$

$$k_i \triangleq \frac{1}{2} [h_i^{\ell} - h_i (\underline{x}^0)] \tag{6.44}$$

Now, by following the same steps as in the last section, one ends up with the following problem:

$$\text{Maximize} \quad r^{1/2}$$

subject to (6.45)

$$\underline{\alpha}_i^T (\underline{x}^0) \, \underline{x}_g - \xi_i \, r^{1/2} \leq k_i \qquad i=1, \ldots, N_s$$

where

$$\xi_i \triangleq \{\underline{\alpha}_i^T (\underline{x}^0) \, [A]^{-1} \, \underline{\alpha}_i \, (\underline{x}^0)\}^{1/2} \tag{6.46}$$

Solving this LP problem one obtains $\underline{x}_g^*$. Now to get the exact solution, we propose an iterative process.

In the kth iteration, after finding $\underline{x}_g^k = \underline{x}_g^*$, the points at which the linear constraints touch $R\ (\underline{x}, \underline{x}_g^k)$ are computed. They are given by

$$\underline{x}_i^{k+1} = \underline{x}_g^k + \lambda_i^k \, [A]^{-1} \, \underline{\alpha}_i \, (\underline{x}^k) \qquad i=1, \ldots, N_s \tag{6.47}$$

These points are then projected into their corresponding hyper-surfaces by computing λ_i^k from:

$$(\underline{x}_i^{k+1})^T \, [H_i] \, (\underline{x}_i^{k+1}) = h_i \qquad i=1, \ldots, N_s \tag{6.48}$$

Equations (6.48) give rise to relations similar to those in (6.26). The resulting points $(\underline{x}_i^{k+1}, \; i=1, \ldots, N_s)$ are then used to re-linearize the constraints and repeat the LP solution.

To converge, one may need to solve a few LP problems. The volume of the computations, however, can be reduced markedly, after the first LP solution. By discarding those constraints whose $r_i^* = (\lambda_i^* \xi_i/2)^2$ exceed r^* by a certain fraction (e.g., 25%), the size of the LP tableau decreases sharply.

After finding the solution to (6.39), one may transform $R(\underline{x}, \underline{x}_g^*)$ into the $\underline{z}$-space using a TSE formula. By choosing the expansion point to be $\underline{x}_g^*$ a rather simple relation results.

Note that in the case $[A] = [I]$, one actually finds the largest hyper-sphere that can be embedded into S_x [60] .

6.3 Filtering the Redundant Constraints

6.3.1 Motivation

Quite often, a substantial number of the constraints describing S_z (implicitly) are redundant, i.e., they can be deleted without affecting S_z. The redundancy in the operating constraints is normally a consequence of implementing certain security measures in a power system in its design (expansion) stage. A common design (expansion) objective is to build into the system the ability to maintain quality service for a range of predicted loads, while certain key generating and transmitting components are inoperative. This obviously requires the system components to have ratings much higher than what is needed during the normal operation. Note that, for a well designed system, a redundant constraint, say, among the constraints describing S_z, will be an active constraint for some other security sets, and vice-versa.

Since in large systems the redundant constraints can constitute more than 75% of the total number of operating constraints [52, 61], their deletion in the security related problems could reduce the volume of the computation drastically. This is certainly true in the case of computing a local or a global subset of S_z. Other examples include the security monitoring process and solving the secure-economic dispatch problem (Section 5.3).

Unfortunately, it is not easy to identify a redundant operating constraint. Various proposed schemes [52,61] seem to involve excessively large amounts of computations. In this section we study this problem in some detail.

6.3.2 Definition and General Approach

Consider a set defined by the following constraints

$$g_j(\underline{x}) \geq 0 \qquad j=1, \ldots, m \tag{6.49}$$

A constraint $g_k(\underline{x}) \geq 0$ $(k \leq m)$ is redundant if and only if the set of points defined by

$$g_j(\underline{x}) \geq 0 \qquad j=1, \ldots, m \; ; \quad j \neq k$$

is equal to that defined by (6.49).

The obvious way of verifying whether or not the constraint $g_k(\underline{x}) \geq 0$ is redundant, is to solve the following problem:

$$\min_{\underline{x}} : \quad g_k(\underline{x})$$

subject to (6.50)

$$g_j(\underline{x}) \geq 0 \qquad j=1, \ldots, m$$

Denoting the solution by $\underline{x}^*$, if $g_k(\underline{x}^*) > 0$, the constraint is redundant, otherwise it is "binding" or "active".

The above procedure is not practical for identification of the redundant constraints in the implicit definition of the security sets.

This is because of the large number of constraints involved in describing each set.

In what follows, we present a practical scheme which is fundamentally different from the above one.

6.3.3 A Simulation-Based Approach

Here, unlike the above scheme which identifies the redundant constraints, we try to sort out the active ones. Consider the following sets:

$$B^j = S_x \cap \{\underline{x} \,/\, \underline{x}^T [H_j] \underline{x} = h_j^\ell\} \qquad j=1, \ldots, N_s \tag{6.51}$$

Clearly, among these sets, the non-empty ones correspond to the active constraints. This means here, that to demonstrate that the kth constraint is active, it is sufficient to find a point belonging to B^k.

The boundary of S_x, denoted by B_x, can be expressed in terms of the above sets, namely,

$$B_x = \bigcup_{j=1}^{N_s} B^j \tag{6.52}$$

From above, it follows that a point belonging to B_x can identify at least one active constraint. This simple property is exploited here to propose an efficient scheme for sorting out the active constraints. Note that, while it is not easy to find points belonging to, say, B^k, points belonging to B_x can be found fairly easily.

Let $\underline{x}^0$ represent a point inside S_x and $\underline{v}$ denote a general direction in the $\underline{x}$ space. The line $\underline{x} = \underline{x}^0 + \alpha\, \underline{v}$ intercepts B_x at least at two points. These two points can be found by solving

$$(\underline{x}^0 + \alpha\, \underline{v})^T\, [H_j]\, (\underline{x}^0 + \alpha\, \underline{v}) = h_j^{\ell} \qquad j=1, \ldots, N_s \tag{6.53}$$

for α and checking if $\underline{x}^0 + \alpha^j\, \underline{v} \triangleq \underline{x}^j \in S_x$, where α^j denotes a solution to the jth equation. The above equations can be rewritten in the form

$$\{\underline{v}^T\, [H_j]\, \underline{v}\}\, \alpha^2 + 2\, \{\underline{v}^T\, [H_j]\, \underline{x}^0\}\, \alpha + \{\underline{x}^{0^T}\, [H_j]\, \underline{x}^0 - y_j^{\ell}\} = 0$$

$$j=1, \ldots, N_s \tag{6.54}$$

To have a computationally viable scheme, $\underline{v}$ has to be chosen such that the terms $\underline{v}^T\, [H_j]\, \underline{v}$ and $\underline{v}^T\, [H_j]\, \underline{x}^0$ can be computed efficiently ($\underline{x}^{0^T}\, [H_j]\, \underline{x}^0$ is assumed to be known). A convenient set of directions are the coordinate axes. When moving away from $\underline{x}^0$ along the ith axis, the line becomes: $\underline{x} = \underline{x}^0 + (x_i - x_i^0)\, \underline{\ell}_i$. Then $\underline{\ell}_i^T\, [H_j]\, \underline{\ell}_i = (h_{ii})_j$ and, by exploiting the special structure of $[H_j]$, $\underline{\ell}_i^T\, [H_j]\, \underline{x}^0$ can be computed quite easily (for further clarification, see Appendix E). As shown in Figure 6.8, by moving along all the coordinate axes one can potentially identify $2\, N_z$ active constraints.

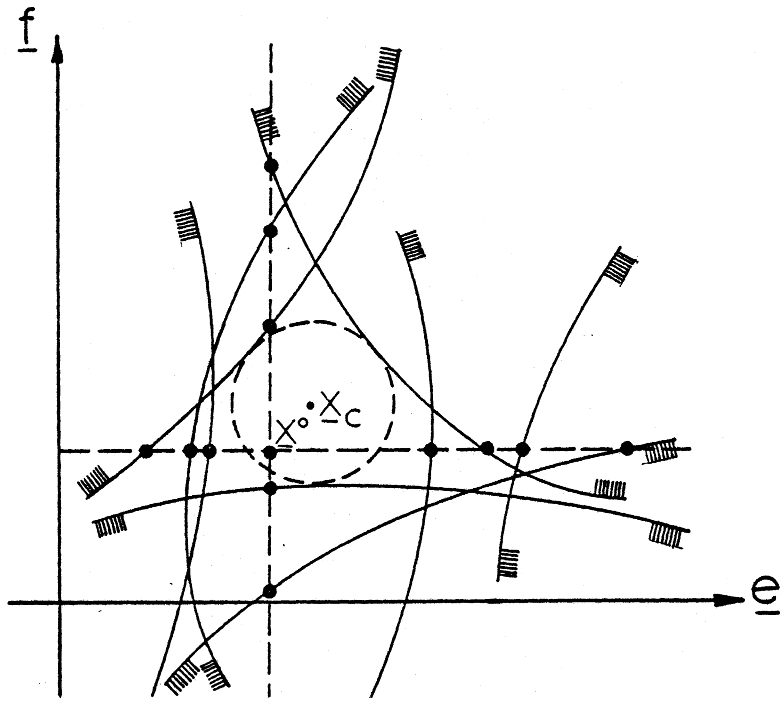

Figure 6.8. Illustration of the basic idea behind the proposed scheme.

The scheme is clearly based on the access to a large number of points inside S_x . It is computationally inefficient to try to get such points by generating points randomly in a large hyper-box containing S_x . Instead, one can use the largest hyper-sphere that can be put inside S_x . As described in Section 6.2.4, that involves solving a LP problem (for an approximate solution) with a tableau containing all the constraints. Points randomly generated inside the hyper-sphere then can be used efficiently to sort-out the active constraints. The basic approach is described in the flow diagram of Figure 6.9. Many details are not given in the flow diagram to present the main idea as clearly as possible.

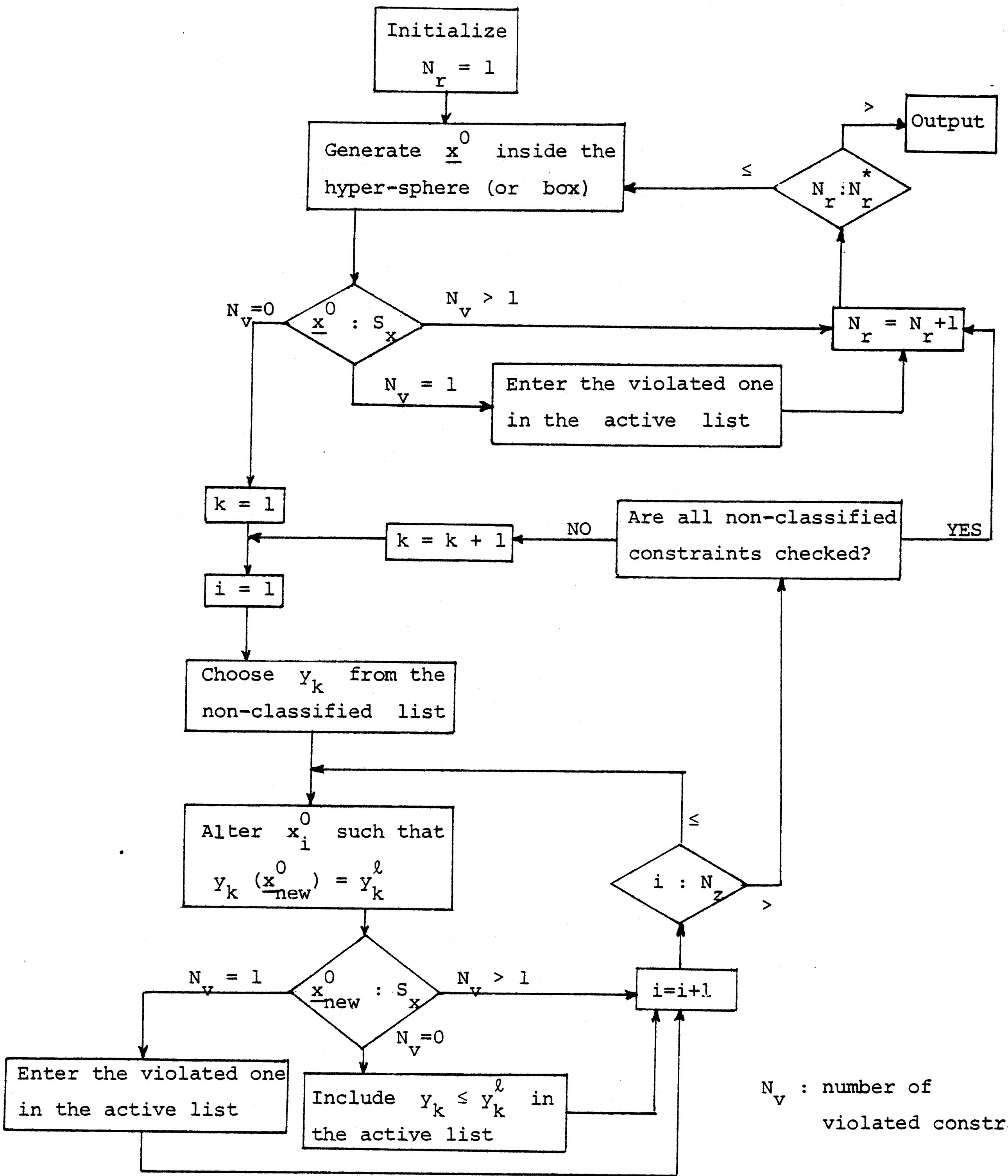

N_v : number of violated constraints

N_r : number of generated random points.

Figure 6.9. The flow diagram for identifying the active constraints forming S_x .

Since S_x is not convex, there is a risk that by confining the random points to the hyper-sphere, some of the active constraints remain undetected. Thus, after generating sufficiently large number of points, it is advisable to replace the hyper-sphere by a hyper-box. A suitable hyper-box is the one whose center coincides with that of the hyper-sphere and its sides are 4 to 5 times the radius of the latter.

It is worth remembering that in the process of finding the largest hyper-sphere, at least, $2\ N_b$ of the active constraints are recognized.

CHAPTER VII

SET-THEORETIC APPROACH TO PREDICTIVE SECURITY ASSESSMENT AND ENHANCEMENT

7.0 Preliminary Remarks

In this chapter we have tried to exhibit how sub-sets of a security set, when available in a simple and explicit form, can facilitate various security related functions of a system. The operating aspects of power systems which are examined in relation to this effort are:

(i) Under vulnerable conditions, the operator needs to compute a stand-by control strategy as quickly as possible. Since, under such circumstances, the economical aspect of the computed controls is not crucial, the use of fast and efficient techniques which produce non-optimal control strategies is justified.

(ii) Under similar environmental, industrial and system conditions, the system trajectory closely repeats itself. Thus, based on past data, the future system trajectory can be estimated within a limited range of accuracy.

(iii) Normally the transition of operating conditions from one state to another is gradual. Thus, the state vector stays in the neighborhood of an immediate past operating state for an appreciable period of time.

Each of the above operating aspects has motivated one of the sections of this chapter.

7.1 Application of Global Sub-Sets to Security Control

7.1.1 Motivation

Consider a normal secure operating point which is vulnerable to a number of the listed contingencies. To correct this operating condition, the operator is faced with the following difficulties:

(i) There is often no control strategy that does not involve load curtailment and can result in an operating point inside S_z^I ;

(ii) The corrective control action, if any, is often economically unattractive. This is compounded by the fact that, in many cases, the probability that a critical contingency actually occur is quite low.

Because of the above difficulties, it has been the policy of many electric power utilities to compute stand-by control actions <u>for each</u> critical contingency, to be used in the event that one of the critical contingencies actually occur [10,102] .

To compute the required control strategies, in theory, one has to solve the following problems:

$$\underset{\underline{z} \in S_z^k}{\text{Minimize}} : \sum_{i=1}^{N_g} f_i\,(p_i^g) + (\underline{d} - \underline{d}_0)^T\,[D]\,(\underline{d} - \underline{d}_0) \qquad k \in K \tag{7.1}$$

The vector $\underline{d}_0$ represents the present system load, while members of the set K identify the critical contingencies. The summation, as before, represents the total generation cost. The role of the diagonal matrix [D] is to make sure that the load curtailment would be considered as the last resort by less-heavily weighing the corresponding term in (7.1).

Solving the above problems on-line is not practical since the required computing time, even for a single problem, may prove excessive. It can be argued, however, that the operator's concern under vulnerable conditions is primarily to make sure that one has access to some feasible control strategies, rather than to seek an optimum solution to (7.1). In other words, minimization of the operating cost does not have the highest priority while the system is in the emergency state.

In this section, a simple and fast procedure for computing feasible, but non-optimal, stand-by control strategies is introduced.

7.1.2 Computing Stand-By Control Strategies

Let $\underline{z}_0$ represent a normally secure operating point which is vulnerable to the r-th contingency, i.e., $\underline{z}_0 \in S_z$ but $\underline{z}_0 \notin S_z^r$. We would like to find a control strategy $\Delta \underline{z}_r^T = [\Delta \underline{u}_r^T, \Delta \underline{d}_r^T]$ such that $(\underline{z}_0 + \Delta \underline{z}_r) \in S_z^r$. By studying Figure 7.1, one notes that there are two distinct classes of operating points which can include $\underline{z}_0$. For one class S_z^r $(\underline{d} = \underline{d}_0)$ is non-empty, while for the other class it is empty. This distinction is important because for the first class $\Delta \underline{d}_r$ can be zero, i.e., no load shedding is required.

Denoting the largest hyper-ellipsoid that can be embedded inside S_z^r by E_z^r, it is clear that if

$$(\underline{z}_0 + \Delta \underline{z}_r) \in E_z^r \Rightarrow (\underline{z}_0 + \Delta \underline{z}_r) \in S_z^r \tag{7.2}$$

A very simple and efficient method of correcting the vulnerability of $\underline{z}_0$ is then by searching for a $\Delta \underline{z}_r$ such that $(\underline{z}_0 + \Delta \underline{z}_r) \in E_z^r$. As will be shown below such a $\Delta \underline{z}_r$ can be found very easily, but the result may be more conservative than if we used an optimal strategy.

Let E_z^r be defined by

$$E_z^r \triangleq \{\underline{z} \,/\, (\underline{z} - \underline{z}_r^*)^T \, [A_r] \, (\underline{z} - \underline{z}_r^*) \leq c_r^*\}$$

Obviously, since $\underline{z}_0 \notin S_z^r$,

$$c_0 = (\underline{z}_0 - \underline{z}_r^*)^T [A_r] (\underline{z}_0 - \underline{z}_r^*) > c_r^* \tag{7.3}$$

To keep the procedure of computing $\Delta \underline{z}_r$ as simple as possible, we move along the line connecting $\underline{z}_0$ to $\underline{z}_r^*$, the center of the ellipsoid, until we intersect the boundary of E_z^r. The line is expressed by

$$\Delta \underline{z} = t \Delta \underline{z}_0 \qquad 0 \le t \le 1$$

where $\Delta \underline{z} \triangleq \underline{z} - \underline{z}_r^*$ and $\Delta \underline{z}_0 \triangleq \underline{z}_0 - \underline{z}_r^*$. The solution is then

$$\Delta \underline{z}_r = [1 - (c_r^* / c_0)^{1/2}] \Delta \underline{z}_0 \tag{7.4}$$

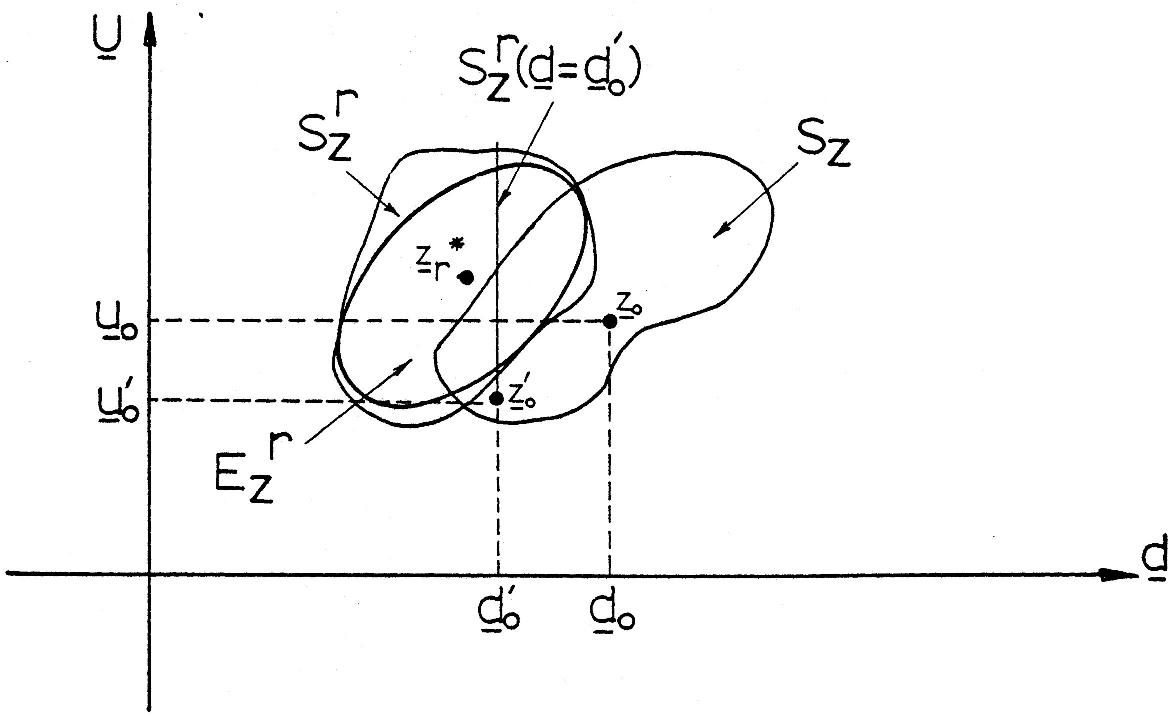

Figure 7.1. Illustration of the two possible situations for a vulnerable operating point.

The above control strategy is undesirable since it generally will result in load shedding. It is thus preferable to try to enforce $\Delta \underline{d}_r = \underline{0}$ by moving along the line

$$\Delta \underline{u} = t \Delta \underline{u}_0 \qquad 0 \leqslant t \leqslant 1$$

where $\Delta \underline{u} \triangleq \underline{u} - \underline{u}_r^*$ and $\Delta \underline{u}_0 \triangleq \underline{u}_0 - \underline{u}_r^*$. The control adjustments, $\Delta \underline{u}_r$, are computed by finding the point where this line intersects the boundary of a secure control set, produced by projecting the cross-section of E_z^r corresponding to $\underline{d} = \underline{d}_0$ into the $\underline{u}$ space. Here, the secure control set is given by

$$\Delta \underline{u}^T [A_{uu}^r] \Delta \underline{u} + 2 \Delta \underline{d}_0^T [A_{ud}^r] \Delta \underline{u} + \Delta \underline{d}_0^T [A_{dd}^r] \Delta \underline{d}_0 \leqslant c_r^* \tag{7.5}$$

where

$$[A_r] = \left[\begin{array}{c:c} A_{uu}^r & A_{ud}^r \\ \hdashline A_{ud}^r & A_{dd}^r \end{array}\right] \quad ; \quad \Delta \underline{d}_0 = \underline{d}_0 - \underline{d}_r^*$$

Inserting $\Delta \underline{u} = t \Delta \underline{u}_0$ into (7.5), and also replacing the inequality sign in (7.5) by an equality sign, one ends up with the following equation for t :

$$t^2 + 2 \alpha_0 t + \alpha_1 = 0 \qquad 0 \leqslant t \leqslant 1 \tag{7.6}$$

where

$$\alpha_0 \triangleq \frac{\Delta\, \underline{d}_0^T\, [A_{ud}^r]\, \Delta\, \underline{u}_0}{\Delta\, \underline{u}_0^T\, [A_{uu}^r]\, \Delta\, \underline{u}_0}$$

$$\alpha_1 \triangleq \frac{\Delta\, \underline{d}_0^T\, [A_{dd}^r]\, \Delta\, \underline{d}_0 - c_r^*}{\Delta\, \underline{u}_0^T\, [A_{uu}^r]\, \Delta\, \underline{u}_0}$$

When equation (7.6) has no real solution, we could use equation (7.4).

Instead of moving along a line, it is possible to minimize $\|\underline{z} - \underline{z}_0\|^2$ or $\|\underline{u} - \underline{u}_0\|^2$ over the set E_z^r or over its projected cross-section, E_z^r $(\underline{d} = \underline{d}_0)$, respectively. However, in that case, the solution must be obtained by a numerical scheme, which could be time consuming.

Note that the underlying assumption here is that if, say, the r-th contingency occurs on the system, the present system configuration would assume the form for which E_z^r is computed.

The matrix $[A_r]$ can be chosen by experimentation. For instance, one can choose $[A_r]$ to be (see Appendix F)

$$[A_r] = \lambda_r^{max}\, [I] - (\lambda_r^{max} - \lambda_r^{min}) \left[\underline{\alpha}_r\, \underline{\alpha}_r^T\right] \qquad 0 < \lambda_r^{min} < \lambda_r^{max} \qquad \|\underline{\alpha}_r\| = 1 \tag{7.7}$$

and experiment with different $\dfrac{\lambda_r^{max}}{\lambda_r^{min}}$ and $\underline{\alpha}_r$. The eigenvalues of the above matrix are all λ_r^{max} except λ_r^{min} which is set less than λ_r^{max}. Since the eigenvector corresponding to λ_r^{min} is $\underline{\alpha}_r$, the resulting ellipsoid will be stretched primarily in the direction of $\underline{\alpha}_r$. This implies that a good choice for $\underline{\alpha}_r$ would be along a direction where S_z^r is known to be "long". Note that the inverse of $[A_r]$ for this case is simply

$$[A_r]^{-1} = \frac{1}{\lambda_r^{max}} [I] + \frac{\lambda_r^{max} - \lambda_r^{min}}{\lambda_r^{max} \lambda_r^{min}} \left[\underline{\alpha}_r \ \underline{\alpha}_r^T \right]$$

The simplicity, the low storage requirements, and the computational efficiency of this particular choice are important factors to consider. Because of these properties, it is more practical to embed a few different ellipsoids, with such $[A_r]$ matrices, inside each S_z^r, rather than to look for an optimal matrix $[A_r]$. Then, when the computation of a stand-by control strategy is needed, one can use these different ellipsoids to compute different control strategies and choose the most appropriate one. The computing efficiency of this choice is due to the fact that one can write

$$(\underline{z} - \underline{z}_r^*)^T [A_r] (\underline{z} - \underline{z}_r^*) = \lambda_r^{max} \|\underline{z} - \underline{z}_r^*\|^2 + (\lambda_r^{max} - \lambda_r^{min}) [\underline{\alpha}_r^T (\underline{z} - \underline{z}_r^*)]^2$$

To keep the storage requirements of $[A_r]$ down, one can also use a diagonal matrix. In that case, the logical choice for $[A_r]$ is $[A_z]$. The diagonal elements of $[A_z]$ are defined by

$$(a_{ii})_z \triangleq 1 / (z_i^M - z_i^m)^2 \qquad i = 1, \ldots , N_z \qquad (7.8)$$

where z_i^M and z_i^m are defined in equation (5.2). The resulting ellipsoid tries to fill up the hyper-box H_z, as much as possible.

7.2 Security Corridors

7.2.1 Motivation

The daily trajectory of a power system is defined by variations of the system's injection vector with time, over a 24-hour period. Many security related problems which arise during the operation of a power system can be best predicted and treated by understanding the relations existing between the system's daily trajectory and its various security sets. This is a well recognized concept which has been studied under the heading of "predictive security assessment", [9,103] .

The predictive security assessment is part of the overall operation planning in a power system. Based on the daily bus load forecasts [104, 105], it tries to predict in advance the critical conditions which may arise during the next day's operation. The approach followed by the industry, to study the steady state aspect of the system response to the predicted loading conditions, is to run a large number of load flows off-line along the predicted trajectory. The control strategies employed in these simulations are computed on the basis of the predicted loading conditions. The resulting data are then studied to find time intervals during which any one of the physical, operating, or security constraints may be violated. Corrective control strategies are computed and stored to be used in the event that the predicted violations actually take place.

Because of the point-wise nature of this scheme, the extremely large volume of the data produced in this process hardly reveals the relation between the system trajectory and the security sets. Moreover, since the actual trajectory always deviates somewhat from the predicted one, this pre-calculated data cannot be used to precisely establish the security of the system during its actual on-line operation.

In this section and the following ones, we examine how the process of predictive security assessment can be carried out by a region-wise approach. Our effort is focused primarily on the potential applications of such an approach to actual on-line security analysis.

7.2.2 Parameters Influencing a Daily Trajectory

Since at each instant, the system trajectory is defined by $\underline{z}^T = [\underline{u}^T ; \underline{d}^T]$, the parameters influencing it are those which affect the daily variations of $\underline{d}$ and $\underline{u}$.

The daily variation of the load, $\underline{d}$, is correlated to various environmental, industrial, and social factors [106, 107, 108] . If these factors do not drastically change from one day to another, the daily load trajectory will be repeated closely.

The daily variation of $\underline{u}$ is tied to the variation of $\underline{d}$, the cost and the extent of the generation available per bus, as well as the network configuration. Variations of $\underline{u}$ are closely linked to those of $\underline{d}$ because of the physical constraints on the system, i.e., at every instant demand must be met with sufficient generation. Since the demand is allocated between the generators primarily on an economic basis, the generation cost and the generation capacity of each generating unit have a profound influence on the daily pattern of $\underline{u}$. This means that losing a generating unit or bringing one on-line, could change the "normal" pattern of $\underline{u}$.

A change in the power network configuration alters, in general, the shape of all the security sets in the $\underline{z}$ space. This in turn affects the control strategy ($\underline{u}$) needed for secure operation, i.e., for keeping the system trajectory inside S_z and other security sets. Very often changes in the "generation status" of the system or in its configuration are required as part of the system's routine maintenance work. These changes are normally scheduled in advance, and their effects on the system trajectory are predictable.

Figure 7.2 illustrates a daily trajectory inside S_z. Note that since $\underline{u}$ is computed primarily based on an economic dispatch strategy, the system trajectory stays, most of the time, on or close to the boundary of S_z.

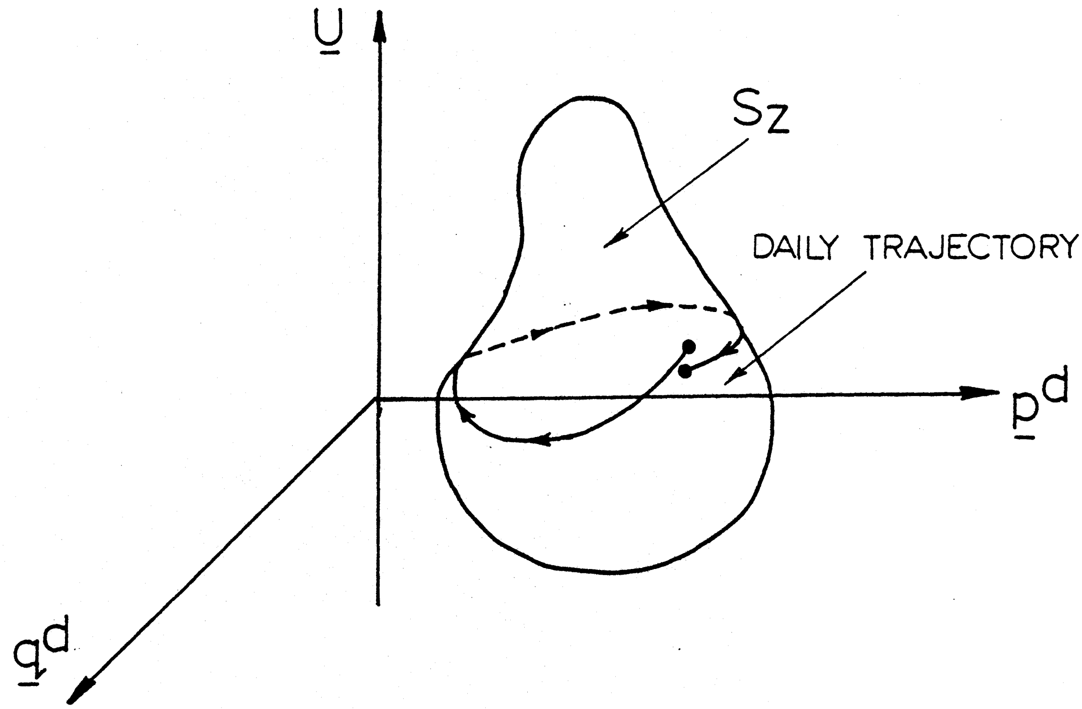

Figure 7.2. The relative position of a daily trajectory with respect to S_z.

An important observation here is that: once the system daily trajectory and the system configuration are predicted, within finite uncertainties, the significant part of S_z will be the neighbourhood surrounding the trajectory. In that case, instead of trying to characterize the whole S_z, it would be sufficient to characterize the part of the set surrounding the trajectory.

7.2.3 The Concept of a Security Corridor

Consider a circular tube in the $\underline{z}$ space whose inner axis coincides with a given (reference) daily trajectory. By proper choice of the size of the circular cross-sections of the tube, one can ensure that all the daily trajectories which stay close to the reference trajectory lie inside the tube. Let the tube be divided into 48 segments each corresponding to a 30 minutes time period marked by the trajectory. Since these segments are quite small, the secure part of each can be described by a small number of constraints. In that case, whenever the actual system trajectory is inside the tube and the system configuration is unchanged, the task of security monitoring will be quite simple. Instead of working with all the constraints defining the security set, the operator would deal with a specific segment of the tube and a small number of constraints which change every 30 minutes.

It is not generally possible to define an explicit circular tube whose inner axis is a general trajectory. This difficulty, however, can be resolved by replacing the tube by a number of over-lapping hyper-ellipsoids. A pictorial illustration of this is given in Figure 7.3. Since the hyper-ellipsoids are expressible by simple, explicit functions and they can be oriented to lie along the trajectory, they seem to be the logical choice for this purpose.

The hyper-ellipsoids replacing the tube are defined by

$$E^i \triangleq \{\underline{z} \,/\, (\underline{z} - \underline{z}_i)^T \, [A_i] \, (\underline{z} - \underline{z}_i) \le c_i\} \quad i = 1, \ldots , n \qquad (7.9)$$

where n is their total number. Their union forms a corridor which is denoted by E^c, i.e.,

$$E^c \triangleq \bigcup_{i=1}^{n} E^i$$

We refer to the secure part of E^c, denoted by E^c_s, as the "security corridor", which is defined by

$$E^c_s \triangleq E^c \cap S_z = \bigcup_{i=1}^{n} E^i_s \qquad (7.10)$$

where E^i_s is the secure part of E^i. Now the major problems to be resolved are the following:

(1) How to choose $[A_i]$, $i = 1, \ldots , n$ to ensure that the hyper-ellipsoids are oriented along the trajectory;

(2) How to ascertain that E^i, $i = 1, \ldots , n$ are overlapping sufficiently;

(3) How to characterize E^i_s, $i = 1, \ldots , n$.

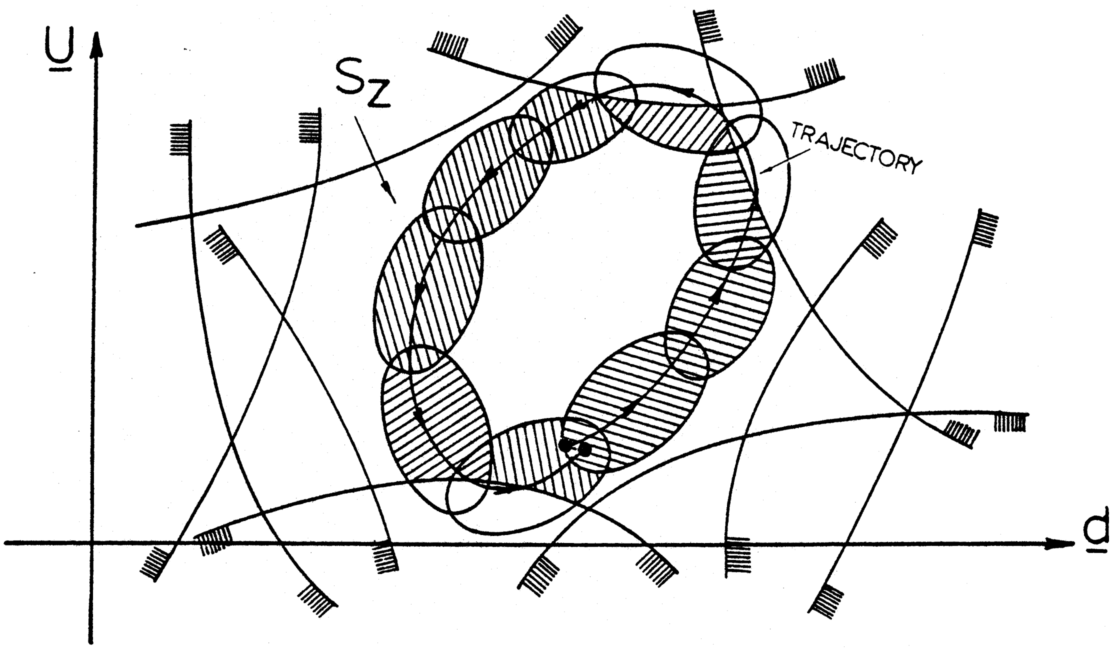

Figure 7.3. A pictorial representation of a reference daily trajectory and its associated security corridor.

7.2.4 Orientation Problem

The center of the hyper-ellipsoids ($\underline{z}_i$ $i = 1, \ldots, n$) are chosen on the reference trajectory. Let the tangents to the trajectory at $\underline{z}_i$ be represented by $\underline{a}_i$. The hyper-ellipsoids are laid along the trajectory by making sure that their major axis lie along $\underline{a}_i$, $i = 1, \ldots, n$. In Appendix F two techniques for constructing $[A_i]$, $i = 1, \ldots, n$ with such a property is discussed. We introduced the first approach earlier in Section 7.1.2 (equation (7.8)). The other approach is based on the Gram-Schmidt orthogonalization process. Both approaches allow efficient computation of $[A_i]$ as well as $[A_i]^{-1}$.

A daily trajectory is normally available only at discrete points, termed the "base points". The trajectory is then approximated by linear interpolation of the base points. As a result, computation of $\underline{a}_i$, $i = 1, \ldots, n$ is quite simple.

7.2.5 Overlapping Problem

Here, two ellipsoids are assumed to be overlapping sufficiently when at least the last quarter of the time period covered by the first ellipsoid is part of the time covered by the second. The time covered by an ellipsoid is defined to be the period that the trajectory is inside that ellipsoid.

The parameters affecting the overlapping of the ellipsoids are primarily c_i, $i = 1, \ldots, n$. For a given c_i, one can find the points where the trajectory enters and leaves E^i. This is particularly simple when the trajectory is given by a piece-wise linear function. First, by checking the membership in E^i of the base points neighbouring $\underline{z}_i$, the two segments of the trajectory which are intercepted by the boundary of E^i are identified (see Figure 7.4). Next by solving two quadratic equations, similar in form to equation (7.6), the intercepting points are computed. If the time of entering and the exit time, respectively, happen to be well inside the time periods covered by E^{i-1} and E^{i+1}, it is clear that sufficient overlapping among E^{i-1}, E^i, and E^{i+1} exists.

If sufficient overlapping is not achieved, either the values of c_{i-1}, c_i, and c_{i+1} must be increased, or the points $\underline{z}_i$ and $\underline{z}_{i+1}$ have to be chosen closer to $\underline{z}_{i-1}$.

7.2.6 Characterization Problem

Consider E^i_s. By definition

$$E^i_s = E^i \cap S_z = E^i \cap \left(\bigcap_{j=1}^{2N_{dp}} Z^j \right) \cap H_z \tag{7.11}$$

We would like to represent E^i_s according to

$$E^i_s = E^i \cap \left(\bigcap_{j\epsilon I^i} Z^j \right) \cap H_z \tag{7.12}$$

The members of the set I^i identify those constraints Z^j which intersect E^i. These constraints can be recognized by solving the following optimization problem:

$$\text{Minimize } c^{\ell}_{ij} = (\underline{z} - \underline{z}_i)^T [A_i] (\underline{z} - \underline{z}_i) \tag{7.13}$$

subject to

$$y_j = y^{\ell}_j \qquad (\ell = M \text{ or } m)$$

for $j = 1, \ldots, N_{dp}$. The above problem is identical to the one discussed in Section 6.1.3. There, it is demonstrated that when y_j is approximated by $\hat{y}_j = \underline{\beta}_j^T (\underline{x}_0)\, \underline{z}$, the solution to the above problem is simply

$$\hat{c}_{ij}^{\ell} = \frac{[y_j^{\ell} - \underline{\beta}_j^T (\underline{x}_0)\, \underline{z}_i]^2}{\underline{\beta}_j^T (\underline{x}_0)\, [A_i]^{-1}\, \underline{\beta}_j (\underline{x}_0)} \qquad \begin{array}{l} \ell = M \text{ or } m \\ j = 1, \ldots , N_{dp} \end{array} \tag{7.14}$$

Then the constraint $\hat{y}_j \leq y_j^M$ is redundant to E_s^i if and only if $\hat{c}_{ij}^M > c_i$. For more accurate results, the proposed algorithms of the last chapter should be employed.

7.2.7 <u>General Remarks on Constructing a Security Corridor</u>

The choice of $\underline{z}_i$ and c_i , $i = 1, \ldots , n$ is crucial to the construction of a security corridor. Some of the important points relevant to their choice are discussed below.

To keep n small, it is essential to choose $\underline{z}_i$ $(i = 1, \ldots , n)$ on long segments of the trajectory, as much as possible, or on segments which do not make large angles with their neighbouring segments. Moreover, to ensure that the resulting E_s^i will not be empty, $\underline{z}_i$ <u>must</u> belong to S_z .

To have an idea of the size of E^i, one can use the formula

$$\% \Delta \; P_d^{max} = \frac{200}{(P_d)_i} \{c_i \underline{\alpha}^T [A_i]^{-1} \underline{\alpha}\}^{1/2} \tag{7.15}$$

The above formula gives the maximum percent change that the total real demand, P_d, can have inside E^i with respect to $(P_d)_i$, the total demand at $\underline{z}_i$. It is derived by solving the following optimization problem:

$$\text{Maximize } P_d = P_1^d + P_2^d + \ldots + P_{N_d}^d = \underline{\alpha}^T \underline{z}$$

subject to

$$(\underline{z} - \underline{z}_i)^T [A_i] (\underline{z} - \underline{z}_i) = c_i \tag{7.16}$$

Computing the percent change inside E^i of various injections along the eigenvectors of $[A_i]$ also gives a good indication of the relative size of E^i.

The size of E^i is obviously a function of c_i. The value of c_i, however, cannot be increased freely. A large value for c_i could increase the number of the constraints defining E_s^i significantly, defeating the prime objective of constructing E_s^c. A small c_i, on the other hand, makes E^c narrow around $\underline{z}_i$ and causes the daily trajectories with slight deviation from the reference trajectory to leave E^c.

The size and shape of E^i depend also on the eigenvalues of $[A_i]$, over which we have control.

We found the following steps for choosing $\underline{z}_i$ and c_i and constructing E_s^i quite practical.

Step 1 : Choose $\underline{z}_i$ on a long segment of the trajectory and run a load flow to ascertain $\underline{z}_i \in S_z$.

Step 2 : Compute $\underline{a}_i$, $[A_i]$, and $[A_i]^{-1}$ (see Appendix F).

Step 3 : Compute values of c_{ij}^M and c_{ij}^m, $j = 1, \ldots, N_{dp}$, using equation (7.14), and tabulate them in ascending order.

Step 4 : Decide on N_i^{max}, the maximum number of elements that I^i can have.

Step 5 : Choose the value of c_i to be the first c_{ij}^{ℓ} in the list (i.e., the smallest c_{ij}^{ℓ}) and compute the time when the trajectory enters and leaves the resulting E^i, as well as the corresponding $\% \Delta P_d$.

Step 6 : Repeat Step 5 for the next N_i^{max} values of c_{ij}^{ℓ} in the list and tabulate the results.

Step 7 : Compare the results with those of E^{i-1} in order to establish what value for c_i should be chosen in order to have:

(a) sufficient overlapping with E^{i-1} ;

(b) comparable size with E^{i-1} ;

(c) a small number of constraints $(< N_i^{max})$ intersecting E^i .

If such a c_i cannot be found, then either change the eigenvalues of $[A_i]$ or choose $\underline{z}_i$ closer to $\underline{z}_{i+1}$ and repeat the relevant steps.

The sixth step above, implies that the value of c_i is actually bounded from above by the restriction on the number of elements in I^i . The largest value that c_i can assume is the value of the $(N_i^{max} + 1)$ - th c_{ij}^{ℓ} , when values of c_{ij}^{ℓ} , $j = 1, \ldots, N_{dp}$, $\ell = M$ or m , are ordered ascendingly. The number of elements in I^i $(i = 1, \ldots, n)$ is limited mainly because of the non-sparsity of the vectors $\underline{\beta}_j(\underline{x}_i)$ $j \epsilon I^i$, $i = 1, \ldots, n$ which tax the available memory in the system heavily.

As a rule of thumb, when the system is lightly loaded (e.g., between 9.00 P.M. to 6.00 A.M.) the points $\underline{z}_i$ $(i = 1, \ldots, n)$ can be chosen far from each other. This is due to the fact that during this

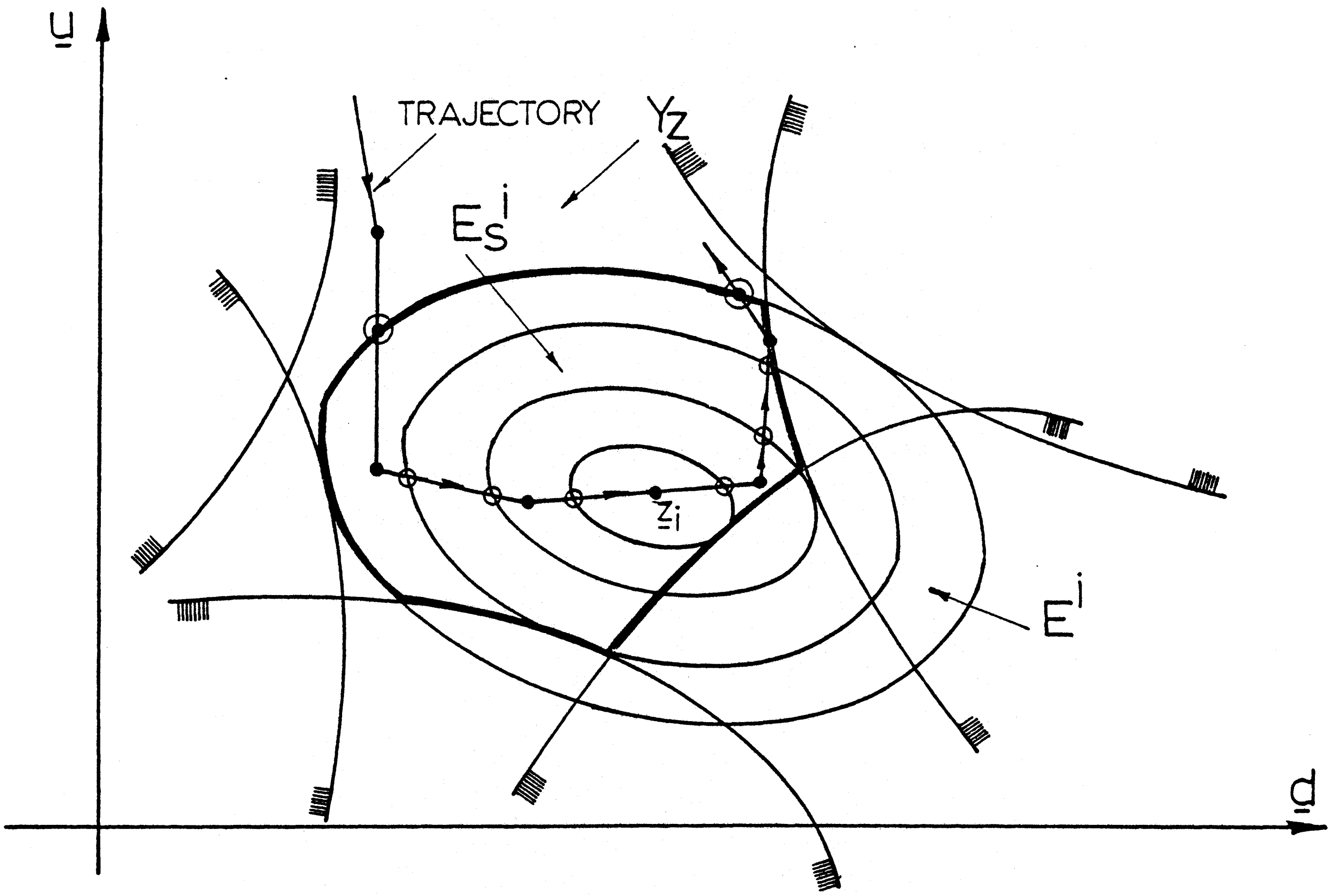

Figure 7.4. An illustration of the way the size of E^i and E_s^i could vary with c_i.

period the trajectory is expected to be well inside Y_z. An ellipsoid under this condition could cover a wide range of operating hours and could be represented with very few or no constraints from Y_z. On the other hand, when the system is heavily loaded (e.g., around noon), the center of the hyper-ellipsoids have to be chosen close to each other in order to keep the number of intersecting constraints per ellipsoid small.

7.2.8 Example

In this section, for a typical reference daily trajectory, the detailed characterization of the secure part of a hyper-ellipsoid and the computation of a security corridor inside S_z for a 5-bus system is presented. The prime objective of this example is to demonstrate the feasibility of the proposed scheme. No attempt is made to produce an "optimal" security corridor.

System Data

(i) Network structure (Figure 7.5).

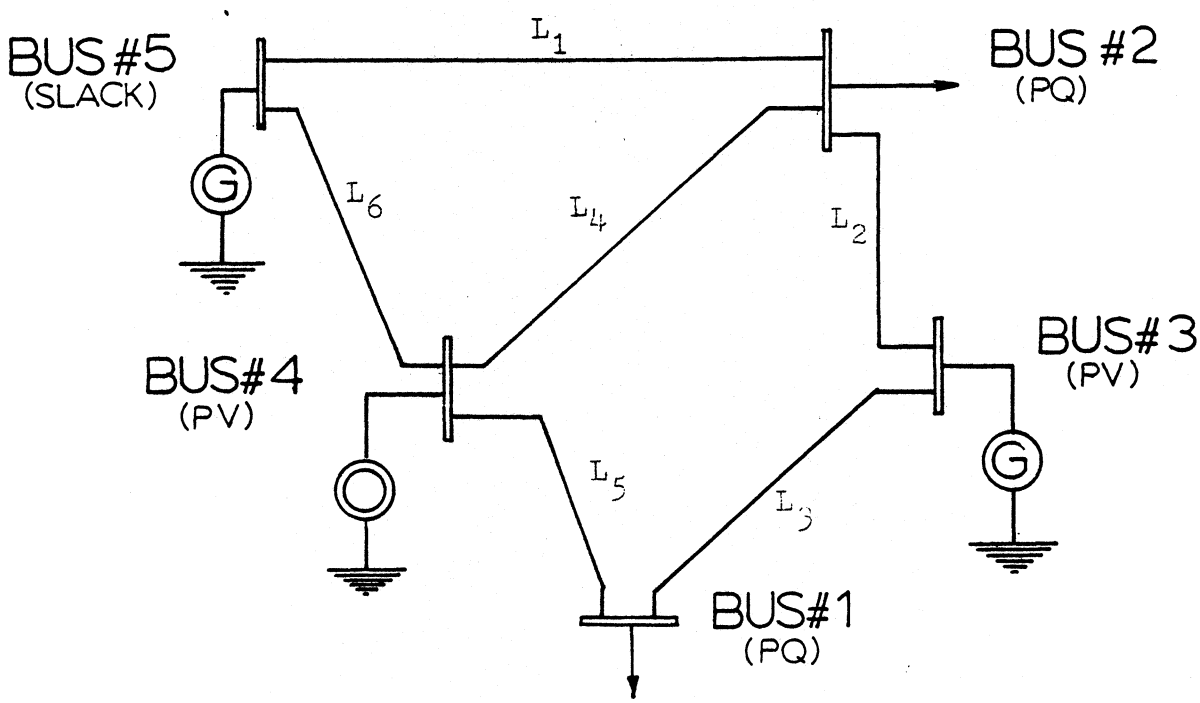

Figure 7.5. Network configuration for the example.

(ii) Network Data

Line	Impedance (p.u)	Susceptance (p.u)
1	0.030 + j 0.100	0 + j 0.015
2	0.020 + j 0.060	0 + j 0.020
3	0.025 + j 0.090	0 + j 0.012
4	0.010 + j 0.030	0 + j 0.008
5	0.025 + j 0.105	0 + j 0.010
6	0.025 + j 0.105	0 + j 0.010

(iii) Operating Constraints

$$\underline{u}^m = \begin{bmatrix} 0.9604 \\ 0.9604 \\ 1.1025 \\ 0.3 \\ 0.0 \end{bmatrix} \le \underline{u} \le \begin{bmatrix} 1.0404 \\ 1.0404 \\ 1.1664 \\ 0.8 \\ 0.0 \end{bmatrix} = \underline{u}^M \qquad \begin{aligned} u_1 &= v_3^2 = z_3 \\ u_2 &= v_4^2 = z_4 \\ u_3 &= v_5^2 = z_5 \\ u_4 &= p_3 = z_8 \\ u_5 &= p_4 = z_9 \end{aligned}$$

$$\underline{d}^m = \begin{bmatrix} 0.0 \\ 0.0 \\ 0.0 \\ 0.0 \end{bmatrix} \le \underline{d} \le \begin{bmatrix} 0.5 \\ 1.0 \\ 1.5 \\ 2.0 \end{bmatrix} = \underline{d}^M \qquad \begin{aligned} d_1 &= -q_1 = z_1 \\ d_2 &= -q_2 = z_2 \\ d_3 &= -p_1 = z_6 \\ d_4 &= -p_2 = z_7 \end{aligned}$$

$$
\underline{y}^m = \begin{bmatrix} 0.9025 \\ 0.9604 \\ -0.1 \\ -0.85 \\ 0.15 \\ 0.8 \\ - \\ - \\ - \\ - \\ - \\ - \end{bmatrix} \le \underline{y} \le \begin{bmatrix} 0.9801 \\ 1.0404 \\ 0.5 \\ 0.0 \\ 1.5 \\ 2.4 \\ 2.1025 \\ 0.25 \\ 0.5625 \\ 0.25 \\ 0.5625 \\ 1.44 \end{bmatrix} = \underline{y}^M
\qquad
\begin{array}{l} y_1 = v_1^2 \\ y_2 = v_2^2 \\ y_3 = q_3 \\ y_4 = q_4 \\ y_5 = q_5 \\ y_6 = p_5 \\ y_7 = |I_1|^2 \\ y_8 = |I_2|^2 \\ y_9 = |I_3|^2 \\ y_{10} = |I_4|^2 \\ y_{11} = |I_5|^2 \\ y_{12} = |I_6|^2 \end{array}
$$

All the values are in p.u.

Reference Trajectory Data

For simplicity, the following control variables are assumed to remain at the following specified values during the operation,

$$z_3 = 1.0 \quad ; \quad z_4 = 1.0 \quad ; \quad z_5 = 1.1664 \quad ; \quad z_9 = 0.0 \ .$$

Variation of the other injections with time over a 24-hour period is given in Figure 7.6. The loads are computed based on a load forecasting

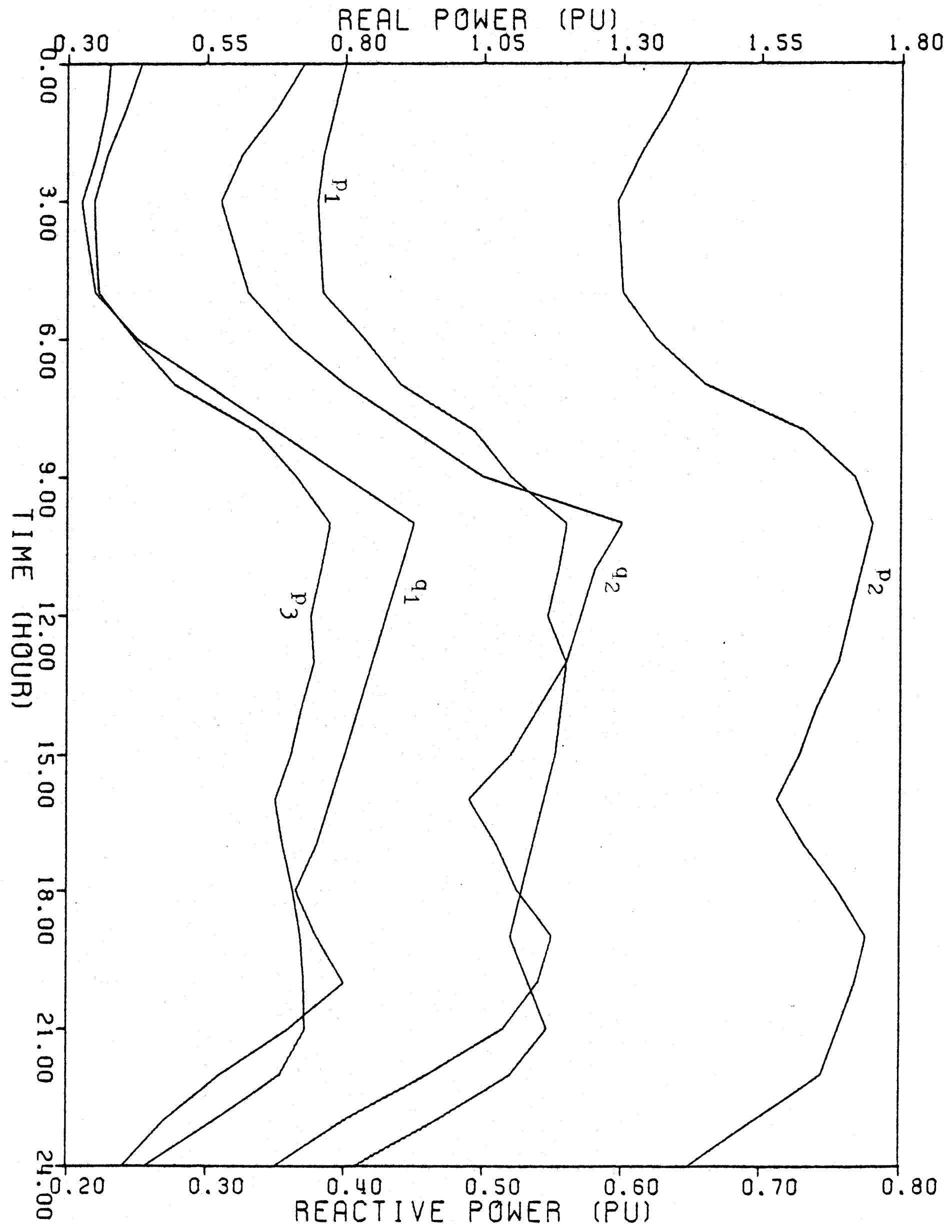

Figure 7.6. Daily variations of the indicated injections for the system in Figure 7.5.

scheme, and the generation is based on an economic dispatch strategy.

Detailed Computation of a Hyper-ellipsoid

The center of E^1 is chosen at $\underline{z}_1$ where

$$\underline{z}_1^T = [-0.227, -0.35, 1.0, 1.0, 1.1664, -0.78, -1.38, 0.403, 0.0] .$$

From Figure 7.6 it can be seen that $\underline{z}_1$ represents the system condition at $t = 1{:}00$. The unit vector tangent at the trajectory at $\underline{z}_1$ is simply:

$$\underline{a}_1^T = [-0.1026, -0.3666, 0.0, 0.0, 0.0, -0.2933, -0.7332, 0.4812, 0.0] .$$

The angle that $\underline{a}_1$ makes with the preceding segment is relatively small and one can easily show that $\underline{x}_1 \in S_x$, where $\underline{x}_1$ is the load flow solution to $\underline{z}_1$, given by

$$\underline{x}_1^T = [0.9732, 0.9972, 0.9972, 0.9979, 1.08, -0.1035, -0.0777, -0.075, -0.06436] .$$

To construct $[A_1]$, we have chosen the approach based on the Gram-Schmidt orthogonalization process, (see Appendix F). The eigenvalues of $[A_1]$ are picked empirically according to

$$\lambda_j = 400 \quad \text{when} \quad |(a_j)_1| = 0.0 \text{ or very small}$$

$$\lambda_j = 1 \quad \text{when} \quad (a_j)_1 = \underset{k}{\text{Max}} \{(a_k)_1\}$$

$$\lambda_j = 16 \quad \text{otherwise}$$

$$j=1, \ldots, N_z \qquad (7.17)$$

For the resulting $[A_1]$, the exact values of all c^{ℓ}_{1j} (using the algorithms of Chapter VI) and their approximate values (equation (7.14)) are computed. Table 7.1 summarizes the first 15 of these values and other relevant information as required in steps 5 and 6 of Section 7.2.7.

A quite similar type of data results when the alternative approach of constructing $[A_1]$ is pursued.

From the table, it is clear that the approximate $(\hat{c}^{\ell}_{1j})$ and the exact values of c^{ℓ}_{1j} are often very close. This is in particular true for those at the top of the list, which happen to be the most important ones.

As can be seen from the table, if one chooses $c_1 = 0.07279$, the set E^1_s will be simply:

$$E^1_s = H_z \cap E^1 \qquad (7.18)$$

TABLE 7.1.

BASIC DATA FOR THE CHOICE OF c_1 AND I^1

CORRESPONDING TO $t_1 = 1{:}00$ AND $N_1^{max} = 14$

(AS REQUIRED IN STEPS 4 TO 6 OF SECTION 7.2.7)

Limiting Constraints j, ℓ	c_{1j}^{ℓ}	$\hat{c}_{1j}^{\ell}$	$\%\Delta P_d^{max}$	t_{in}	t_{out}	$t_{in} - t_{out}$
4, m	0.07279	0.07273	26.35	23:42	6:06	6:24
3, m	0.1195	0.1191	33.76	23:24	6:46	7:22
10, M	0.1726	0.1718	40.57	23:17	6:56	7:39
5, M	0.1880	0.1878	42.35	23:15	6:58	7:43
1, M	0.22016	0.2160	45.82	23:12	7:04	7:52
4, M	0.3337	0.334	56.42	23:01	7:42	8:41
3, M	0.3991	0.4005	61.70	22:53	7:46	8:53
7, M	0.5767	0.5901	74.17	22:13	7:55	9:42
6, M	0.6174	0.6304	76.74	22:12	7:58	9:46
12, M	0.6704	0.6775	79.97	22:10	8:00	9:50
2, m	1.0183	1.059	98.55	21:51	8:58	11:07
2, M	1.0419	1.002	99.69	21:10	8:59	11:49
1, m	1.346	1.412	113.32	21:03	9:23	12:20
8, M	1.4636	1.512	118.16	16:48	9:52	17:04
9, M	1.785	1.822	130.50	15:32	9:58	18:26

$t_1 = 1{:}00$; $N_1^{max} + 1 = 15$.

i.e., no constraint from Y_z is needed to characterize the secure part of E_s^1. The resulting E^1 covers nearly 6 hours of the trajectory, during which the total real power demand can deviate from its expected value up to 26% . This is typical for the periods where the system is lightly loaded.

It is interesting to note that the first constraints [(4, m) and (3, m)] limiting the ellipsoid are those which correspond to the lower bounds on the reactive power generations. This is indicative of the tendency of the generators in the system to reduce their reactive generations (or to generate negative reactive power) under the lightly loaded conditions, where a relatively large amount of positive reactive power is produced by passive elements in the system.

The next constraint limiting E^1, (10, M), corresponds to the upper-bound on a line current magnitude. Obviously the reactive component of the current is responsible for the rise in the current magnitude.

The third type of constraint which limits E^1, under these conditions, are normally those corresponding to the upper bounds on the voltage limits at the load buses. This is again due to the production of a large amount of positive reactive power in the system by the passive elements which tends to rise the voltage level at the load buses.

Computation of a Security Corridor

By choosing other points on the trajectory and repeating the above computations, a security corridor corresponding to the given trajectory is constructed. The important quantities defining the security corridor are tabulated in Table 7.2. Note that in this table t_i, when used in conjunction with Figure 7.6, specifies $\underline{z}_i$, $\underline{a}_i$, and consequently $[A_i]$. For simplicity and reduction in the volume of the data, the eigenvalues of $[A_i]$, i = 1, ... , 11 are all chosen according to (7.17). The negative numbers in I^i, i = 1, ... , 11, indicate that the constraints corresponding to the lower bounds on the relevant dependent variables have to be considered. A positive number implies the alternative.

The ellipsoids forming the corridor are overlapping sufficiently. This can be seen easily by comparing the times that the trajectory enters (t_{in}) and leaves (t_{out}) the ellipsoids. By choosing $N_i^{max} = 5$, i = 1, ..., 11, the number of elements in I^i, i = 1, ... , 11 is kept small.

By expressing each E_s^i according to

$$E_s^i = H_z \cap E^i \cap \{\underline{z} / \underline{\beta}_j^T (\underline{x}_i) \underline{z} \le y_j^\ell \; ; \; j \in I^i\} \qquad i = 1, \ldots, n \tag{7.19}$$

where $\underline{x}_i$ is the load flow solution to $\underline{z}_i$, one can show that the reference trajectory used here is fully inside S_z. This requires

TABLE 7.2

THE CONDENSED DATA FOR A SECURITY CORRIDOR

INSIDE S_z , FOR THE SYSTEM OF FIGURE 7.5.

E^i	t_i	c_i	I^i	$\%\Delta P_d^{max}$	t_{in}	t_{out}
1	1:00	0.1726	{-4, -3}	40.6	23:17	6:56
2	7:00	0.1944	{-4}	43.2	4:37	8:58
3	11:00	0.0823	{9, 6, 4, 7}	21.79	8:12	11:44
4	12:00	0.1022	{10, 4, 9}	10.60	11:14	12:29
5	13:00	0.1045	{4, 6, 7, 9, 10}	22.10	11:52	13:51
6	14:00	0.1093	{4, 6, 7, 9}	22.50	13:11	15:13
7	15:00	0.1237	{4, 6, 3, 7}	25.33	14:18	17:15
8	17:00	0.2173	{10, 4, 3, 6, 7}	22.26	15:26	17:44
9	18:00	0.2117	{10, 4, 7, 6, 3}	19.06	16:19	20:28
10	21:00	0.1211	{9, 4, 6, 7}	21.82	19:04	22:41
11	23:00	0.1955	{-4, -3, 10}	45.67	20:52	02:57

simply checking the base points forming the trajectory against the constraints which define the secure part of the ellipsoids containing them.

Examining the values of $\% \Delta P_d^{max}$ for different hyper-ellipsoids, one observes that a significant deviation in the total real demand with respect to the predicted values on the trajectory can be tolerated inside each hyper-ellipsoid. The smallest permissible deviation is inside E^4 and corresponds to the time period when the system is most heavily loaded. If desired, by changing the eigenvalues of $[A_4]$ and the inclusion of more constraints in the definition of E_s^4, it is possible to increase the $\% \Delta P_d^{max}$ for E^4.

7.3 General Features and Potential Applications of Security Corridors

Suppose the next-day load trajectory is predicted by a bus load forecast routine in the form of a piece-wise linear function in the $\underline{d}$ space. By computing the required controls for the predicted loading conditions and the anticipated system structure at successive short intervals, a daily trajectory can be formed. The controls can be computed simply by a generation constrained economic dispatch routine. As discussed in Section 7.2.1, constructing a security corridor around such a trajectory is tantamount to a region-wise predictive security assessment. In the following, various features and potential applications of a security corridor surrounding the trajectory is discussed.

7.3.1 General Features

(a) Accommodating the Uncertainties

The matrices $[A_i]$, $i = 1, \ldots , n$ can be chosen to correspond to the covariance matrices of the probability errors in the load forecast and in the control settings at $\underline{z}_i$, $i = 1, \ldots , n$. The resulting hyper-ellipsoids would be stretched in the directions where the deviations from the expected values are large. As such, the resulting E^c would try to accommodate the uncertainties in the load forecast and the controls.

This particular choice of the matrices $[A_i]$, $i = 1, \ldots , n$, however, suffers from excessive storage requirements, and results in computational inefficiency.

(b) Identification of Critical Conditions

During the construction of the security corridor, by following the trajectory inside the secure part of each hyper-ellipsoid, one can easily find when the trajectory leaves S_z , what constraints are crossed (violated) by the trajectory, and when the trajectory re-enters S_z . The insecure part of the trajectory then has to be redefined by the operator, by computing new control strategies capable of keeping the trajectory inside S_z . Consequently, during the actual operation, the operator will know approximately when the routine control strategy has to be switched to a new one, what type of strategy has to be used, and for how long the new strategy should be followed.

(c) Identification of Important Constraints

The sets I^i, $i = 1, \ldots, n$ identify the important constraints for different time intervals. These constraints can be expressed linearly in the $\underline{z}$ space with high accuracy by choosing their expansion point to be the center of their relevant ellipsoids. Since their number per ellipsoid is quite small, the computation and storage requirements of $\underline{\beta}_j (\underline{x}_i)$, $i = 1, \ldots, n$, $j \in I^i$, is not excessive.

(d) Load Flow Runs

Since no load flow run is needed to check the security of a point inside a hyper-ellipsoid whose secure part is already characterized, the required number of load flow runs for this approach is relatively small. Under favourable circumstances, the load flow runs, needed to construct a security corridor inside S_z, are limited to the verification of $\underline{z}_i \in S_z$, $i = 1, \ldots, n$.

(e) Predictable Changes in System Configuration and Generation Status

Because of the routine maintenance work, the power system's configuration and generation status can change during the day. These changes are, however, scheduled in advance and can be taken into account in the process of constructing a security corridor.

(f) Treatment of Contingencies

After constructing a security corridor inside S_z and fixing the system trajectory, one can ideally construct a security corridor corresponding to each probable contingency, or equivalently each security set. Then, by finding the time intervals where the trajectory is inside each security set, one can estimate the periods when the system is invulnerable to a given contingency and its monitoring is not needed.

7.3.2 Application to Security Monitoring

As mentioned earlier, security corridors can be used for on-line monitoring of the system conditions. This is possible as long as the system topology is identical to the one for which the security corridors are computed.

Consider an operating point $\underline{z}_g$ and a security corridor E_s^c. The steps which have to be followed for monitoring $\underline{z}_g$ are the following:

Step 1 : Compare the time at which $\underline{z}_g$ occurs with the time interval covered by each ellipsoid forming E^c to identify the relevant ellipsoid.

Step 2 : Let E^k be identified in Step 1. Compute

$$r_g = (\underline{z}_g - \underline{z}_k)^T [A_k] (\underline{z}_g - \underline{z}_k) \tag{7.21}$$

Step 3 : If $r_g < c_k$, find all the constraints defined by I^k for which $c^{\ell}_{kj} < r_g$ ($\ell = M$ or m, $j \in I^k$) .

Step 4 : Check $\underline{\beta}^T_j (\underline{x}_0) \underline{z}_g \le y^{\ell}_j$ only for those constraints identified in Step 3 .

Step 5 : Repeat the above steps for the security corridors constructed for other security sets.

Figure 7.7 demonstrates why in Steps 3 and 4 one needs to check only those constraints for which $c^{\ell}_{kj} < r_g$, $j \in I^k$. For this particular example $I^k = \{1, -2, 3\}$, $c_k = c^m_{4k}$, and for the indicated operating point only the constraint $y_1 \le y^M_1$ must be verified.

Note that as long as $r_g \le c_k$, the operating point is inside or on E^k . When $r_g > c_k$. we cannot use E^k for verifying the security of $\underline{z}_g$ and a load flow run is then needed to check whether or not $\underline{z}_g \in S_z$.

7.3.3 Application to Security Control

Among the control options open to the system operator for security control, are the following major control actions:

(a) Rescheduling of real power generations;

(b) Rescheduling of reactive power generations to:

(1) Reset voltage levels at generation buses;

(2) Allow shunt reactor or capacitor switching;

(c) Changing the network topology via switching actions.

In the following, we examine how such control actions can be computed using the security corridors.

Computation of Stand-by Controls

The ellipsoids forming the security corridors can be used to compute stand-by control strategies. Since the center of the ellipsoids are inside their corresponding security sets, it is possible to compute the required controls based on the approach of Section 7.1.

In Figure 7.7 we have shown graphically how an acceptable control strategy can be computed for an operating point $\underline{z}_0$ outside the secure part of an ellipsoid E^k. The line connecting the center of E^k to $\underline{z}_0$ is intercepted by all those constraints in E^k_s which

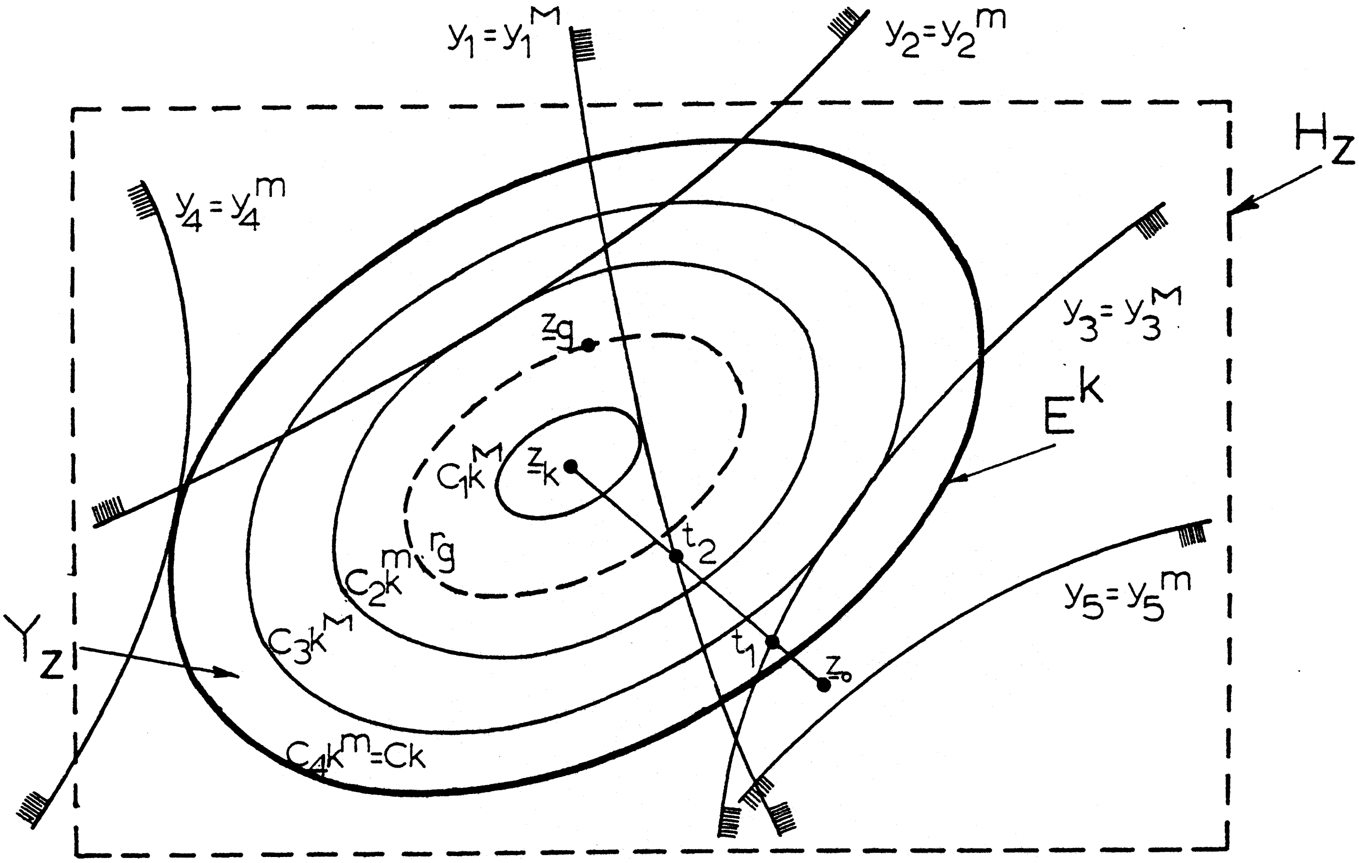

Figure 7.7. Justification of steps 3 and 4 of the security monitoring scheme based on the security corridors.

are violated by $\underline{z}_0$. Since these constraints are represented by linear or quadratic functions of $\underline{z}$, the intercepting points can be easily computed. Among them, the point closest to the center of E^k is on the boundary of E_s^k and represents a feasible solution.

Note that here one can also try to avoid load shedding by fixing the demand part of $\underline{z}$ in the constraints defining E_s^k. (See Section 7.1.2). However, when this fails to produce a solution, one can repeat the approach on other ellipsoids forming the security corridors.

Evaluation of Corrective Controls

Corrective controls are computed when in an emergency state the violated constraint(s) may be tolerated for a limited time period. If the required controls involve only rescheduling of real power operations and altering the voltage levels, as discussed above, they may be computed with the help of a security corridor inside S_z.

Corrective controls may include switching of the shunt reactors or capacitors of the system. When such elements are located at the PQ buses, their switching results in certain changes in the demand components of the operating point. In Appendix G it is demonstrated that these changes can be estimated accurately. Thus, one can use security corridors to verify whether the post switching operating point is secure, or what should be the extent of the changes to ensure security.

Having access to the security corridors corresponding to different system configurations, gives one the opportunity to study the effectiveness of corrective controls based on changing the network topology. Using the security corridors, the operating point which has resulted in an emergency condition can be checked against various security sets. Any network configuration whose associated security set contains that point, represents a possible control strategy. Of course, the feasibility of implementing such switching control strategies must be decided by the system operator.

Note that an emergency, stand-by, or corrective control strategy may consist of a combination of the three listed types of control actions. In that case, the security corridors represent a fast and efficient way of computing, or verifying the effectiveness of, the computed or decided control actions.

7.4 Construction of Security Corridors Using Hyper-Boxes

The use of hyper-boxes in constructing security corridors deserves special attention. The important advantages of using hyper-boxes over the ellipsoids are the following:

(i) To verify the membership of a point in a hyper-box very little computation is required;

(ii) Overlapping of two hyper-boxes can be checked trivially;

(iii) The required computation for characterizing the secure part of a hyper-box is straightforward.

(iv) The redundant constraints existing in the implicit description of the secure part of a hyper-box can be easily identified.

To clarify the last two statements, consider a hyper-box H_b, defined by

$$H_b \triangleq \{\underline{z} \ / \ \underline{z}_b^m \leq \underline{z} \leq \underline{z}_b^M\} \qquad (7.28)$$

Let us expand the dependent variables linearly about $\underline{x}_b$, the voltage solution to $\underline{z}_b = \frac{1}{2}(\underline{z}_b^M + \underline{z}_b^m)$ the center of the hyper-box. To find the constraints intersecting with H_b, one needs to solve the following LP problem :

$$\text{Extremize :} \quad \underline{\beta}_j^T(\underline{x}_b)\,\underline{z} = \sum_{k=1}^{N_z} (\beta_k)_j \, z_k \tag{7.29}$$

subject to

$$(z_k^m)_b \leq z_k \leq (z_k^M)_b \qquad k = 1, \ldots, N_z$$

The above problem has to be solved for all the constraints in Y_z. Consider the case where the objective function must be maximized. By simply examining how it can assume its maximum value over H_b, one arrives at the solution. The solution point, $\underline{z}^*$, is given by

$$\begin{aligned} z_k^* &= (z_k^M)_b \qquad \text{when} \quad (\beta_k)_j > 0 \\ z_k^* &= (z_k^m)_b \qquad \text{when} \quad (\beta_k)_j < 0 \\ & \qquad\qquad k = 1, \ldots, N_z \end{aligned} \tag{7.30}$$

Then if $\underline{\beta}_j^T(\underline{x}_b)\,\underline{z}^* < y_j^M$, one concludes that the constraint $\underline{\beta}_j^T(\underline{x}_b)\,\underline{z} \leq y_j^M$ does not intersect the hyper-box. The minimum of the objective function is also required to fully understand the relation between the hyper-box and the constraints $y_j^m \leq \underline{\beta}_j^T(\underline{x}_b)\,\underline{z} \leq y_j^M$. That can be similarly computed.

Let us denote the secure part of H_b by H_s. It is defined by

$$H_s \triangleq H_z \cap H_b \cap \{\underline{z} \,/\, \underline{\beta}_j^T (\underline{x}_b)\, \underline{z} \le Y_j^{\ell} \,,\quad j \in J^b\} \tag{7.31}$$

where the members of the set J^b represent the constraints from Y_z intersecting H_b. It is clear that one can always pick up $\underline{z}_b^M$ and $\underline{z}_b^m$ such that $H_z \cap H_b = H_b$. Moreover, the redundant constraints among those defined by J^b can be identified easily by solving a few small LP problems (see Section 6.3.2).

In Figure 7.8, the construction of a security corridor using hyper-boxes is demonstrated. The difficulties which are noted in that process are the following:

(i) One needs a large number of hyper-boxes to cover a daily trajectory ;

(ii) To verify the membership of a point to H_s, all the constraints in the set have to be checked (compare with the case where ellipsoids are used, i.e., Section 7.3.2, Step 4).

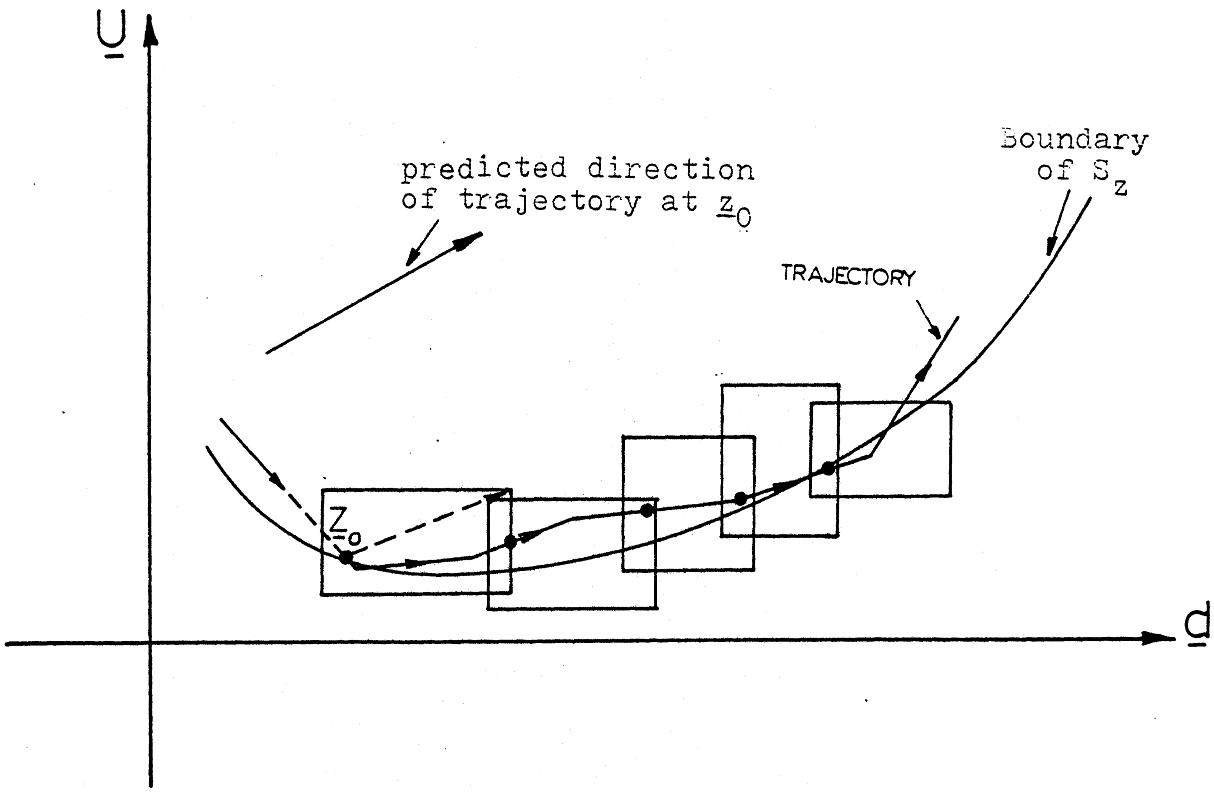

Figure 7.8. Construction of a security corridor, using hyper-boxes.

7.5. A New Monitoring Scheme

Consider the case where the operating point, $\underline{z}_g$, is inside S_z , and load flow runs are used for monitoring the system conditions. In the following, we demonstrate how one can use the result of a load flow run (for $\underline{z}_g$) to characterize the secure part of an ellipsoid surrounding $\underline{z}_g$ fast and efficiently. The operating points following $\underline{z}_g$ then can be monitored using this ellipsoid, often for a significant time duration. When the operating points leave the ellipsoid, a new load flow can then be run and the same procedure repeated.

We emphasize that this monitoring scheme, since it does not require any information on the future load variations, can be used at any time during the operation and represents a new monitoring scheme.

Let E^g represent the ellipsoid surrounding $\underline{z}_g$, the "present" operating point. We define E^g according to

$$E^g \triangleq \{\underline{z} \,/\, (\underline{z} - \underline{z}_g)^T \,[A_z]\, (\underline{z} - \underline{z}_g) \leq c_g\} \tag{7.32}$$

where $[A_z]$ is a diagonal matrix whose non-zero elements are defined in (7.8). The secure part of E^g, denoted by E_s^g, is defined by:

$$E_s^g \triangleq H_z \cap \{\underline{z} \,/\, \underline{\beta}_j^T (\underline{x}_0)\, \underline{z} \leq y_j^\ell \,,\; j \in I^g\} \cap E^g \tag{7.33}$$

Our goal is to make the characterization of E_s^g simple enough so that it can be carried out in a real time environment.

Using the expression (7.14), to characterize E_s^g, one has to compute, first,

$$c_{gj}^\ell = \frac{[y_j^\ell - \underline{\beta}_j^T (\underline{x}_0)\, \underline{z}_g]^2}{\underline{\beta}_j^T (\underline{x}_0)\, [A_z]^{-1}\, \underline{\beta}_j^T (\underline{x}_0)} \qquad \begin{array}{l} j = 1, \ldots, N_{dp} \\ \ell = M \text{ or } m \end{array} \tag{7.34}$$

This computation simplifies greatly, when the following points are noted.

(a) The terms $\underline{\beta}_j^T\ (\underline{x}_0)\ [A_z]^{-1}\ \underline{\beta}_j\ (\underline{x}_0)$, $j = 1, \ldots , N_{dp}$ can be computed in advance. This is due to the fact that the parameters involved in this computation, are all independent of the present or the future operating points. These values, however, should be recomputed, whenever the system topology changes.

(b) Since $\underline{\beta}_j^T\ (\underline{x}_0)\ \underline{z}_g$ is a first order approximation to $Y_j\ (\underline{x}_g)$, ($\underline{x}_g$ is the load flow solution to $\underline{z}_g$), one can replace $\underline{\beta}_j^T\ (\underline{x}_0)\ \underline{z}_g$ by $Y_j\ (\underline{x}_g)$ in (7.34). This may indeed improve the accuracy of the results, because $Y_j\ (\underline{x}_g) = \underline{\beta}_j^T\ (\underline{x}_0)\ \underline{z}_g$, $j = 1, \ldots , N_{dp}$ corresponds to a highly desirable situation, i.e., when $\underline{x}_0 = \underline{x}_g$.

Note that during monitoring the system condition corresponding to $\underline{z}_g$, one actually computes all $[y_j^\ell - Y_j\ (\underline{x}_g)]$, $j = 1, \ldots , N_{dp}$, $\ell = M$ or m . Therefore, by pre-computing the terms $\underline{\beta}_j^T\ (\underline{x}_0)\ [A_z]^{-1}\ \underline{\beta}_j\ (\underline{x}_0)$, the expression in (7.34) can be computed trivially. The major calculation remaining then is the computation of $\underline{\beta}_j\ (\underline{x}_0)$, $j \in I^g$.

By choosing the value of c_g in (7.32) equal to the smallest c_{gj}^ℓ , as shown in Figure 7.7, I^g becomes empty and one does not need to compute any $\underline{\beta}_j\ (\underline{x}_0)$. However, when the resulting ellipsoid is very small (i.e., when $\underline{z}_g$ is approaching the limit on a dependent variable), one may have to choose a larger value for c_g , which then requires computing a few $\underline{\beta}_j\ (\underline{x}_0)$. Our experience shows that, irrespective of the system size, one can compute 5 to 6 different $\underline{\beta}_j\ (\underline{x}_0)$ within the time period needed to solve a load flow problem. Thus, it is quite practical to compute a few $\underline{\beta}_j\ (\underline{x}_0)$ on-line, if needed.

Now consider the case where the value of c_g varies with time according to

$$c_g\ (t) \;=\; [\underline{Z}\ (t) - \underline{z}_g]^T\ [A_z]\ [\underline{Z}\ (t) - \underline{z}_g] \tag{7.37}$$

where $\underline{z} = \underline{Z}\ (t)$ represents the operating point at time t . This also turns the set I^g into a function of time, because it has to represent all those constraints for which $c_g\ (t) > c^{\ell}_{gj}\ (j = 1, \ldots , N_{dp}, \ \ell = M \text{ or } m)$.

To monitor the system condition at time $t = t_0$, then one has to verify the inequalities: $\underline{\beta}^T_j\ (\underline{x}_0)\ \underline{Z}\ (t_0) \leq y^{\ell}_j$, $j \in I^g\ (t_0)$. That can be carried out without computing $\underline{\beta}_j\ (\underline{x}_0)$, $j \in I^g\ (t_0)$. This is due to the fact that one can write (see equation (4.14)),

$$\underline{\beta}^T_j\ (\underline{x}_0)\ \underline{Z}\ (t_0) \;=\; \underline{x}^T_0\ [Y_j]\ \underline{x}_1 \qquad \forall\ j \in I^g\ (t_0) \tag{7.38}$$

where $\underline{x}_1$ is the solution to the system of linear equations

$$[L\ (\underline{x}_0)]\ \underline{x}_1 \;=\; \underline{Z}\ (t_0) \tag{7.39}$$

In other words, monitoring $\underline{Z}(t_0)$ would involve solving (7.39) and computing (7.38).

When the number of elements in $I^g(t)$ gets so large that it is more advantageous to monitor the system conditions by running load flows, because it limits the checks to certain constraints, still a knowledge of $I^g(t)$ is quite useful. This suggests that, even when the monitoring is performed by the conventional methods, to cut down on the number of constraints to be checked, values of c_{gj}^{ℓ} can be computed and updated frequently.

By allowing c_i in (7.9) to vary with time (similar to $c_g(t)$ in (7.37)), the size of the individual ellipsoids forming a security corridor becomes time dependent. This can be viewed as reaching out for the operating points outside the corridor by expanding an appropriate ellipsoid.

CHAPTER VIII

CHARACTERIZATION OF SECURE LOADABILITY SETS

8.0 Preliminary Remarks

A major step in power systems expansion planning is the security analysis of the economically feasible system configurations vis-a-vis the projected future load profiles. This is normally carried out by solving a large number of optimal load flows, corresponding to different plans (i.e., system configurations) and different loading conditions.

In this chapter the concept of secure loadability sets is explored. This concept provides an alternative approach to the problem of assessing the security of various system configurations. The approach is straightforward and does not involve expensive repeated optimal load flows otherwise needed. A secure loadability set defines a region in the $\underline{d}$ space such that for every point of that region there exists, at least, one control vector capable of producing a secure opearting point.

8.1 Secure Loadability Sets

8.1.1 Concept of a Secure Loadability Set

Consider Figure 7.1. From this picture it is clear that not all the loading conditions can *potentially* produce normal operating points. In fact, this property is restricted to those loading conditions which lie inside the projection of S_z into the $\underline{d}$ space. In other words, a given loading condition, $\underline{d}_0$, is normal if and only if S_z $(\underline{d} = \underline{d}_0)$ is non-empty. Thus, denoting the set of normal loading conditions by S_d, it follows that,

$$S_d \triangleq \{\underline{d} \,/\, S_z\,(\underline{d}) \text{ is non-empty}\} \tag{8.1}$$

The set S_d can also be interpreted as the union of the projections of all possible cross-sections of S_z (parallel to the $\underline{d}$ space) into the $\underline{d}$ space. Again, one can similarly define the set of secure loading conditions corresponding to the postulated contingencies, namely,

$$S_d^j \triangleq \{\underline{d} \,/\, S_z^j\,(\underline{d}) \text{ is non-empty}\} \qquad j = 1, \ldots, N_{cg} \tag{8.2}$$

In words, if a loading condition $\underline{d}_0$ belongs to S_d^j, there exists, at least, a control strategy corresponding to $\underline{d}_0$. capable of producing an operating point invulnerable to the jth contingency.

8.1.2 Characterization of Secure Loadability Sets

To project a finite region of the $\underline{z}$ space into the $\underline{d}$ space, one needs to identify the outer-boundary of that region, as seen from the $\underline{d}$ space. Here, the outer boundary of S_z, denoted by O_z, is the collection of the points $\underline{z}^T = [\underline{u}^T, \underline{d}^T]$ whose corresponding control set, $S_z(\underline{d})$, is composed of a finite number of (normally only one) control vectors, i.e.,

$$O_z \triangleq \{\underline{z} \,/\, S_z(\underline{d}) \text{ has a finite number of elements}\} \tag{8.3}$$

The boundary of S_d is simply the projection of all $\underline{z} \in O_z$ into the $\underline{d}$ space. The projection of a point $\underline{z}_0^T = [\underline{u}_0^T, \underline{d}_0^T]$ into the $\underline{d}$ space is simply $\underline{d}_0$.

For a general set, identification of its outer boundary, as well as the description of the boundary of the projected set is quite complicated. This is, however, somewhat simpler for linear security sets.

Consider, for example, $\hat{S}_z$. Since $\hat{S}_z$ is defined by linear constraints, using the algorithm developed by Mattheiss [60, 61], one is able to compute all its vertices and identify those which belong to $\hat{O}_z$. By projecting the vertices belonging to $\hat{O}_z$ into the $\underline{d}$ space, one ends up with the vertices of $\hat{S}_d$. The projected points then can be used to construct a convex hull [111] in the $\underline{d}$ space. In that process all the linear constraints defining $\hat{S}_d$ are computed. Since these computations can be carried out off-line systematically, their relatively large computational requirements should not be considered as a major obstacle.

8.2 Sub-Sets of a Secure Loadability Set

8.2.1 Characterizing Local Sub-Sets

Consider the following optimization problem:

$$\underset{\underline{d}\ \varepsilon\ \text{Ext}\ (\hat{Y}_d)}{\text{Minimize}}\ \mu = (\underline{d} - \underline{d}_0)^T\ [F]\ (\underline{d} - \underline{d}_0) \tag{8.6}$$

where $\hat{Y}_d$ is the orthogonal projection of $\hat{Y}_z$ into the $\underline{d}$ space, and $[F]$ is a symmetric, positive definite matrix. The vector $\underline{d}_0$ is fixed and $\underline{d}_0\ \varepsilon\ \hat{Y}_d$. It is obvious that this problem can be solved by reformulating it in the $\underline{z}$ space and replacing $\hat{Y}_d$ by $\hat{Y}_z$. But, since the objective function is quadratic in $\underline{d}$, that involves solving a rather difficult optimization problem in a much larger space.

Chief among our objectives being simplicity, we thus look for sub-optimal solutions which pose less difficulties. Remembering that, by considering each constraint one at a time, the counter-part of this problem was solved easily (Section 7.2.6) in the $\underline{z}$ space, we are prompted to look into the following problem:

$$\text{Minimize}\ \mu_j = (\underline{d} - \underline{d}_0)^T\ (F)\ (\underline{d} - \underline{d}_0)$$

subject to

$$\underline{\beta}_{ju}^T\ \underline{u}^+ + \underline{\beta}_{jd}^T\ \underline{d} = y_j^{\ell}$$

where $\underline{u} = \underline{u}^+$ is a fixed, feasible, control vector, and $\underline{\beta}_j^T (\underline{x}_0) = [\underline{\beta}_{ju}^T , \underline{\beta}_{jd}^T]$. By solving this problem for all the constraints forming Y_z , one arrives at the following solution:

$$\mu^+ = \underset{j}{\text{Min}} (\mu_j^+)$$

where

$$\mu_j^+ = \frac{[y_j^\ell - \underline{\beta}_{ju}^T \underline{U}^+ - \underline{\beta}_{jd}^T \underline{d}_0]^2}{\underline{\beta}_{jd}^T [F]^{-1} \underline{\beta}_{jd}} \qquad \ell = M \text{ or } m \quad j=1, \ldots , N_{dp}$$

A general interpretation of this solution is given in Figure 8.1. For a general Y_z , μ^+ represents the largest value that the ellipsoid $\mu = (\underline{d} - \underline{d}_0)^T [F] (\underline{d} - \underline{d}_0)$ can assume over Y_z $(\underline{u} = \underline{u}^+)$. The set Y_z $(\underline{u} = \underline{u}^+)$ is a <u>load set</u>, which is defined by the projection of the cross-section of the set Y_z (for $\underline{u} = \underline{u}^+$) into the load space. Clearly, among the feasible control strategies, there is a $\underline{u}^+ = \underline{u}^*$ which makes μ^+ maximum. From Section 6.2.3, we remember that such a $\underline{u}$ can be computed by solving a mini-max problem. There it was demonstrated that for linear constraints the problem reduces to the following simple LP problem:

$$\text{Maximize : } r \tag{8.9}$$

subject to

$$\beta_{ju}^{T}\ \underline{u} + \phi_j\ r \leq y_j^{\ell} - \underline{\beta}_{jd}^{T}\ \underline{d}_0 \qquad \ell = M \text{ or } m$$

$$j=1, \ldots, N_{dp} \qquad (8.10)$$

where $\phi_j \triangleq \{\underline{\beta}_{jd}^{T}\ [F]^{-1}\ \underline{\beta}_{jd}\}^{1/2}$ and $r \triangleq \mu^{1/2}$.

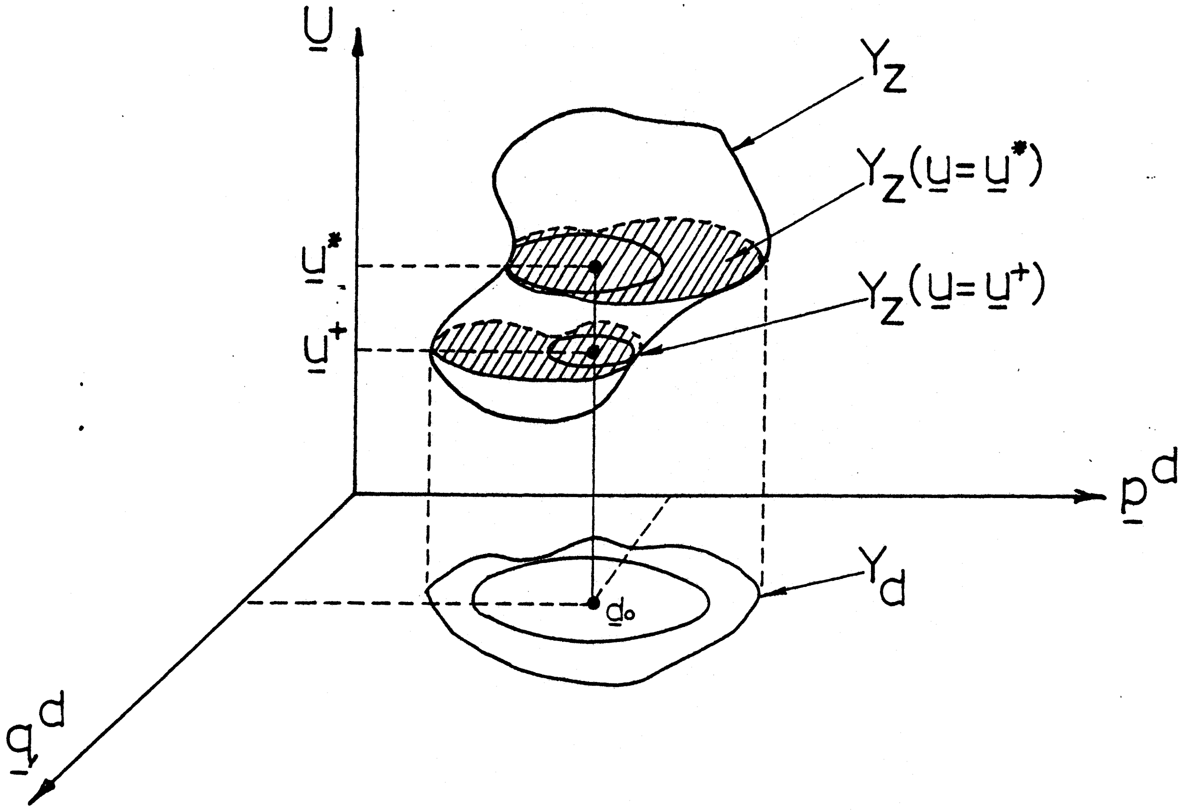

Figure 8.1. Interpretation of the proposed sub-optimal approach.

The above optimization process can be viewed as allowing $\underline{u}^{+}$ to slide along the $\underline{u}$ axis to vary the size of $\hat{Y}_z$ $(\underline{u} = \underline{u}^{+})$ until the cross-section over which μ takes its largest value is found (see Figure 8.1). Note that the resulting solution, $\mu^* = (r^*)^2$, is not an optimal one, because it is restricted to a particular cross-section of $\hat{Y}_z$. Since the set $\hat{Y}_d$ is the union of all such cross-sections, it may offer more room to the ellipsoid to "expand". However, one can easily show that for the cases where $\underline{d}_0$ is close to the boundary of Y_d, very often, the sub-optimal and the optimal solutions produce identical results.

It is interesting to note that by treating $\underline{d}_0$ in (8.10) as an unknown vector, one can also obtain a sub-optimal solution to the problem of embedding the largest ellipsoid inside $\hat{Y}_d$, for a given [F].

8.2.2 Characterizing the Secure-Economical Loadability Set

Suppose, for a given power system, there exists an explicit function $\underline{E}$ relating the demand vector, $\underline{d}$, to its unconstrained (not including the physical equality constraints) optimal control strategy, i.e.,

$$\underline{u} = \underline{E}(\underline{d}) \tag{8.11}$$

Now, consider the intersection of the non-linear manifold $\underline{u} - \underline{E}(\underline{d}) = \underline{0}$ with the set of normal operating points, S_z. As shown in Figure 8.2, the projection of the part of the manifold which is inside S_z into the

$\underline{d}$ space, produces a unique loadability set. When the function $\underline{E}$ represents the economic dispatch of the load, we call the resulting set the set of secure-economical loading conditions, and denote it by S_d^e. Clearly, S_d^e can be defined by

$$S_d^e \triangleq S_z \, [\underline{u} = \underline{E} \, (\underline{d})] \tag{8.12}$$

which implies replacement of $\underline{u}$ by $\underline{E}$ $(\underline{d})$ in every relation defining S_z. Interesting properties of this set include:

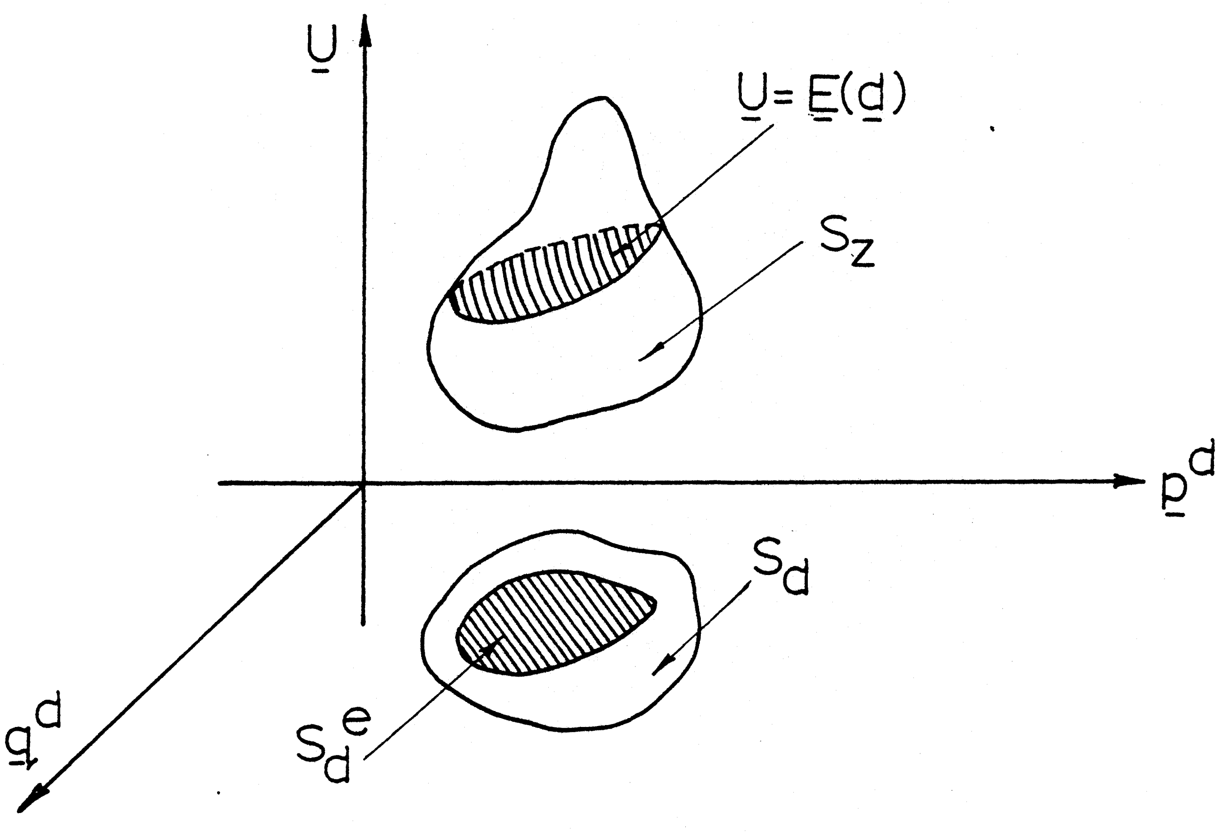

Figure 8.2. Illustration of the relation between the sets S_d and S_d^e.

(i) From the definition of S_d^e, it follows that,

$$S_d^e \subset S_d$$

(ii) The <u>constrained</u> optimal dispatch for any loading condition $\underline{d}_0 \in S_d^e$ is simply given by

$$\underline{u}_0 = \underline{E}(\underline{d}_0)$$

(iii) When $\underline{d}_0 \in S_d^e$, the operating point $\underline{z}_0^T \triangleq [\underline{E}^T(\underline{d}_0), \underline{d}_0^T]$ represents a highly desirable operating condition. This is due to the fact that, under such conditions, not only the system is operated most economically, but none of the system components are under stress. In other words, without risking the violation of any of the operating constraints, the system is being operated in its most efficient economic mode. Thus for planning purposes, it may be desirable to make S_d^e as large as possible.

<u>Derivation of $\underline{E}(\underline{d})$ for a Simple Case</u>

Let the economic dispatch cost function be represented by a quadratic expression in $\underline{P}^g$, the generation vector, and let P_1^g, the slack bus generation, be related to the other bus injections linearly. Under such conditions, the unconstrained generation dispatch is the solution to the following problem:

$$\text{Minimize:} \quad \underline{a}_c^T \, \underline{P}^g + \underline{P}^{g^T} [D_c] \, \underline{P}^g$$

subject to

$$P_1^g = \underline{\beta}_1^T (x_0) \, \underline{z} \tag{8.14}$$

where $\underline{a}_c$ and $[D_c]$ (a diagonal matrix) contain the cost coefficients. For fixed voltage levels $(\underline{v}^2)$ and demand vectors $(\underline{d})$, by partitioning the vector $\underline{\beta}_1 (\underline{x}_0)$, the equality constraint can be rewritten in the form

$$\underline{\gamma}^T \, \underline{P}^g = \underline{\beta}_{1v}^T \, \underline{v}^2 + \underline{\beta}_{1d}^T \, \underline{d} \tag{8.15}$$

where

$$\underline{\beta}_1 (x_0) = \begin{bmatrix} \underline{\beta}_{1v} \\ \underline{\beta}_{1p} \\ \underline{\beta}_{1d} \end{bmatrix} \quad ; \quad \underline{\gamma} \triangleq \begin{bmatrix} 1 \\ \hline -\underline{\beta}_{1p} \end{bmatrix} \quad ; \quad \underline{P}^g = \begin{bmatrix} P_1^g \\ \hline \underline{P}^v \end{bmatrix}$$

With the equality constraint expressed by (8.15), the solution to the unconstrained economic dispatch is simply

$$\underline{P}^g = -\frac{1}{2} [D_c]^{-1} \underline{a}_c + \left[\frac{\underline{\gamma}^T [D_c]^{-1} \underline{a}_c + 2 (\underline{\beta}_{1d}^T \underline{d} + \underline{\beta}_{1v}^T \underline{v}^2)}{2 \, \underline{\gamma}^T [D_c]^{-1} \underline{\gamma}} \right] [D_c]^{-1} \underline{\gamma} \tag{8.16}$$

After deleting the first row in this expression (corresponding to P_1^g), it can be rearranged in the general form:

$$\underline{P}^{v} = \underline{a}_0 + [B_v]\, \underline{v}^2 + [B_d]\, \underline{d} \tag{8.17}$$

where $[B_v]$, $[B_d]$ (rectangular matrices), and $\underline{a}_0$ are functions of $\underline{\beta}_1\,(x_0)$ as well as the generators' cost coefficients. Since $\underline{u}^T = [\underline{v}^{2T}, \underline{P}^{vT}]$, it is evident that for a given voltage level the above expression is a first order approximation to $\underline{u} = \underline{E}\,(\underline{d})$.

8.3 Applications of Secure Loadability Sets

8.3.1 Security Assessment

When characterized explicitly, the secure loadability sets can be employed efficiently to assess the security of the system for a given loading condition. The main factors contributing to this efficiency are the following:

(i) The number of constraints defining, say, $\hat{S}_d$ explicitly is much smaller than those defining $\hat{S}_z$;

(ii) Since the dimension of the $\underline{d}$ space is normally much smaller than the $\underline{z}$ space, the storage and the computational requirements for security assessment of a loading condition is relatively small;

(iii) The security of the system for a given loading condition can be verified without restricting it to a particular set of controls;

(iv) The secure loadability sets allow one to recognize quickly those emergency or vulnerable conditions which can be corrected without resorting to load curtailment.

It has to be re-emphasized, however, that the secure loadability sets are primarily suitable for off-line security assessment. Because of this, their main application is in power system expansion planning.

8.3.2 Power System Expansion Planning

Once the secure loadability sets for different system configurations are characterized, the security assessment for the projected load profiles reduces to simple constraint checks. Thus, there is no need for solving complicated optimization problems. In the following some other applications of these sets in power system expansion planning are touched upon.

Based on the present daily load trajectory and the projected future load levels, one can forecast a future daily load trajectory. This load trajectory, then, can be used to identify the best expansion plan among the economically feasible plans from a security point of view. The best plan should have a normal loadability set (S_d) that embodies the entire trajectory. Moreover, the total time spent by the trajectory inside its S_d^I (the projection of S_z^I into the $\underline{d}$ space) should be longer than the corresponding time for any other plan.

The secure loadability sets can be used for computing the operating range of the required reactive supports for a given expansion plan. This involves treating the sites where the installment of the shunt reactors or capacitors are intended as load points in the system. Then, by altering their corresponding components in $\underline{d}$ and considering the future load profiles, one can determine what ratings of such devices offer "better" security to the future system.

For a well-designed power system, the set of injections which are dynamically stable, should include the set of normal operating points. This can be investigated by transient stability simulations along the boundary of S_d . Of particular interest are those boundary points which are close to the estimated future daily load trajectory.

8.3.3 Load Control

The idea of load control or load management has been around for quite some time [112, 113] . In the past, the implementation of any type of large scale load control has not been considered seriously, mainly, because of its socio-political implications, and the lack of strong motivations. However, the new economical realities have changed the picture considerably. To meet the increasing demand, the power system industry may soon feel that it is necessary to consider a much more efficient use of the available generation capacity in the form of the load management. The public's gradual change of attitude towards compulsory energy conservation measures is also an encouraging sign in this regard.

One of the basic problems in load control is the lack of quantified objectives [114] . This difficulty can be resolved easily by defining the objectives in terms of the loadability sets. For example, depending on the policy of a company, or their feasibility, the objectives can be one, or a combination, of the following:

(i) To ensure operating in the normal state, allow a daily load trajectory which lies entirely inside S_d .

(ii) To operate the system in its most economical mode, with a certain degree of security, restrict the daily load trajectory to the inside of the set S_d^e .

(iii) To have maximum security, allow a load trajectory that lies completely inside S_d^I .

CHAPTER IX

SECURE LOAD FLOW SOLUTIONS

9.0 Introductory Remarks

The difficulty of performing security analysis in the voltage space stems mainly from the fact that in that space the load and control variables are non-linear functions of the dependent voltage vector. This sharply contrasts with the simplicity of the security analysis in the $\underline{z}$-space where the space variables are the load and control variables which are known, independent quantities. The voltage space, nevertheless, offers certain important features which are not present in the $\underline{z}$-space. The most important one from a security point of view is the simplicity in which various network topology changes can be reflected in the security problem formulations. Other significant features include the presence of sparsity in power flow relations as well as their greater accuracy.

In this chapter we look into the possibility of characterizing the set of secure load flow voltage solutions for a given loading condition. The schemes proposed here are based on the original development in [64]. There, the non-linearity of the load flow relations is avoided through an indirect method which reduces the non-linear relations to a set of linear ones without using the standard linearization method. These linear relations retain so many properties of the original ones as to suggest that they could be used to detect unfeasible loading conditions or to find secure load flow solutions.

9.1 Enclosing the Set of Secure Load Flow Solutions by a Linear Set

9.1.1 General Definitions and Motivation

For a specified loading condition, $\underline{d}$, the physical constraints on a power network define a non-linear manifold in the $\underline{x}$-space, i.e., a set in R^{N_z} with fewer degrees of freedom than N_z . Denoting the manifold by the set $M_x(\underline{d})$, based on the notation of Section 2.3.3, it can be defined by

$$M_x(\underline{d}) \triangleq \{\underline{x}/\underline{x}^T [D_j] \underline{x} = d_j \; ; \; j=1, \ldots, N_d\} \tag{9.1}$$

Now, let $S_x(\underline{d})$ denote the set of all voltage vectors satisfying the given demand as well as the operating constraints. From the definition of $M_x(\underline{d})$ and $S_x(\underline{d})$, it follows that,

$$S_x(\underline{d}) \triangleq M_x(\underline{d}) \cap U_x \cap Y_x \tag{9.2}$$

The characterization of $S_x(\underline{d})$, while fundamental to the analysis of various security related problems, is extremely difficult. Simple properties of $S_x(\underline{d})$ such as whether it is empty, though crucial to the computation of corrective controls in an emergency state, cannot be verified unless one actually attempts to compute the required control actions. Thus if $S_x(\underline{d})$ is empty, many precious seconds would be lost seeking a non-existent solution.

Many properties of a non-linear set (such as its shape, relative size, emptiness, etc.), however, may be studied by surrounding it "closely" by simple sets which can be more easily analyzed. In studying the properties of $S_x(\underline{d})$ such a scheme is followed.

9.1.2 The Basic Approach

To study the properties of $S_x(\underline{d})$, first a linear set $L_x^a(\underline{d})$ with the property:

$$L_x^a(\underline{d}) \supset S_x(\underline{d}) \tag{9.3}$$

is sought. The major steps in deriving $L_x^a(\underline{d})$ are:

(i) Expressing the LFE in an appropriate form;

(ii) Using the appropriate form of the LFE to derive necessary linear constraints representing the non-linear operating constraints.

The second step also includes identification and, if possible, adjustment of the factors influencing the degree of tightness with which $L_x^a(\underline{d})$ encloses $S_x(\underline{d})$. These steps are examined in detail in the following sub-sections.

9.1.2.1 LFE in the Nodal Current Form

Using equation (2.1), the rectangular components of the nodal current injections can be related to the bus voltage components, i.e.,

$$\underline{I} \overset{\Delta}{=} \underline{I}^{re}(\underline{x}_r) + j\,\underline{I}^{im}(\underline{x}_r) = \{[G] + j\,[B]\}\,(\underline{e} + j\,\underline{f})$$

or

$$\underline{I}^{re}(\underline{x}_r) = [G]\,\underline{e} - [B]\,\underline{f} \tag{9.4a}$$

$$\underline{I}^{im}(\underline{x}_r) = [G]\,\underline{f} + [B]\,\underline{e} \tag{9.4b}$$

The superscripts "re" and "im" represent respectively the real and imaginary components of a complex quantity. The above expressions indicate that the real and imaginary components of every nodal current injection are linear in $\underline{x}_r$.

Now, using equation (2.2), the net real and reactive power injections at the kth bus can be related to the kth components of $\underline{I}^{re}(\underline{x}_r)$ and $\underline{I}^{im}(\underline{x}_r)$, namely,

$$S_k = p_k + j\,q_k = V_k\,I_k^*$$

$$= (e_k + j\,f_k)[I_k^{re}(\underline{x}_r) - j\,I_k^{im}(\underline{x}_r)]$$

From above, it follows that,

$$p_k = e_k I_k^{re}(\underline{x}_r) + f_k I_k^{im}(\underline{x}_r) \tag{9.5a}$$

$$q_k = f_k I_k^{re}(\underline{x}_r) - e_k I_k^{im}(\underline{x}_r) \tag{9.5b}$$

Solving these equations for $I_k^{re}(\underline{x}_r)$ and $I_k^{im}(\underline{x}_r)$, one arrives at:

$$I_k^{re}(\underline{x}_r) = \left(\frac{p_k}{v_k^2}\right) e_k + \left(\frac{q_k}{v_k^2}\right) f_k \tag{9.6a}$$

$$I_k^{im}(\underline{x}_r) = \left(\frac{p_k}{v_k^2}\right) f_k - \left(\frac{q_k}{v_k^2}\right) e_k \tag{9.6b}$$

Combining equations (9.4) with the above relations, one obtains the nodal current form of the LFE . Since the terms appearing in their right-hand-side are the only non-linear terms, these equations are regarded as a quasi-linear version of the LFE.

9.1.2.2 Derivation of Linear Necessary Conditions

A thorough examination of equations (9.6) reveals that by establishing limits on the quantities $\left(\frac{p_k}{v_k^2}\right)$ and $\left(\frac{q_k}{v_k^2}\right)$ one can obtain linear constraints on $I_k^{re}(\underline{x}_r)$ and $I_k^{im}(\underline{x}_r)$. The resulting linear constraints would define the set $L_x^a(\underline{d})$. The basic steps in deriving these relations are illustrated below, while a detailed derivation is deferred.

Let us assume that the kth bus is a PV bus. In that case, the operating constraints at that bus are normally

$$0 < p_k^m \le p_k \le p_k^M \tag{9.7a}$$

$$0 < q_k^m \le q_k \le q_k^M \tag{9.7b}$$

$$(v_k^m)^2 \le v_k^2 \le (v_k^M)^2 \tag{9.7c}$$

Using these relations, one can write:

$$\left(\frac{v_k}{v_k^M}\right)^2 p_k^m \le p_k^m \le p_k \le p_k^M \le \left(\frac{v_k}{v_k^m}\right)^2 p_k^M \tag{9.8a}$$

$$\left(\frac{v_k}{v_k^M}\right)^2 q_k^m \le q_k^m \le q_k \le q_k^M \le \left(\frac{v_k}{v_k^m}\right)^2 q_k^M \tag{9.8b}$$

or, considering only the outer bounds,

$$\frac{p_k^m}{(v_k^M)^2} \le \frac{p_k}{v_k^2} \le \frac{p_k^M}{(v_k^m)^2} \tag{9.9a}$$

$$\frac{q_k^m}{(v_k^M)^2} \le \frac{q_k}{v_k^2} \le \frac{q_k^M}{(v_k^m)^2} \tag{9.9b}$$

Now assuming that both e_k and f_k are positive, one can multiply the above inequalities by e_k and f_k respectively and add the results to get:

$$\frac{p_k^m e_k + q_k^m f_k}{(v_k^M)^2} \leq \frac{p_k}{v_k^2} e_k + \frac{q_k}{v_k^2} f_k \leq \frac{p_k^M e_k + q_k^M f_k}{(v_k^m)^2}$$

Using equation (9.6a) in the above relation, one arrives at the following linear constraints

$$I_k^{re}(x_r) \geq (p_k^m e_k + q_k^m f_k) / (v_k^M)^2 \tag{9.10a}$$

$$I_k^{re}(x_r) \leq (p_k^M e_k + q_k^M f_k) / (v_k^m)^2 \tag{9.10b}$$

Similarly, by multiplying the inequalities in (9.9) by f_k and $-e_k$ and adding up the new constraints, and exploiting equation (9.6b), one obtains:

$$I_k^{im}(\underline{x}_r) \geq \frac{p_k^m}{(v_k^M)^2} f_k - \frac{q_k^M}{(v_k^m)^2} e_k \tag{9.10c}$$

$$I_k^{im}(\underline{x}_r) \leq \frac{p_k^M}{(v_k^m)^2} f_k - \frac{q_k^m}{(v_k^M)^2} e_k \tag{9.10d}$$

Note that (9.10) are linear inequalities in $\underline{x}_r$ and represent a set of necessary conditions on the voltage solutions.

9.1.2.3 Factors Influencing the Enclosing Set

Two factors influence how tightly the inequalities (9.10) enclose the set $S_x(\underline{d})$. These factors are:

(1) The range of v_k ;

(2) The size of the ratio e_k / f_k .

The range of v_k influences the resulting inequalities by affecting $\left(\frac{v_k}{v_k^m}\right)^2$ and $\left(\frac{v_k}{v_k^M}\right)^2$, the coefficients enlarging the bounds on p_k and q_k in (9.8). Since v_k^M and v_k^m are normally quite close, these coefficients will stay close to unity provided that the constraints $(v_k^m)^2 \le v_k^2 \le (v_k^M)^2$ are explicitly enforced.

The second factor comes into the picture when, in deriving (9.10), the inequalities in (9.9) are first multiplied by e_k and f_k , and then the results are added and subtracted. The impact of these operations on the resulting inequalities is illustrated in Figure 9.1 for two simple inequalities: $X^m \le X \le X^M$, and $Y^m \le Y \le Y^M$. These inequalities are initially multiplied by two positive numbers A and B such that after being added and subtracted, they produce the following relations

$$AX^m + BY^m \le AX + BY \le AX^M + BY^M \tag{9.11a}$$

$$BX^m - AY^M \le BX - AY \le BX^M - AY^m \tag{9.11b}$$

As shown in Figure 9.1, for different values of $\sigma = A/B$ the above constraints define different regions in the X-Y plane, which all enclose the region defined by the original constraints. Moreover, the larger the ratio A/B, the tighter the resulting inequalities enclose the original region.

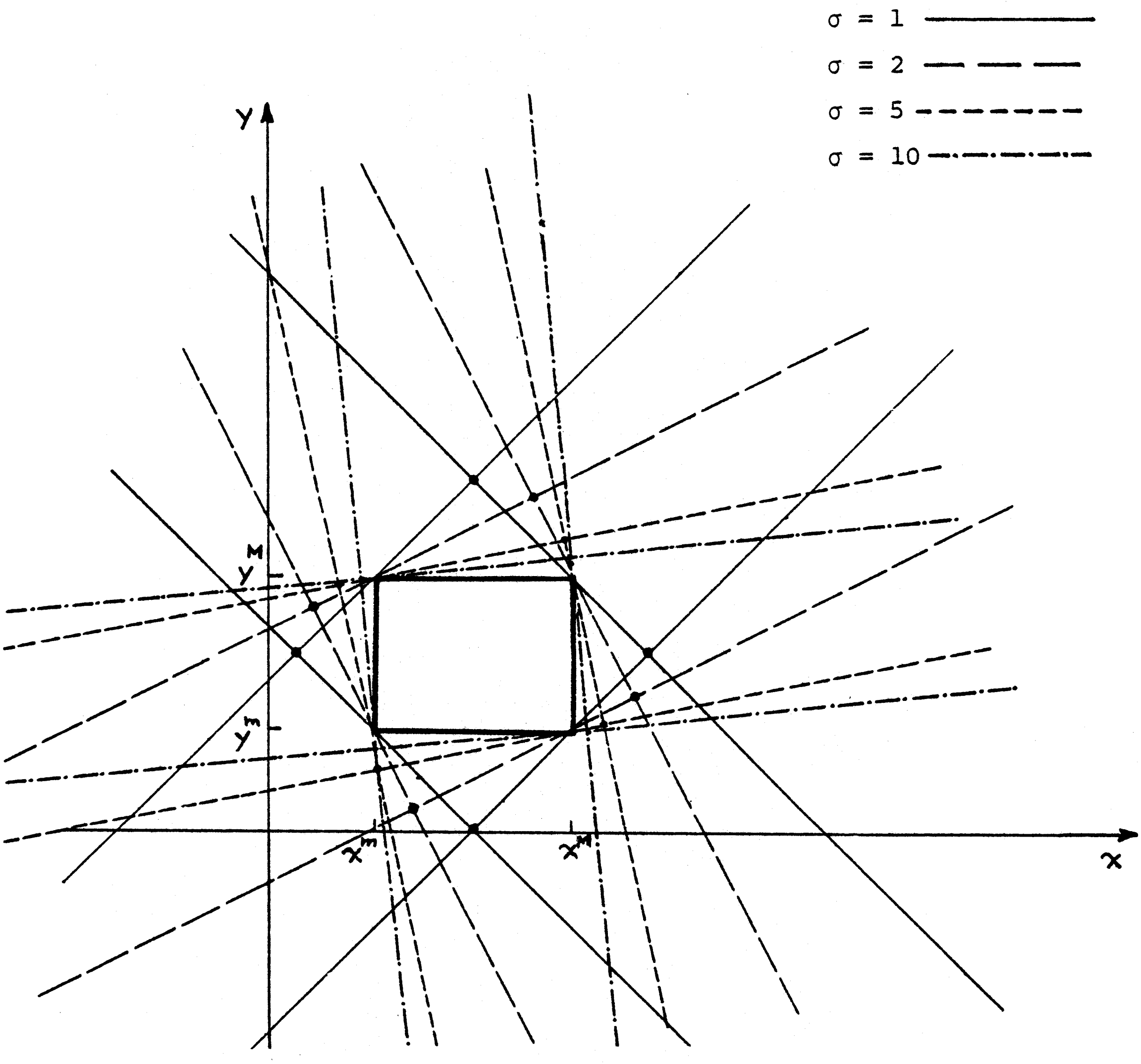

Figure 9.1. The effect of different choice of $\sigma = A/B$ on the constraints enclosing the set $\{x^m \le x \le x^M \; ; \; y^m \le y \le y^M\}$.

By comparison, larger ratios of $\frac{e_k}{f_k}$ produce tighter inequalities to enclose $S_x(\underline{d})$.

Figure 9.1 indicates that to have a reasonably tight enclosure of the original region, one should have $\sigma > 5$. By imposing this condition on $\frac{e_k}{f_k}$ the assumptions so far made on the values of e_k and f_k can be listed as:

$$e_k > 0 \quad ; \quad f_k > 0 \quad ; \quad \frac{e_k}{f_k} > 5 \tag{9.12}$$

Obviously, it is not easy to guarantee the validity of all the assumptions in (9.12), unless one follows a more general approach involving adjustable parameters in the problem formulation. Such an approach is detailed below.

Consider a linear combination of $I_k^{re}(\underline{x}_r)$ and $I_k^{im}(\underline{x}_r)$, namely,

$$\alpha\, I_k^{re}(\underline{x}_r) + \beta\, I_k^{im}(\underline{x}_r) = (\alpha\, e_k + \beta\, f_k)\, \frac{p_k}{v_k^2} + (\alpha\, f_k - \beta\, e_k)\, \frac{q_k}{v_k^2} \tag{9.13a}$$

where α and β are a pair of arbitrary adjustable parameters, which can be different for each bus. To establish an exact analogy between A and B in (9.11) and the terms multiplying $\frac{p_k}{v_k^2}$ and $\frac{q_k}{v_k^2}$ in (9.13a), we also form:

$$(\alpha\, f_k - \beta\, e_k)\, \frac{p_k}{v_k^2} - (\alpha\, e_k + \beta\, f_k)\, \frac{q_k}{v_k^2} = -\beta\, I_k^{re}(\underline{x}_r) + \alpha\, I_k^{im}(\underline{x}_r) \tag{9.13b}$$

Now, instead of e_k and f_k, one can multiply the inequalities in (9.9) by $(\alpha\, e_k + \beta\, f_k)$ and $(\alpha\, f_k - \beta\, e_k)$, and use relations (9.13) to arrive at a new set of linear inequalities, namely,

$$\alpha\, I_k^{re}(\underline{x}_r) + \beta\, I_k^{im}(\underline{x}_r) \geq (\alpha\, e_k + \beta\, f_k)\, \frac{p_k^m}{(v_k^M)^2} + (\alpha\, f_k - \beta\, e_k)\, \frac{q_k^m}{(v_k^M)^2} \tag{9.14a}$$

$$\alpha\, I_k^{re}(\underline{x}_r) + \beta\, I_k^{im}(\underline{x}_r) \leq (\alpha\, e_k + \beta\, f_k)\, \frac{p_k^M}{(v_k^m)^2} + (\alpha\, f_k - \beta\, e_k)\, \frac{q_k^M}{(v_k^m)^2} \tag{9.14b}$$

$$-\beta\, I_k^{re}(\underline{x}_r) + \alpha\, I_k^{im}(\underline{x}_r) \geq (\alpha\, f_k - \beta\, e_k)\, \frac{p_k^m}{(v_k^m)^2} - (\alpha\, e_k + \beta\, f_k)\, \frac{q_k^M}{(v_k^m)^2} \tag{9.14c}$$

$$-\beta\, I_k^{re}(\underline{x}_r) + \alpha\, I_k^{im}(\underline{x}_r) \leq (\alpha\, f_k - \beta\, e_k)\, \frac{p_k^M}{(v_k^m)^2} - (\alpha\, e_k + \beta\, f_k)\, \frac{q_k^m}{(v_k^M)^2} \tag{9.14d}$$

The assumptions in (9.12) consequently change to

$$\alpha\, e_k + \beta\, f_k > 0 \tag{9.15a}$$

$$\alpha\, f_k - \beta\, e_k > 0 \tag{9.15b}$$

$$\frac{\alpha\, e_k + \beta\, f_k}{\alpha\, f_k - \beta\, e_k} > 5 \qquad (9.15c)$$

Now, one could adjust the parameters α and β such that the new assumptions remain valid for all feasible values of e_k and f_k .

9.1.3 Linear Necessary Conditions on Bus Voltage Levels

As pointed out earlier, to keep the bounds on $\frac{p_k}{v_k^2}$ and $\frac{q_k}{v_k^2}$ tight, the constraint $(v_k^m)^2 \leq v_k^2 \leq (v_k^M)^2$ has to be enforced. To represent this constraint linearly, one needs a large number of linear constraints, unless the possible values of e_k and f_k can be restricted to certain parts of the $(e_k\ ,\ f_k)$ plane. Let ψ_k represent an estimate of the average value of θ_k over $S_x(\underline{d})$ (see Section 9.1.4), and let δ_k denote an upper bound on the possible deviation of θ_k from ψ_k , i.e.,

$$\left|\ \theta_k - \psi_k\ \right| < \delta_k \qquad k = 1, \ldots, N_b \qquad (9.16)$$

As shown in Figure 9.2, this relation restricts the values of e_k and f_k to a rather small area in the (e_k, f_k) plane. When δ_k is small, one can <u>surround</u> this area by 5 lines with sufficient accuracy. The linear constraints corresponding to these lines are:

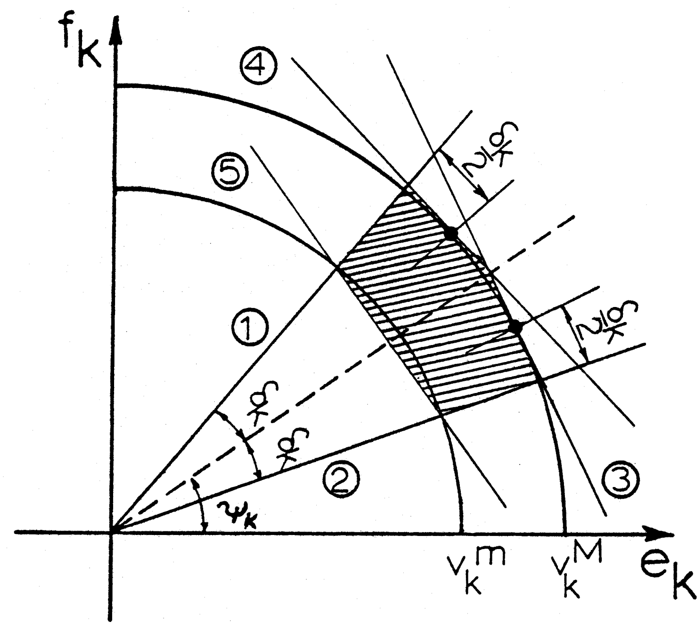

Figure 9.2. Linear necessary constraints corresponding to the bounds on a voltage level.

1: $$\sin(\psi_k + \delta_k)\, e_k - \cos(\psi_k + \delta_k)\, f_k \geq 0 \tag{9.17a}$$

2: $$-\sin(\psi_k - \delta_k)\, e_k + \cos(\psi_k - \delta_k)\, f_k \geq 0 \tag{9.17b}$$

3: $$\cos(\psi_k + \delta_k/2)\, e_k + \sin(\psi_k - \delta_k/2)\, f_k \leq v_k^M \tag{9.18a}$$

4: $$\cos(\psi_k + \delta_k/2)\, e_k + \sin(\psi_k + \delta_k/2)\, f_k \leq v_k^M \tag{9.18b}$$

5: $$\cos(\psi_k)\, e_k + \sin(\psi_k)\, f_k \geq v_k^m \cos(\delta_k) \tag{9.18c}$$

At the reference bus, in addition to the constraints on the voltage magnitude, one has to enforce

$$\tan(\theta_r)\, e_r - f_r = 0 \qquad (9.19)$$

This relation, however, permits one to reduce the constraints on $v_r^2 = e_r^2 + f_r^2$ to two equivalent linear inequalities, namely,

$$v_r^m \cos\theta_r \leq e_r \leq v_r^M \cos\theta_r \qquad (9.20)$$

9.1.4 Choice of the Adjustable Parameters

Using relations (9.16) and (9.17b), one can easily show that for $\alpha = \cos(\psi_k - \delta_k)$, $\beta = \sin(\psi_k - \delta_k)$, and $\delta_k \leq 45^\circ$, assumptions (9.15a) and (9.15b) are always valid. Relation (9.15c), however, imposes a much more restrictive condition on δ_k. This can be demonstrated by noting that

$$\frac{\alpha\, e_k + \beta\, f_k}{\alpha\, f_k - \beta\, e_k} = \text{cotan}\, (\theta_k - \psi_k + \delta_k > \text{cotan}\, (11.3^\circ)$$

where we have made use of the fact that $\tan(\theta_k) = f_k/e_k$ and $5 \simeq \text{cotan}\, (11.3^\circ)$. The above relation is equivalent to

$$(\theta_k - \psi_k) + \delta_k < 11.3^\circ$$

which in view of relation (9.16) leads to

$$\delta_k \leq 5.35^\circ \tag{9.21}$$

In short, to enclose the set $S_x(\underline{d})$ sufficiently tight by the linear constraints in (9.15), one should be able to estimate an average value for θ_k by ψ_k within the accuracy of $\pm 5.35^\circ$.

Such estimates are usually known from operational experience on the network. When the network buses are electrically close, one can choose $\psi_k = \theta_r$ for $k=1, \ldots, N_b$. This assumes that all the phase angles in the network are not going to deviate more than 5.35° from the reference angle. One can also choose a set of feasible real power injections and run a DC load flow to compute an often very good estimate of the phase angles.

Note that the estimation accuracy of (9.21) is not highly demanding, though it can be further relaxed by decreasing the lower limit in (9.15c). This would however give a more conservative enclosure of $S_x(\underline{d})$ by $L_x^a(\underline{d})$.

9.1.5 Linear Necessary Conditions on Power Injections at a Generation Bus

The relations derived in (9.13) correspond to a generation bus. For the suggested choice of α and β, those inequalities can be rearranged to read

$$\geq \left[\frac{p_k^m - \xi_k\, q_k^m}{(v_k^M)^2}\right] e_k + \left[\frac{\xi_k\, p_k^m + q_k^m}{(v_k^M)^2}\right] f_k \tag{9.22a}$$

$$I_k^{re}\,(\underline{x}_r) + \xi_k\, I_k^{im}\,(\underline{x}_r)$$

$$\leq \left[\frac{p_k^M - \xi_k\, q_k^M}{(v_k^m)^2}\right] e_k + \left[\frac{\xi_k\, p_k^M + q_k^M}{(v_k^m)^2}\right] f_k \tag{9.22b}$$

$$\geq \left[\frac{p_k^M}{(v_k^m)^2} - \eta_k\,\frac{q_k^m}{(v_k^M)^2}\right] e_k + \left[\frac{q_k^m}{(v_k^M)^2} + \eta_k\,\frac{p_k^M}{(v_k^m)^2}\right] f_k \tag{9.22c}$$

$$I_k^{re}\,(\underline{x}_r) + \eta_k\, I_k^{im}(\underline{x}_r)$$

$$\leq \left[\frac{p_k^m}{(v_k^M)^2} - \eta_k\,\frac{q_k^M}{(v_k^m)^2}\right] e_k + \left[\frac{q_k^M}{(v_k^m)^2} + \eta_k\,\frac{p_k^m}{(v_k^M)^2}\right] f_k \tag{9.22d}$$

where $\xi_k \triangleq -\frac{1}{\eta_k} \triangleq \tan\,(\psi_k - \delta_k)$. Note that for the reference bus $\xi_r = \tan\,(\theta_r)$.

9.1.6 Linear Constraints Enclosing the Load Manifold

At a PQ bus, one normally has

$$p_k = p_k^{spec} < 0 \tag{9.23a}$$

$$q_k = q_k^{spec} < 0 \tag{9.23b}$$

$$(v_k^m)^2 \leq v_k^2 \leq (v_k^M)^2 \tag{9.23c}$$

Thus, one can write

$$\frac{p_k^{spec}}{(v_k^M)^2} \geq \frac{p_k}{v_k^2} \geq \frac{p_k^{spec}}{(v_k^m)^2} \tag{9.24a}$$

$$\frac{q_k^{spec}}{(v_k^M)^2} \geq \frac{q_k}{v_k^2} \geq \frac{q_k^{spec}}{(v_k^m)^2} \tag{9.24b}$$

These inequalities are different from those of (9.9) in the direction of the inequality signs. Thus, by setting $p_k^m = p_k^M = p_k^{spec}$, and $q_k^m = q_k^M = q_k^{spec}$ in (9.22) and reversing the direction of the resulting inequalities, one obtains linear constraints which tightly surround the load manifold.

9.1.7 Linear Necessary Conditions on Line Power Flows

For a transmission line connecting bus k to j, the line current (from k to j) is given by

$$I_{kj}\,(\underline{x}_r) = \frac{1}{2} V_k\, Y_\ell^{sht} + (V_k - V_j)\, Y_\ell^{ser}$$

$$\triangleq I_{kj}^{re}\,(\underline{x}_r) + j\, I_{kj}^{im}\,(\underline{x}_r) \tag{9.25}$$

where ℓ is the line index. Obviously $I_{kj}^{re}(\underline{x}_r)$ and $I_{kj}^{im}(\underline{x}_r)$ are linear functions of $\underline{x}_r$.

Now consider the power flowing from bus k to bus j, that is

$$S_{kj} = p_{kj} + j\, q_{kj} = V_k\, I_{kj}^*$$

$$= (e_k + j\, f_k)\, [I_{kj}^{re}\,(\underline{x}_r) - j\, I_{kj}^{im}\,(\underline{x}_r)]$$

As in Section 9.1.2.1, the above relation leads to

$$I_{kj}^{re}\,(\underline{x}_r) = \left(\frac{p_{kj}}{v_k^2}\right) e_k + \left(\frac{q_{kj}}{v_k^2}\right) f_k \tag{9.26a}$$

$$I_{kj}^{im}\,(\underline{x}_r) = \left(\frac{p_{kj}}{v_k^2}\right) f_k - \left(\frac{q_{kj}}{v_k^2}\right) e_k \tag{9.26b}$$

Now starting from the constraints $|p_{kj}| \le p_{kj}^M$, $|q_{kj}| \le q_{kj}^M$, and

$(v_k^m)^2 \le v_k^2 \le (v_k^M)^2$, one can follow the same steps leading to (9.22) to obtain:

$$|I_{kj}^{re}(\underline{x}_r) + \xi_k\, I_{kj}^{im}(\underline{x}_r)| \le [\frac{p_{kj}^M - \xi_k\, q_{kj}^M}{(v_k^m)^2}]\; e_k + [\frac{q_{kj}^M + \xi_k\, p_{kj}^M}{(v_k^m)^2}]\; f_k \qquad (9.27a)$$

$$|I_{kj}^{re}(\underline{x}_r) + \eta_k\, I_{kj}^{im}(\underline{x}_r)| \le -\,[\frac{p_{kj}^M + \eta_k\, q_{kj}^M}{v_k^m}]\; e_k + [\frac{q_{kj}^M - \eta_k\, p_{kj}^M}{(v_k^m)^2}]\; f_k \qquad (9.27b)$$

9.1.8 Summary of the Constraints Forming the Enclosing Set

The linear constraints forming $L_x^a(\underline{d})$ are summarized in Table 9.1. Constraints (9.17) are not included in the table, because they simply represent relation (9.16), which is assumed to be true. The set $L_x^a(\underline{d})$ is thus comprised of $3N_b$ constraints corresponding to the voltage magnitudes, and $4(N_b + N_\ell)$ constraints due to the restrictions on the nodal power injections and the line power flows. For example, for a 15 bus system with 24 lines $L_x^a(\underline{d})$ is defined by 200 inequality constraints and 1 equality (i.e., equation (9.19)) .

Since the basic tool available for analyzing linear sets is the simplex method, it is advisable to choose $\theta_r = 45^\circ$. This choice of θ_r generally ensures that $\underline{x}_r \ge \underline{0}$ which fits into the conventional formulation of the LP problems.

TABLE 9.1

SUMMARY OF THE LINEAR CONSTRAINTS FORMING $L_x^a(\underline{d})$

$$\left[\xi_k = -\frac{1}{\eta_k} = \tan(\psi_k - \delta_k)\right]$$

Bounds on Generations:

$$I_k^{re}(\underline{x}_r) + \xi_k I_k^{im}(\underline{x}_r) \begin{cases} \geq \left[\dfrac{p_k^m - \xi_k q_k^m}{(v_k^M)^2}\right] e_k + \left[\dfrac{\xi_k p_k^m + q_k^m}{(v_k^M)^2}\right] f_k \\[2ex] \leq \left[\dfrac{p_k^M - \xi_k q_k^M}{(v_k^m)^2}\right] e_k + \left[\dfrac{\xi_k p_k^M + q_k^M}{(v_k^m)^2}\right] f_k \end{cases}$$

$$I_k^{re}(\underline{x}_r) + \eta_k I_k^{im}(\underline{x}_r) \begin{cases} \geq \left[\dfrac{p_k^M}{(v_k^m)^2} - \eta_k \dfrac{q_k^m}{(v_k^M)^2}\right] e_k + \left[\dfrac{q_k^m}{(v_k^M)^2} + \eta_k \dfrac{p_k^M}{(v_k^m)^2}\right] f_k \\[2ex] \leq \left[\dfrac{p_k^m}{(v_k^M)^2} - \eta_k \dfrac{q_k^M}{(v_k^m)^2}\right] e_k + \left[\dfrac{q_k^M}{(v_k^m)^2} + \eta_k \dfrac{p_k^m}{(v_k^M)^2}\right] f_k \end{cases}$$

Bounds on Demands: Set $p_k^m = p_k^M = p_k^{spec}$ and $q_k^m = q_k^M = q_k^{spec}$ in the above relations and change the direction of the inequalities.

Bounds on Line Power Flow:

$$\left|I_{kj}^{re}(\underline{x}_r) + \xi_k I_{kj}^{im}(\underline{x}_r)\right| \leq \left[\frac{p_{kj}^M - \xi_k q_{kj}^M}{(v_k^m)^2}\right] e_k + \left[\frac{q_{kj}^M + \xi_k p_{kj}^M}{(v_k^m)^2}\right] f_k$$

$$\left|I_{kj}^{re}(\underline{x}_r) + \eta_k I_{kj}^{im}(\underline{x}_r)\right| \leq -\left[\frac{p_{kj}^M + \eta_k q_{kj}^M}{(v_k^m)^2}\right] e_k + \left[\frac{q_{kj}^M - \eta_k p_{kj}^M}{(v_k^m)^2}\right] f_k$$

TABLE 9.1 (cont'd)

Voltage Limits:

$$\cos(\psi_k - \delta_k/2)\, e_k + \sin(\psi_k - \delta_k/2)\, f_k \le v_k^M$$

$$\cos(\psi_k + \delta_k/2)\, e_k + \sin(\psi_k + \delta_k/2)\, f_k \le v_k^M$$

$$\cos(\psi_k)\, e_k + \sin(\psi_k)\, f_k \ge v_k^m \cos(\delta_k)$$

For the reference bus:

$$v_r^m \cos\theta_r \le e_r \le v_r^M \cos\theta_r$$

$$\tan(\theta_r)\, e_r - f_r = 0$$

9.2 Characterizing Subsets of the Set of Secure Load Flow Solutions

The approach presented in the last section can be modified to obtain an approximate subset of $S_x(\underline{d})$, denoted by $L_x^b(\underline{d})$. The required modifications are of two types:

(i) Instead of enclosing the set $U_x \cap Y_x$ by linear constraints, embedding a linear set inside that set is attempted.

(ii) Full representation of the physical constraints is replaced by using certain linear cross section of the load manifold.

The details of the above modifications when applied to various system constraints are given in the following sub-sections.

9.2.1 Derivation of Linear Sufficient Conditions

When embedding subsets in the set of operating constraints, $U_x \cap Y_x$, one should make sure that no point exterior to $U_x \cap Y_x$ will be included in the enclosed subset. Thus, for instance, instead of using relations (9.9), one starts with the following conditions:

$$0 < p_k^m \le \left(\frac{v_k}{v_k^m}\right)^2 p_k^m \le p_k \le \left(\frac{v_k}{v_k^M}\right)^2 p_k^M \le p_k^M \tag{9.28a}$$

$$0 < q_k^m \le \left(\frac{v_k}{v_k^m}\right)^2 q_k^m \le q_k \le \left(\frac{v_k}{v_k^M}\right)^2 q_k^M \le q_k^M \tag{9.28b}$$

or, considering only the inner bounds,

$$\frac{p_k^m}{(v_k^m)^2} \le \frac{p_k}{v_k^2} \le \frac{p_k^M}{(v_k^M)^2} \tag{9.29a}$$

$$\frac{q_k^m}{(v_k^m)^2} \le \frac{q_k}{v_k^2} \le \frac{q_k^M}{(v_k^M)^2} \tag{9.29b}$$

Now, to derive linear constraints using (9.29), one has to modify the guide-line (9.11) such that the resulting relations define a subset of the original set. It is easy to show that the appropriate sufficient relations in this case are

$$A\,Y^m + B\,X^M \le B\,X + A\,Y \le A\,Y^M + B\,X^m \tag{9.30a}$$

$$A\,X^m - B\,Y^m \le A\,X - B\,Y \le A\,X^M - B\,Y^M \tag{9.30b}$$

Thus any X and Y satisfying the above, also satisfy $X^m \le X \le X^M$ and $Y^m \le Y \le Y^M$. For $\dot{\sigma} = A/B = 10$, this is illustrated in Figure 9.3 .

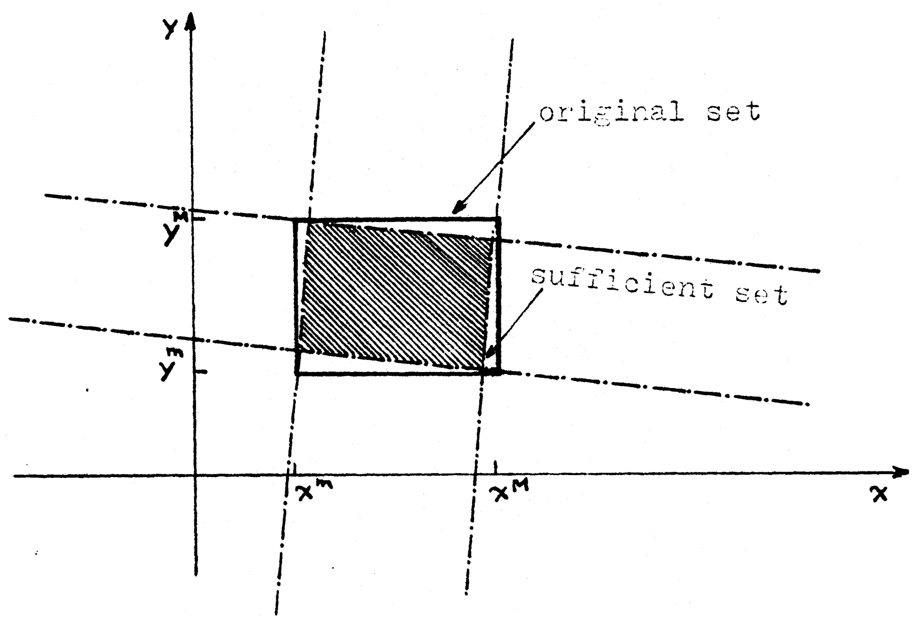

Figure 9.3. Relation between the set $\{x^m \le x \le x^M;\ Y^m \le Y \le Y^M\}$ and its subset, derived based on the sufficient conditions in (9.30) for $\sigma = 10$.

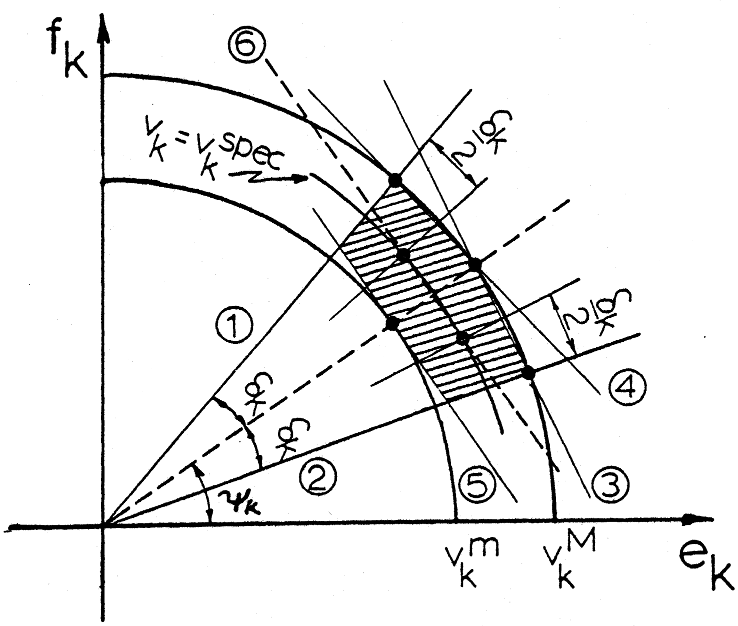

Figure 9.4. Linear sufficient constraints corresponding to the bounds on a voltage level.

Now following the same steps as detailed in the previous section, inequalities (9.29) and the guideline (9.30) can be used to derive a set of linear sufficient conditions. The resulting inequalities will be identical to those of (9.22), except for the following changes:

(i) All v_k^M and v_k^m are replaced by v_k^m and v_k^M respectively.

(ii) ξ_k is defined by $\xi_k = -\frac{1}{\eta_k} = \tan(\psi_k + \delta_k)$.

The second change is due to the fact that here, instead of relation (9.17b), relation (9.17a) is used. The linear, sufficient conditions corresponding to the line power flows are obtained by making the same changes in equations (9.27).

Also, instead of relations (9.18), representing necessary conditions on the voltage levels, one has to use the following sufficient conditions:

$$\text{(iii)} \quad [-\sin(\psi_k) + \sin(\psi_k + \delta_k)]\, e_k + [\cos(\psi_k) - \cos(\psi_k + \delta_k)]\, f_k \le v_k^M \sin(\delta_k) \tag{9.31a}$$

$$\text{(iv)} \quad [\sin(\psi_k) - \sin(\psi_k - \delta_k)]\, e_k$$

$$- [\cos(\psi_k) - \cos(\psi_k - \delta_k)]\, f_k \le v_k^M \sin(\delta_k) \tag{9.31b}$$

$$\text{(v)} \quad \cos(\psi_k)\, e_k + \sin(\psi_k)\, f_k \ge v_k^m \tag{9.31c}$$

The relation between these constraints and the original bounds on v_k^2 is shown in Figure 9.4.

9.2.2 Load Manifold Representation

At the PQ buses, we fix the value of the voltage magnitude. As a result, the load manifold becomes the intersection of a number of hyper-planes of the form:

$$(v_k^{spec})^2\, I_k^{re}(\underline{x}_r) = p_k^{spec}\, e_k + q_k^{spec}\, f_k \tag{9.32a}$$

$$(v_k^{spec})^2\, I_k^{im}(\underline{x}_r) = p_k^{spec}\, f_k - q_k^{spec}\, e_k \tag{9.32b}$$

where v_k^{spec} is chosen inside the range $v_k^m \le v_k \le v_k^M$. Obviously, the resulting load manifold is the cross-section of the original manifold for $v_k = v_k^{spec}$.

To have results consistent with the specified value of voltage levels, these should be enforced. For this purpose, we use the equality constraint:

$$\text{(vi)} \quad \cos(\psi_k)\, e_k + \sin(\psi_k)\, f_k = v_k^{spec} \cos(\delta_k / 2) \tag{9.32c}$$

The relation between the above line and the constraint $v_k = v_k^{spec}$ is illustrated in Figure 9.4 by line 6 .

9.2.3 Numerical Considerations

Inequality (9.29a) is valid if p_k^M , p_k^m , v_k^M and v_k^m satisfy

$$\left(\frac{v_k}{v_k^m}\right)^2 p_k^m \leq \left(\frac{v_k}{v_k^M}\right)^2 p_k^M \tag{9.33}$$

Since values of p_k^M and p_k^m are normally far apart while v_k^M and v_k^m are quite close, the above condition is almost always satisfied. The same argument applies to other inequalities in (9.29).

In replacing the nonlinear constraint $v_k = v_k^{spec}$ by the linear constraint in (9.32c), a certain amount of error is introduced. Assuming, however, that relation (9.16) holds, the % error lies in the interval:

$$\{-\ 200\ \sin^2\ (\delta_k/4),\ -\ 100\ +\ 100\ \cos\ (\delta_k/2)\ /\ \cos\ (\delta_k)\} \tag{9.34}$$

For $\delta_k = 5.65^{\circ}$ this interval is $[-0.122\ ,\ 0.366]$, which is rather insignificant. Note that since $v_k = v_k^{spec}$ cannot be enforced exactly, points belonging to $L_x^b(\underline{d})$ satisfy the demand with a small error. Also, to be consistent with the actual bounds on v_k , v_k^{spec} has to be chosen from the range

$$v_k^m\ /\ \cos\ (\delta_k/2) \leq v_k^{spec} \leq v_k^M\ \cos\ (\delta_k)\ /\ \cos\ (\delta_k/2) \tag{9.35}$$

The above relation is derived by demanding that the segment of the line (9.32c) satisfying (9.16) should also satisfy $v_k^m \leq v_k \leq v_k^M$.

In the present formulation, every PQ bus introduces 3 equality constraints into $L_x^b(\underline{d})$. There is also an equality constraint due to the reference bus (equation (9. 19)) . Thus, for an N_b - bus system with m PQ buses, in order $L_x^b(\underline{d})$ to be more than a single point (if not empty), one should have

$$3\ m + 1 < 2\ N_b$$

where $2\ N_b$ is the dimension of $\underline{x}_r$. Therefore, a 15 bus system must have less than 10 and a 50 bus system should have less than 33 PQ buses in the system in order for this method to be applicable.

9.3 Applications

9.3.1 Potential Applications of an Enclosing Set

The set $L_{x}^{a}(\underline{d})$, being defined by inequalities linear in $\underline{x}_r$, can be analyzed via linear programming. Once $L_{x}^{a}(\underline{d})$ is formed, it can easily provide the following information on $S_x(\underline{d})$:

(i) Existence of Secure Load Flow Solutions

The absence of a voltage vector $\underline{x}_r$ satisfying the inequalities defining $L_{x}^{a}(\underline{d})$ indicates that $L_{x}^{a}(\underline{d})$ and hence that $S_x(\underline{d})$ are empty. Note that the existence of $L_{x}^{a}(\underline{d})$ does not necessarily imply the existence of a secure load flow solution, but rather indicates that "near" secure voltage solutions exist.

(ii) Size and Shape of $S_x(\underline{d})$

For a given loading condition $\underline{d} = \underline{d}_0$, the "width" of the set $S_x(\underline{d}_0)$ in any direction $\underline{c}$ can be estimated approximately from the solutions of the following problem:

$$\text{Extremize} \; : \; \underline{c}^T \underline{x}_r$$

$$\underline{x}_r \in L_{x}^{a}(\underline{d}_0) \tag{9.36}$$

(iii) Near Secure Load Flow Solutions

Since $L_{x}^{a}(\underline{d})$ surrounds $S_x(\underline{d})$ "tightly", its vertices often represent possible near secure solutions. To obtain "better" solutions, one can maximize and minimize a linear objective function over $L_x^a(\underline{d})$ (i.e., solve (9.36)) to obtain two extreme points of $L_x^a(\underline{d})$. The line segment joining these two points lies entirely inside $L_x^a(\underline{d})$. One then can search along such a line to find a point at which the line either intersects or is very close to the load manifold.

(iv) Starting Points for Optimal Load Flow Algorithms

Suppose the objective function of an optimal load flow problem can be expressed, or approximated, by a linear function in $\underline{x}_r$. Then, by minimizing (or maximizing) that objective function over $L_x(\underline{d})$, one obtains an approximate solution to the original problem. Such a solution could prove invaluable to the optimal load flow schemes which require good starting points [90 , 91] .

9.3.2 Potential Applications of an Embedded Set

The set $L_x^b(\underline{d})$ offers equally interesting possibilities. The most important ones are:

(i) Secure Load Flow Solutions

The set $L_x^b(\underline{d})$, when non-empty, contains an infinite number of secure load flow solutions. Thus, it can be used in an emergency state to compute a corrective control strategy. The choice of the voltage levels at the PQ buses, however, is crucial under such circumstances. When voltage levels are not chosen properly, the set $L_x(\underline{d})$ will be empty. One can, nevertheless, hope that the system operator can use his experience, or use the past data, to assign voltage levels to the PQ buses appropriate to the existing loading condition. A suitable objective function can be used to avoid solutions which lead to economically poor system performance.

The fact that such computations can be carried out entirely by the highly efficient and reliable LP routines, suggests that the set $L_x^b(\underline{d})$ can be used for on-line computations. Note that the required tableau once computed, requires little effort to accommodate changes in the loading condition, network configuration, or the operating limits.

(ii) Starting Points for Optimal Load Flow Algorithms

Certain classes of the algorithms designed to solve constrained optimal problems require starting points satisfying all the constraints in the problem [90 , 97] . Such points are usually found by "ad hoc" procedures which are basically trial and error in nature. The set $L_x^b(\underline{d})$ allows a systematic approach for finding such solutions. It is clear that when the objective function can be expressed linearly in $\underline{x}_r$, the resulting solution would also represent an approximate solution to the original optimization problem.

9.4 Examples

In this section, the results of analyzing the sets $L_x^a(\underline{d})$ and $L_x^b(\underline{d})$ for a three bus system are presented. It has to be emphasized that these results pertain to those typical properties of $L_x^a(\underline{d})$ and $L_x^b(\underline{d})$ which are observed in various studied systems.

9.4.1 System Data

(i) Network Configuration (Figure 9.5)

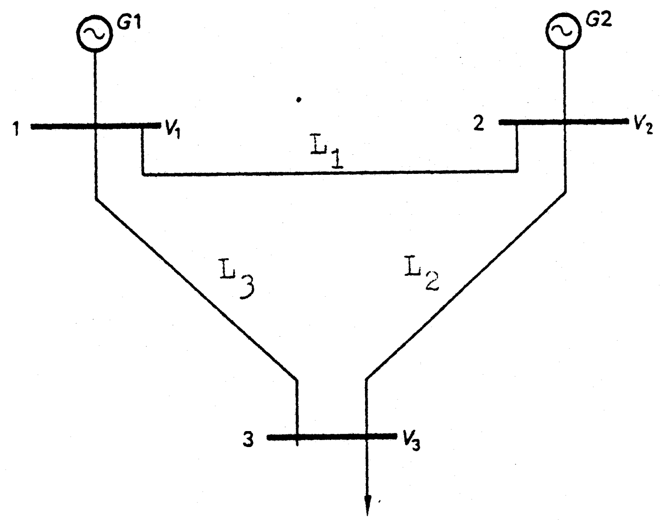

Figure 9.5. Network configuration for the example.

(ii) Network Data (in p.u.)

Line	Susceptance	Impedance
1	0 + j 0.015	0.030 + j 0.100
2	0 + j 0.020	0.020 + j 0.060
3	0 + j0.010	0.025 + j 0.105

(iii) System Constraints (in p.u.)

$0.1 \le p_1 \le 1.0$ $\qquad$ $0.1 \le p_2 \le 1.0$

$005 \le q_1 \le 0.4$ $\qquad$ $005 \le q_2 \le 0.5$

$0.97 \le v_1 \le 1.03$ $\qquad$ $0.97 \le v_2 \le 1.03$

$p_3 = -1.2$ $\qquad$ $q_3 = -0.5$ $\qquad$ $0.94 \le v_3 \le 0.98$

$|p_{12}| \le 0.2$ $\qquad$ $|q_{12}| \le 0.1$

$|p_{23}| \le 1.0$ $\qquad$ $|q_{23}| \le 0.5$

$|p_{31}| \le 0.8$ $\qquad$ $|q_{31}| \le 0.4$

(iv) Value of the Adjustable Parameters

Since the buses in the chosen power network are electrically close, one can allow

$$\psi_1 = \psi_2 = \psi_3 = \theta_r$$

Value of the other adjustable parameters are set at

$$\theta_r = \theta_1 = 45^\circ \quad ; \quad \delta_1 = 0^\circ \quad ; \quad \delta_2 = \delta_3 = 5^\circ$$

Here, bus No. 1 represents both the slack and the reference bus.

9.4.2 Properties of the Computed Enclosing Set

For the given system data linear inequalities forming $L_x^a(\underline{d}_0)$ are computed. The following LP problems are then solved:

$$\underset{\underline{x}_r \,\varepsilon\, L_x^a(\underline{d})}{\text{Maximize}} : \pm \underline{C}_0^T \underline{x}_r = \pm \sum_{i=1}^{2N_b} (x_i)_r \qquad (9.37)$$

The solutions of the above problems are two extreme vertices of $L_x^a(\underline{d})$ which, corresponding to the sign of the objective function, are denoted by $\underline{x}_r^+$ and $\underline{x}_r^-$. The line segment connecting these two points is given by

$$\underline{x}_r = \underline{x}_r^+ + t\,(\underline{x}_r^- - \underline{x}_r^+) \qquad 0 \le t \le 1 \qquad (9.38)$$

Table 9.2 indicates that for $\underline{x}_r^+$ (t=0) and $\underline{x}_r^-$ (t=1) some of the system constraints (marked by *) are violated. This is obviously due to the fact that $L_x^a(\underline{d}) \supset S_x(\underline{d})$. By the same argument, one can hope that as the vector $\underline{x}_r$ moves into the set $L_x^a(\underline{d})$ along the line (9.38), it enters into the set $U_x \cap Y_x$. This is verified by searching along the line. The search, as recorded in Table 9.2, has shown that part of the line (9.38) identified by $0.31 \le t \le 0.92$ is indeed inside the set $U_x \cap Y_x$. This range of t is also reflective of the degree of "tightness" with which $S_x(\underline{d})$ is surrounded by $L_x^a(\underline{d})$, along the direction $\underline{C}_0$.

Next, by minimizing the function

$$f(t) = \sum_{k=N_{g+1}}^{N_b} \{\lambda_k\, [p_k(t) - p_k^{spec}]^2 + \gamma_k\, [q_k(t) - q_k^{spec}]^2\} \qquad (9.39)$$

$$0.31 \le t \le 0.92$$

we tried to find a point on the secure portion of the line (9.38) close to the load manifold, $M_x(\underline{d})$. In (9.39), the positive constants λ_k and γ_k are appropriate weights, while the functions $p_k(t)$ and $q_k(t)$ represent the variation of p_k and q_k along the line (9.38). Since the demand variables are quadratic in $\underline{x}_r$, their variation with t is also quadratic. Thus, to compute, say, $p_k(t)$ it is sufficient to have its value at three points along the line (9.38). For this example, using $\lambda_3 = \gamma_3 = 1.0$, the function $f(t)$ has a minimum at $t \simeq 0.485$. Value of various relevant quantities for t = 0.485 is also given in Table 9.2.

TABLE 9.2.

VOLTAGE SOLUTIONS AND CORRESPONDING VALUES OF SYSTEM VARIABLES

FOR IMPORTANT POINTS ALONG A LINE JOINING TWO VERTICES OF $L_x^a(\underline{d})$

Variable	t = 0.00	t = 0.31	t = 0.485	t = 0.92	t = 1.00
e_1	0.726946	0.714220	0.706831	0.689178	0.686894
e_2	0.727010	0.709045	0.698614	0.673695	0.669060
e_3	0.730550	0.714724	0.705535	0.683585	0.679500
f_1	0.726946	0.714220	0.706831	0.689178	0.685894
f_2	0.701069	0.700970	0.700912	0.700775	0.700750
f_3	0.653328	0.650685	0.649151	0.645481	0.644804
V_1	$1.028\angle 45.00^\circ$	$1.010\angle 45.00^\circ$	$0.999\angle 45.00^\circ$	$0.974\angle 45.00^\circ$	$0.970\angle 45.00^\circ$
V_2	$1.010\angle 43.96^\circ$	$0.997\angle 44.67^\circ$	$0.989\angle 45.09^\circ$	$0.972\angle 46.13^\circ$	$0.969\angle 46.32^\circ$ *
V_3	$0.980\angle 41.80^\circ$	$0.966\angle 42.31^\circ$	$0.958\angle 42.61^\circ$	$0.940\angle 43.36^\circ$	$0.937\angle 43.50^\circ$ *
P_1	0.83983	0.59797	0.46125	0.14568	0.08869 *
P_2	0.48952	0.66205	0.76010	0.98796	1.02936 *
P_3	-1.30439 *	-1.23800 *	-1.20028	-1.11267 *	-1.09676 *

TABLE 9.2 (cont'd)

Variable	t = 0.00	t = 0.31	t = 0.485	t = 0.92	t = 1.00
q_1	0.44531 *	0.39969	0.37382	0.31387	0.30300
q_2	0.14553	0.14975	0.15429	0.17134	0.17548
q_3	-0.54682 *	-0.51695 *	-0.49968	-0.45863 *	-0.45103 *
p_{12}	0.22466	0.08913	0.01259	-0.16385	-0.19568
p_{23}	0.71233	0.75063	0.77241	0.82308	0.83230
p_{31}	-0.60352	-0.50017	-0.44151	-0.30537	-0.28066
q_{12}	0.11233 *	0.09720	0.08864	0.06881	0.06522
q_{23}	0.26729	0.26021	0.25682	0.25093	0.25017
q_{31}	-0.29410	-0.27588	-0.26478	-0.23674	-0.23128

(Violated constraints for the given solution points are marked by stars (*)) .

Existence of the Set $L_x^a(\underline{d})$

By increasing the real demand from -1.2 to -1.55 and changing the range of allowable voltage level at the load bus to $1.0 \le v_3 \le 1.05$, the set $L_x^a(\underline{d})$ disappears. The absence of $L_x^a(\underline{d})$ implies that the load manifold, $M_x(\underline{d})$, is not intersecting the set $U_x \cap Y_x$, and, thus, $S_x(\underline{d})$ must be empty. Note that the assumed loading condition and the voltage limits do not correspond to abnormal loading conditions or voltage profiles on the studied system. In fact, the system seems to have sufficient generation and transmission capacity to meet the specified demand. A small increase in $p_{12}^M = 0.2$, however, causes the set $L_x^a(\underline{d})$ to reappear.

9.4.3 Properties of the Computed Embedded Set

In the same three bus system, under the loading condition and operating constraints stated in Section 9.4.1, the set $L_x^b(\underline{d})$ is formed. We have tried however to keep the voltage level on the demand bus at $v_3 = 0.96$.

Any voltage vector $\underline{x}_r \in L_x^b(\underline{d})$, represents a secure load flow solution. Two such points are computed by maximizing and minimizing the objective function in (9.37) over $L_x^b(\underline{d})$. These solutions are identified in Table 9.3 by $t = 0$ and $t = 1$ respectively. The mid-point of the line segment connecting these two solutions is also included in the table to represent a point inside $L_x^b(\underline{d})$.

The values of various system variables computed for the tabulated points are fully indicative of the fact that, within the introduced approximations, $S_x(\underline{d}) \supset L_x^b(\underline{d})$. Since the loading condition is enforced by equality constraints, the load is (approximately) satisfied along any line connecting two points belonging to $L_x^b(\underline{d})$. The small imbalance between the actual demand and those implied by the solutions, is due to the linear enforcement of $v_3 = 0.96$. The amount of imbalance is generally small (here about %0.5) and for various tested systems has not been observed to exceed %2 .

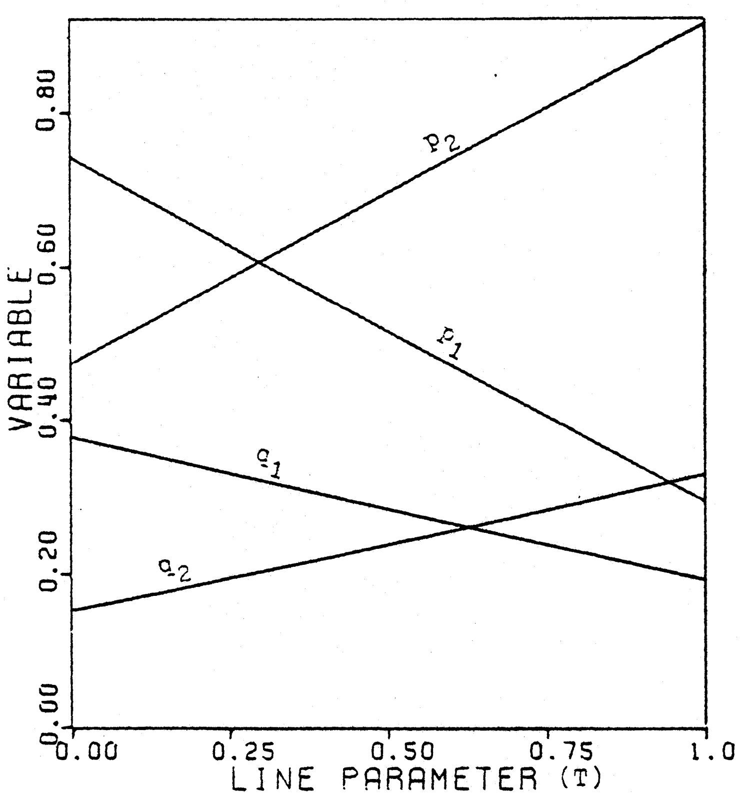

Figure 9.6. Variation of some of the system variables along a line joining two vertices of $L_x^b(\underline{d})$.

TABLE 9.3

VOLTAGE SOLUTIONS AND CORRESPONDING VALUES OF SYSTEM VARIABLES FOR TWO VERTICES OF $L_x^b(\underline{d})$ AND THEIR MID-POINT

Variable	t = 0.0	t = 0.5	t = 1.0
e_1	0.707967	0.703669	0.699370
e_2	0.711990	0.706558	0.701125
e_3	0.711990	0.706558	0.701125
f_1	0.707967	0.703669	0.699370
f_2	0.685959	0.697076	0.708192
f_3	0.640488	0.645921	0.651353
V_1	$1.001\angle 45.00^\circ$	$0.995\angle 45.00^\circ$	$0.989\angle 45.00^\circ$
V_2	$0.986\angle 44.06^\circ$	$0.989\angle 44.78^\circ$	$0.993\angle 45.49^\circ$
V_3	$0.957\angle 41.97^\circ$	$0.957\angle 42.43^\circ$	$0.957\angle 42.89^\circ$
P_1	0.74162	0.51694	0.29495
P_2	0.47412	0.69681	0.91903
P_3	-1.19421	-1.19328	-1.19250

TABLE 9.3 (cont'd)

Variable	t = 0.0	t = 0.5	t = 1.0
q_1	0.37796	0.28454	0.19224
q_2	0.15313	0.23946	0.33187
q_3	-0.49759	-0.49720	-0.49687
p_{12}	0.18898	0.04954	-0.08822
p_{23}	0.66177	0.74622	0.83057
p_{31}	-0.54284	-0.46023	-0.37821
q_{12}	0.08670	0.03313	-0.01978
q_{23}	0.25020	0.28695	0.32601
q_{31}	-0.25967	-0.23081	-0.20068

The voltage solution in Table 9.3 corresponding to $t = 0.0$ represents a vertex of the set $L_x^b(\underline{d})$. Restricted variables forming this vertex are: p_3, q_3, v_3, q_1, p_{12}, and q_{12} . Comparing the value of the last three variables at that vertex with their corresponding original limits indicates that this vertex is fairly close to the boundary of $S_x(\underline{d})$.

Figure 9.6 shows the variation of some of the unspecified variables along the line segment connecting the voltage solutions in Table 9.3 . The large amount of variations that the real power injections exhibit is suggestive that for this example $L_x^b(\underline{d})$ is a relatively large set. Cleraly, under such circumstances, $L_x^b(\underline{d})$ can be used to obtain a very good starting point to any optimal load flow problem.

CHAPTER X

CONCLUSIONS AND SUGGESTIONS FOR FURTHER INVESTIGATION

10.1 Conclusions

A general approach to the analysis and the explicit characterization of those operating conditions under which a bulk-power system is steady-state secure is put forward in this thesis. Theoretical and numerical tools basic to this study have been developed by exploiting the analytical properties of the mathematical model of the system. The implications and potential applications of the results with regard to various security related problems have been investigated. The validity of the proposed schemes and their potential applications are demonstrated through a number of numerical examples.

Significant results and notable developments in this thesis are the following:

(i) The general steady-state invulnerability set in the space of the network parameters and the specified nodal injections possesses important properties which qualify it as a basis for a unified approach to the treatment of various security related functions of a power system.

(ii) The security sets in the injection space are the consequence of two successive mathematically well-defined transformations on a number of simple, elementary sets.

(iii) Using Taylor series expansion formula, approximate expressions, relating dependent load flow variables to the nodal injection vector, can be derived systematically. It is shown that the resulting linear relations have adequate accuracy, while the quadratic relations are highly accurate.

(iv) The approximate relations derived based on the Taylor series expansion formulae have their major applications in:

(1) Constructing steady-state security regions in the injection space;

(2) Functional representation of the impact of the load-generator outages on the pre-outage operating points;

(3) Systematic derivation of highly accurate loss formulae;

(4) Expanding the scope of some efficient secure-economic dispatch algorithms which are based on the DC load flow model or decoupled load flow schemes.

(v) When a security set is non-empty, there exists only a certain class of expansion points for the approximate relations which lead to the correct description of the set in the injection space.

(vi) In theory, security regions in both voltage and injection spaces can be disjoint.

(vii) The steady-state security regions are not invariant under the choice of the location of the slack or the reference bus.

(viii) The problem of characterizing part of a security region by a simple, explicit function has been formulated as an optimization problem. When the explicit function is a general ellipsoid, two efficient numerical schemes for solving the resulting problem have been developed and tested.

(ix) The problem of embedding the largest set inside a security set for a given explicit function has been formulated as a mini-max problem. For the case where the set is linear and the function is a general ellipsoid, it is demonstrated that the problem is reducible to a simple standard LP problem.

(x) An efficient scheme has been suggested for screening out the redundant constraints among those defining a security set. The scheme is based on the random generation of points inside the set and does not involve excessive computations.

(xi) A simple technique has been proposed to compute various stand-by control strategies for a system under vulnerable conditions.

The technique requires pre-computing the largest ellipsoids that can be put inside various security sets.

(xii) The concept of a security corridor and numerical schemes required for its computation have been developed. A security control is composed of a number of overlapping explicit security sets covering a predicted daily trajectory. As long as the actual trajectory stays inside a security corridor, security is guaranteed and no additional computations are required. Construction of a security corridor has been shown to be virtually a systematic region-wise predictive security assessment scheme with results which can significantly improve various security functions of a system. Through numerical examples it is demonstrated that:

1. To form a security corridor, only a small number of explicit security sets are required;

2. Compared to running load flows, the residence of the actual trajectory inside (or outside) a security corridor can be verified trivially;

3. For the greater part of the predicted trajectory, a typical security corridor is "wide" enough to allow large deviations of the actual trajectory from the predicted one inside its boundary.

(xiii) A new monitoring scheme which involves infrequent detailed security analysis has been proposed. The scheme is based on new developments suggesting that by using the information on the security of an operating point and pre-computing a number of coefficients, part of the security region surrounding the operating point can be characterized trivially.

(xiv) The concept of a secure loadability set with notable applications to system expansion planning and load management has been introduced. A secure loadability set contains all the loading conditions for which there exist at least one control strategy capable of producing a secure operating point. For the case where the security set is linear, an approach for characterizing its secure loadability set has been outlined. Techniques are also developed to characterize sub-sets of a secure loadability set. One such sub-set is the set of secure-economical loadability set with important implications in power system expansion planning.

(xv) Simple techniques are developed to enclose, or to characterize a subset of, the set of secure load flow solutions by a linear set. The validity and the performance of these techniques are verified through numerical examples. It is demonstrated that:

1. The degree of "tightness" of an enclosing set can be partly influenced by adjusting certain parameters;

2. The emptiness of the enclosing set is a sufficient condition for the non-existence of a secure load flow solution;

3. The linear subsets can provide easy access to voltage vectors satisfying all the equality and inequality constraints. Thus, they serve as a systematic means for computing starting points to optimization algorithms which require such points as their starting points.

10.2 Suggestions for Further Investigation

Since a large portion of this thesis is devoted to analytical studies, some numerical aspects of the proposed schemes may have not been fully explored. Future research efforts thus can be directed toward further investigation of the efficiency and performance of the proposed schemes on larger systems and under more realsitic operating conditions.

Other suggestions for further research include:

(i) The modification of the system's mathematical model to include the transformer turn ratios as part of the control variables. This leads to more general results and, in particular, to more practical loss formulae.

(ii) The application of approximation formulae in network equivalencing. Approximate relations can be derived to express explicitly the power flows in the tie-lines connecting a system to its neighbouring system in terms of the nodal injections in both systems. Thus, - with the availability of communication links between control centers of the neighbouring systems - the impact of changes inside one system on a neighbouring system can be easily accounted for by computing changes in the relevant tie-line power flows.

(iii) The development of a new numerical scheme for obtaining all the solutions to a load flow problem. This problem can be related to the algorithms developed in Chapter VI by formulating it in the following form:

$$f\ (\varepsilon) \;=\; \underset{\underline{x}}{\text{Min}} : \;\{[L\ (\underline{x})\ ]\ \underline{x} - \underline{z}^{spec}\}^{T}\{[L\ (\underline{x})]\ \underline{x} - \underline{z}^{spec}\}$$

subject to

$$(\underline{x} - \underline{x}_0)^T(\underline{x} - \underline{x}_0) \;=\; \varepsilon$$

Zeros of the scalar function $f\ (\varepsilon)$ occur at various load flow solutions and thus can be found by increasing value of ε from zero in steps and solving the resulting problems.

(iv) Exploring the possibility of using the explicit global and local sub-sets of a security set in solving optimization problems involving that set. A possible approach may involve first substituting the set by its global sub-set and solving the optimization problem, and then refining the resulting approximate solution by successive use of the local sub-sets.

(v) The development of fast and efficient numerical schemes to compute the coefficients

$$\underline{\beta}_j^T\,(\underline{x}_0)\;[A_z]^{-1}\;\underline{\beta}_j\,(\underline{x}_0) \qquad j=1,\ \ldots,\ N_{dp}$$

directly in terms of $\underline{x}_0$, $[Y_i]$ and $[A_z]$, without actually computing $\underline{\beta}_j\,(\underline{x}_0)$. The availability of such schemes could greatly reduce the required computation time for up-dating these coefficients in case of a change in network topology or drastic departure of the operating points from the neighbourhood of $\underline{z}_0 = [L\,(\underline{x}_0)]\,\underline{x}_0$.

(vi) The formulation of a generalized security corridor in the space of network parameters and nodal injections. In this space a security corridor may accommodate deviations from the expected values both in the injections and in the network parameters.

(vii) The development of more efficient schemes to characterize a secure loadability set. The scheme proposed in Chapter VIII involves rather excessive off-line computations and may prove to be highly expensive.

(viii) The investigation into the possibility of combining the derivation of $L_x^a(\underline{d})$ and $L_x^b(\underline{d})$ in such a way that the factors influencing $L_x^a(\underline{d})$ offset each others' effect. The resulting set should be able to produce better approximate solutions for optimization problems involving $S_x(\underline{d})$.

REFERENCES

[1] Ewart, D.N., "Whys and Wherefores of Power System Blackouts," IEEE Spectrum, Vol. 15, p. 36, April 1978.

[2] "Economy-Security Functions in Power System Operations," Prepared by IEEE Working Group on Operating Economics and presented at IEEE Winter Power Meeting, January 1975 (IEEE Publ. 75 CH0969-5 PWR).

[3] Elgerd, I.O., An Introduction to Electric Energy Systems, McGraw-Hill, pp. 200-271, 1971.

[4] "Electric Power in Canada - 1978," Electrical Section, Energy Publicity Sector, Department of Energy, Mines and Resources, Cat. No.: M 24-5, 1979.

[5] Wilson, G.L., Zarakas, P., "Anatomy of a Blackout," IEEE Spectrum, Vol. 15, No. 2, pp. 39-46, February 1978.

[6] Corwin, J.L., Miles, W.T., "Impact Assessment of the 1977 New York City Blackout," Systems Engineering for Power, Division of Electrical Energy Systems, U.S. Department of Energy, July 1978.

[7] Schweppe, F.C., "Power Systems '2000' : Hierarchical Control Strategies," IEEE Spectrum, Vol. 15, No. 7, July 1978.

[8] Fink, L.H., Carlson, K., "Operating Under Stress and Strain," IEEE Spectrum, Vol. 15, No. 3, March 1978.

[9] Debs, A.S., Benson, A.R., "Security Assessment of Power Systems," Engineering Foundation Conference on Systems Engineering for Power : Status and Prospects, Henniker, N.H., pp. 144-176, August 1975.

[10] Hajdu, L.P., Podmore, R., "Security Enhancement for Power Systems," Engineering Foundation Conference on Systems Engineering for Power : Status and Prospects, Henniker, N.H., pp. 177-195, August 1975.

[11] DyLiacco, T.E., "The Adaptive Reliability Control System," IEEE Trans. on Power Apparatus and Systems, Vol. PAS-86, p. 517, 1967.

[12] DyLiacco, T.E., "Real Time Control of Power Systems," IEEE Proceedings, Vol. 62, No. 7, pp. 884-891, July 1974.

[13] DyLiacco, T.E., "System Control Centre Design," Proceedings Engineering Foundation Conference on Systems Engineering for Power : Status and Prospects, Henniker, N.H., pp. M 6 - 232, August 1975.

[14] Galiana, F.D., Glavitch, H., and Fiechter, A., "A General Compensation Method for the Study of Line Outages in Load Flow Problems," presented at the Fifth Power System Computation Conference, Cambridge, England, 1975.

[15] El-Abiad, A.H., and Stagg, G.W., "Automatic Evaluation of Power System Performance - Effects of Line and Transformer Outages," AIEE Trans. Power App. Syst., Vol. PAS - pp. 712-715, February 1963.

[16] Limmer, H.D., "Techniques and Applications of Security Calculations Applied to Dispatching Computers," presented at the Third Power Systems Computation Conference, Rome, Italy, June 23-27, 1969.

[17] Stott, B., "Review of Loadflow Calculation Methods," IEEE Proceedings, Vol. 62, No. 7, pp. 916-929, 1974.

[18] Taylor, D.G., "A Linear Programming Model Suitable for Power Flow Problems," Proc. Third PSCC, Rome, Italy, Paper OM2, 1969.

[19] Brown, H.E., "Contingencies Evaluated by a Z-matrix Method," IEEE Trans. Power App. Syst., Vol. PAS - 88, pp. 409-412, April 1969.

[20] Stott, B., "Decoupled Newton Load Flow," IEEE Trans. Power App. Syst., Vol. PAS - 91, pp. 1955-1959, September / October 1972.

[21] Stott, B., Alsac, O., "Fast Decoupled Loadflow," IEEE Trans., Vol. PAS - 73, May / June 1974.

[22] Peterson, N.M., Tinney, W.F., Bree, D.W., "Iterative Linear A.C. Power Flow Solution for Fast Approximate Outage Studies," IEEE Trans., Vol. PAS - 91, pp. 2048-2056, September / October 1972.

[23] Daniel, H., and Chen, M.S., "An Optimization Technique and Security Calculations for Dispatching Computers," IEEE Trans. on Power App. Syst., Vol. PAS - 91, pp. 883-888, May / June 1972.

[24] Stagg, G.W., and Phadke, A.G., "Real Time Evaluation of Power System Contingencies - Detection of Steady-State Overloads," presented at IEEE Summer Power Meeting July 1970.

[25] Sachdev, S.M., and Ibrahim, S.A., "A Fast Approximate Technique for Outage Studies in Power System Planning and Operation," presented at IEEE PES Summer Meeting, Vancouver, B.C., Canada, July 15 - 20, 1973, (Paper T 73 469-4).

[26] Zaborszky, J., et al, "Fast Contingency Evaluation Using Concentric Relaxation," Paper F 79 688-3, IEEE PES Summer Meeting, Vancouver, B.C., Canada, July 15 - 20, 1979.

[27] Zaborszky, J., and Subramanian, A.K., "On the Emergency Control of the Large Power System : Structure, State and Stability," Proceedings, 1977 Joint Automatic Control Conference, p. 737.

[28] Kaltenbach, J.C., and Hajdu, L.P., "Optimal Corrective Rescheduling for Power System Security," IEEE Trans., Vol. PAS - 90, pp. 843-851, March / April 1971.

[29] Peschon, J., et al, "Optimal Solution Involving System Security," in Proc. 7th PICA Conference, Boston, Massachusetts, pp. 210-218, 1971.

[30] Sachdev, M.S., and Ibrahim, S.A., "An Approach for Preventing System Insecurity Arising from Line Outages," paper presented at IEEE Winter Power Meeting, New York, January 1975.

[31] Blaschak, J.G., Heydt, G.T., and Bright, J.M., "A Generation Dispatch Strategy for Power Systems Operating under Alert Status," Paper A79 474-8, IEEE PES Summer Meeting, Vancouver, B.C., Canada, July 15 - 20, 1979.

[32] Carpentier, J.W., "Differential Injections Method : A General Method for Secure and Optimal Load Flows," Proc. IEEE 8th PICA Conference, Minneapolis, Minnesota, June 4 - 6, 1973.

[33] Carpentier, J.W., "Total Injection Method : A Method for the Solution of the Unit Commitment Problem Including Secure and Optimal Load Flow," <u>ibid</u>, pp. 412-420.

[34] Abadie, J., and Carpentier, J., "Generalization of the Wolfe Reduced Gradient Method to the Case of Nonlinear Constraints," <u>Optimization</u>, pp. 37-47, Academic Press, 1969.

[35] Abadie, J., "On the GRG Method for Nonlinear Optimization and Its Application to Control Problems," presented to the Advanced Study Institute on Integer and Nonlinear Programming, Ile de Bendon, June 1969 (Proceedings, North Holland Publishing Company, 1970).

[36] Peschon, J., Piercy, D.S., Tinney, W.F., Treit, O., "Sensitivity in Power System," IEEE, Vol. PAS - 87, pp. 1687-1695, August 1968.

[37] Peschon, J., et al, "Optimum Control of Reactive Power Flow," IEEE Trans. Power App. Syst., Vol. PAS - 87, October 1968.

[38] Peschon, J., et al, "Optimum Power Flow for Systems with Area Interchange Controls," Submitted to the IEEE for presentation at the Summer Power Meeting, 1971.

[39] Dommel, H.W., Tinney, W.F., "Optimal Power Flow Solutions," IEEE Trans., Vol. PAS - 87, pp. 1866-1876, October 1968.

[40] Dommel, H.W., "Constrained Optimal Control of Real and Reactive Power Dispatch," Symposium on Optimal Power-System Operation, University of Manchester, Institute of Science and Technology, U.K., September 8 - 12, 1969.

[41] Sasson, A.M., Aboytes, F., Gardenas, C., Gomez, R., Viloria, F., "A Comparison of Power System Static Optimization Techniques," Proceedings of the Power Industry and Computer Applications (PICA), pp. 328-340, Boston, May 1971.

[42] Sasson, A.M., and Merill, H.M., "Some Applications of Optimization Techniques to Power System Problems", IEEE Proceedings, Vol. 62, No. 7, pp. 959-972, 1974.

[43] Wells, D.W., "Method for Economic Secure Loading of a Power System," Proc. IEE, Vol. 115, No. 8, pp. 1190-1194, August 1968.

[44] Shen, C.M., and Laughton, M.A., "Power System Load Scheduling with Security Constraint Using Dual Linear Programming," Proc. IEE, Vol. 117, No. 11, pp. 2117-2127, November 1970.

[45] Jolissant, C.H., Arvanitidis, N.V., and Luenberger, D.G., "Decomposition of Real and Reactive Power Flows : A Method Suitable for On-Line Applications," IEEE Trans. Power App. Syst., Vol. PAS - 91, pp. 661-670, March / April 1972.

[46] Ejebe, G.L., Puntel, W.R., Wollenberg, B.F., "A Load Curtailment Algorithm for the Evaluation of Power System Adequacy," Paper A77 505-1, IEEE Summer Power Meeting, Mexico, July 1977.

[47] Stott, B., Hobson, E., "Power System Security Control Applications Using Linear Programming, Part I and II," IEEE Vol. PAS - 97, pp. 1713-1731, September / October 1978.

[48] Stott, B., Marinho, J.L., "Linear Programming for Power System Network Security Application," IEEE Trans. Vol. PAS - 98, pp. 837-848, May / June 1979.

[49] Lasdon, L.S., Optimization Theory for Large Systems, MacMillan Company, 1970.

[50] Chan, S.M., Schweppe, F.C., "A Generation Reallocation and Load Shedding Algorithm," IEEE Trans. Vol. PAS - 98, pp. 26-34, January / February 1979.

[51] Chan, S.M., and Yip. E., "A Solution of the Transmission Limited Dispatch Problem by Sparse Linear Programming, Paper F78 568, presented at the IEEE PES Summer Meeting, Los Angeles, California, July 1978.

[52] Hnyilicza, E., Lee, S.T.Y., Schweppe, F.C., "Steady State Sesurity Regions : Set-Theoretic Approach," Proceedings of the Power Industry and Computer Applications (PICA), pp. 347-355, New Orleans 1975.

[53] Brown, H.E., "Interchange Capability and Contingency Evaluation by a Z-matrix Method," IEEE Trans., Vol. PAS - 91, pp. 1827-1832, September / October 1972.

[54] Landgren, G.L., et al, "Transmission Interchange Capability - Analysis by Computer," IEEE Trans., Vol. PAS - 91, pp. 2405-2414, November / December 1972.

[55] Landgren, G.L., and Anderson, S.W., "Simultaneous Power Interchange Capability Analysis," IEEE Trans., Vol. PAS - 92, pp. 1973-1989, November / December 1973.

[56] Pang, C.K., Koivo, A.J., and El-Abiad, A.H., "Application of Pattern Recognition to Steady-State Security Evaluation in a Power System," IEEE Trans., Vol. SMC - 3, pp. 622-630, November 1973.

[57] Pang, C.K., et al, "Security Evaluation in Power System Using Pattern Recognition," IEEE Trans., Vol. PAS - 93, pp. 969-976, May / June 1974.

[58] Crevier, D., "A Simulation-based Separation Surface Method for Power System Stability Assessment," Paper A78 226-3, IEEE Winter Power Meeting, New York, February 1978.

[59] Crevier, D., Nourmoussavi, M.A., "Steady State and Transient Stability Domains of Power Systems," presented at the IEEE Canadian Communications and Power Conference, Montreal, Quebec, October 18-20, 1978.

[60] Mattheiss, T.H., "An Algorithm for Determining Irrelevant Constraints and All Vertices in Systems of Linear Inequalities," Operations Research, Vol. 21, pp. 247-260, 1973.

[61] DeMaio, J.A., Fischl, R., "Fast Identification of the Steady State Security Regions for Power System Security Enhancement," Paper No. A76-076, IEEE Winter Power Meeting, New York, January 1976.

[62] Fischl, R., Ejebe, G.C., and DeMaio, J.A., "Identification of Power System Steady-State Security Regions under Load Uncertainty," Paper No. A76 495-2, IEEE PES Summer Meeting, Portland, Oregon, July 18-23, 1976.

[63] Fischl, R., "The Identification of Feasible Strategies in the Presence of Uncertainties for Planning and Operating of Power Systems," Department of Electrical Engineering, Drexel University, March 1979.

[64] Galiana, F.D., "Analytic Properties of the Loadflow Problem," Proceedings of the IEEE International Symposium on Circuits and Systems, pp. 802-816, Phoenix, Arizona, April 25, 1977.

[65] Shalaby, A., Carvalho, V.F., "Personal Communication," Ontario Hydro, Toronto.

[66] Galiana, F.D., "Power Voltage Limitation Imposed by the Network Structure of a Power System," Proceedings of the Power Industry and Computer Applications (PICA), pp. 356-365, 1975.

[67] Galiana, F.D., Lee, K., "On the Steady State Stability of Power System," Proceedings of the Power Industry and Computer Applications (PICA), pp. 201-210, Toronto, May 1977.

[68] Galiana, F.D., Jarjis, J., "Feasibility Constraints in Power Systems," Paper A78 560-5, IEEE Summer Power Meeting, Los Angeles, July 1978.

[69] Jarjis, J., Galiana, F.D., "Quantitative Analysis of Steady State Stability in Power Networks," Paper F79 753-5, IEEE Summer Power Meeting, Vancouver, July 1979.

[70] Galiana, F.D., Banakar, M., "Approximation Formulae for Dependent Load Flow Variables," Paper A79 078-7, IEEE Winter Power Conference, New York, February 1979 (F80 200-6, IEEE Winter Power Conference, New York, February 1980).

[71] Strang, G., <u>Linear Algebra and Its Applications</u>, Academic Press, New York, 1976.

[72] Rechtschaffen, E.E.M., "Algebraic Properties of Bus and Line Power Equations with Application in Network Planning and Analysis," Proceedings of the Sixth Power System Computation Conference, Darmstadt, Germany, August 21, 1978.

[73] Nobel, B., Applied Linear Algebra, Prentice-Hall Inc., Englewood Cliff, N.J., 1969.

[74] Podmore, R., "Economic Dispatch with Line Security Limits," IEEE Trans., PAS. Vol. 93, pp. 289-295, January / February 1974.

[75] Happ, H.M., "Optimal Power Disptach," Engineering Foundation Conference on Systems Engineering for Power: Status and Prospects, Henniker, N.H., pp. 36-51, August 1975.

[76] Kirchmayer, L.K., Economic Operation of Power Systems, John Wiley and Sons, Inc., New York 1958.

[77] Podmore, R., Peterson, N.W., Stanton, K.W., "Economic Dispatch and Scheduling," Energy Control Centre Design, IEEE Tutorial Course 77 TU0010-9-PWR, pp. 28-35, 1977.

[78] Happ, H.M., "Optimal Power Dispatch - A Comprehensive Survey," IEEE Trans. PAS. Vol. 96, No. 3, pp. 841-854, May / June 1977.

[79] Alsac, O., Stott, B., "Optimal Loadflow with Steady State Security," IEEE Trans. PAS. Vol. 93, pp. 745-751, May / June 1974.

[80] Kron, G., "Tensorial Analysis of Integrated Transmission Systems - Part II: Off-Nominal Turn Ratios," AIEE Trans. Power Apparatus and Systems, Vol. PAS-71, pp. 505-512, 1952.

[81] Early, E.D., Watson, R.E., "A New Method of Determining Constants for the General Transmission Loss Equation," AIEE Trans. Power Apparatus and Systems, Vol. PAS-74, pp. 1417-1423, 1956.

[82] Kirchmayer, L.K., Happ, H.H., Stagg, G.W., Hohenstein, J.F., "Direct Calculation of Transmission Loss Formula," Part I is in AIEE Trans. Power Apparatus and Systems, Vol. PAS-79, pp. 962-969, 1960. Part II is in IEEE Trans. Power Apparatus and Systems, Vol. PAS-83, pp. 702-707, 1964.

[83] Meyer, W.S., Albertson, V.D., "Improved Loss Formula Computation by Optimally-Ordered Elimination Techniques," IEEE Trans. Power Apparatus and Systems, Vol. PAS-90, pp. 62-69, 1971.

[84] Shoult, R.R., Grady, W. Mack, Helmick, S., "An Efficient Method for Computing Loss Formula Coefficients Based Upon the Method of Least Squares," Paper F 78 739-5, Summer Power Meeting, Los Angeles, 1978.

[85] Stevenson, W.D., <u>Elements of Power System Analysis,</u> Second Edition, McGraw-Hill, New York, 1962.

[86] Land, A., and Powell, S., <u>Fortran Codes for Mathematical Programming: Linear, Quadratic and Discrete,</u> John Wiley and Sons, London, 1973.

[87] Sasson, A.M., "Combined Use of the Powell and Fletcher Powell Non-Linear Programming Methods for Optimal Loadflows," IEEE Trans. PAS. Vol. 88, pp. 1530-1537, October 1969.

[88] Sasson, A.M., "Non-Linear Programming Solution for Loadflow, Minimum Loss and Economic Dispatching Problems," IEEE Trans. PAS. Vol. 88, pp. 357-409, April 1969.

[89] Handschin, E., Reichert, K., "A Convergent Loadflow Algorithm Using Non-Linear Optimization Techniques: Theory and Experience," Brown Boveri, Switzerland.

[90] Gill, P.E., Murray, W., (Eds.), Numerical Methods for Constrained Optimization, Academic Press, 1974.

[91] Luenberger, D.G., Introduction to Linear and Non-Linear Programming, Addison Wesley, 1973.

[92] Fiacco, A.V., McCormick, G.P., Nonlinear Programming: Sequential Unconstrained Minimization Techniques, John Wiley, New York, 1968.

[93] Fletcher, R., Powell, M.J.D., "A Rapidly Descent Method for Minimization," Computer Journal, Vol. 6, pp. 163-168, 1963.

[94] Fletcher, R., Reeves, R.M., "Function Minimization by Conjugate Gradiants," Computer Journal, Vol. 7, No. 21, pp. 149-154, 1964.

[95] Bandler, J.W., Charalambous, C., "Nonlinear Programming Using Minimax Techniques," J. Optimiz. Theory Appl., Vol. 13, 1974.

[96] Einarsson, O., "Minimax Optimization by Algorithms Employing Modified Lagrangians," IEEE Trans. Microwave Theory Tech., Vol. MTT-23, pp. 838-841, October 1975.

[97] Wolfe, P., "Methods of Nonlinear Programming" in Recent Advances in Mathematical Programming, Graves, R.L., Wolf, P., (Eds.), McGraw-Hill, New York, 1963.

[98] Ishizaki, Y., Wantanbe, H., "An Iterative Chebyshev Approximation Method for Network Design," IEEE Trans. on Circuit Theory, Vol. CT-15, No. 4, pp. 326-336, December 1968.

[99] Director, S.W., Hachtel, G.D., "The Simplicial Approximation Approach to Design Centering," IEEE Trans. on Circuits and Systems, Vol. CAS-24, No. 7, July 1977.

[100] Marqwardt, D.W., "An Algorithm for Least Squares Estimation of Nonlinear Parameters," SIAM Journal, Vol. 11, 1963.

[101] Bandler, J.W., et al, "Minimax Optimization of Networks by Grazor Search," IEEE Trans. Microwave Theory Tech., Vol. MTT-20, pp. 596-604, September 1972.

[102] IEEE Committee Report, "Control Criteria and Practices Related to Capacity Emergencies," IEEE Trans. on Power Apparatus and Systems, Vol. PAS-98, p. 536, 1979.

[103] Banakar, M.H., Galiana, F.D., "Power System Security Corridors: Concept and Computation," Accepted for presentation at the PICA Conference, 1981.

[104] Pyne, R.A., "Short-Term Bus Load Forecasting and Its Intended Use in Scheduled Outage Analysis," Proc. 1974 IEEE Conference on Decision and Control, pp. 593-598, November 1974.

[105] Lijesen, D.P., et al., "Forecasting of Hourly Loads to Improve Operating Decisions in Power Systems," Paper presented at the IEEE Winter Power Meeting, 1971.

[106] Sullivan, R., <u>Power System Planning,</u> McGraw-Hill, New York, N.Y., 1977.

[107] Galiana, F.D., "An Application of System Identification and State Prediction to Electric Load Modeling and Forecasting," M.I.T., Cambridge, Massachusetts, Electric Power Systems Engineering Laboratory, Report No. 28, March 1971.

[108] Gupta, P.C., Yamada, K., "Adaptive Short-Term Forecasting of Hourly Loads Using Weather Information," Trans. IEEE, PAS-91, pp. 2085-2094, September / October 1972.

[109] Hill, E.F., Stevenson, W.D., "A New Method of Determining Loss Coefficients," IEEE Trans. on Power Apparatus and Systems, Vol. PAS-87, No. 7, pp. 1548-1553, July 1968.

[110] Galiana, F.D., Vojdani, A.F., "Analytic Solution of the Economic Dispatch Problem," Proc. of the Canadian Communication and Power Conference, Montreal, pp. 387-391, October 1978.

[111] Grunbaum, B., Convex Polytopes, Wiley-Interscience, New York, 1967.

[112] Friedlander, G.D., "Matching Utility Outputs to Customer Demand," IEEE Spectrum, Vol. 13, No. 9, September 1976.

[113] Platts, J., "Electrical Load Management: The British Experience," IEEE Spectrum, Vol. 16, No. 2, February 1979.

[114] Kaplan, G., "Two-Way Communication for Load Management," IEEE Spectrum, Vol. 14, No. 8, August 1977.

APPENDIX A

A BRIEF SURVEY ON PURELY NUMERICAL SCHEMES USED FOR SECURITY ANALYSIS AND CONTROL

A.1 Security Analysis

One of the earliest line-outage calculation methods is the "distribution factor method" developed by El-Abiad and Stagg [15] in early 1960's. It is based on the DC load flow approximation and is strictly a sensitivity analysis method. This method has been used for a number of years in power utilities [16] and, apart from poor accuracy and lack of information on reactive flows, has interesting features for on-line application.

The "exact DC outage method" [17, 18] is basically an improved version of the distribution factor method. The improved accuracy, though not substantial, is offset by extra computational requirements. An AC load flow routine would have to be called occasionally to check (or verify) the DC load flow solutions.

The so-called Z-matrix method is an approximate version of a load flow scheme known by the same name. This method was suggested by Brown in the late 1960's [19] . Its accuracy is slightly better than the DC load flow based methods.

Two general load flow schemes which, because of their special features, are currently used extensively for contingency evaluation are Stott's "fast decoupled load flow" [20, 21] and the "iterative linear load flow" scheme of Peterson et al [22] . These schemes can predict efficiently the post-fault value of all key variables, while their accuracy is controlled by the number of iterations.

The decoupled load flow scheme takes advantage of the relative insensitivity of the real power injections to the voltage magnitudes and of the reactive power injections to the voltage phase angles. The weak coupling between these variables allow an approximation of the Jacobian matrix, when a Newton-type algorithm is employed. In the iterative load flow methods the sine and cosine functions of the voltage phase angles are expressed as their Taylor series expansion formulae. The number of terms used (from the series) is in general an accuracy control parameter, but quite often the first two terms are employed. The above two methods appeared in the literature in the early 1970's and both exploit the sparsity as well as the symmetry present in the power flow equations.

In 1972 Daniel and Chen [23] proposed changing the <u>real power</u> injections at the system buses to simulate a line outage. Some numerical improvements to this scheme was then suggested by Stagg and Phadke [24] . The final modification came from Sachdev and Ibrahim [25] who used both real and reactive power injection changes to simulate a line outage. The important aspect of this scheme is that it allows using the same mathematical model for pre-fault as well as post-fault calculations.

A recent work by Zaborszky et al [26] has opened a new avenue to researchers interested in contingency evaluation. In this work the concept of concentric relaxation is exploited by making analogy between a large power system at steady-state and a quiet pond. A fault on the system then corresponds to the fall of a pebble into the pond. This suggests that voltage at buses which are far from the fault position are not going to be affected considerably and can be set at their pre-fault values. Furthermore, by choosing a few "tiers" (corresponding to concentric waves) and localizing the effect of the fault to each tier in turn and then "relaxing" it, relatively accurate solutions can be obtained. The main feature of this approach is the reduced system size due to localizing the effect of the fault. This concept is also expected to have applications in emergency control [27] .

A.2 Security Control

As mentioned in Section 1.3.2.2, because of the excessively large dimension associated with the preventive control problem, it is normally reduced to another problem which tries to take into account the security constraints indirectly. Kaltenbach and Hajdu [28], for instance, proposed that the security constraints can be introduced into a constrained optimization problem concerning only the intact network, through modifying the operating constraints. Peschan et al [29] suggested a similar approach but requiring a simplified special-purpose optimal load flow algorithm. Heuristic approaches based upon adapting objective functions which tend to reduce the power flow or current magnitude in the critical lines are also suggested. The most basic one in this category is introduced by Sachdev and Ibrahim [30] and the most recent one is developed by Blaschak and Heydt [31] . To be effective, such approaches demand considerable insight and familiarity with the power network.

When the computation of corrective controls are desired, the enforcement of the violated constraints is given the highest priority, thus allowing the security constraints to be ignored. This still does not permit an exact optimal rescheduling due to the limited time available for the considerable computation burden.

While the first optimal power flow programs (OPF) were developed primarily as tools for system planning, with the advent of large and fast dispatch computers, their potential value for the system operation was quickly recognized. The first concrete approaches to OPF were developed in France by Carpentier [32, 33] and Abadie [34, 35] . They proceeded in developing a new gradient algorithm, the method of "Generalized Reduced Gradient", in which dependent and independent variables are exchanged in case of constraint violations. This work was later followed in the U.S. by Peschon and others [35, 37, 38] . Another research group in the U.S. (Domel and Tinney) also suggested a gradient projection technique for the reduced gradient of the control parameters [39, 40] . Their method incorporates constraint violations on the dependent variables into the objective function as penalty terms. Here, there is no exchange between the dependent and independent variables except for reactive generation limit violations which are handled by bus type switching. A comprehensive review on OPF techniques is provided in references [41] and [42] . A key element in these approaches is their reliance on fast sparsity oriented Newton-type power flow routines.

A different approach to corrective control (security dispatch) based on the use of approximate linear power flow models, which permits the employment of linear programming (LP) routines, was pursued independently in the Great Britain [43, 44] and the U.S. [45 - 48] . The principal motive for the use of LP arised from the shortcomings of nonlinear programming methods. These deficiencies include:

(i) Unreliability or slowness of convergence;

(ii) The need for sophisticated algorithms and tuning procedures;

(iii) The need for a feasible starting point;

(iv) Complicated sparsity manipulation of matrices;

(v) In the case of using penalty functions, difficulties in recognizing infeasibility.

The main attractions of LP, in contrast, are inherent computational reliability and speed. Furthermore, the duality property of LP formulation allows the large number of constraints present in the corrective control problem to be handled efficiently and systematically.

A major difficulty in this approach is that the formulation of objective functions must be in accord with the framework of LP problems. In the case of total generation cost minimization, for example, quite often piece-wise linear functions are used to represent the cost function of individual generators. This may require assigning a variable to each cost segment, thus increasing the number of variables significantly. Moreover, the constraints are to be transformed into the chosen operating space. The computation required in this step renders this approach unattractive for on-line use. These difficulties were later overcome largely by Stott and Marinho [48] . They combine the relaxation technique [49] with their "reduced basis" approach to decrease drastically the number of required constraint transformation. Another significant contribution of their work is the efficient treatment of piece-wise cost functions, requiring no extra variables in the program. It is possible to generalize their approach to include preventive control, but the required computation still would be excessive.

The approximate linear model, used in the above approaches, takes into account only the real-power injections and the voltage angles. Results in most cases show good agreement between the real power flows predicted by the linear model and that found by an AC power flow solution of the new operating point. This model is nevertheless inadequate for applications which involve changes in the voltage profile or rescheduling of reactive power generations.

A recent work [50], which permits manipulation of all control variables, now seems to be getting wide acceptance. This approach can be viewed as a marriage between the nonlinear OPF and those using linear network models. It is based on successive linearization of the power flow equations and application of LP . The key factor here is the treatment of all variables (dependent or independent) as decision variables. This eliminates the need for transforming the dependent variables into the "operating space". Furthermore, the increase in the problem size due to the inclusion of reactive power generations and voltage magnitudes is offset by the employment of an efficient LP algorithm which exploits the preserved sparsity of the full linear formulation and the use of the "upper-bounding" technique [51] . After every LP iteration, however, a power flow run is needed to ensure staying on the load manifold as the algorithm proceeds toward the optimum solution.

Through suitable formulation of the objective function the corrective and emergency control calculations (e.g., generation rescheduling and load shedding option) are often combined into a single problem [37 - 41] . By proper weighting of the terms defining the objective function, one can assign different priorities to different control actions. Thus by assigning the lowest priority to emergency control actions these controls are evaluated only in the event that corrective controls fail to relieve the existing over-loads. As a result, the numerical approaches cited for corrective control calculations, depending on the available time, could be used for emergency control evaluation as well.

APPENDIX B

FUNCTIONAL REPRESENTATION OF A LOAD OR GENERATOR OUTAGE

Shortly after the occurrence of a load or generator outage, the system responds to it in the form of a frequency shift, Δf. Thus, the change in the system state, to the first order, is

$$\Delta z_i^k = \mu_i \Delta f + \varepsilon_i^k z_i \qquad i = 1, \ldots, N_z \tag{B.1}$$

where ε_i^k is defined in Section 5.2.2, and $\mu_i \triangleq \left(\frac{\partial z_i}{\partial f}\right)_{f=f^o}$ is assumed to be known (e.g., the slope of a generator droop curve). To account for the possible variations in the slack bus real power injection due to the outage, one has to allow also a Δp_1^g of the form:

$$\Delta p_1^g = \mu_s \Delta f + \varepsilon_s^k p_1^g \tag{B.2}$$

To be physically feasible, the resulting new state should satisfy the LFE. This can be ensured approximately by demanding the enforcement of the relation

$$\Delta p_1^g = \underline{\beta}_1^T (\underline{x}_0) \Delta \underline{z} = \sum_{j=1}^{N_z} (\beta_j)_1 \Delta z_j \tag{B.3}$$

The above relation is simply the incremental form of relation (8.14). Adding that to equations (B.1) and (B.2), one has enough equations to solve for Δf, Δz_i and Δp_1^g. After some elementary manipulation of equations (B.1 - B.3), one arrives at the following solutions:

$$\Delta z_i^k = [\sigma_i \underline{\Gamma}^k + \varepsilon_i^k \underline{\ell}_i]^T \underline{z} \qquad i = 1, \ldots, N_z \tag{B.4}$$

where

$$\Gamma_i^k \triangleq (\beta_i)_1 (\varepsilon_i^k - \varepsilon_s^k)$$

$$\sigma_i \triangleq \mu_i [\mu_s - \underline{\beta}_1^T (x_0) \underline{\mu}]^{-1}$$

and $\underline{\ell}_i$ is defined in (4.1). Using (B.4), $\Delta \underline{z}^k$ is expressible in the form of equation (5.12).

<u>Special Case</u>

Since μ_s is proportional to the equivalent inertia of the slack bus generators, in the case where slack bus generators are significantly larger than other generators in the system, one often has

$$\mu_s >> \underline{\beta}_1^T (\underline{x}_0) \underline{\mu}$$

As a result $\sigma_i \approx 0$. This reduces equations (B.4) to

$$\Delta z_i^k \simeq \varepsilon_i^k \, \underline{\ell}_i^T \, \underline{z} = \varepsilon_i^k \, z_i \qquad i = 1, \ldots, N_z$$

i.e., there will be no significant frequency change in the system. For the slack bus, however, from equation (B.3), one obtains:

$$\Delta p_1^g = \sum_{j=1}^{N_z} (\beta_j)_1 \, \varepsilon_j^k \, z_j \tag{B.5}$$

In words, all the variations in the load or generations will be absorbed by the slack bus generators.

APPENDIX C

UP-DATING A LINEAR TSE FORMULA

Here we would like to demonstrate that $\underline{\beta}_j\ (\underline{x}_0)$ can be up-dated for a new expansion point $\underline{x}_i$, using an available decomposed based Jacobian, $[L\ (\underline{x}_0)]$. A direct computation of $\underline{\beta}_j\ (\underline{x}_i)$ involves solving

$$[L\ (\underline{x}_i)]^T\ \underline{\beta}_j\ (\underline{x}_i) = [y_j]\ \underline{x}_i \tag{C.1}$$

for $\underline{\beta}_j\ (\underline{x}_i)$. Defining,

$$\Delta\ \underline{x} \triangleq \underline{x}_i - \underline{x}_0$$

$$\Delta\ \underline{\beta}_j \triangleq \underline{\beta}_j\ (\underline{x}_i) - \underline{\beta}_j\ (\underline{x}_0)$$

one can rewrite equation (C.1) in the form:

$$[L\ (\underline{x}_0 + \Delta\ \underline{x})]^T[\underline{\beta}_j\ (\underline{x}_0) + \Delta\ \underline{\beta}_j] = [y_j]\ (\underline{x}_0 + \Delta\ \underline{x}) \tag{C.2}$$

Using the property (2.25) and the definition of $\underline{\beta}_j\ (\underline{x}_0)$, equation (C.2) reduces to

$$[L\ (\underline{x}_0)]^T\ \Delta\ \underline{\beta}_j = [y_j]\ \Delta\ \underline{x} - [L\ (\Delta\ \underline{x})]^T[\underline{\beta}_j\ (\underline{x}_0) + \Delta\ \underline{\beta}_j] \tag{C.3}$$

The above equation can be solved iteratively for $\Delta \underline{\beta}_j$ according to the iteration rule

$$[L\ (\underline{x}_0)]^T\ \Delta\ \underline{\beta}_j^{k+1} = \Delta\ \underline{b} - [L\ (\Delta\ \underline{x})]^T\ \Delta\ \underline{\beta}_j^k \tag{C.4}$$

where

$$\Delta\ \underline{b} \stackrel{\Delta}{=} [y_j]\ \Delta\ \underline{x} - [L\ (\Delta\ \underline{x})]^T\ \underline{\beta}_j\ (\underline{x}_0) \tag{C.5}$$

Since the term $[L\ (\Delta\ \underline{x})]^T\ \Delta\ \underline{\beta}_j^k$ is of second order, the suggested algorithm normally converges very fast.

APPENDIX D

OPTIMALITY CONDITIONS

Setting $\rho = 0$, the first order optimality conditions for the optimization problem stated in (6.13) take the following form:

(i) $$\left(\frac{\partial L}{\partial \underline{x}}\right)_{\underline{x} = \underline{x}^*} = \underline{0} \quad \text{or}$$

$$[L\,(\underline{x}^*)]^T\,\underline{\alpha}\,(\underline{x}^*) - \frac{1}{2}\lambda^*\,[Y_j]\,\underline{x}^* = \underline{0} \tag{D.1}$$

where

$$\underline{\alpha}\,(\underline{x}^*) \triangleq [A]\,\{[L\,(\underline{x}^*)]\,\underline{x}^* - \underline{z}_g\} \tag{D.2}$$

(ii) $$\left(\frac{\partial L}{\partial \lambda}\right)_{\underline{x} = \underline{x}^*} = 0 \quad \text{or}$$

$$Y_j\,(\underline{x}^*) = Y_j^{\ell} \tag{D.3}$$

(iii) $$\lambda^* > 0 \tag{D.4}$$

The second order optimality condition for this problem can be presented as follows:

(iv) For every vector $\underline{v}$ satisfying

$$\underline{v}^T [Y_j] \underline{x}^* = 0 \tag{D.5}$$

the relation

$$\underline{v}^T \left[\frac{\partial^2 L}{\partial \underline{x}^2}\right]_{\substack{\underline{x} = \underline{x}^* \\ \lambda = \lambda^*}} \underline{v} \geq 0 \tag{D.6}$$

must hold, where

$$\left[\frac{\partial^2 L}{\partial \underline{x}^2}\right] = 2 [L(\underline{x})]^T [A] [L(\underline{x})] + [Z(\underline{\alpha})] - \lambda [Y_j] \tag{D.7}$$

The vector $\underline{\alpha} = \underline{\alpha}(\underline{x})$ is introduced in (D.2). The condition (D.6) is checked by finding a set of N_z-1 orthogonal vectors satisfying (D.5) . This is carried out by using the Gram-Schmidt orthogonalization process, which is discussed in Appendix F .

APPENDIX E

NUMERICAL CONSIDERATIONS IN IDENTIFYING NON-REDUNDANT CONSTRAINTS

The term which requires special attention in obtaining equation (6.54) is $\underline{\ell}_i^T\ [H_j]\ \underline{x}_0$. For a variable $h_j = \underline{x}^T\ [H_j]\ \underline{x}$, one can write

$$\underline{x}^T\ [H_j]\ \underline{\ell}_i = \frac{1}{2}\ (\frac{\partial\ h_j}{\partial\ \underline{x}})\ \underline{\ell}_i = \frac{1}{2}\ \frac{\partial\ h_j}{\partial\ x_i} \tag{E.1}$$

Thus, one can compute $\underline{\ell}_i^T\ [H_j]\ \underline{x}_0$ by direct partial difference of h_j and evaluating the result at $\underline{x} = \underline{x}_0$. The number of terms present in $\frac{\partial\ h_j}{\partial\ x_i}$ is normally less than four. However, when h_j represents a real or reactive power injection at bus j and $j = i$ or $j = i + N$, the number of terms defining $\frac{\partial\ h_j}{\partial\ x_i}$ could be significantly larger. In that case, one can simplify the derivatives by expressing them in terms of the relevant power injections, that is:

$$\frac{\partial\ p_k}{\partial\ e_k} = [g_{kk} + \frac{p_k}{v_k^2}]\ e_k + [B_{kk} + \frac{q_k}{v_k^2}]\ f_k \tag{E.2}$$

$$\frac{\partial\ p_k}{\partial\ f_k} = [g_{kk} + \frac{p_k}{v_k^2}]\ f_k - [B_{kk} + \frac{q_k}{v_k^2}]\ e_k \tag{E.3}$$

$$\frac{\partial\ q_k}{\partial\ e_k} = [g_{kk} - \frac{p_k}{v_k^2}]\ \ f_k + [B_{kk} - \frac{q_k}{v_k^2}]\ e_k \tag{E.4}$$

$$\frac{\partial\, q_k}{\partial\, f_k} = -\,[g_{kk} - \frac{p_k}{v_k^2}]\; e_k + [B_{kk} - \frac{q_k}{v_k^2}]\; f_k \qquad (E.5)$$

Knowing the values of $p_k = P_k\ (\underline{x})$ and $q_k = Q_k\ (\underline{x})$ at $\underline{x} = \underline{x}_0$ makes the computation of the above derivatives trivial. Note that the first step in the proposed algorithm is to ascertain $\underline{x}_0 \ \varepsilon\ S_x$, which involves computing all $P_k\ (x_0)$ and $Q_k\ (x)$.

Relations (E.2) to (E.5) can be derived easily by exploiting the special structure of load flow equations in their current from (see Section 9.1).

APPENDIX F

EVALUATION OF THE MATRICES REQUIRED IN CONSTRUCTION OF SECURITY CORRIDORS

Here, one would like to compute a positive definite matrix $[A_i]$ in such a way that its eigen-vector corresponding to the smallest eigenvalue lies along a given vector $\underline{a}_i$. In the following, two different approaches to this problem are introduced.

Approach 1 :

Consider the following choice for $[A_i]$:

$$[A_i] = \lambda_i^{max} [I] + (\lambda_i^{min} - \lambda_i^{max}) [\underline{a}_i \underline{a}_i^T] \tag{F.1}$$

By choosing $\lambda_i^{max} > \lambda_i^{min} > 0$, the above matrix satisfies all the requirements stated for $[A_i]$. This can be proved easily by noting that for a general vector $\underline{w}$, one can write

$$[a_i \underline{a}_i^T] \underline{w} = (\underline{a}_i^T \underline{w}) \underline{a}_i \tag{F.2}$$

Thus, with $\|\underline{a}_i\| = 1$,

$$[A_i] \underline{a}_i = \lambda_i^{max} \underline{a}_i + (\lambda_i^{min} - \lambda_i^{max}) (\underline{a}_i^T \underline{a}_i) \underline{a}_i = \lambda_1^{min} \underline{a}_i \tag{F.3}$$

and for any vector $\underline{b}$ satisfying $\underline{a}_i^T \underline{b} = 0$,

$$[A_i]\,\underline{b} \;=\; \lambda_i^{max}\,\underline{b} + (\lambda_i^{min} - \lambda_i^{max})\;(\underline{a}_i^T\,\underline{b})\;\underline{a}_i \;=\; \lambda_i^{max}\,\underline{b} \tag{F.4}$$

In words, $\underline{a}_i$ and N_z-1 possible independent vectors perpendicular to it (a full basis for the null space of $[\underline{a}_i\ \underline{a}_i^T]$) form the eigen-vectors of $[A_i]$. Furthermore, except for λ_i^{min}, all the other eigenvalues of $[A_i]$ are equal to λ_i^{max}.

Applying the matrix inversion lemma, one can show readily that

$$[A_i]^{-1} \;=\; \frac{1}{\lambda_i^{max}}\,[I] + \frac{(\lambda_i^{max} - \lambda_i^{min})}{\lambda_i^{max}\,\lambda_i^{min}}\;[\underline{a}_i\ \underline{a}_i^T] \tag{F.5}$$

Note that here one has control only over λ_i^{min} and λ_i^{max}. By specifying these two parameters, all the eigenvalues of the matrix $[A_i]$ will be fixed.

<u>Approach 2 :</u>

A positive definite matrix $[A_i]$ can be expressed generally in the form:

$$[A_i] \;=\; [M_i]^T\;[\Lambda_i]\;[M_i] \tag{F.6}$$

The eigen-vectors of $[A_i]$ are the columns of the matrix $[M_i]$, and $[\Lambda_i]$ is a diagonal matrix containing the eigenvalues. To have the required properties, $\underline{a}_i$ must be one of the orthonormal columns of $[M_i]$. Moreover, all the eigenvalues must be positive and the smallest one should correspond to $\underline{a}_i$.

We start with the following set of independent vectors

$$\{\underline{a}_i, \underline{\ell}_2, \ldots, \underline{\ell}_i, \ldots, \underline{\ell}_{N_z}\} \tag{F.7}$$

where $\underline{\ell}_i$ has 1 in the ith position and zeros elsewhere. This set of independent vectors then can be converted into a set of orthogonal vectors by the Gram-Schmidt process: First $\underline{m}_1 = \underline{a}_i$, and then each $\underline{m}_k$ is computed according to

$$\underline{m}_k = \underline{\ell}_k - \frac{\underline{m}_1^T \underline{\ell}_k}{\|\underline{m}_1\|^2} \underline{m}_1 - \ldots - \frac{\underline{m}_{k-1}^T \underline{\ell}_k}{\|\underline{m}_{k-1}\|^2} \underline{m}_{k-1} \tag{F.8}$$

The final vectors, when normalized, can represent the columns of $[M_i]$. At that stage, $\underline{a}_i$ need not be the first column of $[M_i]$. Note that

$$[A_i]^{-1} = [M_i]^T [\Lambda_i]^{-1} [M_i] \tag{F.9}$$

The specific choice of the original set of vectors, introduced in (F.7), facilitates the required computations considerably.

APPENDIX G

COMPUTATION OF THE CHANGES IN THE INJECTION VECTOR DUE TO SHUNT REACTOR OR CAPACITOR SWITCHING

Suppose, in order to modify the operating point $\underline{z}_0$, some reactive devices at the load buses j, k, and ℓ are switched into the system. The reactive power injections at these buses change according to

$$\Delta Q_i = - \Delta B_{ii} v_i^2 \qquad i = j, k, \ell \tag{G.1}$$

where v_i^2 represents the post-switching voltage level at bus i . The values of ΔB_{ii} $i = j, k, \ell$ are known in terms of the reactance of the switched devices. From Section 4.5.2 we know that the voltage levels at the load buses can be expressed accurately by a linear function of the injection vector. Thus, one can write

$$v_i^2 = \underline{\beta}_i^T (\underline{x}_0) (\underline{z}_0 + \Delta \underline{z}) = (v_i^0)^2 + \underline{\beta}_i^T (\underline{x}_0) \Delta \underline{z} \qquad i = j, k, \ell \tag{G.2}$$

where $(v_i^0)^2$ is the pre-switching voltage level at bus i and

$$\underline{\beta}_i (\underline{x}_0) = [L (\underline{x}_0)]^{-T} [V_i] \underline{x}_0 \tag{G.3}$$

Since ΔQ_j, ΔQ_k, and ΔQ_ℓ are the only changes in the injection vector, it follows that

$$\underline{\beta}_i^T \, (\underline{x}_0) \; \Delta \, \underline{z} \;=\; (\beta_r)_i \; \Delta \, Q_j + (\beta_m)_i \; \Delta \, Q_k + (\beta_n)_i \; \Delta \, Q_\ell \qquad \text{(G.4)}$$

$$i = j,\ k,\ \ell$$

where $(\beta_r)_i$, $(\beta_m)_i$, and $(\beta_n)_i$ are respectively components of $\underline{\beta}_i \, (\underline{x}_0)$ corresponding to $\Delta \, Q_j$, $\Delta \, Q_k$, and $\Delta \, Q_\ell$ in $\Delta \, \underline{z}$. By using relations (G.2) and (G.4) into (G.1), one ends up with a system of linear equations for the unknowns $\Delta \, Q_j$, $\Delta \, Q_k$, and $\Delta \, Q_\ell$.

APPENDIX H

POSITIVE SEMI-DEFINITENESS OF THE MATRIX $[E(\underline{x}_0)]$ WHEN COMPUTED FOR THE NETWORK LOSSES

For the network losses, the matrix $[E(\underline{x}_0)]$ is given by

$$[E_\ell(\underline{x}_0)] \triangleq [Y_\ell] - [Z(\underline{\beta}_\ell)] \tag{H.1}$$

where

$$\underline{\beta}_\ell(\underline{x}_0) = [L(\underline{x}_0)]^{-T} [Y_\ell] \underline{x}_0 \tag{H.2}$$

and $[Y_\ell] \geq 0$. We would like to prove $[E_\ell(\underline{x}_0)] \geq 0$ when $\underline{x}_0$ is chosen sufficiently "close" to $\underline{x}_f$, the flat voltage profile. The proof is based on the following proposition:

For any matrix $[A]$ and vector $\underline{y}_1$ satisfying

$$\underline{y}_1^T [A] \underline{y}_1 > 0 \tag{H.3}$$

there exists a $\varepsilon > 0$ such that any $\underline{y}_2$ satisfying

$$\|\underline{y}_1 - \underline{y}_2\| < \varepsilon \tag{H.4}$$

is guaranteed to satisfy

$$\underline{y}_2^T \, [A] \, \underline{y}_2 > 0 \tag{H.5}$$

The proof also uses the facts that

$$[E_\ell \, (\underline{x}_0)] \, \underline{x}_0 = \underline{0} \tag{H.6}$$

$$[Y_\ell] \, \underline{x}_f = \underline{0} \tag{H.7}$$

To use the above proposition, first one needs to prove that:

$$\varepsilon_1 \, (\underline{x}_f) = \underline{x}_f^T \, [E_\ell \, (\underline{x}_0)] \, \underline{x}_f > 0 \tag{H.8}$$

This is easy to verify once one notes that $\varepsilon_1 \, (\underline{x}_f)$ can be written in the form

$$\varepsilon_1 \, (\underline{x}_f) = \Delta \, \underline{x}^T \, [Y_\ell] \, \Delta \, \underline{x} + \Delta \, \underline{x}^T \, [Y_\ell] [L \, (\underline{x}_0)]^{-1} [L \, (\Delta \, \underline{x})] \, \Delta \, \underline{x} \tag{H.9}$$

where $\Delta \, \underline{x} = \underline{x}_f - \underline{x}_0$. The second term in this expression is of third order in $\Delta \, \underline{x}$; therefore, for small $\Delta \, \underline{x}$, the first term is always dominant. The first term, however, represents the network losses at $\Delta \, \underline{x}$ and is positive when $\Delta \, \underline{x} \neq \underline{x}_f$. This implies that for all $\underline{x}_0$ sufficiently close to $\underline{x}_f$ relation (H.8) is always true.

Now we prove by contradiction that $[E(\underset{\sim}{x}_0)] \geq 0$. Starting from the assumption that $[E(\underset{\sim}{x}_0)] < 0$, one can assume that $\underset{\sim}{x}_0$ can be chosen so close to $\underset{\sim}{x}_f$ that $[E(\underset{\sim}{x}_0)]$ has only one negative eigenvalue. This is a realistic assumption considering the fact that for $\underset{\sim}{x}_0 = \underset{\sim}{x}_f$, $\underset{\sim}{\beta}_\ell(\underset{\sim}{x}_0) = \underset{\sim}{0}$ and $[E(\underset{\sim}{x}_0)] = [Y_\ell] \geq 0$. Denoting this eigenvalue by λ_m, and its corresponding eigenvector by $\underset{\sim}{x}_m$, it follows that

$$\underset{\sim}{x}_m^T [E(\underset{\sim}{x}_0)] \underset{\sim}{x}_m = \lambda_m \|\underset{\sim}{x}_m\|^2 < 0 \tag{H.10}$$

Since $\underset{\sim}{x}_0$ satisfies (H.6), the vector $\underset{\sim}{x}_m$ must be very "close" to $\underset{\sim}{x}_0$. On the other hand, $\underset{\sim}{x}_0$ is chosen very "close" to $\underset{\sim}{x}_f$. This implies that one can always choose $\underset{\sim}{x}_0$ sufficiently close to $\underset{\sim}{x}_f$ to satisfy

$$\|\underset{\sim}{x}_f - \underset{\sim}{x}_m\| < \delta \tag{H.11}$$

where δ is a positive constant. But, relations (H.8) and (H.11) according to the aforementioned proposition imply that

$$\underset{\sim}{x}_m^T [E(\underset{\sim}{x}_0)] \underset{\sim}{x}_m > 0 \tag{H.12}$$

which contradicts (H.10).

Q.E.D.